U.PORTO

FEUP FACULDADE DE ENGENHARIA
UNIVERSIDADE DO PORTO

MIT Portugal

Advanced forecast and scheduling of power systems with highly variable sources

PhD Program in Sustainable Energy Systems

Pedro Miguel Neves da Fonte, *M.Sc.*

Dissertation submitted to the Faculty of Engineering of University of Porto
in partial fulfilment of the requirements for the degree of
Doctor of Philosophy

Supervisor: Professor Fernando Pires Maciel Barbosa, Ph. D.

Co-supervisor: Professor Cláudio Domingos Martins Monteiro, Ph. D

Department of Electrical and Computer Engineering,
Faculty of Engineering, University of Porto

January, 2015

À Paula, à Carolina e ao Rodrigo

Acknowledgments

It was a long, challenging and sometimes difficult path that allowed me to conclude this thesis. This thesis was only possible thanks to many people and institutions, who helped me in several ways to reach this goal. I owe my thanks to all of them.

First of all, I would like to express my gratitude to my scientific adviser, Professor Fernando Maciel Barbosa; to his commitment and dedication as well as his valuable advice. It was his constant support and advice that kept me moving forward and steadfast, even in times of great frustration.

A very special thanks to my co-adviser Professor Cláudio Monteiro, for all his support from the beginning and throughout this work and, in particular for having placed at my disposal, his insight and scientific ability. Without his advice, I would not have reached my goals. I would like to highlight both his human and scientific qualities.

To the São Miguel's power company, *EDA – Electricidade dos Açores*, a special acknowledge for providing the data used in this work.

To the Smartwatt team, a great acknowledgement for their team spirit, and all support. I have to give special thanks to Bruno Santos for his infinite patience in helping me during the implementation of the case studies. Without his efforts, this work would have had a different ending. With his scientific and human abilities, I predict that he will have a future full of success.

To my PhD colleagues, Pedro Almeida, Manuel Rocha, Julia Vasiljevska, Antero Moreira da Silva, Joel Soares and Pedro Melo, who have demonstrated a spirit of friendship and companionship. This spirit will never be forgotten.

My thanks to professor João Peças Lopes, for his kindness and comprehension revealed when he received me for the first time in the PDSEE program.

To all my colleagues of the ISEL's Electrical Machines Group. First my thanks goes to Professor José Carlos Quadrado, who influenced me to follow a teaching and researching career. Very special thanks to Rita Pereira and Ricardo Luís, for all their incredible support, their tolerance and encouragement during hard times. To them I wish the biggest success in their PhD research. To Professor Sérgio Abrantes Machado whose technical and human competencies are a source of inspiration and an example to follow. A special thanks for the remaining colleagues of the ISEL's Electrical Machines Group, for all the words of encouragement to pursue the work.

The most special acknowledgment goes to my family. To my parents and brother, who throughout my life inspired my accomplishments, on a personal and professional level. I would

like to make my greatest thanks to the encouragement and trust that they have in me. I hope I deserve that trust.

Lastly I thank Paula, my always present wife, my life mate for more than twenty years, who has always supported me in both good and bad times, and always in her own detriment. During all these years she has been my pillar of support.

Finally to my children, Carolina and Rodrigo, hoping that, someday, they will be able to understand all the moments during which I was not present and I hope that this work can one day serve as an inspiration to their long lives.

To all those that I did not mention but are in my mind I give great thanks.

A todos, um grande Obrigado.

Abstract

Management of electric energy production is one of the most important issues in electric grids operation. With this management it is intended to feed the load ensuring the generation/consumption equilibrium in a most economical way, simultaneously respecting technical constraints. In addition to this technical/economical management it is mandatory to ensure the system reliability in order to safeguard the continuity of service in case of some fault, or catastrophe of some of the power system components, whether they are on generation level, transportation or loads. All this management is done through the unit commitment and economic dispatch, to be able to decide which generation units have to be connected to the power grid as well as the allocated load to each one. This process, based in mature and well dominated technology, became a new challenge with the massive introduction of electric energy generation based in renewable power sources. These, are predisposed to depend on variable and hard to control resources, adding a large amount of uncertainty to the decision process. This problem is enhanced in systems with low rated power, as is the case of islands without connection to the large continental grids, without storage capacity or quick starting generation units. Generally this problem is addressed by two different approaches which, in the end, complement each other. One is at a forecasting level; researching improvements in performances of forecasting as well as the apprehension of the renewable production uncertainties. The second pursues the development of scheduling models which potentiate information obtained by the forecast, as well as the increment of velocity.

Most recent researching works focus on the application of stochastic programming models in order to decide the unit commitment of the units as well as in production and reserve's allocation and security levels.

This work intends to develop a complete methodology including the forecasting of renewable generation and load, with respective characterization of the uncertainty, complemented with scheduling based in a risk assessment model. The case study refers to the production power system of São Miguel Island (Azores, Portugal).

During the development of this work, an overview about the techniques and mathematical formulation of scheduling models (deterministic and stochastic) as well as some state of the art solving techniques was done. It is also presented an overview concerning the renewable production and load forecasting, together with models to represent the uncertainty. It was done a detailed study about some of these techniques, namely concerning the choice of forecasting models and explanatory variables as well as a short sensibility analysis about the influence of explanatory variables. Thus, it was developed a model of aggregate forecasts in order to indicate the thermal production necessities. Then it is presented an original contribution of a scheduling

model based on risk assessment based on formulation of the production system of São Miguel. Also, characterization of thermal production is done, introducing the concept of equivalent optimal generation unit. In parallel, it is presented a metaheuristic based on a cloud of particles to solve the economic dispatch problem, with its performances being compared with some results presented in biography.

At the end it is shown a real case study where detailed explanation is presented, under a real context, the developed methodology. Finally, it is done a comparison with the scheduling proposed by the system operator of São Miguel Island and conclusions are drawn.

In short, this work proposes a complete methodology since the forecasting up to the generation scheduling for an isolated system with large penetration of renewable generation.

Keywords: Metaheuristics; Power generation scheduling; Power forecasting; Risk assessment; Power system operation in islands

Resumo

A gestão da produção de energia elétrica é uma das questões mais importantes na operação de redes de energia. Com esta gestão pretende-se alimentar a necessidade de carga mantendo o equilíbrio produção/consumo da forma mais económica e ao mesmo tempo respeitando as restrições técnicas. Para além desta gestão técnico/económica é necessário garantir a fiabilidade do sistema de modo a garantir a continuidade de serviço no caso de mesmo no caso de alguma falha, desde que não catastrófica, de alguns componentes do sistema de potência, sejam eles a nível da geração, transporte ou cargas. Toda esta gestão é feita através do comissionamento de grupos e despacho económico de modo a decidir quais a unidade que devem estar ligadas à rede bem como a alocação de carga a cada uma delas. Todo este processo baseado em tecnologia madura e bem cimentada tornou-se num desafio com a introdução em massa de geração de energia elétrica com base em energias renováveis. Estas tendencialmente dependem de recursos variáveis e difíceis de controlar. Nesse sentido foi adicionado uma grande quantidade de incerteza ao processo de decisão. Este problema é potenciado em sistemas com baixa potência instalada como é o caso de ilhas sem ligação às grandes redes continentais e sem capacidade de armazenamento de energia ou unidades produtoras com arranques rápidos.

Este problema geralmente é abordado por duas perspectivas diferentes que no fim se complementam. Uma a nível da previsão, com a procura de uma melhoria nas performances da previsão e captura da incerteza da produção renovável. A outra no desenvolvimento de modelos de comissionamento para potenciar a informação obtida pelas previsões bem como o incremento da sua rapidez.

Os trabalhos mais recentes apostam na aplicação de modelos de programação estocástica com vários níveis de modo a decidir o comissionamento de grupos, bem como a alocação de produção e reservas, e níveis de segurança.

Neste trabalho desenvolveu-se uma metodologia completa que passa pela previsão da produção renovável e carga com a respetiva caracterização da incerteza e pelo comissionamento da geração baseado numa análise de riscos. O caso estudado é referente ao sistema produtor da ilha de São Miguel nos Açores (Azores/Portugal).

Durante o desenvolvimento deste trabalho foi feito uma visão geral acerca das técnicas e formulações matemáticas dos modelos de agendamento (determinístico e estocástico) bem como de algumas técnicas de resolução presentes no estado-da-arte. É também apresentada uma visão geral acerca das técnicas de previsão de produção renovável e carga, bem como dos modelos para representar a sua incerteza. Foi feito um estudo detalhado acerca de algumas dessas técnicas, nomeadamente acerca da escolha dos modelos de previsão e das variáveis explicativas bem como uma pequena análise de sensibilidades acerca da influência das variáveis explicativas.

Foi desenvolvido um modelo de previsões agregadas de modo a se conhecer qual a necessidade de produção térmica.

Seguidamente é apresentada uma contribuição original de um modelo de agendamento baseado na análise de risco tendo por base de formulação o sistema produtor de São Miguel. É feita uma caracterização da produção térmica com a introdução do conceito de (unidade geradora equivalente ótima) *equivalent optimal generation unit*. Paralelamente é apresentada uma meta heurística baseada em nuvens de partículas para a resolução do problema de despacho económico sendo as suas performances comparadas com alguns dos resultados presentes na bibliografia.

Por fim é apresentado um caso estudado real onde se explica com algum detalhe e num contexto real a metodologia desenvolvida, feita a comparação com o comissionamento proposto pelo operador do sistema elétrico da ilha de São Miguel e tiradas conclusões.

Em suma este trabalho propõe uma metodologia completa desde a previsão até ao comissionamento da geração para um sistema isolado com grande penetração de produção renovável.

Palavras-chave: Análise de risco; Gestão de produção de energia; Meta-heurísticas; Previsão de Potência; Operação de sistemas de energia em ilhas

List of contents

List of figures

List of tables

List of abbreviations and symbols

AGC – Automatic Generation Control

ALADIN – Aire Limitee Adaptation Dynamique development InterNational

ANFIS – Artificial Neuro Fuzzy Inference System

ANN – Artificial Neural Networks

ANN_CC – Cascade Correlation

ANN_CG – Conjugate-Gradient

ANN_LM – Levenberg-Marquardt

ARMA – Auto Regressive Moving Average

ARIMA – Autoregressive Integral Moving Average

ARMAX – Auto-Regressive with Exogenous Input

BMGP – Below Minimum Generation Probability

BP – Back propagation

CCPSO – Chaotic sequences and Crossover operation PSO

CEP – Classical Evolutionary Programming

CFD – Computational Fluid Dynamic

CGRG – *Central Geotérmica Ribeira Grande*

CGPV – *Central geotérmica do Pico Vermelho*

CHTN – *Central Hídrica dos Túneis*

CHTB – *Central Hídrica dos Tambores*

CHFN – *Central Hídrica da Fábrica Nova*

CHCA – *Central Hídrica do Canário*

CHFR – *Central Hídrica Foz da Ribeira*

CHRP – *Central Hídrica Ribeira da Praia*

CHSC – *Central Hídrica do Salto do Cabrito*

COPSO – Crossover Operation PSO

CSPSO – Chaotic Sequences PSO

DED – Dynamic Economical Dispatch

DP – Dynamic programming

ED – Economic dispatch

EDA – *Eletricidade dos Açores*

EP – Evolutionary Programming

ESO – Evolutionary Strategy Optimization

EV – Expected Value

FS-SCUC – Full Scenario-Security Constrained Unit Commitment

FEP – Fast Evolutionary Programming

GA – Genetic Algorithms
GENSET – Generators Set
HPP – Hydrological Power Potential
IFEP – Improved Fast Evolutionary Programming
IPSO – Improved Particle Swarm Optimization
ISO – Independent System Operator
ITS – Improved Taboo Search
KDE – Kernel Density Estimator
LHS – Latin Hypercube Sampling
LS – Load Shed
LOLE – Loss Of Load Expectation
LOLP – Loss Of Load Probability
LOWP – Loss Of Wind Probability
MAE – Mean Absolute Error
MAPE – Mean Average Percentage Error
ME – Mean Error
MIP – Mixed Integer Programming
MILP – Mixed Integer Linear Programming
MLP – Multi layer perceptron
MOS – Model Output Statistics
MPSO – Modified PSO
MSE – Mean Squared Error
MRI – Meteo Risk Index
NO – Normal Operation
NOC – Normal Operation Cost
NMAE – Normalized Mean Absolute Error
NMAPE – Normalized Mean Absolute Percentage Error
NPRI – Normalised Prediction Risk Index
NPSO – New Particle Swarm Optimization
NPSO – LRS - New Particle Swarm Optimization with Local Random Search
NRMSE – Normalized Root Mean Squared Error
NW – Nadaraya-Watson
NWP – Numerical Weather Prediction
ORR – Outage Replacement Rate
PE – Percentage Error
PSO – Particle Swarm Optimization

PSO-CEP – PSO embebbed in CEP

PSO-LRS – Particle Swarm Optimization with Local Random Search

QR – Quantile Regression

RBF – Radial Based Functions

RCED – Reliability Constraint Economic Dispatch

RCUC – Reliability Constraint Unit Commitment

RES – Renewable Energy Sources

RMSE – Root Mean Squared Error

SCADA - Supervisory Control And Data Acquisition

SCED – Security Constrained Economic Dispatch

SFEP – Swarm direction Fast Evolutionary Programming

SF – Skill Forecasting

SCO – Sensing Cloud Optimization

SCUC – Security Constrains Unit Commitment

SHPP – Small Hydro Power Plant

SONARX – Self-Organizing Nonlinear Auto-Regressive model with eXogenous input

SSCUC – Stochastic Security Constrained Unit Commitment

s.t. – subject to

UC – Unit commitment

WPF – Wind power forecast

WPP – Wind power production

WS – Wait-and-See

W2P – Wind to Power

WRF – Weather Research Forecasting

List of variables

A	Matrix of coefficients in linear programming
A	Incremental response of the power generation to the precipitation
a_i	Coefficient of cost function of thermal unit *i*
a_{ik}	Coefficient of cost function of thermal unit *i* with fuel *k*
A_i	Non-load cost, thermal unit *i*
$AS_{i,t}$	Boiler cool down coefficient of unit *i* at time *t*
B	Hydro generation decay in dry days
b_i	Coefficient of cost function of thermal unit *i*
b_{ik}	Coefficient of cost function of thermal unit *i* with fuel *k*
b	Vector of coefficients in linear programming formulation
$BM_{i,t}$	Base value of maintenance cost of unit *i* at time *t*
$BS_{i,t}$	Boiler start-up cost of unit *i* at time *t*
C	Vector of coefficients in linear programming formulation
c_i	Coefficient of cost function of thermal unit *i*
c_{ik}	Coefficient of cost function of thermal unit *i* with fuel *k*
$C_i^d(k)$	Shut-down cost, thermal unit *i*, period *k*
$C_i^p(k)$	Production cost, thermal unit *i*, period *k*
$C_i^{p,s}(k)$	Production cost, thermal unit *i*, period *k*, scenario *s*
$C_i^u(k)$	Start-up cost, thermal unit *i*, period *k*
$cw_j(k)$	Wind generation shed, wind unit *j*, period *k*
C_{BO}	Blackout cost
CC_i	Cold starting cost, thermal unit *i*
C_{GENSET}	GENSET cost
$C_{WC,h}$	Cost of wind curtailment, hour *h*
$C_{LS,h}$	Cost of load shed, hour *h*
$C_{min\|WC,h}$	Cost of production below the generators minimum, hour *h*
D	Recourse matrix of stochastic programming
$D(k)$	Load, period *k*
D_t^f	Load at time *t*
$D_{i,t}$	Number of hours that the unit *i* is off-line
DR_i	Decrement ramp rate of unit *i*
e_i	Coefficient of cost function of thermal unit *i*
e_{ik}	Coefficient of cost function of thermal unit *i* with fuel *k*

E	Expected value
f_i	Coefficient of cost function of thermal unit *i*
f_{ik}	Coefficient of cost function of thermal unit *i* with fuel *k*
$f_{t+k\|t}$	*Pdf* look-ahead time *t+k* done at time *t*
$F_{i,t}$	Cost function of each unit *i* at time *t*
$\boldsymbol{F}$	Set of feasible solutions
$F_{t+k\|t}$	*Cdf* look-ahead time *t+k* done at time *t*
$\hat{F}_{t+k\|t}$	Forecasted cumulative distribution at time *k* done at time *t*
FC	Fuel cost
$FC_{i,t}(P_{i,t})$	Generic energy production cost of each on-line thermal unit *i*
F_{S1}	Enlarging factor of inverted sigmoid
F_{S2}	Enlarging factor of inverted sigmoid
H	Shrinkage factor of inverted sigmoid
HC_i	Hot starting cost, thermal unit *i*
H_h	Hydrological power potential
H_{new_h}	Refreshed value of hydrological power potential
h_c	Sigmoid function coefficients
h_o	Minimum value of hydrologic power potential
h_m	Maximum value of hydrologic power potential
h_s	Sigmoid function coefficients
h_p	Bandwidth for variable *p*
h_j	Bandwidth of each Kernel *j*
$IM_{i,t}$	Incremental value of maintenance cost of unit *i* at time *t*
$\hat{I}^{(\beta)}_{t+k\|t}$	Forecasted interval with nominal coverage β
K	Number of periods under commitment
K_i	Incremental shutdown cost of unit *i*
k	Number of iterations of SCO
$KP_{i,t}$	Incremental shut-down cost
L	Set of feasible states in dynamic programming
L_N	*Net load*
L_{NW}	*Net load* after wind curtailment
M	Number of the cloud particles
$MC_{i,t}$	Maintenance cost of unit *i* at time *t*
$MC_{l,i}$	Marginal cost, block *l*, thermal unit *i*

$MS_{i,t}$	Start-up maintenance cost of unit *i* at time *t*
min_{GENSET}	Minimum power limit of each GENSET
max_{GENSET}	Maximum power limit of each GENSET
n	Number of samples
$n_{k,1}^{\alpha}$	Number of "hits" within the interval forecast α, to instant *k*
$n_{k,0}^{\alpha}$	Number of "fails" in the interval forecast α, to instant *k*
N	Number of problem dimensions
N_G	Number of thermal generators
N_L	Number of line of the network
N_{PZ}	Number of prohibited zones
Ns	Number of scenarios
N_W	Number of wind generators
P_{est_h}	Forecasted hydro power production
$P_{i,t}$	Power production of unit *i* at hour *t*
$P_{i,t}^{0}$	Power production form unit *i* at the beginning of the hour *t*
$P_{i,1}^{LB}$	Lower bound of 1st prohibited zone
$P_{i,j}^{LB}$	Lower bound of j^{th} prohibited zone
$P_{i,j-1}^{UB}$	Upper bound of$(j\text{-}1)^{th}$ prohibited zone
$P_{i,Npz}^{LB}$	Lower bound of *last* prohibited zone
$P_{i,t}^{\max}$	Maximum technical limit of unit *i* at hour *t*
$P_{i,t}^{\min}$	Minimum technical limit of unit *i* at hour *t*
$P_{ik,t}^{\min}$	Minimum technical limit of unit *i* with fuel *k* at hour *t*
P_L	Power losses
$P_{LF,j,t}$	Power flow at line *j* at time *t*
$P_{LF,j,t}^{\max}$	Maximum power flow at line *j* at time *t*
$\underline{PT}_i$	Minimum capacity, thermal unit *i*
$\overline{PT}_i$	Maximum capacity, thermal unit *i*
$pt_i(k)$	Power generation, thermal unit *i*, period *k*
$pt_i^s(k)$	Power generation, thermal unit *i*, period *k*, scenario *s*
$\underline{pt}_i(k)$	Minimum feasible generation, thermal unit *i*, period *k*

$\overline{pt_i}(k)$	Maximum feasible generation, thermal unit *i*, period *k*
$\overline{pt_i^s}(k)$	Maximum feasible generation, thermal unit *i*, period, scenario *s*
$PW_j^f(k)$	Wind power forecast, unit *j*, period *k*
$pw_j(k)$	Wind generation, unit *j*, period *k*
$pw_j^s(k)$	Wind generation, unit *j*, period *k*, scenarios *s*
$\hat{p}_{t+k\|t}$	Power forecasted to time t+*k* done at time *t*
P_w	Wind power production
q	Penalty factor
$q^{\alpha}_{t+k\|t}$	Quantile with nominal coverage α_i to time t+*k* done at time *t*
$r(k)$	Reserve, period *k*
$\hat{q}(\tau)$	Forecasted quantile with nominal coverage τ
$R^2_{fitness(i)}$	Determination coefficient of second-order trend line, dimension *i*
$R^2_{\varphi(i)}$	Determination coefficient of first-order trend line, dimension *i*
R_h	Forecasted precipitation
R_t	Power reserve at time *t*
RD_i	Ramping limit (down), thermal unit *i*
RU_i	Ramping limit (up), thermal unit *i*
s	Scenario *s*
$\boldsymbol{S}$	Set of scenarios *s*
$SD_{i,t}$	Shut-down cost of unit *i* at time *t*
$ST_{i,t}$	Start-up cost of unit *i* at time *t*
SU_i	Start-up ramp limit, thermal unit *i*
T	Set of planning horizons *t*
T_i^{dn}	Minimum down time limit, thermal unit *i*
T_i^{up}	Minimum up time limit, thermal unit *i*
$T_i^{up,0}$	Minimum up time limit, thermal unit *i*
T_i^{up-1}	Minimum up time limit, thermal unit *i*
$t_{off,i,t}$	Minimum down time of unit *i* at time *t*
$T_{off,i}$	Minimum down time of unit *i*
$t_{on,i,t}$	Minimum up time of unit *i* at time *t*
$T_{on,i}$	Minimum up time of unit *i*
$t_{p(i)}$	Minimum value of second-order regression for the dimension *i*

$TS_{i,t}$	Turbine start-up costs of unit *i* at time *t*
$u_i(k)$	Binary variable on/off, thermal unit *i*, period *k*
$u^s_i(k)$	Binary variable on/off, thermal unit *i*, period *k*, scenario *s*
U_i	Average unavailability of unit *i*
$U_{i,t-1}$	Binary variable on/off, thermal unit *i* at time *t-1*
$U_{i,t}$	Binary variable on/off,thermal unit *i* at time *t*
UR_i	Incremental ramp rate of unit *i*
v	Wind speed
$\boldsymbol{x}$	Vector of variables
$x_{b(i)}$	Position of the best particle on dimension *i*
$x_{\max(i)}$	Maximum limit of search space, dimension *i*
$x_{\min(i)}$	Minimum limit of search space, dimension *i*
$X_{q(i)}$	Central point of the cloud of particles, dimension *i*
$x_{t+k\|t}$	Generic explanatory variable to time *t+k*
$\mathbf{Z}$	Vector of scenarios
$Z_t^{(s)}$	Scenario (*s*) at time (*t*)
α_i	Quantile α
α_l	Lower bound nominal proportion
α_u	Upper bound nominal proportion
$\hat{\alpha}_k^{\alpha}$	Percentage of "hits" in nominal coverage α, to instant *k*
α_h	Coefficient α of Beta distribution for hour *h*
α_{h1}	Coefficient α of Beta distribution for hour *h*, after wind curtailment
$\hat{\beta}(\tau)$	Predicted coefficients in quantile regression
$\beta_i(\tau)$	Regressor coefficients in quantile regression
β_h	Coefficient β of Beta distribution for hour *h*
β_{h1}	Coefficient β of Beta distribution for hour *h*, wind curtailment
$\overline{\Delta}_{l,i}$	Maximum generation block *l*, thermal unit *i*
$\delta_{l,i}(k)$	Thermal generation, block *l*, unit *i*, period *k*
$\delta^s_{l,i}(k)$	Thermal generation, block *l*, unit *i*, period *k*, scenario *s*
$\delta^{\alpha}_{t+k\|t}$	Size of the interval forecast with nominal coverage rate α
$\overline{\delta}_k^{\alpha}$	Mean size of the distance between quantiles
λ_f	Forgetting factor
λ_i	Failure rate of unit *i*

μ_i	Repair rate of unit *i*
$\sigma_{\varphi(i,j)}$	Standard deviation of $\varphi_{(i,j)}$
$\sigma_{\text{fitness}(i,j)}$	Standard deviation of fitness values of $\varphi_{(i,j)}$
$\sigma^2_{(i)}$	Variance of the dimension *i* of the cloud of particles
ω	Uncertain parameters
Ω	Set of uncertainty realizations of ω
ξ	Set of uncertainty parameters
$\xi_k^{\alpha_i}$	Indicator variable for observed proportions
$\xi(\omega)$	Realization of the uncertainty

Operators

$\frac{\partial f(\bullet)}{\partial \bullet}$	Partial derivative operation
F_t^{-1}	Inverse cumulative distribution
Unif	Uniform distribution
min	minimization
$\mathscr{L}$	Lagrange function
K_j	Kernel function for variable *j*
$f_{x,y}(x_i,y_i)$	Joint density function
$f_x(x)$	Marginal density
$\nabla\varphi_{(i)}$	Gradient of linear regression
$\rho_\tau(u)$	Loss function

CHAPTER 1

Introduction

Contents

In this chapter the motivation and the conceptual lines of this work, as well as the main research questions and challenges, are presented. The hypothesis and chosen methodologies are described. Finally the thesis objectives are delineated and present the thesis outline with a brief introduction to each chapter.

1. Introduction

Power systems have been changing significantly during the last decades and they will keep changing in the near future. Changes occur due to several reasons, namely: environmental obligations, security of supply, new generation technologies, technological development mainly in communications and control, and the need of new market opportunities and deregulation. Although in real life the forecasting procedures imply some uncertainty around the load and renewable production, such as wind/solar forecasts (caused by forecast errors and variability), up to a very recent past, a single expected value for each forecasting horizon, called deterministic, *spot* or *point forecast* are provided and were used in the generation dispatch and commitment procedures [1]. As load and generation can deviate from their forecasts, it becomes increasingly unclear (particularly, with the increasing penetration of renewable resources) if the system will be able to meet the conventional generation requirements within the look-ahead horizon, such as reserves, ramps, minimum up times, minimum down times and power balance. Additional balancing efforts are needed as it gets closer to the real time and additional costs will be incurred by those needs. Although there are several works developing the incorporation of these uncertainties into power system operations, large proportion of these efforts are limited to wind generation uncertainties and ignore the fact that there are additional sources of uncertainty, such as other renewable and intermittent generation and unexpected generation or transmission lines outages.

Increasingintroduction of electric energy production with renewable sources, mainly those with high variability, has created several challenges to the market operator and/or energy networks operators, predominately in the scheduling chapter. Both have to do their scheduling, with different detail levels, depending on technical or economic objectives in order to minimize the operation cost, taking into account the problem restrictions: reserve managing, reliability guarantee, management of consumption and management of independent power producers. These optimization problems take the form of unit Commitment (UC) and Economic Dispatch (ED) problems. When speaking about UC and ED in a generic way it must be considered that there are different levels such as Security Constrains Unit Commitment (SCUC), Reliability Constraint Unit Commitment (RCUC), Security Constrained Economic Dispatch (SCED) and Reliability Constraint Economic Dispatch (RCED).

This problem is enhanced in low power networks, especially in islands without any connection to continental networks. Due to its large implementation, generally, wind generation is considered the main source of variability on renewable generation but there are other sources that can introduce much faster variations, as solar generation [2]. On the other

hand, hydro generation, with easier operation control, may depend on economic strategies, disconnected from available resource. If there is a small storage capacity, the production can be temporally disconnected from the rainfall. Still in island context, a large variation on renewable production can lead to stability problems in the network, which can create generation and/or load shed and, at limit, blackouts. This way, and for security, the scheduling is generally done by a conservative way, with low risk but sometimes far away from an optimal operation. Consequently, reserve levels are greater and the possibility of wasting renewable production leads to a more expensive operation.

An efficient use of accurate short-term probabilistic forecast of renewable energy sources (RES) and load can allow optimal committed/dispatched thermal generators, avoiding generation, load shed or even blackouts.

Motivated by the importance of these topics, there are a number of research works related to this area, [1],[3]–[16] , among many other cited throughout the text:

- Characterisation of spatial and temporal uncertainties related to renewable sources (wind, hydro and solar):I is necessary to understand the variability and uncertainty associated with those resources, considering different levels of temporal and spatial resolution and for different levels of aggregations. It is also required the evaluation of optimal trade-off between cost and details of information used in these new scheduling approaches;

- Forecast models for wind, hydro and solar generation: There is a considering number of research works for wind forecast but a better comprehension of characteristics (such as: spatial resolution, temporal granularity, time horizon, optimal forecast refreshment, error and information requirements) is needed. These studies are necessary to characterise the best configurations of the forecasts to be used in the scheduling.

- Performance of the actual forecasts services in use: Improvement of studies of real time series of forecasts, characterizing the accuracy of the different forecast types (wind, solar, small-hydro and consumption) is needed as well as evaluation of the value of these different forecasts for the system.

- Modelling and processing of uncertainties related with forecasts: There is a portion of researches in this area but difficulties in the integration of this information on the decision process associated with the scheduling are an issue

- Scheduling specifications in market environment approaches: Scheduling resulting from the different market sessions is itself a specification of the initial and base

solution for the scheduling optimization. It is necessary the integration of this specification on the scheduling optimization structure.

- Scheduling optimisation solutions must be improved in order to increase velocity, precision, temporal resolution and time horizon. Work on new structures of the scheduling process which use several parallel scheduling runs, using different resolutions and horizons in order to use incremental information procedures is a necessity. These approaches will improve the performance for realistic scheduling operations.
- Faster and more precise scheduling optimization algorithms with the aim of solving larger problems with high number of variables.

1.1 Selected research questions

There are several questions that should be answered before the formalization of the final case study. The research must be split in smaller problems, which will contribute to get the global problem solution.

1.1.1 Which is the most adequate probabilistic forecasting model to each forecast horizon?

Due to the increment of the renewable power sources in the electric systems, there is a remarkable concern about the forecasting of renewable production. Firstly, the efforts were focused in spot forecasts which evolved to models incorporating uncertainties. Nowadays, researchers try to improve models, pursuing forecasts which will better capture uncertainties related to the resource. There are researches in areas such as solar [17], small hydro, wind or even waves [18] but stronger efforts are focused on wind generation. Nevertheless, the uncertainty models that are used in the wind forecast area can be used, subjected to their own specifications, to other renewable resources forecasts.

Hypothesis

Considering the above, in this work, the studies related with wind forecast will serve as base to remaining forecasts. The Numerical Weather Prediction (NWP) is the main source for forecast uncertainty and, secondarily, amplification and damping effect of the non-linear relation between wind speed and wind power [1]. Following the same author, there are several approaches to model these uncertainties by probabilistic techniques. Following a parametric approach, as demonstrated in [19] , through the 4º moment (kurtosis), the shape of parametric probability density functions (*pdf*) of forecast errors changes with the forecast horizons. It is

also shown that a Beta distribution can be used to model wind power generation errors [19]. However, errors are not always following a Beta distribution [20],[21]. In [22] a study comparing the Beta distribution with the Extreme Value distribution is presented and the authors concluded that Beta distribution outperforms the Extreme Value distribution to low and medium ranges of wind power, being the Extreme Value more adequate to high values of wind power. Aiming wind speed forecasts, several distributions such as Weibull, Rayleigh, Beta, Gama and Normal were tested to model the uncertainty [23]. On the other hand several authors such as [9],[13],[24] and [25], among others, prefer a non-parametric approach, not having to take any decision in advance regarding which distribution should be chosen.
This way, the understanding of the probabilistic models and the selection of one sufficiently robust, to represent the uncertainties in a satisfactory way, is a necessity.

1.1.2 What is the aggregation role of RES for the scheduling process?

Several studies have demonstrated the decrease of forecast errors and power variability with the renewable power sources aggregation. However, due to its large implementation, the spatial wind power aggregation has been the most studied [26]–[28]. Some studies concerning not only wind aggregation but also other renewable resources were done but generally in small scale or in hybrid solutions [29],[30].

Hypothesis

In this work, a mix of renewable power sources aggregation will be studied, with the objective of understanding its impact on variability and forecast errors. It is expected that this reduction should depend on the aggregated power sources and the revelation of each one.
In the scheduling process, on a renewable context, aggregation of renewable energy sources (RES) is typically subtracted from load (Load-RES) in order to produce the *net load* which then can be used to compute the thermal generator requirements [31],[32]. Considering that the forecasts are independent from each other, aggregations will be done by the convolution.

1.1.3 Which optimization tools should be used?

Unit commitment and ED are the base of the power systems scheduling processes. Although being solved at the same time, the UC intends to define which and how long the generation units should be online and the ED proposes to define the production of each on-line unit to meet the load at the minimum operation costs. Improvements on unit generation scheduling can lead to significant cost savings, simultaneously ensuring operational restrictions are not violated. The dynamic economical dispatch (DED) is an extension of conventional ED problem, taking into account the ramp rate limits of generating units [33].

Traditional approach to the ED problem considers, for simplicity, that the cost function for each unit is approximately represented by a single quadratic function. The essential assumption is that the incremental cost curves were monotonically, increasing piecewise-linear function, which could be solved by conventional programming methods and optimization techniques, as the Gradient method, Lagrangian function, Lambda-iteration method, base point and participation factor methods, dynamic programming, Newton's method Linear and Quadratic Programming and Interior Point method, among others [34]–[36]. Generally, these mathematical methods require the derivative information of cost functions. However, the generation cost functions of recent thermal units are not continuous, not convex, neither differentiable due to valve-point loading effect, multi-fuel burn systems and operational prohibited zones. Thus, the ED problem becomes a non-convex optimization problem with constrains, which cannot be solved directly by some of the traditional mathematical methods. A deep survey regarding these issues can be found in [37].

Regarding UC, generally its formulation contains binary variables, defining which units must be online. The traditional algorithms demand the usage of integer programming as mixed integer linear/non-linear programming which can be time consuming. In the case of scheduling with uncertainty, when the uncertainty is modeled by scenarios, it is mandatory to solve each one independently multiplying the computation time.

Hypothesis

With respect to units cost functions with non-convex, the problem solution becomes much more complex. To overcome this problem, over the past years, metaheuristic tools have gained more and more importance in optimization problems as unit commitment and economic dispatch. Heuristic usually refers to a procedure that seeks an optimum solution but does not guarantee that it will find it or even if it exists. Metaheuristics are general frameworks for heuristics in solving hard problems. Meta-heuristics do not stop in the first local optimum as a simple heuristic does and can be classified into two groups: those performing a single walk using special procedures, trying not to be trapped in a local optimum and those performing multiple walks. As a result of this, several heuristic methods were proposed to solve this kind of problems, such as Genetic Algorithms (GA) [34], Simulated Annealing, Taboo Search, Evolutionary Programming (EP), Evolutionary Strategies, Particle Swarm Optimization (PSO), Bacteria Foraging Optimization [38],[39], Ant Colony Optimization [33],[38],[39], and Artificial Neural Networks (ANN) approach with Hopfield Networks and hybrid artificial intelligence methods [40]. From the base algorithms several improved approaches and hybrid were proposed, as Improved Taboo Search [34]**,** Fast Evolutionary Programming and Improved Fast Evolutionary Programming [41], Improved

Particle Swarm Optimization [40] and hybrids as PSO with Evolutionary programming [42], PSO with crossover operations [40], Fast Evolutionary programming with Swarm Direction [33], New Particle Swarm Optimization with Local Random Search(NPSO-LRS) [40] and Real Coded Genetic Algorithm – Ant Colony Optimization [43], among many others [44].
Understanding which optimization model should be used is intended at the end of this work.
Concerning the scheduling, it can be accelerated by decoupling the UC and ED in order to avoid the necessity of run the ED to each set of feasible solutions of each hour of each scenario.

1.2 Challenges

This work will be developed under real context and with real information. One of the challenges will be dealing with the quality of information. The data set will incorporate measured values of load, wind, hydro and geothermal production, these values can be "polluted" by wrong measures, absence of measured values, unexpected production profiles provoked by outages, malfunctions, amongst others. Also, there is the natural dynamic of power systems with outages due to maintenance, which change the profile of production systems and can skew the datasets used in forecasts. In some of these situations it will be necessary to do some pre-processing to some data set values in order to prevent deviations.
On the scheduling context, results will be compared with those obtained by the system operator, implying the discovery of a comparing platform. The dataset is composed by hourly average values, consequently it is not possible to analyse some fast dynamics inside the hour.

1.3 Chosen methodologies

Generally, the scheduling process has complex formulations. Due to the dimension and required precision, it becomes extensive and with a big computational effort. Considering this, all the optimization process can be accelerated only using the sufficient calculus resolution to the existing uncertainty level in each moment. Accordingly, it is verified that the information about the uncertainty is useful to accelerate the calculation procedure as well as the forecast information, which is also essential for the scheduling process. At the end it is expected that the process can be accelerated with the new optimization algorithm.
The chosen methodology for solving the problem and verifying the hypothesis will be:

- Test the forecasting techniques to be applied in the scheduling;
- Evaluate the uncertainty to be applied in the scheduling;
- Develop adequate optimization methods to be applied in the scheduling;
- Evaluate performances of the optimization methods;

- Evaluate the benefits of new scheduling method.

1.4 Thesis objective

The main objective of this thesis is to develop an integrated set of mathematic techniques aiming the optimisation of electric energy systems operation with significant penetration of high variability resources. In particular, it is intended to specify the characteristics of forecasting systems which best suit the purpose, namely defining types of input data, mathematical models to include uncertainty and the representation of this uncertainty. A new generation scheduling process based on risk assessment for fast solving the scheduling with convex or non-convex cost function is also an objective.

With this thesis, the contribution for the mitigation of the economic and environmental impact from the uncertainty related to the operation variables, which affect the scheduling, is expected to be significant.

The final results of this research work will be an approach of advanced scheduling integrating:

- Forecast of renewable sources, based on state-of-the-art models;
- Uncertainties associated with forecasts;
- Innovative optimization approaches;
- Scheduling optimization tools.

The final result should be a complete method built to give a full answer to the energy scheduling systems with high integration of variable power resources. An application will be developed to study the management of the information from a power production perspective.

The innovation of this thesis is spread in several parts of the problem but the main added value will be the aggregation of all the components in the global scheduling approach.

1.5 Thesis outline

The research work developed within the scope of this thesis is structured in 6 chapters:

Chapter 1 In this chapter it is outlined the motivation and conceptual lines as well as the main research questions and challenges. Some hypotheses for solving the research questions and chosen methodologies are described. Finally the thesis objectives are outlined.

Chapter 2 This chapter begins with an overview concerning the power generation scheduling, first under a classical deterministic approach and posteriorly under uncertainty.

The mathematical formulations are shown and the importance of the reserves is highlighted. It is also presented a brief overview concerning the latest researches in this area.
The second part consists of several aspects concerning the stochastic optimization with the manifold approaches, namely recourse problems, distribution problems, chance-constraints problem and worst-case constraints problems are represented.
In the third part of the chapter it is done an overview about renewable power production forecast, namely wind, hydro and solar. Lastly, some techniques for power forecasts uncertainty estimation are presented.

Chapter 3 This chapter presents an introduction to the case study and an explanation of the necessity of accurate forecasts.
In the second part all the steps for achieving renewable and load forecast with associated uncertainty are described. It is explained how the prediction models are chosen, as well as the choice of explanatory variables and some evaluation criteria.
Finally the results from wind, hydro and geothermal power forecasts coupled with the load and their aggregation are presented.

Chapter 4 This chapter presents the full methodology for the generation scheduling under uncertainty, based on risk assessment.
In the first part it is described the case study thermal generation characterization and it is introduced the concept of equivalent optimal generation unit. Next, it is announced an original metaheuristic based on cloud of particles in order to solve non-convex problems.
Finally it is presented the scheduling formulation based on risk assessment.

Chapter 5 - In this chapter the case studies centered on the proposed methodology are presented. A net load forecasting is done followed by a single-period and a multi-period unit commitment based on risk assessment. The São Miguel Island's system operator proposed scheduling is presented and the results are compared with those from the proposed methodology.

Chapter 6 - In this chapter the overall conclusions are drawn and the original contribution is presented. Conclusions concerning the research questions and formulated hypothesis are addressed and some future research perspectives are also discussed.

Annex - In annex are presented some intermediate results which, due to their length, were not included in remain chapters.

CHAPTER 2

Scheduling – General Overview

Contents

This chapter is a general overview concerning the schedule process regarding the unit commitment problem and economic dispatch under deterministic and stochastic approach. It is also an outline of stochastic programming methods.

Finally, it is done an overview concerning the renewable power forecast and uncertainty modelling

2. General Overview of scheduling

2.1 Introduction

Scheduling and control actions of an electric power system are processes which involve several agents and are carried out at different time horizons in a progressive close-up approach before the moment of operational control action [45]. The process intends to specify how the generation resources should be used to fulfill with security and economic criteria. It is a procedure that has to be done in advance and it must provide information concerning the generation units namely, whom and when should be online. In addition to how much energy will be produced, the costs and the uncertainty related with the availability of the resource must also be considered. Other important information is the extra potential and services that the online units can provide when is necessary [45].

The scheduling horizon and time steps may differ, depending on the country or market environment, but generally fulfil the following steps [45],[46] and [47]:

- **48h before** – The market agents collect availability of power plants and resources information. They need information about the independent variables for their own system and, if possible, information about the management of systems by competing agents. Information about renewable forecast, system consumption forecast, availability and technical constraints in power plants is needed;
- **42h before** – The agents present the day-ahead market bids, using the scheduling obtained in the previous period. To reduce uncertainty, the most recent information about forecasts and generation availability must be used. The Independent System Operator (ISO) also receives information about scheduling constrains for each unit (e.g. ramping rates, start-up and shutdown costs/times, minimum up-time and down-time, efficiency curves, among others);
- **40 h before** – The Market Operator clears the market for the day-ahead. The clearing process is done in coordination with the ISO in several steps: first, based on bids and on generation variability it defines the requirements of reserve; second, a SCUC is done for day-ahead; third, a SCED is done, finding the optimal scheduling and complying with generation constraints, network restrictions and multi-period constraints;
- **24 h before** – Before starting the operational day, a RCUC is done by the ISO, using updated load forecasts and renewable forecasts. At this stage, more detailed information about generation can be integrated. After this moment, ISO can decide to

change the scheduling mechanisms of compensation, which were defined by the deviation relatively to the clearing price;

- **12 hours before** – Before each intraday market, the agents prepare the internal scheduling optimization to bid in intraday market. Information about errors in forecast and clearing prices in the previous market session is very useful for the intraday market.
- **8 hours before** – After each intraday-market and after receiving the bids for intraday market, the same process as described in point 3 is repeated. For this phase more detailed SCUC and SCED is done, providing the information about clearing prices and deviations. This information can be used by the agents in the next intraday market bids.
- **1 to 4 hours before** – For each interval in the operation day, a SCED is permanently refreshed for each short period over the operating day. The scheduling is continuously refreshed (e.g. every 5 min) for the next few hours (e.g. 4 hours). In this scheduling the optimization variables are limited and most of the variables are non-dispatchable generation. This permanent and close-up scheduling adjustment has, as a goal, to guarantee the load following and the adjustments to a very short-term generation changes prediction.
- **Present** – Operational control action, it is the instant of generation action for which all the scheduling has been planned before.

Following these time periods, it is clear that the scheduling is based on optimization algorithms in order to optimize the application of the available resources, based on economic criteria and subjected to technical, security, environmental and regulatory restrictions.
It is also clear the necessity of power forecasts with different time horizons and with different levels of data to provide a chain of information and its refreshment with new data. This information can also include more recent data which was not available in previous forecasts, such as changes in units' availability, more recent meteorological information with on-line data, as well as power and load forecast uncertainties. Aiming this, the deterministic approach for scheduling has been updated to a stochastic methodology in order to integrate the uncertainties resulting from the increment of renewable power generation. Despite the advances on power forecast permit good accuracies, possible differences between the forecasts' values, used to run the UC and the real generated values must be taken into account. It should be bear in mind that the uncertainty is intrinsic to the forecasting process and it is essential for the decision process. At the end only one optimal is chosen and, this

way, the decision agent needs to know what is the associated risk, (of not obtaining the real optimum), to its decision.

2.2 Generation scheduling

2.2.1 Unit commitment

As discussed above, the generation schedule is essentially composed of two problems, the UC and the ED. The main objective of UC is fundamentally to stipulate which units must be kept on-line and for how long, to feed the forecasted load. Despite the apparent simplicity, this problem is not trivial, mainly because there are several restrictions that must be considered. Taking this into consideration, the basic formulation of UC can be transformed into a Reserve Constrained Unit (RCU) problem which includes constraints about the minimum value of reserves, Security Constrained Unit Commitment (SCUC), including constraints about the minimum reserve and network constraints, and the Reliability Constrained Unit Commitment (RCUC), including constrains about generation and network reliability [45],[47].

Bounded with the UC, ED intends to allocate the generation profile of each on-line unit to obtain the lowest production cost and, generally, both problems are solved simultaneously. The UC problem is discrete due to the start-up and shut-down operations and for this it can be much more difficult to solve than ED, because of its binary on/off variables.

There are different mathematical formulations for the UC, where the major differences lie in the constraints used to capture the dynamics of the generation units, (ramp limits for instance), or in the assumptions regarding cost models (linear or nonlinear) or solving algorithm (mixed integer linear or nonlinear programming, heuristics, among others).

The objective is to minimize the cost of supplying the hourly load (assuming that the load is fully fed) by N_G thermal units during an interval T, and can be analyzed considering two main components, cost function and restrictions. The cost function (2.1) can be defined by the energy production cost of each on-line thermal unit $FC_{i,t}(P_{i,t})$, startup costs (hot or cold) $ST_{i,t}(P_{i,t})$, shutdown costs $SD_{i,t}(P_{i,t})$ and maintenance costs $MC_{i,t}(P_{i,t})$. The variable $U_{i,t}$ is the binary on/off variable of thermal unit i at time t [37],[48].

$$\min \sum_{t=1}^{T} \sum_{i=1}^{N_G} \left[FC_{i,t}\left(P_{i,t}\right) + ST_{i,t}\left(P_{i,t}\right) + SD_{i,t}\left(P_{i,t}\right) + MC_{i,t}\left(P_{i,t}\right) \right] U_{i,t} \tag{2.1}$$

The energy production cost function is modeled regarding several approaches, as continuous or non-continuous, convex or non-convex and differentiable or non-differentiable all over the entire domain. Its characterization will later be deeply discussed in this work.

The maintenance cost is described by equation (2.2) where $BM_{i,t}$ is the base maintenance cost, and $IM_{i,t}$ the incremental maintenance cost is.

$$MC_{i,t}\left(P_{i,t}\right) = BM_{i,t} + IM_{i,t}P_{i,t} \tag{2.2}$$

The startup cost $ST_{i,t}$ of equation (2.3) will depend on several factors, where $TS_{i,t}$ the turbine start-up cost is, $BS_{i,t}$ the boiler start-up cost, $MS_{i,t}$ the start-up maintenance cost and $AS_{i,t}$ the boiler cool down coefficient. However, generally, one of the most important pieces of information is the number of hour's offline, $D_{i,t}$.

$$ST_{i,t} = TS_{i,t} + \left(1 - e^{\left(D_{i,t}/AS_{i,t}\right)}\right)BS_{i,t} + MS_{i,t} \tag{2.3}$$

Finally the shutdown cost is also envisaged by the equation (2.4), where K_i is the incremental shutdown cost of unit i.

$$SD_{i,t} = K_i P_{i,t} \tag{2.4}$$

The minimization problem of equation (2.1) must be subjected to several constraints, which are the minimum and maximum production limits (2.5), minimum up time (2.6) (certain number of hours $T_{on,i,t}$ before it can shut down), minimum down time (2.7) (certain number of hours $T_{off,i,t}$ before it can be brought back on-line), and power balance (forecasted load D^f_t plus power losses $P_{L,t}$) (2.8). Equation (2.9) represents the units' generation ramp limits between two consecutive time steps, where $P^0_{i,t}$ is the power production of unit i at the beginning of period t, while DR_i and UR_i indicate the maximum downward and upward ramp limits, respectively [4],[37],[45],[48] and [49].

$$U_{i,t}P^{\min}_{i,t} \le P_{i,t} \le U_{i,t}P^{\max}_{i,t} \tag{2.5}$$

$$\left(U_{i,t-1} - U_{i,t}\right)\left(t_{on,i,t} - T_{on,i}\right) \ge 0, \forall i, \forall t \tag{2.6}$$

$$\left(U_{i,t} - U_{i,t-1}\right)\left(t_{off,i,t} - T_{off,i}\right) \ge 0, \forall i, \forall t \tag{2.7}$$

$$\sum_{i=1}^{N_G}\left(U_{i,t}P_{i,t}\right) = D^f_t + P_{L,t} \tag{2.8}$$

$$\max\left(P^{\min}_i, P_{i,t-1} - DR_i\right)U_{i,t} \le P_{i,t} \le \min\left(P^{\max}_i, P_{i,t-1} + UR_i\right)U_{i,t} \tag{2.9}$$

In equations (2.5) up to (2.9), $U_{i,t}$ represents the binary on/off variable of thermal unit i at time t, while in the equations (2.6) and (2.7), $U_{i,t-1}$ represent the binary variables i for time $t-1$.

Updating the previous formulation to a SCUC, other restrictions have to be added, such as minimum reserve R_t (2.10) and power flow limits in the network (2.11), where $P_{LF,j,t}$ is the active power flow at branch j at time t.

$$\sum_{i=1}^{N_G}\left[\min\left(P_{i,t}^{\max}-P_{i,t},P_{i,t-1}+UR_i\right)U_{i,t}\right]\geq R_t \tag{2.10}$$

$$\left|P_{LF,j,t}\right|\leq P_{LF,j,t}^{\max}\qquad j=1,2,...,N_L \tag{2.11}$$

Other restrictions can be added as “must run units” (prescheduled units which must be online due to operational reliability and/or economic aspects) and “must out units” which are in forced outages due to maintenance and consequently unavailable for commitment. In some models, even crew constrains are assessed, considering certain power plants may have limited crew members to simultaneous startup and/or shutdown of several units at the same power plants [37],[49].

In the case of deregulated environment the previous formulation have to experience two changes: the objective function instead of minimizing the costs, will maximize the profits and the balance equation (2.8) must take the form of equation (2.12) [37].

$$\sum_{i=1}^{N_G}\left(U_{i,t}P_{i,t}\right)-P_L\leq D_t^f \tag{2.12}$$

There are several methods for solving the UC problem (some of them not feasible in large power systems) such as exhaustive enumeration, priority listing, dynamic programming, integer and linear programming, branch and bound, lagrangian relaxation, interior point optimization, taboo search, simulating annealing, fuzzy systems, ANN, genetic algorithms, evolutionary programming, ant colony search algorithm and hybrid models [37],[50]. The biggest challenge, which is transversal to all approaches, is the computational burden, since the effort depends on the number of simulation periods, the number of units, restrictions and the dependencies between periods.

Following the equation (2.10), during the scheduling and operation processes, it is necessary to ensure a certain amount of reserves to face load variation and any kind of unpredictable situations, such as forecast errors, last-time unavailable scheduled generation unit, deviation of generation or transmission lines outages. Therefore, the reserve management is a very important issue since it can have great impact on operational security and economic achievement. There are different levels of reserve with objectives and time response. In figure 2.1 a diagram with the operating reserves is shown [47].

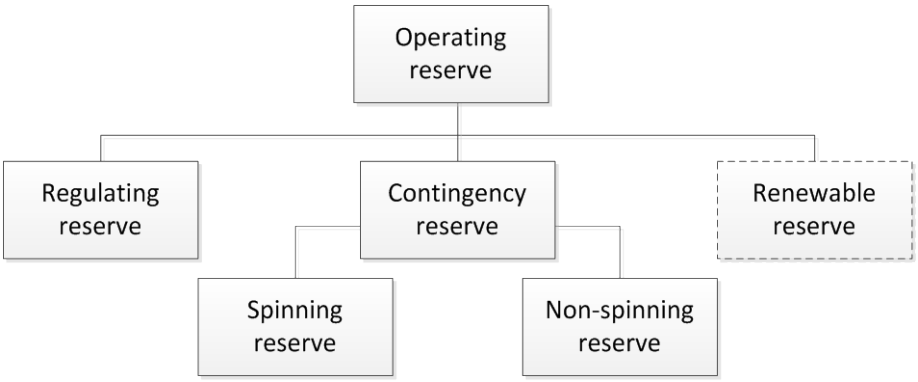

Figure 2.1 – Diagram of operating reserves

Traditionally, operating reserves can be divided in regulating and contingency reserves. But, nowadays, renewable sources power plants, being on the rise, begin to have an important contribute to the reserves [47]. With regulating reserves it is intended to guarantee the following of loads and any variable generation. On the other hand, contingency reserves aim to ensure the security of the system when a contingency occurs (generating units or lines outages). Those can be spinning reserves or non-spinning (complementary) reserves, where in the first case, the units are already synchronized with the network, while in the second case the units are offline but have the capacity of quick start, such as gas or diesel turbines or hydro power plants. Beside the controllable generation reserves, there are others consumption based, namely interruptible loads, demand response, and consumer generation.

In the perspective of control response, the reserves are split on primary, secondary and tertiary. The primary reserve is stored in kinetic energy of the spinning mass of the turbine and generator, which is able to be disposable in less than 30 seconds [45]. The amount of primary reserve allocated is determined by reliability of the system, namely the risk of fault in the generation system. This way, spinning masses must have enough stored energy to deal with any outage, at least until the secondary reserve actuates.

The secondary reserve role is injecting extra energy, controlled by the Automatic Generation Control (AGC), restoring the frequency after the primary reserve actuation. This reserve should respond between 30 and 60 seconds and is selected by rank order or using the interconnection capacity. Generally, the secondary reserve is available from gas and hydro power turbines and its value results from the primary reserve plus the generation, which being lost, can trigger the frequency and voltage protections. The secondary reserve requirement is mainly driven by the *N*-1 criterion and short-term demand variation [51]. It must be understood that the primary reserve is only temporary energy transference, while the secondary reserve must restore the energy balance by injecting more energy into the system. In interconnected systems the interconnection capacity can also be used as secondary reserve.

The tertiary reserve has as main objective to guarantee the regulation control, changing the generation by adjusting the scheduling, whose process should be done between 15 minutes and 1 hour after the contingency. This additional reserve is calculated by adding the variation in load with the variation in variable generation. Although being not so important as the primary and secondary reserves, as the contingency reserve must be maintained permanently, the regulating reserve is an additional reserve with additional cost [45].

Traditionally, it is not common to use renewable power sources as reserves, mainly as primary and secondary reserves, since there is resource waste, but it can give a support to the tertiary reserve.

There are several approaches to define the amount of reserves. In a deterministic point of view it can be defined as a given percentage of forecasted load, a percentage of renewable production forecasts, equal to the amount of the most loaded unit [47],[52] (generally for the primary reserve) or a mix of some of the previous rules [52]. In the case of probabilistic approach, it uses a function of the probability of not having enough generation to meet the load (due to load and production forecasting errors), or also using approaches based on standard deviation of load forecasting errors, among others.

2.2.2 Economic dispatch

The economical dispatch problem is one other important issue in the power system scheduling. Fundamentally, it is intended to evaluate the value that each on-line unit should generate with the lowest cost respecting the technical and load constraints. The ED uses as a basis the UC solution, excluding from the optimization the generation units that are offline. Opposing the UC, which solutions can result from constant costs (in the case of simple ranking of priority), ED characteristics' of production costs can be nonlinear. Consequently, the optimum is an allocation of generation between the units.

On the majority of publications that strictly analyze the subject of ED, the online generation units are already known and commonly the case studies are done using a single period (sometimes to present new solution algorithms). The multi-period analysis is less addressed since it presents a more difficult solution. In reality, ED is done in a dynamic way (Dynamic Economical Dispatch) [33],[53] as it takes into account the variation of demand over time, as shown in equation (2.13), where $FC_{i,t}$ is the cost function of each unit i during interval T, and N_G represents the number of on-line units [39].

$$\min \sum_{t}^{T} \sum_{i=1}^{N_G} FC_{i,t}\left(P_{i,t}\right) \tag{2.13}$$

The basic formulation includes the production limits of each unit as shown in (2.5) or (2.9) and balance equations as (2.8) or (2.12). As for the UC, the ED can include several kinds of constraints, such as SCED which deal with reserves and network constraints and RCED, including constraints about generation and network reliability.

Merging the problem of UC with the problem of ED using Mixed Integer Programming optimization algorithms is a widely adopted approach. One of the advantages is the fact that the non-linear details in the ED can justify a change in the solution of the UC. On the other hand, the ED can integrate UC costs considering the fix costs of the generation [45].

Over the past decades, many methods have been developed to solve the ED problem. There are the traditional methods such as Gradient, Lagrangean, Lambda-iteration, Dynamic Programming, Newton's, Linear Programming and Interior Point, among other methods [34]. Some of these methods are used under the assumption that the thermal unit's costs functions are convex, continuous, differentiable and monotonically increasing, along the domain.

Real thermal units can present cost functions with different characteristics from those mentioned above. For instance, steam turbines can present valve-point effects and some units' burn different type of fuels resulting in a different function for each fuel. In this case the cost function can take the form equation (2.14), for *k* types of fuel.

$$FC_{i,t} = \begin{cases} a_{i1}P_{i,t}^2 + b_{i1}P_{i,t} + c_{i1} + \left| e_{i1} \times \sin\left(f_{i1} \times \left(P_{i1,t}^{\min} - P_{i1,t} \right) \right) \right|, & \text{for fuel 1, } P_{i1}^{\min} \le P_i \le P_{i1} \\ a_{i2}P_{i,t}^2 + b_{i2}P_{i,t} + c_{i2} + \left| e_{i2} \times \sin\left(f_{i2} \times \left(P_{i2,t}^{\min} - P_{i2,t} \right) \right) \right|, & \text{for fuel 2, } P_{i1}^{\min} < P_i \le P_{i2} \\ \vdots & \\ a_{ik}P_{i,t}^2 + b_{ik}P_{i,t} + c_{ik} + \left| e_{ik} \times \sin\left(f_{ik} \times \left(P_{ik,t}^{\min} - P_{ik,t} \right) \right) \right|, & \text{for fuel } k, \ P_{ik-1} < P_i \le P_i^{\max} \end{cases} \quad (2.14)$$

Due to possible vibration in the shafts or problems with the continuous start and stop of the coal mills, there are prohibited operation zones were the thermal units cannot work at steady state. Taking this into account, the constraints can be non-continuous as shown in equation (2.15),

$$P_{i,t} \in \begin{cases} P_i^{\min} \le P_{i,t} \le P_{i,1}^{LB} \\ P_{i,j-1}^{UB} \le P_{i,t} \le P_{i,j}^{LB} \quad j = 2,3,..,N_{pz} \\ P_{i,N_{pz}}^{LB} \le P_{i,t} \le P_i^{\max} \end{cases} \quad (2.15)$$

where $P_{i,j}^{LB}$ are the lower bound of the j^{th} prohibited zone of unit *i* and $P_{i,j-1}^{UB}$ is the upper bound of the $(j\text{-}1)^{th}$ prohibited zone of the same unit. Thus, the ED problem becomes a non-convex optimization problem with constraints, which cannot be solved directly by some of the traditional mathematical methods. Dynamic programming can solve this kind of problem, but

can suffer with the dimension and the time needed to solve it [35],[36] and [54]. On the other hand, commercial tools, which are able to solve economical dispatch for thermal units, always require convex cost functions. This condition can be attributed to the limitations of the optimizing tool or the need of rapidity and non-convex algorithms tend to be slow. To overcome this problem, sometimes the technique is to split the space solution in convex sub-spaces and then use conventional algorithms. This technique may create a vast number of solutions, some possible, others not, and the best solution must be found inside the set of feasible results.

Alongside, several heuristic methods were proposed to solve this kind of problem such as Genetic Algorithms, Simulated Annealing, Taboo Search, Evolutionary Programming, Evolutionary Strategies, Particle Swarm Optimization, Bacteria Foraging Optimization, Ant Colony Optimization, Artificial Neural Networks approach with Hopfield Networks, and hybrid artificial intelligence methods. From the base algorithms several improved approaches and hybrid were proposed, as Improved Taboo Search [35]**,** Fast Evolutionary Programming and Improved Fast Evolutionary Programming [42], Improved Particle Swarm Optimization [55] and hybrids as PSO with Evolutionary programming [54], PSO with crossover operations [38] and Fast Evolutionary programming with Swarm Direction [39], among many others.

2.2.3 Unit commitment and economic dispatch under uncertainty

In a classical approach (deterministic), without the integration of renewable source power plants with their intermittent and variability profile, the source of uncertainties is only related to the load forecast or some unexpected unit or line outage. As a consequence, security of a power system refers to its ability to survive to contingencies, while avoiding any undesirable disruption of service. As a security measure, the so called *N*-1 security criterion is commonly used, where the system is considered to be *N*-1 secure if any single component outage does not lead to an overloaded component or to other operational violations.

When renewable power sources are included, the amount of uncertainty increases, due to the variability and errors introduced by the forecast process. As a consequence scheduling becomes a much more challenging problem. However, even when considering renewable power sources, if a *spot forecast* (point forecast) is assumed, the problem can be considered as deterministic too.

The difference between uncertainty and variability is a matter that must be taken into consideration; the variability is related to the type of resource, which can, by its nature, change without any capacity of management like in wind or solar sources. While uncertainty is linked with the forecasting, which, considering the nature of the resource, can be hard to forecast with a appropriate certainty. The scheduling process has to deal, in distinct ways,

with both cases. Regarding variability the problem impact can be reduced with fast scheduling processes, giving solutions in advance.

Forecasting errors, characterized as the difference between the values used to the unit commitment and the real ones available in the real time dispatch, can cause serious difficulties for the system operator, who must balance the positive or negative deviations of an intermittent production.

To deal with uncertainties, various stochastic analyses have been developed. In a stochastic approach, the main question, cited from [4], "*What is the level of operating reserves that should be imposed at the UC stages, to take into account the additional uncertainty from the renewable power sources ?*" must be addressed.

Nowadays, even when considering the increase of solar and small hydro capacity, wind resource is clearly the most important issue for scheduling systems with high penetration of renewable energy. Correspondingly, the vast majority of publications are focused on wind power generation. Works addressing this matter focus on three main concerns:

- How to improve forecasting techniques;
- How to model the uncertainty and its impact on the reserves and consequently on the scheduling;
- How to make the scheduling process faster with less computational burdens.

There are many models concerning UC, which fundamentally differ from how the constraints are formulated to capture the dynamic performances of generation units or in the cost models. The overview below gives a general idea about the more recent research lines regarding these themes.

In [56], a comparison between different probabilistic forecasting and scenario reduction methods to solve the UC and assess operating reserves is done. The scenarios are generated from probabilistic density functions created by Quantiles Regression (QR) and Kernel Density Estimators (KDE) (based on *Nadaraya-Watson* (NW) estimator), using the wind power forecast as explanatory variable. The results from stochastic and deterministic UC are compared. It is concluded that a higher number of scenarios improve the performance of the stochastic UC strategy in spite of increasing several times the computational efforts. Their case study showed that the random scenario reduction is in line with other techniques like those resulting from Kantorovich distance. It is also concluded that the dynamic reserve derived from NW outperforms the one resulting from QR. The scenarios created from NW outperform the scenarios created with QR, in the case of UC.

Similarly, in [16], and in [4], the probabilistic method was based in scenarios where the focus was the impact of wind power uncertainty on power systems operation as UC, ED, and

reserves management. It is done a comparison between a stochastic approach and a deterministic approach with different levels of reserves and conclusions are that the deterministic formulation from a certain value of reserves requirement onwards, reaches results comparable with the stochastic approach. It is also concluded that wind power forecast errors have a great impact on the scheduling of generation units in a day-ahead market with implications on the real-time economic dispatch. They do not address other uncertainties, such as load uncertainty and transmission line or generator outages (It is considered that the reserves based on classic criteria are sufficient to deal with those uncertainties).

In [15] it is presented a deterministic formulation for the UC and its extension to stochastic programming formulation. Wind generation is considered as the source of uncertainty, where the wind speed uncertainty is estimated with the use of ensemble approach, while the load has no uncertainty. The network model and forced outages are not considered. The authors sustain that when using stochastic formulation to represent the wind uncertainty, the requisite of a previous value of reserves can be strongly reduced. In fact, a comparison of robustness is done between an explicit value of reserves and the implicit amount of reserves that result from the stochastic formulation.

In [57] an SCUC with wind power generation is analyzed to test how the power system reacts by re-dispatching thermal units in real time when the actual power is different than the forecasted. It is pointed out that the ramping of the thermal units is crucial for accommodating the uncertainty and variability of wind power generation. In this case the wind uncertainty was formulated with generated scenarios, including a Latin Hypercube Sampling (LHS) technique in the simple Monte Carlo simulation. Concerning the uncertainty, the assumption is wind power errors follow a normal distribution and the mathematical formulation does not include load shed neither wind curtailment. Transmission network constraints are also included in the problem. In figure 2.2 the flowchart of proposed SCUC is shown.

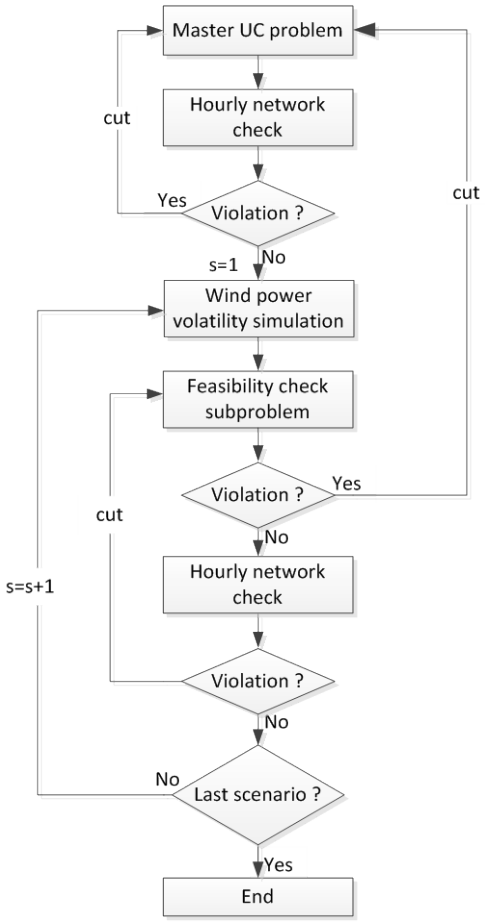

Figure 2.2 –Security-constrained unit commitment with wind power

The SCUC is solved as a master problem with the wind power generation spot forecasting and

a second problem is solved simulating scenarios to represent the wind power uncertainty, both solved by Mixed Integer Programming (MIP). The large scale mixed integer UC is solved as a master problem followed by a network security check sub-problem. In case of any violation of the sub-problem, the Benders cut is formed and added to the master problem.

As in [57], paper [58] presents a combined model of optimal reserve ED considering uncertainty of wind power generation. The SCUC and reserve dispatch problem based on forecasted wind power is settled in the master problem. In the sub-problems the obtained generation dispatch has to meet the requirements due to the uncertainty of wind power. The volatility of wind power was simulated by scenarios generated by LHS technique in the Monte Carlo simulation (based on normal distribution). The difference is the introduction of wind curtailment and load shed into the original formulation of [57]. It was verified that incrementing wind curtailment costs, the amount of wind energy scheduled increases and, naturally, the cost of reserves increases too.

Reference [59] presents a full-scenario security-constrained unit commitment (FS-SCUC) when considering wind generation and load variability.

Following the line of [57], the Benders decomposition of the whole problem into a main problem and two sub-problems is proposed, aiming the reduction of the scale of UC and improve the computational speed using Mixed Integer Linear Programming (MILP). The main problem solves the UC without network security constraints. Subsequently, the first sub-problem checks whether the commitment and dispatch solution of the master problem can satisfy the network security constraints or not. The second sub-problem checks if the worst-case security constraints can be satisfied with the obtained schedule on the master problem. In the formulation, active and reactive powers are incorporated. The wind power generation and node load are treated as volatile loads (the wind power is considered as a negative load) and the uncertainty is modeled by forecasting intervals which will originate scenarios. Reserves are implicitly determined by a specific commitment schedule corresponding to the full-scenario security constraints. As in [57] and [58] it is concluded that cost decreases if wind power curtailment is allowed and the curtailment compensation is small. In figure 2.3 a flowchart of overall FS-SCUC is represented.

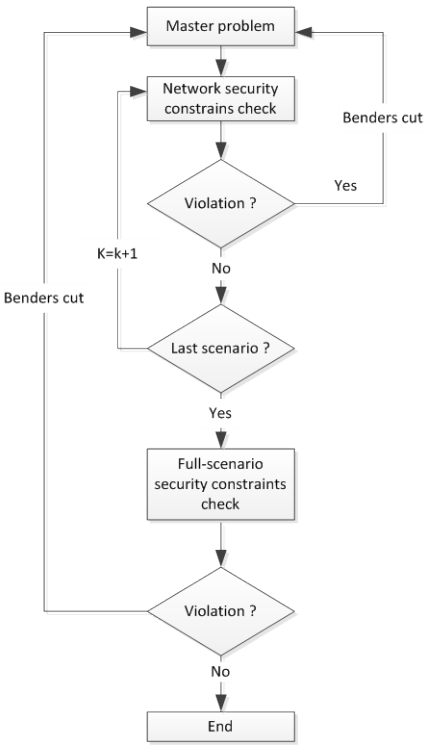

Figure 2.3 – Overall procedure of SCUC

In [60] it is proposed a Constrained Ordinal Optimization (COO) method for solving a scenario-based Stochastic Security Constrained Unit Commitment (S-SCUC). Consideration of Ordinal Optimization aims the facilitation of the scenario-based solution method, since its goal is to seek *good enough solutions* with high probability instead of searching the best solutions with absolute certainty. In this specific case, it is used a Weibull distribution for the wind speed, which is converted into power by a wind turbine power curve, and load forecast errors are modeled by normally distributed functions with constant standard deviation. Random outages of generation units and transmission lines are both considered. The wind curtailment is allowed and load shedding is also considered but only as the last resort to maintain the system reliability. As in previous methods, the corresponding Security Constrained Economic Dispatch (SCED) is repeated for all scenarios until a feasible UC is obtained. In figure 2.4 the flowchart of a feasibility model is shown.

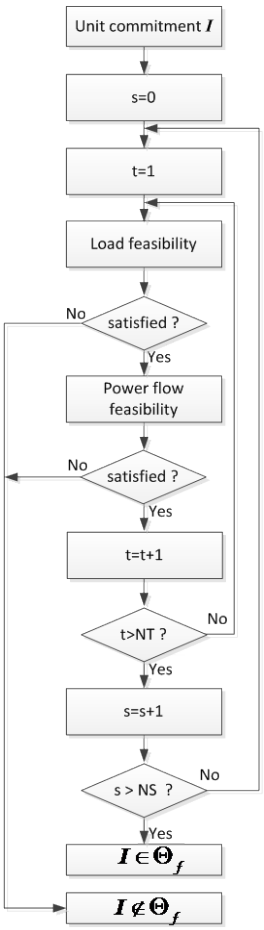

Figure 2.4 – Flowchart of the feasibility model

Generally, the final solution may not be the optimal for the stochastic SCUC problem but the purpose of the proposed COO method is to find a good enough solution with a high probability instead of an optimal solution. As conclusion, the proposed COO demonstrated to be computationally more efficient than an MILP-based approach, showing a remarkable decrease of computational time.

Commonly, in many approaches, it is required that the load must be fed, even in the worst cases, leading to high levels of reserve. In [31] a Chance-Constrained Unit Commitment is proposed, when considering that the demand should be met in any plausible scenario, leaving out extreme scenarios in order to reduce the cost of dispatched energy. The chance constraint problem is formulated subjected to stochastic demand for the scheduling of energy and spinning reserves with a α-quantile and *n-K* criteria. The proposed chance constraints are the risk measure of not meeting the demand with a certain confidence level α. As in [59], wind generation is considered as a negative load creating the variable *net load*, resulting from the subtraction of wind generation from load, both defined by normal distributions with fixed standard deviations. The scenarios of *net load* are generated by a LHS technique based on the normal distribution of *net load*. In a single period case, it is evaluated the total cost versus wind energy penetration.

On the formulation, some probability of generation outages is also considered but the network model is not considered. The formulation is done in two stages: firstly it solves the UC with up/down reserve scheduling, and secondly the real demand has to be met under a certain probability. There are reserves to deploy the real demand, but load shedding or wind curtailment are allowed and the chance constraints are defined as reliability constraints of system, limiting the load shedding and wind curtailment.

In [61] a Chance-Constrained Unit Commitment is also proposed. The problem is formulated as a chance-constrained two-stage stochastic programming and a combined sample average approximation (SAA) algorithm was developed to solve the model efficiently The idea behind SAA is to approximate the real distribution of random variables by a Monte Carlo sampling empirical distribution. The authors state that the model ensures, with high probability, that a large portion of the wind power output at each operation time is used. Wind power is the only source of uncertainty since the load is considered deterministic. The wind power uncertainty is represented by scenarios obtained from a normal distribution, with standard deviation equal to a percentage of the expected values. Compared with [31] the network is also considered in the model but the outages are omitted.

In [62] a comparison between a scenario-based and interval optimization approaches to stochastic SCUC is done. The scenario based stochastic SCUC problem is decomposed into a main problem and three sub problems. The main problem is an UC without network security constraints and serves as base case. Then a first sub problem addresses the hourly network evaluation of the main problem solutions for the base case. A second sub problem does the hourly feasibility check for each scenario, checking possible violations of the main UC solution in each scenario. Finally, the third sub problem checks the optimality of master UC solution in each scenario. In figure 2.5 a scheme of the proposed scenario-based approach is shown.

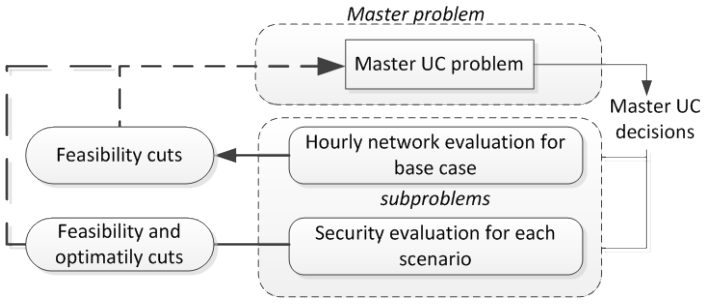

Figure 2.5 – Scenario-based approach

The reserve requirements are implicitly represented by deviations in the dispatch solutions of the base case and scenarios and are optimally determined via preventive and corrective actions.

Different from the scenario-based approach, the interval optimization doesn't need any pre-knowledge of wind generation probability distribution. In this case only the wind power forecast has uncertainty. The interval optimization requires less computational efforts to generate upper and down bounds to the objective value. However, the choice of the uncertain interval coverage rate can dramatically change the optimal solutions. It is also not appropriated to simulate discrete random variables as units or transmission lines outages. The wind speed scenarios generation are based on a Weibull distribution and converted to power by a turbine power curve. In the case of intervals, the uncertainty is considered as a percentage of installed capacity.

The authors conclude that the scenario-based approach provides a more suitable solution. Yet, it can be a large scale problem with high computation burdens. Although the scenario case needs more computational efforts, it is less sensitive to the starting values. On the other hand the uncertainty interval reveals to be faster than scenario-based, being equivalent to two scenarios, but is very sensitive to the assumed uncertainty interval.

In [32] it is stated that traditional UC with deterministic spinning reserve requirements are inadequate, given the variability and uncertainty of wind power. Thus, a new probabilistic model of SCUC is proposed to minimize the energy cost, spinning reserve and load shedding (Expected Energy Not Served (EENS)), using the determination of additional spinning reserve due to the integration of wind generation. The formulation of EENS takes into account the probability distribution of forecast errors of wind and load, and the outage replacement rate (ORR) of several generation units. There is not any assumption about spinning reserve constraint because its value is based on an internal cost/benefit analysis. The *net load* (load minus wind power) forecast errors are assumed to be normally distributed with zero mean and a fixed standard deviation. The proposed approach determines the optimal amount of spinning reserve, which minimizes the total cost of system operation (balancing energy costs, start-up cost, reserve and expected cost of load shedding), reaching the trade-off between economy and reliability of the system. It is concluded that, even increasing the amount of EENS, comparing with those obtained by the traditional constant reserve UC, the operating cost is lower as well as the total cost. The reserves are strongly dependent on value of loss of load and ORR and less dependent from load and wind forecasts errors.

In paper [63], unlike the previously mentioned, it is analyzed a different approach.. Pumped-storage and wind unit generation are coordinated and optimized with a stochastic SCUC model through several coordination strategies. The proposed optimization problem is formulated as a Mixed Integer Problem (MIP). The Benders decomposition technique is used to decompose the original large-scale problem into a more tractable master MIP problem and several Linear Programming (LP) subproblems. The subproblems check the power flow

which results from the master problem solution in the base case and all scenarios. If there is any violation, the corresponding feasibility Benders cuts are generated and fed back to the master problem, for the solution of the next iteration. The stochastic SCUC for coordinated scheduling of wind-pumped-storage units is shown in figure 2.6.

Forecast errors of wind and load and random outages of generators and transmission lines are taken into consideration. The load forecast errors are represented by a truncated normal distribution with a fixed standard deviation and the average is equal to the hourly power forecast. The wind power forecast is modeled by Auto Regressive Moving Average (ARMA) and the uncertainty is equal to a fixed percentage of the wind power forecast. The scenarios are generated with LHS technique in the Monte Carlo simulation and the forced outage rate of transmission line and generation units are defined by a low percentage value.

It is shown that a correct coordination of wind-pumped storage, due to the reduction of variation of thermal generation commitment, may lead to lower total operation costs, wind curtailment and corrective actions in scenarios costs.

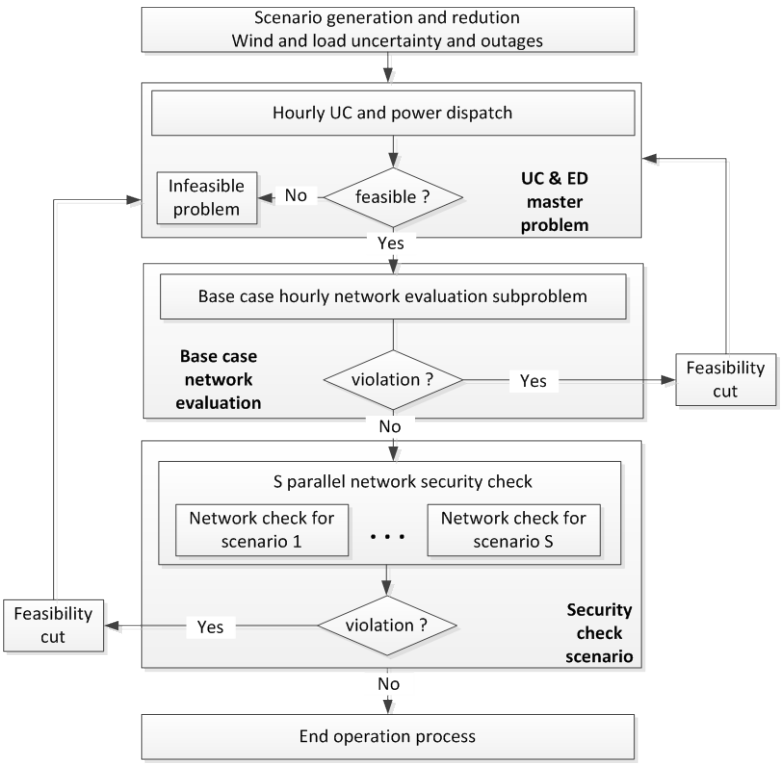

Figure 2.6 – Stochastic SCUC for coordinated scheduling of wind pumped-storage units

A different approach from stochastic programing is proposed in [64], namely the robust scheduling based on Robust Optimization (RO). In this approach, the solution is considered robust if it remains "close" to optimal for all scenarios and robust model if it remains "almost" feasible for the same scenarios. Being so, there are not unfeasible solutions since RO finds the solution which violates the constraints by the last amount. With the extreme

scenarios concept introduction, knowledge of wind power probabilistic distribution, necessary to create scenarios in stochastic programming, is avoided. The extreme scenarios set is derived from the uncertainty confidence interval of wind power output and is based on the worst case outcomes (defined as a fixed percentage of wind power forecast). Although it is secure, it can be too far conservative for some kind of problems.

In paper [65] a Reduced SCUC (R-SCUC) regarding wind power uncertainty is presented. The main goal of the proposed method is reducing the computational burden associated with the calculation of the reserves deployment. The notation of *loadability set* is introduced and it consists of a set of loads, which can be fed by the scheduled generation units exposed to all security constraints. This way, neither load shed nor wind curtailment is considered. These loads, defined as residual demand scenarios, result from the subtraction of wind power scenarios from the expected demand. Wind power scenarios are generated from normal wind power probability distribution functions. On the problem formulation, network transmission congestions are also taken into account. For situations of heavy congested cases the authors developed an extension of R-SCUC (three-stages), namely R-SCUC+.

Facing standard SCUC, R-SCUC reached comparable results of scheduled generation and reserve capacity and reached remarkable reductions in time processing (almost 20 times).

In a market trend, in [46] it is analyzed how demand dispatch combined with probabilistic wind power forecast can help the accommodation of large amounts of wind power. The purpose is to estimate dynamic operating reserve requirements in function of the uncertainty forecast level. This approach differs from the previous because the load, instead of being considered a fixed value, is dynamic. The term “demand dispatch” is introduced in order to characterize loads with sufficient flexibility to be price responsive, which are modeled as generation units with negative output.

The wind power forecast and associated uncertainty is done by a time-adaptive KDE in order to define its probability density function, which allows to calculate a set of quantiles for estimation of the dynamic operating reserves requirements. In the formulation, load shed is allowed as well as wind curtailment, lines or generation units’ outages and load forecasting errors are not addressed. Applied to a realistic case in Illinois, authors concluded that demand dispatch clearly improves the ability to handle wind power uncertainty and variability. Even low values of demand dispatch improve reliability in terms of reserve, load shedding and wind curtailment. At the end it is stated that the future of load forecasts passes for predicting both the firm and price-responsive components of the load.

In table 2.1 a summary of publications analyzed in the overview, concerning the uncertainty sources, outages criteria, and stochastic sources, among others is shown. It can be seen that the overview covers a wide range of the latest techniques for solving the scheduling and

assess the reserves. It is verified that the majority of the authors propose scenarios to model the uncertainties of wind power forecast, though confidence intervals are also proposed. Albeit several renewable power sources can introduce uncertainty during the scheduling process, throughout the publications search, all authors consider the wind generation as e main source, which is always present. In some cases the load forecast may also introduce uncertainty. In the RSCUC formulation, network lines or generation unit's outages are also considered.

Table 2.1 – Overview of techniques of scheduling with uncertainty

Ref.	Year	Uncertainty	Multi-periods	Network	Outages criteria	Reserves	Stochastic	Shedding
[4]	2009	Wind power	yes	no	no	fixed	Scenarios	load and wind
[56]	2011	Wind power (QR and NW_ KDE)	yes	no	no	fixed and dynamic	Scenarios	load and reserves
[15]	2009	Wind speed (ensembles)	yes	no	no	fixed	Scenarios	no
[16]	2011	Wind power (quantile)	yes	no	no	fixed	Scenarios	load and reserves
[57]	2008	Wind power (normal)	yes	yes	no	fixed	Scenarios	no
[58]	2013	Wind power (normal)	yes	yes	no	dynamic	Scenarios	load and wind
[59]	2012	Wind power & load (intervals)	yes	Yes	no	dynamic	Scenarios	wind
[60]	2013	Wind (Weibull) load (normal)	yes	yes	gen. lines	-	Scenarios	wind and load
[31]	2013	*Net load* (normal)	yes	no	gen.	fixed	Scenarios	load and wind
[61]	2012	Wind power (normal)	yes	yes	no	fixed	Scenarios	wind
[62]	2012	Wind (Weibull and % of rated power)	yes	yes	no	dynamic	scenarios intervals	no
[32]	2012	*Net load* (wind and load normal)	yes	yes	gen.	dynamic	scenarios	load
[63]	2013	Wind (%forecast) Load (normal)	yes	yes	gen. lines	dynamic	scenarios	wind
[64]	2012	Wind (conf. intervals)	yes	yes	no	fixed	extreme scenarios	no
[65]	2013	*Net load* (normal)	yes	yes	no	dynamic	scenarios	no
[46]	2013	Wind power (quantiles)	yes	yes	no	dynamic	scenarios	load and wind
[66]	2011	Wind power (quantiles)	yes	no	gen.	fixed	scenarios	load

The authors in [66] presents a work exclusively committed to the reserves assessment. It is intended to set the adequate operating reserve in power systems with large integration of wind generation. It is proposed a risk evaluation in order to describe the consequences of each possible reserve level through a set of risk indices in order to inform the decision-maker.
With this model it is proposed the definition of the operating reserves needed for the daily and intraday market. The load forecasting uncertainty is based on a normal distribution approximated by a set of quantiles, while conventional generation is modeled by a probability mass function (*pmf*). The wind power uncertainty is modeled by a set of quantiles. It is defined the system generation margin probability distribution as a discrete probability distribution by the convolution between the probability distribution of load, conventional generation and wind power generation. As the convolution is done and assuming the complete distribution, the tails of the distribution were modeled with exponential functions.
Authors conclude that it is not only the level of wind generation which has impact on reserve needs, but also the amount of wind generation uncertainty and the shape of its distribution.
Generally speaking, the author's concerns reside on reserves assess, the study of the response of power systems to the variability of renewable generation, the quantification of the load shed or wind curtailment or even the increment of algorithms velocity. In conclusion, it is necessary to find a compromise between the detail, the quickness and the robustness of the solutions. For instance, high detailed models not including uncertainties in the results (favouring the accuracy), may result in loss of result's meaning due to the uncertainty. On the other hand, models integrating uncertainty and risk assessment can lose the detail needed for the system operators. Very detailed models can be too much slow for the system operator needs.
Other conclusions can be achieved, namely:

- Using only deterministic power forecasts can conduce to high levels of unserved load and reserve;
- In the deterministic case, a dynamic reserves based on uncertainty reveal better performances than a fixed level of additional reserve;
- All the authors scenarios, stress out the necessity of scenario reduction because a large number can increase the computational efforts; on the other hand few numbers of scenarios can result in a poor approximation;
- The scenarios are useful to integrate the interdependence between time periods;

- Depending on the size of the balancing areas, geographical distribution of wind resources and market clearing intervals, the wind power increases the cost of ancillary services.

2.2.4 Deterministic scheduling formulation

The following Mixed-Integer Linear Programming (MILP) formulation is based on [48] whose formulation is widely used in several publications, as those presented above.
From (2.16) up to (2.39) it is presented a deterministic formulation of the UC to be solved. The power output of each thermal generator *i* at time *k* is defined by $pt_i(k)$ while the wind power generation, to the same period, by each unit *j* is characterised by $pw_j(k)$. Both must generate enough power to equal the load at time *k*, represented by $D(k)$ in equation (2.17).

$$\sum_{k=1}^{K}\sum_{i=1}^{N_G} C_i^p(k) + C_i^u(k) + C_i^d(k) \tag{2.16}$$

s.t.

$$\sum_{j=1}^{N_W} pw_j(k) + \sum_{i=1}^{N_G} pt_i(k) = D(k) \tag{2.17}$$

$$\sum_{i=1}^{N_G}\left[\overline{pt}_i(k) - pt_i(k)\right] \geq D(k).r(k) \tag{2.18}$$

In the function (2.16) it is assumed that wind generation cost is null being only contemplated the thermal energy production $C_i^p(k)$, and start-up and shutdown costs, $C_i^u(k)$ and $C_i^d(k)$ respectively. In (2.18) $pt_i(k)$ is a continuous variable which represents the power production of each thermal unit *i* at time *k* in order to model the requirements of spinning reserves defined by $r(k)$. Those requirements are modelled by the difference $\overline{pt}_i(k) - pt_i(k)$, where $\overline{pt}_i(k)$ is the maximum production of unit *i* at time *k* (in order to ensure the reserves of equation (2.18)).
This model includes the option of wind curtailment defined for each wind generator *j* at time *k* by $cw_j(k)$, by (2.19). The wind curtailment is the difference between the wind power point forecast $PW^f_j(k)$ for unit *j* to the hour *k* and the real production $pw_j(k)$.
As discussed in 2.2.2, the production cost function of each thermal generator depends on several aspects, like specific consumption, number of fuels, steam valve-effects, among others. However, generally, the most common model is defined by a second order polynomial or a piecewise linear model as (2.20), where $MC_{l,i}$ is the cost of each linearized segment *l* of

thermal unit i cost function and A_i is the non-load cost [16],[49]. The binary variable $u_i(k)$ represents the on/off status of thermal generator i at time k. The total thermal production results from (2.21), by summing the lower production limit of each on-line unit i to the generation $\delta_{l,i}$ at period k. Restrictions (2.22) and (2.23) represent the first and last piecewise segment of linearized function.

$$pw_j(k) + cw_j(k) = PW_j^f(k) \tag{2.19}$$

$$C_i^p(k) = A_i u_i(k) + \sum_{l=1}^{L} MC_{l,i}(k).\delta_{l,i}(k) \tag{2.20}$$

$$pt_i(k) = \underline{PT}_i.u_i(k) + \sum_{l=1}^{L} \delta_{l,i}(k) \tag{2.21}$$

$$\delta_{l,i}(k) \le \overline{\Delta}_{l,i} \tag{2.22}$$

$$\delta_{l,i}(k) \ge 0 \tag{2.23}$$

If the cost function is defined by a single linear segment, equations (2.20) to (2.21), become simpler, being defined as an ordinary linear function.

The second term of equation (2.16) intends the incorporating of start-up costs of thermal generators. As explained before, in equation (2.3) the starting up costs are strongly dependent on the temperature of the boiler and, therefore, the time that has passed since the units were turned off. In (2.24) and (2.25) CC_i and HC_i are respectively the cold start and hot start costs. In (2.24), N is the sum of time for cold start with minimum down time. The third term of (2.16) represents the shutting down costs as formulated by (2.27). It is intended that any thermal unit i is able to complete the shutting down manoeuvre within the time period k.

$$C_i^u(k) \ge CC_i.\left[u_i(k) - \sum_{n=1}^{N} u_i(k-n)\right] \tag{2.24}$$

$$C_i^u(k) \ge HC_i.\left[u_i(k) - u_i(k-1)\right] \tag{2.25}$$

$$C_i^u(k) \ge 0 \tag{2.26}$$

$$C_i^d(k) \ge C_i.\left[u_i(k-1) - u_i(k)\right] \tag{2.27}$$

$$C_i^d(k) \ge 0 \tag{2.28}$$

Concerning the operational issues of thermal units, the power output $pt_i(k)$ of each unit must satisfy the constraints (2.29) and (2.30) where $\underline{PT}_i$ and $\overline{PT}_i$ are respectively, the minimum and maximum capacity of unit i.

$$\underline{PT}_i.u_i(k) \le pt_i(k) \le \overline{pt_i}(k) \tag{2.29}$$

$$0 \le \overline{pt_i}(k) \le \overline{PT}_i.u_i(k) \tag{2.30}$$

Each thermal unit has its own thermal inertia as well as a particular heat rate (owing to thermodynamic processes). With this it is not possible to increment or decrement the production more than a certain value within a time interval. Equations (2.31) to (2.33) model the up/down ramp limits, where RU_i and RD_i are the up and down ramp limits of each unit i, respectively, and SU_i and SD_i are the start-up and shutdown ramp limits.

$$\overline{pt_i}(k) \le pt_i(k-1) + RU_i.u_i(k-1) + SU_i.\left[u_i(k) - u_i(k-1)\right] + \overline{PT}_i.\left[1 - u_i(k)\right] \tag{2.31}$$

$$\overline{pt_i}(k) \le \overline{PT}_i.u_i(k+1) + SD_i.\left[u_i(k) - u_i(k+1)\right] \tag{2.32}$$

$$pt_i(k-1) - pt_i(k) \le RD_i.u_i(k) + SD_i.\left[u_i(k-1) - u_i(k)\right] + \overline{PT}_i\left[1 - u_i(k)\right] \tag{2.33}$$

Additionally to the previous constraints, some thermal units once turned on (or off) must remain in this state for a specific period of time. The minimum up time is modelled from (2.34) up to (2.36) while minimum down time is modeled from (2.37) up to (2.39),

$$\sum_{k=1}^{T_i^{up,0}} \left[1 - u_i(k)\right] = 0 \tag{2.34}$$

$$\sum_{n=k}^{k+T_i^{up}-1} u_i(n) \ge T_i^{up}.\left[u_i(k) - u_i(k-1)\right] \tag{2.35}$$

$$\sum_{n=k}^{T} \left\{u_i(n) - \left[u_i(k) - u_i(k-1)\right]\right\} \ge 0 \tag{2.36}$$

where T_i^{up} is the minimum up time limit of each unit and $T_i^{up,0}$ is the number of on-line periods of unit i before the beginning of the scheduling period.

$$\sum_{k=1}^{T_j^{dn,0}} u_i(k) = 0 \tag{2.37}$$

$$\sum_{n=k}^{k+T_j^{dn}-1} \left[1 - u_i(n)\right] \ge T_i^{dn}.\left[u_i(k-1) - u_i(k)\right] \tag{2.38}$$

$$\sum_{n=k}^{T} \left\{1 - u_i(n) - \left[u_i(k-1) - u_i(k)\right]\right\} \ge 0 \tag{2.39}$$

On the other hand, T_i^{dn} and $T_i^{dn,0}$ are minimum down-time limits and the number of periods that unit i was initially off-line.

The presented model is quite complete, taking into account the power ramp limits, minimum up/down times and the contributions of each unit to the spinning reserve. Clearly, there are other modified formulations that follow the same line, considering the spinning reserve as a percentage of the total production, assign cost to the reserves, allow load shed, among others. The ramp limits have a specific role allowing the study of the response of thermal units in the presence of changes in generation and load or even forced generation outages. Nevertheless, the model can be improved introducing the network model and consequent power flow, evolving to complete security and reliability formulations.

2.2.5 Stochastic scheduling formulation

The deterministic formulation presented in 2.2.4, can be generalized to stochastic formulation running several scenarios of wind power or load, instead of only one. The differences from the deterministic formulation are basically in the objective function and in the notation. There is the introduction of the notation *s*, in the formulation (2.40) up to (2.52), which correspond to the scenario number [4],[15],[46],[47] and [56].

$$\min \sum_{s=1}^{S} prob^{s} \left(\sum_{k=1}^{K} \sum_{i=1}^{N_G} C_i^{p,s}(k) + C_i^{u}(k) + C_i^{d}(k) \right) \tag{2.40}$$

s.t.

$$\sum_{j=1}^{N_W} pw_j^s(k) + \sum_{i=1}^{N_G} pt_i^s(k) = D(k) \tag{2.41}$$

$$\sum_{i=1}^{N_G} \left[\overline{pt_i}^{s}(k) - pt_i^s(k) \right] \geq D(k).r(k) \tag{2.42}$$

$$pw_j^s(k) + cw_j^s(k) = PW_j^{f,s}(k) \tag{2.43}$$

$$C_i^{p,s}(k) = A_i u_j(k) + \sum_{l=1}^{L} MC_{l,i}(k).\delta_{l,i}^s(k) \tag{2.44}$$

$$pt_i^s(k) = \underline{P}_j.u_i^s(k) + \sum_{l=1}^{L} \delta_{l,i}^s(k) \tag{2.45}$$

$$\delta_{l,i}^s(k) \leq \overline{\Delta}_{l,i} \tag{2.46}$$

$$\delta_{l,i}^s(k) \geq 0 \tag{2.47}$$

$$\underline{PT}_i.u_i(k) \leq p_i^s(k) \leq \overline{pt_i^s}(k) \tag{2.48}$$

$$0 \leq \overline{pt_i^s}(k) \leq \overline{PT}_i.u_i(k) \tag{2.49}$$

$$\overline{pt_i^s}(k) \le pt_i^s(k-1) + RU_i.u_i(k-1) + SU_i.\left[u_i(k) - u_i(k-1)\right] + \overline{PT}_i.\left[1 - u_i(k)\right] \quad (2.50)$$

$$\overline{pt_i^s}(k) \le \overline{PT}_i.u_i(k+1) + SD_i.\left[u_i(k) - u_i(k+1)\right] \quad (2.51)$$

$$pt_i(k-1) - pt_i(k) \le pt_i^s(k) + RD_i.u_i(k) + SD_i.\left[u_i(k-1) - u_i(k)\right] + \overline{PT}_j\left[1 - u_i(k)\right] \quad (2.52)$$

The minimum up/down time equations (2.34) up to (2.39) do not suffer any changes in the formulation.

Further, this scheduling formulation can be extended, considering corrective actions on the thermal generation units taking into account the uncertainty of wind power plants, loads, generation and transmission outages. The problem can be transformed into two (or more) stages stochastic programming as proposed in [15],[57]–[63] and [65]. In the first stage it is intended to decide the value of the thermal power output and the commitment profiles over the entire scheduling horizon. The power outputs are considered as nonanticipatory (*here and now*) because it is assumed that the forecasted values are known.

The formulation of second-stage is done regarding multi realizations of the forecasted variables in order to meet scenario dependent thermal power output (*wait-and-see*) [15].

In order to keep the problem computationally tractable, the commitment variables are not scenario dependents. If the committed unit's remains on/offline in the second stage, it means that, in practice, an economic dispatch is being run to each scenario.

2.3 Stochastic optimization

In an environment without uncertainty, many deterministic model-based approaches have been developed. Depending on the objectives, decision variables and constraints, the deterministic optimization problems can be formally classified as Linear Programing (LP), Integer programming (IP), Mixed Integer LP (MILP), Non-Linear Programming (NLP), and Mixed Integer NLP (MINLP), among others. These model-based approaches are often impossible to implement in "real world" due to the high modelling complexity or, if there is some kind of uncertainty. This uncertainty can be introduced due to the stochastic nature of objective functions, variables or constraints, especially in the case of dynamic and complex systems. These may have parameters where, usually, the uncertainty is generating large effects on the objective functions and constraints. This is the case of power production scheduling, where there is the necessity to take decisions for the future, depending on the load and power production forecast uncertainty unexpected outages. Hence, it is always present the great challenge of taking decisions future operations. As a consequence,it is necessary to implement models of optimization under uncertainty.

The Stochastic Programming or stochastic optimizing problems are a sort of optimization where the stochastic properties of the uncertainties on the data and the model are taken into account. Stochastic programming is a mathematical technique which explicitly incorporates uncertainty of some parameters, underlying the optimization model. It can be used in financial planning, supply chain management, transportation logistics, telecommunications, network designs and energy systems planning, among others [67].

There are two main modelling issues in the stochastic programming, namely the optimal resources allocation model and randomness model, as presented in figure 2.7 [67].

The optimum decision model, together with the constraints, constitutes the core of the problem, which must be solved and it depends on the specific characteristics of each application problem. The model of the randomness and scenario generation is the major issue in the application of stochastic programming, it is the representation of the underlying random process.

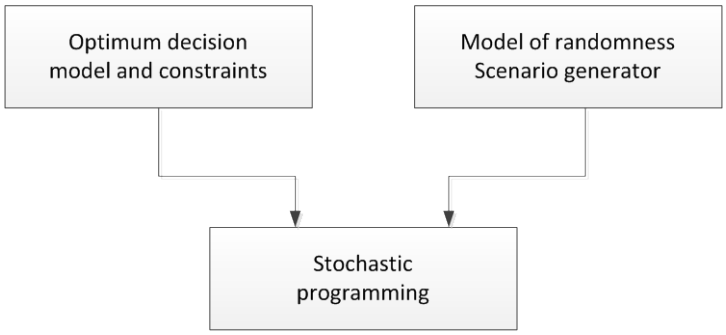

Figure 2.7 –Breakdown of stochastic programming

In figure 2.8 is presented a classification of stochastic programming models which can be applied both to linear and non-linear programming [67]. They are classified considering the way which the uncertainty is defined and how the problem is adapted to the optimization model.

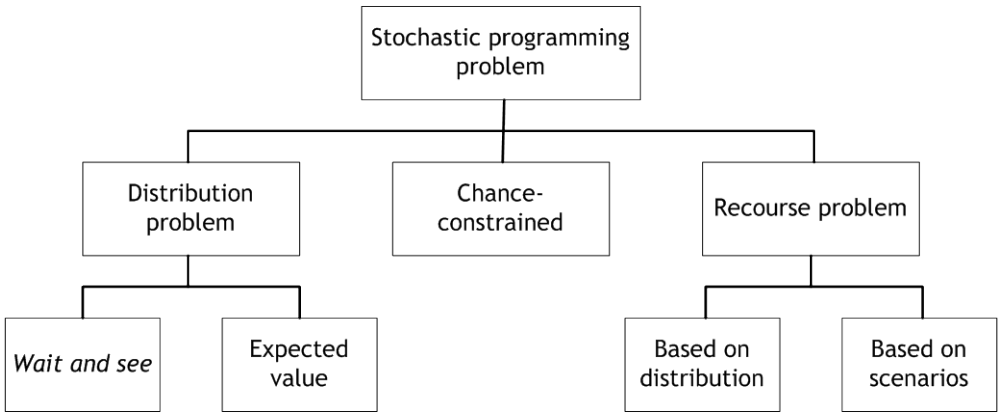

Figure 2.8 –Classification of stochastic programming problems

To illustrate this kind of problems the analysis can be initiated with the formulation of a linear problem defined by (2.53), where $\mathbf{A} \in R^{m \times n}$, $\mathbf{C}$, $x \in R^n$ and $\mathbf{b} \in R^m$ [67].

$$\begin{aligned} &\min \mathbf{C}x \\ &\quad s.t. \\ &\quad\quad \mathbf{A}x \geq \mathbf{b} \\ &\quad\quad x \geq 0 \end{aligned} \tag{2.53}$$

Lets also consider a discrete probability space represented by $(\Omega, \Im, P)$ and the realization of the uncertain parameters denoted by $\xi(\omega)$ with $\omega \in \Omega$. For each event ω, the realization of the parameters **A**, **b** and **C** is defined as $\xi_\omega = (\mathbf{A}, \mathbf{b}, \mathbf{C})_\omega$. The probabilities associated with these realizations can be denoted by $P(\xi(\omega))$ or only $P(\omega)$ [67].

2.3.1 Distribution problems

Distribution problems are broadly known as those which provide the distribution values of cost function for different realizations of the random parameters and also for the expected values of such parameters. The distribution problems can even be split in *Expected Value* (EV) and *Wait and See* (WS).

Expected value

The expected value model is built by changing the random parameters with their expected values as shown in (2.54). This way the model of EV can be considered as a linear problem, in fact, the uncertainty is handled before its introduced into the underlying optimization model. Despite not representing the full distribution and uncertainty, the usage of EV formulation, can be used in order to gain some sensibility regarding the decision problem.

$$\begin{aligned} &\min \mathbf{C}x \\ &\quad s.t. \\ &\quad\quad \mathbf{A}\left[E\left(\xi(\omega)\right)\right]x \geq \mathbf{b}\left[E\left(\xi(\omega)\right)\right] \\ &\quad\quad x \geq 0 \end{aligned} \tag{2.54}$$

Wait-and-see

In *wait-and-see* problem it is assumed that the decision-makers are capable of delaying their decisions, waiting until an observation is made on the random element and then solve it as a deterministic problem. Therefore, this approach is based on perfect information about the future [67]. In such cases when additional measurement information on the uncertainties becomes available, the operational strategy can be adopted. This strategy requires the solution

of several deterministic optimization problems in order to find the deterministic optimal decision at each scenario or random sample. However, *wait-and-see* strategy does not consider the uncertainty properties and has some drawbacks, such as the actions, which are always taken *a posteriori*. Furthermore, a feedback control cannot ensure constraints on open-loop variables [68]. Since the complete future realizations are rarely known, this approach is not suitable for handling time-varying processes, as power generation scheduling.

These models are often used to analyse the probability distribution of the objective values and belong to linear programming models family, being each one connected with an individual scenario [67]. The formulation for WS problem can be depicted as in (2.55).

$$\begin{aligned} &\min \mathbf{C}x \\ &\quad s.t. \\ &\quad\quad \mathbf{A}\left(\xi(\omega)\right)x \geq \mathbf{b}\left(\xi(\omega)\right) \\ &\quad\quad x \geq 0 \end{aligned} \tag{2.55}$$

2.3.2 Recourse problems (*here-and-now problems*)

The recourse problems are also known as *here-and-now* problems. While in the distribution problems approach, the expected values of the uncertainties are used in the problem formulation, the *here-and-now* problems involve the definition of both the objective function and constraints in terms of some probabilistic representation (expected value, variance, and quantiles). Moreover, the decision variables are separated from uncertain parameters.

In the recourse formulation, it is allowed the constraints violation, but are penalized through a penalty term in the objective function. (This approach is only recommended when the objective function and constraints are able to be described by the same measurement). If the cost model is hard to model or when the constraints are associated with safety requirements, it is better to not compensate for violations by additional costs. In these cases it is encouraged to maintain a high level of reliability. This means that constraints have to be satisfied at least with a probability exceeding some pre-selected value.

As it is a recourse problem it can be solved in several stages. The single stage, solution of the objective function by stochastic programming model can be formulated as (2.56) [67], where $x \in F$.

$$\begin{aligned} &\min E\left[\mathbf{C}\left(\xi(\omega)\right)x\right] \\ &F = \bigcap_{\omega \in \Omega} F^{\omega} \end{aligned} \tag{2.56}$$

The optimal value of (2.56) represents the minimum expected cost of the stochastic problem, and the optimal solution $x^* \in F$ hedges against all possible events of ω that may occur in the future [68]. The standard formulation of the two-stages stochastic programming model with recourse is done by (2.57)[68]. The intention is that the sum of first stage costs and the expected value of the random second stage, or recourse costs, is minimized [69],[70]. The objective is to choose the first stage variables in a manner that the sum with expected value of the second stage cost is minimized.

$$\begin{aligned} &\min \mathbf{C}x + Q\left(x, \xi(\omega)\right) \\ &\quad s.t. \\ &\quad \mathbf{A}x \geq \mathbf{b} \\ &\quad x \geq 0 \end{aligned} \tag{2.57}$$

where,

$$\begin{aligned} Q(x,\omega) = \min E_{\omega}\left[\mathbf{q}\left(\xi(\omega)\right)\mathbf{y}\left(\xi(\omega)\right)\right] \\ s.t. \\ \mathbf{D}\left(\xi(\omega)\right)\mathbf{y}\left(\xi(\omega)\right) = \mathbf{h}\left(\xi(\omega)\right) + \mathbf{B}\left(\xi(\omega)\right)x \\ \mathbf{y}\left(\xi(\omega)\right) \geq 0 \\ \omega \in \Omega \end{aligned} \tag{2.58}$$

The vectors **A** and **b** from (2.57) are known without any uncertainty. The function $Q(x,\xi(\omega))$ represents a non-linear term, which is referred to as the recourse function. The matrix $\mathbf{B}(\xi(\omega))$, $\mathbf{D}(\xi(\omega))$(recourse), the vectors $\mathbf{h}(\xi(\omega))$ and $\mathbf{q}(\xi(\omega))$ may be random.

For a given first stage decision *x*, the corresponding recourse actions $\mathbf{y}(\xi(\omega))$ are obtained solving the sub-problem associated with recourse function $Q(x,\xi(\omega))$. The future unfolds in several sequential steps and subsequent recourse actions are taken dealing with the generalization of the two-stage recourse problem, known as multistage stochastic programming problem with recourse. A decision made in stage *t* should take into account all future realizations of the random parameters and such decisions only affect the remaining decisions in stages *t*+1..*T* [67],[68]. The general formulation of a multistage recourse problem is set out in equation (2.59),

$$\min_{x_1}\left\{C_1x_1+E_{\xi 2}\left[\min_{x_2}C_2x_2+E_{\xi 3|\xi 2}\left[\min_{x_3}C_3x_3+.....+E_{\xi T|\xi T-1|..|\xi 2}\min C_Tx_T\right]\right]\right\}$$

$$\begin{aligned} &s.t.\\ &\mathbf{A}_{11}x_1 && && && && \geq \mathbf{b}_1\\ &\mathbf{A}_{21}x_1 && \mathbf{A}_{22}x_2 && && && \geq \mathbf{b}_2\\ &\mathbf{A}_{31}x_1 && \mathbf{A}_{32}x_2 && \mathbf{A}_{33}x_3 && && \geq \mathbf{b}_3\\ &\vdots && && && \ddots && \\ &\mathbf{A}_{T1}x_1 && \mathbf{A}_{T2}x_2 && \mathbf{A}_{T3}x_3 && \mathbf{A}_{TT}x_T && \geq \mathbf{b}_T\\ &l \leq x_t \leq u_t \end{aligned} \tag{2.59}$$

where t =1,…,T represents the stage in the planning horizon, and the vectors ξ_t = ($\mathbf{b}_t$,c_t,$\mathbf{A}_{t1}$,…,$\mathbf{A}_{tT}$) with $\forall t \in [2,...,T]$ are random vectors on a probability space $(\Omega, \Im, P)$.

This approach already gets better values than those obtained by the expected value approaches of distribution problems. If any feasible solution obtained by the expected value exists, it is already contemplated in the *here-and-now* model.

The two-stage recourse problem was used in works presented in [15],[58] and [63], while in [65] a three-stage problem was used (all referenced in table 2.1).

Another approach for obtaining worthy solutions is the sample average approximation (SAA) method [69]. A sample ξ_1,…, ξ_N of N realizations of random vector $\xi(\omega)$ is generated and with this, the real distribution ξ is replaced by an empirical distribution corresponding to a Monte Carlo sampling (2.60). This technique was explicitly used in [15] and [31].

$$\begin{aligned} &\min \mathbf{C}x+\frac{1}{N}\sum_{i=1}^{N} Q\left(x,\xi_i(\omega)\right)\\ &s.t.\\ &\mathbf{A}x \geq \mathbf{b}\\ &x \geq 0 \end{aligned} \tag{2.60}$$

2.3.3 Chance-constraints problem

Other method of stochastic programming is the probabilistic or chance-constrained which focuses on the system reliability. The reliability is the system ability to remain feasible in an uncertain environment. It can be expressed as the minimum requisite of the probability of satisfying the system constraints. This optimization technique deals with random processes where one (or several) constraints or an objective function must be satisfied with high probability, as defined in equation (2.61). Therefore there are two main reasons for the problem to become intractable; the formulation of the constraint can be hard and the feasible

search space limited by the chance-constraint is generally not convex even if the constraints are convex in x for each realization ξ of ω [31]. In the case of α equal to 1 the problem is equivalent to a deterministic one.

$$\begin{aligned} &\min \mathbf{C}\left(\xi(\omega)\right)x \\ &s.t. \\ &P\left\{A\left(\xi(\omega)\right) \geq b\left(\xi(\omega)\right)\right\} \geq \alpha \\ &x \geq 0 \end{aligned} \tag{2.61}$$

This approach was used in [31] and [61] to solve an UC with wind power uncertainty.

2.3.4 Worst-case constraints

To deal with the *a priori* unknown operating reality, two general methods are widely used, the worst-case and the base-case. While in the base case it is used the nominal (mean) value of the uncertainty variables, the worst-case is a simplified approach for evaluation of the robustness and feasibility. Generally, it is applied to problems where the distribution is unknown. It is assumed that all the variations can occur simultaneously in the worst combination possible. It is a very conservative analysis, since it considers that worst cases of variables or parameters deviations will occur simultaneously. Nevertheless, and although the reachable "low profit", the worst-case is widely used in the optimization areas due to its simplicity and reliability in ensuring the constraints. This is the case of [59] and [64] where it is defined a set of extreme scenarios for description of wind power uncertainty.
After this study some conclusions could be obtained and are presented in table 2.2.

Table 2.2 – Overview of stochastic programming

Expected value	Chance-constraint	Worst case
Solution not robust	Robust solution	Absolutely robust solution
Solution at low cost	Not too expensive	Extremely expensive
Easy to solve	Often difficult to solve	Cannot even exist

So far it is verified that there are several sources of uncertainty in the power systems scheduling. Some authors include uncertainty related with generation unit's outages or transmission lines, uncertainty in load forecast and/or in renewable power forecast in their formulations. However, it is a constant presence in different formulations or solutions techniques, the uncertainty related with renewable power production, namely wind power generation. The renewable power production forecast is based on several techniques which may depend on the type of the renewable source, the available information, forecasting

horizon, among others. To understand these issues an overview concerning renewable production and load power forecast is done.

2.4 Power forecast methodologies

Despite not existing a unique definition for classifying the temporal horizon of forecasting, it is current to consider three temporal scales: very-short-term (up to 6h or even 9h) [71], short-term (6h to 72h) and mid-term (3 days to 10 days) [71]–[73]:

Very short-term forecast: The application of this time horizon depends on the market rules with the forecasts being useful for trading in intraday markets. For the system operator, the usefulness of these forecasts is related to the ancillary services management of the power system, as well as for UC and ED refreshment. It is also useful in the management of rapid conventional power plants (very usual in isolated systems as islands);

Short-term forecast: Forecast for a time horizon between 6 and 72 hours. This time horizon is strongly related with the power system scheduling, namely UC and ED. This time horizon is of great importance for the input in the electricity daily market. In this case the forecast horizon is defined by the requirement of market operator. The short-term forecasts can also be used for maintenance scheduling, particularly when the time horizon is 72 h;

Mid-term forecast: From 72 hours up to 7 days allowing programming maintenance operations.

In an energy system integration level, the power forecast can have the most varied applications, namely [71],[72]:

- Optimization of energy grid management at the level of economic dispatch or pre-dispatch of power plants, dynamic security assessment, reserves allocations, power flow with neighbouring systems, water storage in power plants reservoir, etc. The forecasting horizons depend on the production system size and conventional power plants type.
- Optimization of energy trade in the energy market environmental. The producers at market, energy suppliers, energy traders and independent producers define generation schemes for the time horizons set by the market rules, usually with 48 hours in advance, suffering penalties for deviations from these plans;

- Power plants or transmission lines maintenance planning, for which longer forecasting horizons can reveal interest, though the acuteness of the meteorological predictions strongly decreases from 5 to 7 days.

2.4.1 Reference models

Any new model or forecasting method to predict power can only be considered satisfactory if it obtains better results, i.e. smaller errors than the reference considered methods. The simplest method is the persistence where it is considered that the forecasted value to instant $t+k$ is equal to the one measured at instant t (2.62).

$$\hat{p}_{t+k|t} = p_t \tag{2.62}$$

Despite of its simplicity, this method is hard to beat in very short-term horizons [71]–[74]. The generalization of persistence leads to the moving average method, which provides a future value with the average of n past values. At the limit, the average is all available past data. Another method considered as reference is based in climatological concepts [72]-[76], and use the average of the meteorological statistics accumulated during several years, to a specific location during a defined time interval. This method combines the persistence and the mean $\overline{p}$ as shown in equation, where the weight a_k is a function of the correlation between the last measured value p_t and the previous values.

$$\hat{p}_{t+k|t} = a_k p_t + (1 - a_k)\,\overline{p} \tag{2.63}$$

Typically, this method obtains better performances than the persistence method in cases of forecasts from 12 to 18 hours [73],[74]. The drawback of this method is the need to estimate a_k which has to be done under some assumptions.

2.5 Wind power forecast models

In the prediction of very short-term and short-term, fundamentally there are two paths; one uses physical models and the other uses statistical models. However, there are systems using the combination of both methods, since, in reality, both are necessary to the forecasting success [72],[74].

2.5.1 Physical models

The physical models try, as much as possible, to only use physical considerations to achieve the best estimates to a specific place and, in certain cases, to use statistical models as Model

Output Statisics (MOS) to reduce the remaining errors [71],[72]. The type of information for providing a physical model can be characterized as dynamic and static:

Dynamic information**:** is based in numerical methods (Numerical Weather Predictions - NWPs) and obtained from very complex models run on computers with large processing capacity. The numerical weather forecast is a specific area of the forecasting based on meteorological concepts which are studied and developed by meteorologists whose results serve as base for renewable power production forecasts. Typically, the information indicated by the meteorological services is: temperature, atmospheric pressure, wind speed and direction, precipitation, among others. Generally, measures of real-time data are rarely used to adapt the statistical models (MOS).

Static information: Wind power plant plants description, number of wind turbines, power curves, description of terrain, including topography, roughness, turbines placement and obstacles, among others.

In figure 2.9 is presented a simplified block diagram with the steps for the power forecast based in physical models [71],[72].

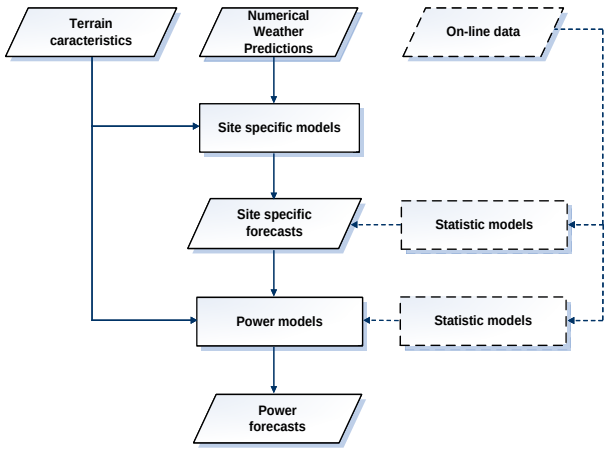

Figure 2.9 – Block diagram to wind power forecast from physical models

Despite several model types exist, they all are based on the same physical principles, basically changing the way the grid is structured and the used numerical method to solve the equations. Depending of NWP type, these predictions are given with a resolution of few kilometres, generally 10 to 15 Km, depending on the distance between meteorological stations. If the forecasts are provided for far away points from the wind power plant, the resolution can be insufficient, as shown in figure 2.10. In this case it is necessary to model the site in order to individualise the predictions for the geographic location where the wind turbines are deployed. The first step is to obtain site-specific models using the interpolation of values provided for wind prediction (and other variables such as direction) to the location of power

plant at a reference height, which is usually 10 meters. This can be achieved by using mesoscale and microscale models [72]–[74] and [76], depending on the resolution which is intended to reach for increasing the predictions resolution. Use of micro and mesoscale models may be needless if the forecasts with NWP models are good enough. The opposite may also occur in cases where the mesoscale and microscale resolution are too coarse to solve specific site fluctuations. In this case additional physical considerations about the wind flow may help. However, it should be remarked that collecting this information is one of the greatest difficulties for implementing physical models.

On the other hand, there are some models where the results of the NWPs are provided by the meteorological services directly to the wind power plants localization by interpolation, as shown in Figure 2.11.

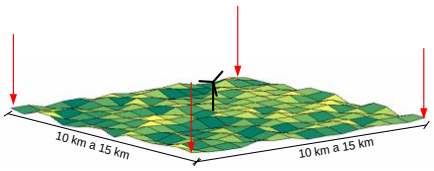

Figure 2.10 – Wind speed prediction with NWP to grid points around the wind power plant

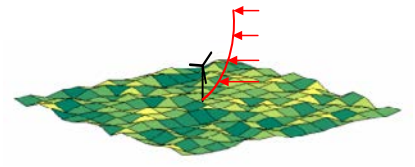

Figure 2.11 – Wind speed predictions with NWP with direct interpolation to the wind power plant

If these interpolations are based on simple mathematical relationships, not taking into account the nonlinearities introduced by the terrain, significant errors can be introduced. After knowing wind speed values to each local, the power models are elaborated. As wind turbines are located in friction layer, the wind speed is influenced by surface roughness, increasing the speed as they move away from the surface. The effect of the frictional force will fade, almost vanishing from 1000 meters, at higher heights it is considered free atmosphere [77]. Generally, the predicted values are provided at 10 meters height but wind speed varies with altitude and roughness of the soil. To calculate the wind speed to the height of the turbine the Prandtl law must be used. After knowing the values at turbine height, they are converted to electrical power through several models. These models can be a simple power curve given by the manufacturer or through more elaborated processes like artificial neural networks, fuzzy logic, among others [71]–[74]. Finally, depending on their availability and the forecast horizon, the measured power, obtained by Supervisory Control and Data Acquisition (SCADA) systems data can be used as input, since in many cases it helps statistical models (MOS) to improve the residual errors. Though using statistical methods, the global model is considered physical since best performances come from physical considerations.

The use of the models above depends on the purpose of the forecasts and so on, a trade-off between NWP costs and the utility of the forecast should be measured. As an example, if the

forecasts are inputs to an ED problem for horizons ranging from 10 minutes up to 1 hour, the use of very-short forecasts is enough and no additional costs with NWP are necessary.

2.5.2 Statistic models

The majority of alternatives to the physic methods to the power forecast, are based in models purely statistics. Thus, the blocks relating to the terrain specifications and power models represented in figure 2.9 are replaced by a single step that directly converts the input in power, usually employing recursive techniques, as shown in figure 2.12. In the very short-time approach, the models are based on the time series approach, such as the Kalman Filters, Autoregressive Moving Average (ARMA), Autoregressive Integral Moving Average (ARIMA), Autoregressive Moving Average with Exogenous inputs (ARMAX), Auto-Regressive with Exogenous Input (ARX), among others. These type of models, generally, take only as input past values from the forecasted variable (e.g., wind speed and power generation). At the same time, they also can use other explanatory variables (e.g., wind direction, temperature), which can minimize the forecast error [71],[72] and [78].

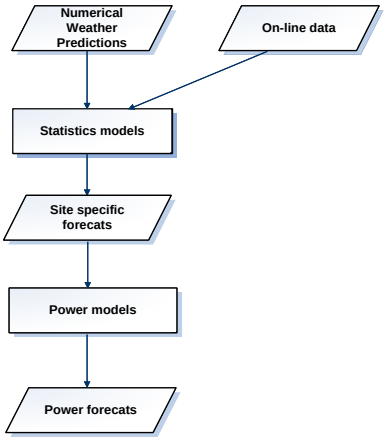

Figure 2.12 – Block diagram to wind power forecast from statistical models

The major problem of this method is defining analytic expressions and the determination of their numerical coefficients. More sophisticated statistical models, such as "black box", including artificial neural networks, can find complex relationships between the values of input and output [74] in order to produce better forecasts than simplest models, such as regression methods. There are also, some methods joining the physical and statistical models, exploring the knowledge of wind production properties and helping the structure definition of a “grey box” model. Though the ultimate aim is the power forecast, many statistical models are used for wind prediction, calculating the power in a second step. This intermediate step is often overlooked, being developed a single model that provides directly the power.

2.5.3 Models ensemble

Currently, different approaches are used, based on the assembling of various models. The final objective is to obtain the benefits and advantages of each model and get the optimum performance for the horizon desired. The combinations can be either [79]:

- Combination of physical and statistical approaches;
- Combination of very short-term models (0 to 6h) and short-term (6 to 72h);
- Combination of alternative statistical models.

All models start from wind speed and direction forecast, among others, through numerical models and in some cases with real time data, only deviating in the way of such data is processed. The combination of the two methods can extract the best from each, improving the forecasts quality.

2.5.4 Regional forecasting (*upscaling*)

In most cases, it is not possible to have NWP predictions for all wind farms in an area, due to the high computational effort and costs involved. To overcome this problem, *upscaling* approaches have been developed to forecast regional/national wind generation from a set of reference wind farms. Furthermore, the aggregation of wind farms appears to reduce the forecast error as a result of spatial smoothing effects [28],[71] and [80]. The *upscaling* intention is to extrapolate the total wind generated power, from predictions carried out for a number of representative (or reference) wind farms. This aggregation can be done under several approaches:

Direct up scaling: the *upscaling* model is designed and trained to provide forecasts for the regional wind power, using direct inputs from reference wind farms. This approach is essentially based on statistical modelling and the main difficulty is that the function has to be updated if new wind farms are added to the system.

Cascaded approach: this is mainly used for *upscaling* today. It considers two forecasting stages: first, the generation of the reference wind farms is estimated and, then, the sum is extrapolated to the total regional/national generation

Cluster or sub regions approach: it is based on the aggregation of wind farms into clusters that contain neighbouring wind farms or wind farms belonging to the same sub region. A model is developed for each cluster or sub region based on input from the reference wind farms in that cluster/sub region. Finally, the sum of the clusters' generation forecasts provides the total forecast for the region.

On-line (OL) persistence for *up scaling* models: The OL-Persistence method is defined as the sum of the production of the representative wind farms with SCADA, scaled to the total wind power (using nominal power).

The previous prediction models approaches, generally provide point forecasts since only a single value of wind power is estimated. The main drawback of point forecasts is no information is being provided on the dispersion of observations around the predicted value. Recent research efforts have focused in associating uncertainty estimates with point forecasts, taking into account the form of probabilistic forecasts [5],[16],[26] and [71], among others. Due to the large implementation of wind power, almost all works are focused in the uncertainty of wind power forecast but the same approaches can be applied to other renewable power sources.

2.6 Hydro power forecast models

The mini-hydro power plants are characterised as power facilities with low rated power (up to 10 MW) localised in rivers, which compared with reservoirs of large hydro power plants, have relatively reduced water flows and low storage capacity. If they are of run-of-river type, the flow regulation capacity is neglected. In a very simple approach, it can be considered that energy production in this kind of facilities depends mainly on the water level stored in the reservoirs, when in presence of facilities with reservoir or from the inflow, in the case of run-of-river power plants. In both cases the main variable is rainfall being the relationship between rainfall and inflow highly nonlinear [81]–[83]. Oppositely to wind production, where the wind speed and the power produced are connected, in the hydro power plants the rainfall may not correspond with the power production as shown in figure 2.13.

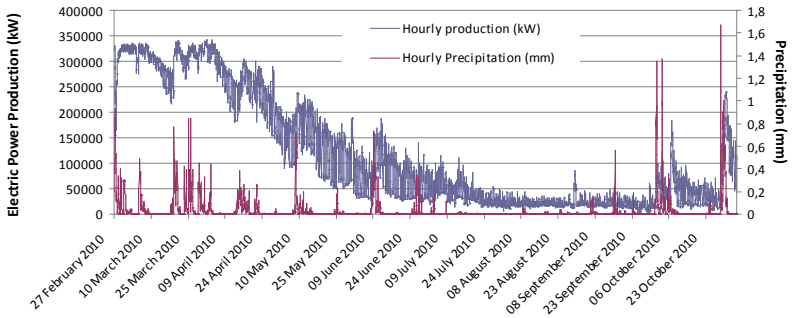

Figure 2.13 –Hourly average power production and hourly average rainfall

With this in mind, several authors [81],[82] and [84]–[89] among others, dedicated their studies to develop inflows forecast methods, taking into account predictions scopes and physical features which characterize the watershed area, inflow characteristics and operation strategies and forecast horizons. Generally, it is concluded that the water inflow doesn't depend only from rainfall, but also from environment temperature and, in more specific cases, snow melting, air humidity and, in large watersheds, localized storms. Just like in wind forecast models, it can be divided in three large sets:

- Physical models
- Statistical models
- Ensemble of models

2.6.1 Physical models

These models simulate the physic processes, usually incorporating simplified forms of physical laws and generally are non-linear, time-invariant, and deterministic. Incorporate parameters that are representative of watershed characteristics but ignore the spatially distribution, time-varying, and stochastic properties of the rainfall–runoff process. The implementation and calibration of such a model can typically present various difficulties, which require sophisticated mathematical tools, significant amounts of calibration, and some degree of expertise and experience with the models. The problem with conceptual models is that empirical regularities or periodicities are not always evident and can often be masked by noise. However, it is generally considered that conceptual watershed models are reliable in forecasting the most important features of the hydrography.

2.6.2 Statistical Models

The statistic models look for strong relations between historical data of inflow or power production and measured values, using recursive techniques. It is a different approach from physical models, since only a single module is used to transform the existent information in inflow or power forecast. It is important to highlight that statistical models have as an advantage the fact of being needless of physical information. However, to the parameter estimations process it is necessary to know a large set of historical data and information in real time.

The ANN's, in spite of not being a pure statistical method, has intrinsically the capacity to reach nonlinear mathematical relations, contained in the watershed models. Additionally, show a relative facility of implementation, being one of the most common tools used in the inflows and power production forecasting in hydro power stations.

In [85],[87], and [88] it was proposed a reservoir inflow forecasting for a mini-hydro power plant based on rainfall forecasting. Two temporal horizons were considered, very short-term using historical data of rainfall and inflow measured along the watershed and short-term, based in rainfall forecasting and, consequently, inflow to reservoir. In both cases the values are subsequently processed using ANN of Multi-Layer Perceptron (MLP) [88], as presented in figure 2.14.

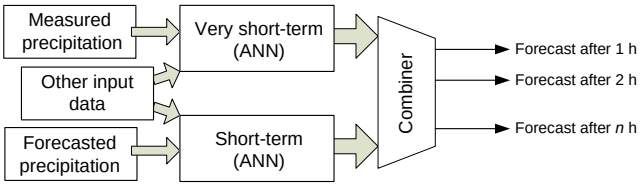

Figure 2.14 – Reservoir inflow forecasting for a mini-hydro power plant based on rainfall forecasting

In [90] it was applied an ANN of MLP with backpropagation learning algorithm using as input the date (month and day), the inflows and the level of storage to provide the daily production for the next month. In [82] it is presented a study for daily river inflow forecasting, without considering power production, where a study has been done for comparing two forecast methods, namely Self-Organizing Neural Networks and Auto Regressive Moving Average (ARMA) based in time series. In another different approach, [91] studied the use of ANN of MLP to rainfall prediction for 6 h ahead. It is intended to know the inflows and avoid flash floods, mainly in small watersheds. It even was stated that in very small watersheds, sensible to flash floods, the predictions by numerical method may not be the most advisable. Many other topics based in ANN were studied, as Echo State Network, Self-Organizing Nonlinear Auto-Regressive model with eXogenous input (SONARX), ANN Radial Based Functions (RBF) and Artificial Neuro Fuzzy Inference System (ANFIS)[86].

In [92], the author also used ANN with several learning algorithms, as: Backpropagation (ANN_BP), Conjugate-Gradient (ANN_CG), Cascade Correlation (ANN_CC) and Levenberg-Marquardt (ANN_LM) to short-term forecast diary stream flow. In [93], are presented inflow forecasts based on gradient descendent method, Resilient Backpropagation, Scaled Conjugate Gradient and Levenberg-Marquardt which results were compared with the ARIMA method. Similar studies were presented in [94] where the daily forecast of inflows using ANN type MLP and RBF are presented. In this case, it was used as network inputs, past values of rainfall and runoff to forecast the inflow with MLP. As conclusion, in [92] and [95] it is sustained that, in average, 90% of hydrological studies applications use MLP with BP.

2.6.3 Ensemble of models

Depending on the time horizon and available information and resources, there are several forecasting methods which can be used. However, they all have limitations, such as the need for large amount of historical data or the low ability to handle with non-linearity. With this, selecting combined models with their different characteristics and applications in order to contribute for the improvement of forecasting processes is a must.

With the exposed, it is verifiable that there are several works proposing inflow forecasts with different time horizons, from hours up to months, but without proposing any kind of power

production strategies. These issues were recently outlined in [96] where it is presented an original short-term forecasting model for hourly average electric power production of small-hydro power plants. The proposed method takes into account operation strategies of the small-hydro power plants and starts with the estimation for the daily average power production, followed by hourly average power production.

2.7 Solar photovoltaic forecast models

The electric power production in photovoltaic devices depends mainly on two variables, irradiance and cells temperature. The irradiance has direct influence on the cells current, keeping the voltage relatively constant during a large interval of irradiance values. As to the cell temperature, its increase causes a decreasing in the voltage, keeping the current almost constant. There is also another meteorological factor that indirectly has influence on the power production; the wind speed cools the cells' surface consequently decreasing the cells' temperature. Externally, there are other factors contributing to the power production, as the geographic position, the panel's angle, among others. However, it can be considered that the solar power production depends mainly on global irradiance, which is composed by three components: direct irradiance, due to the direct incidence of solar radiation, diffuse irradiance due to the radiation that comes from atmosphere (although not being directly from the sun) and albedo resulting by the direct irradiance reflected from soil around.

2.7.1 Global irradiance forecast models

Images from geostationary satellites have been used to determine and forecast the solar irradiance conditions in certain locations. This method is based on clouds shapes' structure during time intervals, proceeding later to the extrapolation of its motion. The result is a prediction of clouds' position and hence a prediction of solar irradiance to the studied site [97]. Solar predictions are done to very short-term based in satellite images and short-term with numerical weather predictions. In figure 2.15 a simplified process model is shown. Other approaches, based on ANN are proposed in [97] where ANN_BP, ANN_LM, ANN_RBF, recurrent networks and ANFIS to hourly solar irradiance forecast are used. In [98] are used ANN_BP, ANN conjugate gradient algorithm, ANN quasi-Newton algorithm and ANN_LM to the daily irradiance forecast.

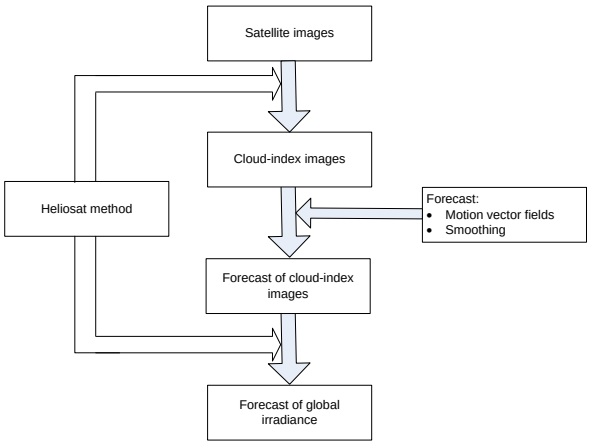

Figure 2.15 – Example of cloud position prediction

Several other authors as [99]–[103] used time series models as ARMA and ARIMA with satisfactory results for short time intervals. In [104] it is considered that for very short-term, satellite images and ARMA and ARIMA can be used, in spite of the modelling of the daily irradiance, which cannot incorporate the clouds influence.

2.7.2 Irradiance splitting forecast models

As mentioned before, all presented models predict the global irradiance in a horizontal plan, which is necessary to split into their components, namely, direct, diffuse and albedo. This step can be surpassed if the predictions are directly made in their components. In [105] it was proposed the forecast of daily and monthly diffuse components of global irradiance. Correlations between diffuse portion (quotient between diffuse and global irradiance) and clarity index (quotient between extra-terrestrial and global irradiance) were developed in a daily scale. In [106] several experiments were done with ANN, with several combinations of inputs to predict the hourly diffuse irradiance.

2.7.3 Power production forecast models

To avoid the need of more calculations after the solar irradiance forecast, several authors presented models to predict directly the power production as those shown in figure 2.16. Starting with the numerical weather forecasts, with the predictions locally refined by statistical models associated with local meteorological stations. Next it is interpolated to solar power plants localization. After, it is necessary to simulate the photovoltaic system, considering its orientation and angle to convert the horizontal incident irradiance to an angular plan and split it in the irradiance components. Finally, the complete electrical system is modelled.

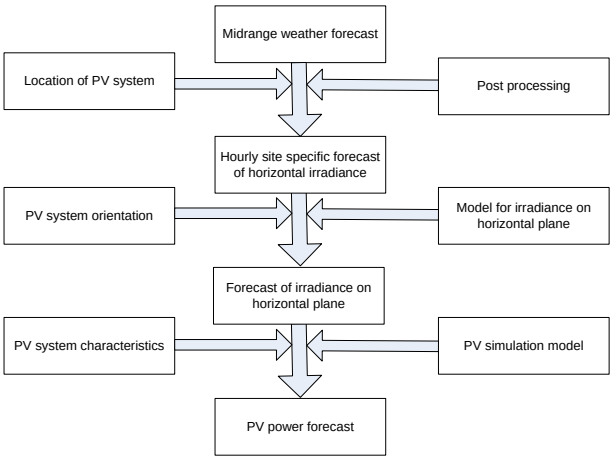

Figure 2.16 – Power production forecasted model

In [107] the predictions are done in a perspective of energy production and the errors between individual power plant forecasts and aggregated forecasts are compared. It is concluded that the RMSE to one day ahead forecast is almost three times higher than to a national aggregation.

2.8 Load forecast models

Load forecasting is another crucial component for the scheduling and operation of power systems. In operational framework such as power system scheduling, there is the need of knowing the load, which has to be fed by the units to be committed, as well as to estimate load flows for decreasing the risk of overloading, which leads to improvement of *net load* reliability and decreases the probability of occurrences of lines or units outages and blackouts. In planning framework it helps to make important decisions, namely decisions on purchasing electric power, load switching or infrastructure development. Said this, its accurate forecast is extremely important for energy suppliers, ISO, financial institutions and other participant's on electric energy generation, transmission, distribution and markets.

Comparing with some renewable power production, namely wind and solar, generally the load profile presents much less variability. It follows a well-defined pattern during the days with clear variations along the day between peak and off-peak periods. Over the years, generally, the great differences are in the load amplitude and some temporal shift linked with seasons and Winter/Summer hour.

As referred in point 2.4, there is not a unique definition for classifying the temporal horizon of forecasting. In [108] it is stated that load forecasts can be split into three time frameworks,

namely short term forecast (form 1 hour to one week), medium-term forecast from a week up to a year and long-term forecast (longer than a year).

In all time frames the majority of forecasting methods are based on statistical techniques as regression, or artificial intelligence algorithms such as ANN, fuzzy logic and expert systems [108]–[110]. In the particular case of medium and long-term forecasting, the so-called end-use and econometric approach or their combination is broadly used. These models use description of appliance used by costumers, size of houses, technology changes, equipment age, age costumer behavior and population dynamics. Also, economic factors as employment levels, per capita incomes and electricity prices are used. Although the variety of methods include several applicable to medium and long-term load forecasting, in this work only the short-term load forecasting methods will be addressed.

In the case of short-term load forecasting there are three main aspects, such as time factors, weather data, and costumers classes [108]. The time factors include the week of the year, the day of the week, and the hour of the day. The week of the year gives information about the period of the year under study, as an example: it is harder to forecast during the holidays than non-holidays due to consumption profiles not following the frequent pattern. The day of the week describes the differences between working days and weekends as well as the different behaviors in working days, namely the Mondays and Fridays, which present a structurally different load from the rest of the days. This behavior has higher impact during summer.

Concerning the weather, the temperature is the most important data, followed by the humidity and wind speed. The binomial temperature/humidity has more importance during summer and temperature/wind speed during the winter.

The costumer classes is more significant at a local level since it gives significance to the type of costumers, such as residential, commercial, and industrial.

Following [108], there is a large variety of statistical intelligence techniques which have been developed for short-term load forecasting such as similar-day approach, regression methods, time series, ANN, expert systems and fuzzy logic.

The similar-day approach is based on searching historical data for days with similar characteristics as weather, day of the week and date. With this, the load of similar day is considered as a forecast.

Regression methods based on time series are widely used as statistical techniques. Different authors introduce different explanatory variables such as, weather, type of the day, costumer classes, among others, in order to find their relation with load consumption. Methods such as ARMA, ARIMA, ARMAX and ARIMAX are often used [108]. In [110] semi-parametric approach to model nonlinear relationship combining temperature with time and type-of-day using ARIMA is addressed.

In [109] it is proposed the use a feedforward backpropagation ANN, which combines load profiles and temperature in order to find the non-linear relation between them and predict the load 24 hours ahead. There is other ANN which can be used, such as Radial Basis Functions (RBF), Hopfield, Boltzmann machine, among others. However, the feedforward backpropagation is still the most used.

The expert systems are molten with fuzzy logic, since both are based in heuristic techniques, where the forecasting is based in rules and proceeding is defined by human experts. In these cases there is not any associated mathematical model, being the relation between the explanatory variables, weather and time, among others, being the load defined by linguistic rules.

2.9 Uncertainty estimation

Thus far, in all the forecast techniques, whether they are renewable production or load, only a single forecasted value is provided. The main disadvantage is that no information about possible deviations from the predicted value is available. For the decision makers the benefits are quite limited, mainly in the applications based on risk assessment or stochastic optimization, as it could be seen in point 2.3. For this, it is much desirable for the decision-makers having an idea about the uncertainty associated with each forecasting period.

When a forecast is done, there are always associated errors which can result from several factors, such as incorrect or incomplete models, wrong parameters, extreme events, incorrect starting conditions, variations of sources, dynamics over the forecast period, amongst others. The models developed for load forecast generally get good results with lower deviations from the measured values because load profiles follow a characteristic pattern. Comparing with load forecast, the prediction of RES, due to its variability, presents much bigger challenges.

In the RES chapter, due to its high installed power capacity all over the World and high variability and uncertainty, wind power forecast gathers the majority of the attention of researchers and the major number of published works. Though addressing other types of RES (namely solar and hydro), wind generation is presented as the main source of generation uncertainty in power systems scheduling, grid operation and market environment.

In wind power forecast, there are three major factors which have influence on the uncertainty, namely, the NWP, the conversion of wind to power (due to the nonlinearity of the power curve) and terrain complexity. On the other hand, the NWP and the clouds dynamic are the main source of uncertainty in the case of solar photovoltaic since conversion is well defined. In the case of hydro power forecasting systems, the uncertainty generally propagates from the

NWP model through the rainfall-run-off model. The rainfall-run-off models are limited by their representation of flow dynamics, whose main problem is not the representation of the dynamic but knowing the local parameters [111].

In this analysis one must keep in mind that there is a difference between how to capture the uncertainty of forecasts and the way to represent the uncertainty of those predictions (by probabilistic models or scenarios). A very comprehensive analysis can be found in [1] and a very extended and complete in [71]. The following examples are focused in wind power production but can easily be extrapolated to other power sources.

In figure 2.17 the based on NWP point forecast approach is depicted. In this case only a single point forecast is done to each look-ahead time, (generally wind speed and direction, atmospheric pressure, precipitation, temperature, among others). As represented in figure 2.17, with this data two paths are available, or it applies the data directly to the probabilistic model or it previously converts the NWP to wind power spot forecast (WPF) using a wind-to-power (W2P) model, calculates the errors and only then applies the probabilistic model. As a single spot forecast is not enough to characterize the uncertainty, on this approach it is mandatory having a historical data set of power production, or errors and corresponding explanatory variables, which must be updated by the time each new value is known. Since wind power generation is a nonstationary process, a time adaptive and recursive estimation method can be applied [11],[71],[112] and [113]. These upgrades are very important when in presence of changes in the production profiles due to the installation of new generators, long outages owed to big maintenances or even something as natural as changes in the vegetation on the surroundings of the wind facility. There are several probabilistic models that can be used in order to represent the uncertainty of forecasts, which will be discussed in point 2.10.

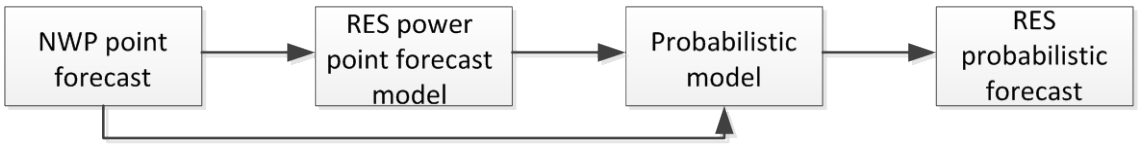

Figure 2.17 – Approach based on NWP point forecast

Other approach for determining the probabilistic forecast is to produce ensembles. This method is different from the previous: instead of a spot forecast an ensemble of forecasts is provided. There are, fundamentally, two methods: one consists on different runs of a NWP model with different initial conditions or different numerical representation of the atmosphere, the other consists on using a different NWP modeling, or different forecasts made at different times [115],[116]. Basically, there are three different methods to attain the probabilistic forecast from NWP ensembles, the “filtering approach”, the “direct approach”

and the “dimension reduction”.

In figure 2.18 is shown the filtering approach. After the knowledge of the NWP ensembles, it is done the conversion to wind power ensembles. If the ensembles are resultant from the perturbation of a single NWP model, only one conversion model is generally considered, since the ensembles may be considered, in general, indistinguishable. Otherwise, in the case of different NWP modeling or different forecasts models made at different times, it is used one conversion model for each ensemble member.

Figure 2.18 – Filtering approach

The output values of conversion models must be calibrated by a post-processing method in order to convert the uncelebrated power ensembles into probabilistic forecasts [1].

In figure 2.19 and 2.20 the direct and dimension reduction approaches are respectively shown. As in the case of figure 2.17, in the direct approach the probabilistic model can be fed directly with NWP outputs. However, in this case, it is used an ensemble instead of a single spot forecast. The main shortcoming is the increase of model complexity (when the number of input variables is big) without remarkable increment of results, even with the growth of sample number [1].

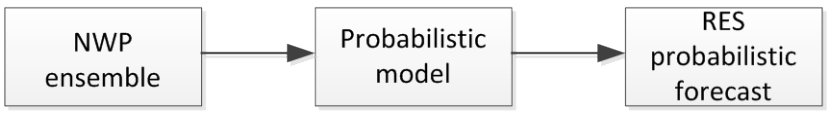

Figure 2.19 – Direct approach

To reduce the complexity and transform it in a more tractable problem, a dimension reduction approach can be done before feeding the probabilistic model, as depicted in figure 2.20. In this case, the number of ensemble members can be reduced by aggregation or converting the ensembles into two values (mean and variance, for instance).

Figure 2.20 – Dimension reduction approach

2.10 Uncertainty models

As explained above, despite the advances in power forecast, there always are associated errors which depend of the resources that are forecasted, the prediction models, forecasting horizons and extreme conditions. The uncertainty created by these errors has a great impact on power systems scheduling since the forecasted values at the beginning of the scheduling process can be quite different from those in the operation periods. In a traditional and conservative point of view, generally, the uncertainties are compensated using conservative decisions, like over-designing the equipment or overestimating the operational parameters basing them on worst-case of the uncertainty parameters. This approach, though being secure, may lead to significant results' deterioration from the optimization problem. To overcome this situation, more complete uncertainty models must be provided, based on probabilistic forecasts, scenarios or risk indices.

The probabilistic forecasts consist of estimating the future uncertainty of power resource expressed as a probability measure. The power production uncertainty can be described using random variables, which may be expressed by many forms, such as [1],[71]:

- Moments of distributions (mean, variance, skewness, kurtosis);
- A set of quantiles and interval forecasts;
- Probability mass function (*pmf*);
- Probability density functions (*pdf*) or cumulative distribution functions (*cdf*) (parametric and non-parametric).

The use of any of the previous uncertainty representations is a case dependent, which should be determined by the nature of the decision-making problem or by the end user's request.

2.10.1 Moments of distributions

The moments of distributions can be used to represent parametrically the uncertainty in decision-making problems [71]. The moments are an acceptable way to the determination of the expected errors and are widely used due to its simplicity and easy calculation from the data sets. The data is shortened in classes of forecasted power and then the standard deviations are calculated [114]. The drawback of this method is the discontinuity between classes and the parameterization (number of bins and width). On the other hand, the standard deviation by itself does not give any information about the probability of a forecast error falling out within a specific interval.

2.10.2 Quantiles and intervals forecast

The probabilistic forecast based on quantiles is a non-parametric approach which avoids the errors introduced by the wrong choice of a parametric distribution [115]. To introduce the concept of quantile forecast let's consider f_{t+k} as the probability density function of the random variable P_{t+k} as well as F_{t+k} as the cumulative distribution function. The forecasted quantile to look-ahead time $t+k$ done at time t, $\hat{q}^{\alpha}_{t+k|t}$ with nominal proportion $\alpha \in [0,1]$ can be defined as $\hat{q}^{\alpha}_{t+k|t} = \hat{F}^{-1}_{t+k|t}(\alpha)$ [71],[112]. When a single quantile forecast $\hat{q}^{\alpha}_{t+k|t}$ with nominal coverage α is defined, it only gives the information that the random variable P_{t+k} has a probability α of being less than $\hat{q}^{\alpha}_{t+k|t}$. As such, it is not given any information concerning any confidence interval. However, with more than one quantile it is possible creating confidence intervals (or prediction intervals) $\hat{I}^{(\alpha)}_{t+k|t}$ bounded by the forecasted quantiles, as shown in equation (2.64), [5],[112],[116] and [117].

$$\hat{I}^{(\alpha)}_{t+k|t} = \left[\hat{q}^{(\alpha_l)}_{t+k|t}, \hat{q}^{(\alpha_u)}_{t+k|t} \right] \tag{2.64}$$

These intervals define a range of possible values within which it is projected that observed values p_{t+k} falls with a certain probability. This probability is defined by the nominal coverage (1-α) with α defined within [0,1]. These prediction intervals, centered on the median, are defined by its lower and upper forecasted quantiles, with lower and upper nominal proportions α_l and α_u respectively, and calculated by (2.65) and (2.66) [71].

$$\alpha_u - \alpha_l = 1 - \alpha \tag{2.65}$$

$$\alpha_l = \frac{1-\alpha}{2} \tag{2.66}$$

Generalizing this process and calculating n interval forecasts with various nominal coverage rates, allows the definition of predictive distributions. Thus, a probabilistic forecast made at time t for leading time $t+k$ is given by the set of corresponding 2n predictive quantiles as shown in equation (2.67), or in a compact form in (2.68) [8].

$$\hat{f}_{t+k|t} \equiv \left\{ \hat{q}^{(\alpha_n/2)}_{t+k|t}, \hat{q}^{(\alpha_{n-1}/2)}_{t+k|t}, ..., \hat{q}^{(\alpha_1)}_{t+k|t}, \hat{q}^{(1-\alpha_n/2)}_{t+k|t}, ..., \hat{q}^{(1-\alpha_{n-1}/2)}_{t+k|t}, \hat{q}^{(1-\alpha_n/2)}_{t+k|t} \right\} \tag{2.67}$$

$$\hat{f}_{t+k|t} \equiv \left\{ \hat{q}^{(\alpha_1)}_{t+k|t}, \hat{q}^{(\alpha_2)}_{t+k|t}, ..., \hat{q}^{(\alpha_{2n})}_{t+k|t} \right\} \tag{2.68}$$

In order to show the intervals forecast evolving along the forecasting intervals, some quantile regression techniques can be addressed. There are fundamentally three approaches, namely

linear quantile regression (LQR), Spline quantile regression (SQR) and Quantile Regression Forest (QRF) (which intends to be more robust than the previous) [118]–[120].

Local quantile regression and spline quantile regression model the relationship between the quantile and the explanatory variables as a linear combination of known basis functions (linear or cubic B-splines). This methods provides estimation of one quantile at a time, if several quantiles are required, the procedure has to be repeated for each one [118].

The model for a multivariate linear regression quantile is defined with equation (2.69) or more generically with (2.70).

$$\hat{q}(\tau) = \beta_0(\tau) + \beta_1(\tau) x_1 + ... + \beta_p(\tau) x_p \tag{2.69}$$

$$\hat{q}(\tau) = \sum_{i=1}^{p} \hat{\beta}_i(\tau) x_i + \hat{\beta}_0(\tau) \tag{2.70}$$

The regressor $\hat{q}(\tau)$ can be calculated solving the linear problem (2.71), where x_i are the p explanatory variables and $\hat{\beta}_i(\tau)$ are unknown coefficients depending on τ. The parameter $\rho_\tau(u)$ represents the loss function given by equation (2.72) whose generic progressing is depicted in figure 2.21.

$$\hat{\beta}(\tau) = \arg\min_{\beta} \sum_{i=1}^{N} \rho_\tau\left(y_i - \hat{q}(\tau)\right) \tag{2.71}$$

$$\rho_\tau(u) = \begin{cases} \tau u & u \geq 0 \\ (\tau - 1)u & u < 0 \end{cases} \tag{2.72}$$

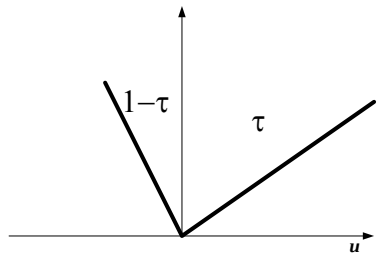

Figure 2.21 – Generic loss function

The other models differ from this regarding the mathematical formulation of regressor α. In figure 2.22 a generic power forecast to 30 hours ahead associated with a set of interval forecasts with 90,70,50,20 and 10% of confidence intervals is shown.

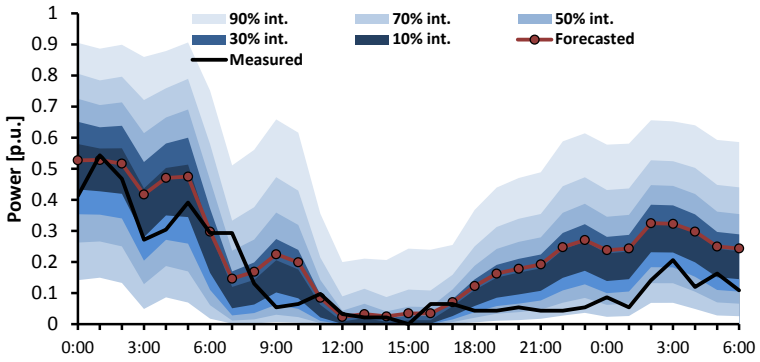

Figure 2.22 – Example of interval forecast

2.10.3 Probability density functions

There are several models of probabilistic estimator models in the literature regarding power forecast with uncertainty.

The classic approach for determining a probability density function is assuming a parametric distribution. The biggest challenge is to find the most adequate parametric function as well as the parameters. Those parameters depend on the explanatory variables and can be hard to calculate. On the other hand the non-parametric approaches have been gaining importance such as KDE [1],[6],[11],[112] and [121].

The KDE is a non-parametric conditional density estimator where no distribution parameters must be assumed. This is the main advantage since it limits the estimation errors connected to incorrect hypothesis on the underlying distribution family. The main drawback of non-parametric approaches is that they require larger data sets than the parametric ones to accomplish equivalent estimations [6].

The estimative of the future conditional density function has a very important role, since it describes the relation between explanatory and target variables. The conditional density estimation can be seen as a generalization of regression, since conditional density estimation aims at obtaining the full probability density function $f_{y|x}(y|x)$, while the regression aims at estimating the conditional mean $E(y|x)$ [25]. This concept is based on the *Nadaraya-Watson* estimator represented by equation (2.73) which allows estimating a random variable Y, when the explanatory random variable X is equal to x [11],[122].

$$f_{Y|X}\left(y\middle|x\right)=\frac{f_{Y,X}\left(y,x\right)}{f_X\left(x\right)} \tag{2.73}$$

Where $f_{Y,X}(y,x)$ is the joint density function of (Y,X) and $f_X(x)$ is the marginal density function of X. In the case of power or load forecast, it consists on the estimation of the future conditional *pdf* of a random variable for each look-ahead time step $t+k$, given a set with N

pairs of samples (p_n,x_n) summarizing all information available up to instant *t*. Each pair consists on a set of explanatory variables X_n and the corresponding value of variable to be predicted P_n. In this process it is assumed explanatory variables $x_{t+k|t}$ are known for each time-step ahead for the desired forecast, resulting in equation (2.74) where p_{t+k} is the power forecasted for look ahead time $t+k$.

$$\hat{f}_P\left(p_{t+k}\left|x_{t+k|t}\right.\right)=\frac{\hat{f}_{P,X\left(p_{t+k},x_{t+k|t}\right)}}{\hat{f}_{X\left(x_{t+k|t}\right)}} \tag{2.74}$$

Since the joint and marginal densities are not known, a nonparametric kernel estimation of the regression function can be used [122].

As renewable power production can depend on several variables (for instance wind speed and direction for wind power forecast, or solar radiation and temperature for solar power forecast) a multivariate KDE can be used [11],[122]. For a given independent and identical distributed multivariate data (X_{1d},….,X_{nd}) from *d* different variables from an unknown multivariate density function *f*, the multivariate KDE is given by (2.75),

$$\hat{f}\left(x_1,....,x_d\right)=\frac{1}{n}\sum_{i=1}^{n}\prod_{j=1}^{d}\frac{1}{h_j}K_j\left(\frac{x_j-X_{ij}}{h_j}\right) \tag{2.75}$$

where *n* is the number of samples, *d* the number of variables and K_j is the kernel function to each variable *j*. In (2.75) h_j is the bandwidth (smoothing parameter) of each kernel around each sample X_{ij} which controls the smoothness of the estimation. The function is placed on each sample point in order to define its contribution to the density. The distribution is obtained by summing up all these contributions. Using *Nadaraya-Watson* estimator, the conditional density is given by (2.76).

$$\hat{f}_{P_{t+k}\left|X_{t+k|t}\right.}\left(p,x\right)=\sum_{i=1}^{n}K\left(\frac{p-P_i}{h_p}\right).\frac{\prod_{j=1}^{d}K_j\left(\frac{x_j-X_{ij}}{h_j}\right)}{\sum_{i=1}^{n}\left[\prod_{j=1}^{d}K_j\left(\frac{x_j-X_{ij}}{h_j}\right)\right]} \tag{2.76}$$

In the case of deterministic forecast, to estimate the conditional mean $\hat{p}_{t+k}=E(p_{t+k}\left|x_{t+k|t}\right.)$ *Nadaraya-Watson* is also used to estimate P_{t+k} as a locally weighted average (2.77).

$$\hat{p}_{t+k}=E\left(p_{t+k}\left|x_{t+k|t}\right.\right)=\sum_{i=1}^{n}\frac{\prod_{j=1}^{d}K_j\left(\frac{x_j-X_{ij}}{h_j}\right)}{\sum_{i=1}^{n}\left[\prod_{j=1}^{d}K_j\left(\frac{x_j-X_{ij}}{h_j}\right)\right]}.P_i \tag{2.77}$$

Due to the non-stationary behavior of wind or changes in available power (number of units), the characteristics may change along the time. Face this situation in [9] and [11] it is proposed a time adaptive model which may be modeled by equation (2.79). Thus the static NW estimator is transformed into a time-adaptive estimator as equation (2.80). This technique allows the introduction of new samples while forgetting older data.

$$\hat{f}_n(x) = \lambda \hat{f}_{n-1}(x) + \frac{(1-\lambda)}{h} K\left(\frac{x - X_i}{h}\right) \tag{2.78}$$

$$\hat{f}_t(p|X = x) = \frac{\lambda_f \hat{f}_{t-1}(x, p) + (1-\lambda_f)\left[K\left(\frac{x - X_i}{h_x}\right) K\left(\frac{p - P_i}{h_p}\right)\right]}{\lambda_f \hat{f}_{t-1}(x, p) + (1-\lambda_f) K\left(\frac{x - X_i}{h_x}\right)} \tag{2.79}$$

The forgetting factor λ controls how quickly or slowly the exponential smoothing adapts to the new data. Other variations to the KDE concept, as evolutionary local kernel regression are presented in [123]. A more complex methodology is proposed in [124] and [125], where the authors use the copula theory in order to model the stochastic dependence between random variables.

2.10.4 Scenarios Power Generation

Following the authors cited in table 2.1, among others [71],[112],[113] and [126], when one is dealing with time dependent problems, such as scheduling of a power production under uncertainty, information is needed about the temporal interdependence of random variables. It is stated that the use of probabilistic forecasts, produced independently for each look-ahead time, cannot provide useful information regarding temporal development of the forecasts. In figure 2.23 a) to d) some examples of the temporal relation between hourly average wind power produced at a time *t* and those produced 1, 3, 5 and 7 hours ahead are shown. These examples reveal that the changes of power production are relatively low up to an hour ahead, growing with the increasing of the horizon. It can be seen that the changes in the power production are not totally randomness, presenting significant temporal interdependence. It means that, when the scenarios of power generation are built, these temporal interdependences have to be modelled. In a simplified form, power generation forecasts from one hour to the ne cannot “jump” from a value to another in a completely random form.

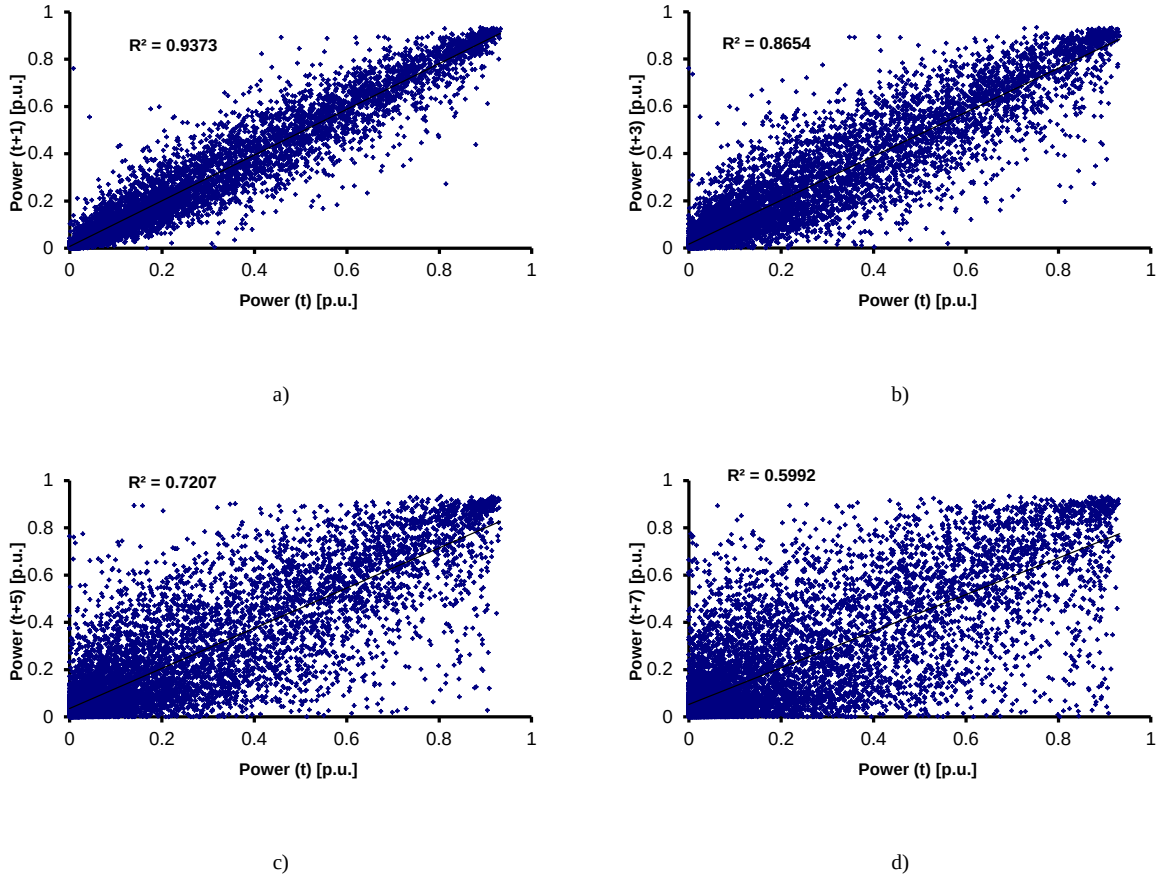

Figure 2.23 – Relation between power values measured at different time horizons

In [112] and [126] it is proposed a Monte Carlo sampling, based on the inverse transform method to simulate random values for wind power by equation (2.80). They consider that the cumulative distribution function for each hour ahead is known, as well as its inverse $\hat{F}^{-1}_{t+k|t}$. In [112] the probabilistic forecast is considered non-parametric and produced with adaptive quantile regression. In the case of [126] they considered a parametric approach defined by a Beta distribution.

$$\hat{p}^{s}_{t+k|t} = \hat{F}^{-1}_{t+k|t}\left(Y^{s}_{t,k}\right) \tag{2.80}$$

The vector $Y^{s}_{t,k}$ is uniformly distributed between 0 and 1 and results from equation (2.81).

$$Y^{s}_{t,k} = F\left(X^{s}_{k}\middle|\mu_k,\sigma_k\right) \tag{2.81}$$

It is introduced a new random variable X^{s}_{k} which must follow a standard normal distribution with zero mean and unitary standard deviation. This value is created by a multivariate Gaussian random number generator, which simulates the forecasting errors behaviour. The

information about the forecasting errors and the interdependence of the errors is concentrated in a covariance matrix **Σ.**

Assuming that the joint distribution of $\mathbf{X}_k$ in equation (2.82) follows a multivariate normal distribution, as in equation (2.83), where $\boldsymbol{\mu}_0$ is a vector of zero's and **Σ**, is the covariance matrix,

$$\mathbf{X}_k = \left(Z_1, Z_2, ..., Z_K\right)^T \tag{2.82}$$

$$\mathbf{X}_k \sim N\left(\boldsymbol{\mu}_0, \boldsymbol{\Sigma}\right) \tag{2.83}$$

results on a positive semi definite matrix with diagonal equal to one. The multivariate normal distribution $\mathbf{X_k}$ is uniquely identified by **Σ**. The challenge in this process is to create X_k (with k = 1,..,K) in order to capture the temporal interdependence of the random variable. For this it is necessary to determine the joint distribution of possible wind power to different look-ahead time t, by the determination of the covariance matrix **Σ**. This way, the random value of each power forecast $\hat{p}_{t+k|t}$ presents a temporal interdependency between forecast intervals, instead of being totally random. Thus, it is more advantageous because it is easier to represent the stochastic process using the joint distribution of a multivariate normal distribution preserving the marginal distribution of P_{t+k}, which denotes the uncertainty of wind power output [113].

In figure 2.24 a) and b) an example of covariance and correlation matrices is shown.

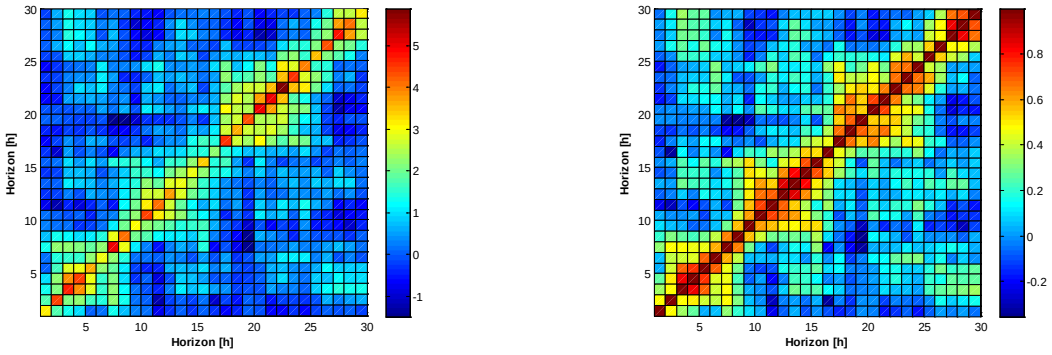

a) b)

Figure 2.24 – Example covariance matrix a) and correlation matrix b)

The covariance matrix and the correlation matrix allow to estimate and track the interdependence structure of prediction errors [112].

In figure 2.25 is shown an example of wind power forecast scenarios for 30 hours-ahead. The initial number of generated scenarios was 1000 and were reduced to 23 following the method described in [5].

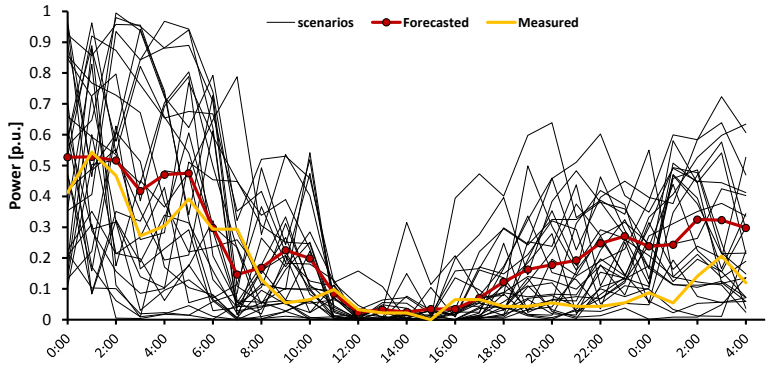

Figure 2.25 – Wind power forecast scenarios (23 scenarios from 1000)

With the creation of these scenarios it is possible to represent the generation ramps' limits between two time steps. This analysis is clearly explained in [112] and [113].

2.10.5 Risk Indices or Skill Forecasting

In the case of power forecasts based on meteorological phenomena, even with adequate and precise forecasting methods, when the weather stability is low, a new source of errors is introduced due to the powerlessness of the forecasting methods to deal with extreme weather conditions. This is the case of small hydro power production when facing wind power under unstable atmospheric conditions or unexpected floods due to snow melting. In the case of solar production, even in sunny days with sparse clouds, the cover of the solar panels during a few minutes can rapidly change the production.

In meteorology environment and following the glossary of meteorology of *American Meteorological Society*, the skill forecasting (SF) or skill score, shown in equation (2.84) , is a measure which relates the forecast accuracy of a certain forecasting model in a comparison with a reference model. The result is a single value which gives an idea about the forecast accuracy of a certain forecast model comparing to some reference model [127].

$$SF = 1 - \frac{SCORE_{Forecast}}{SCORE_{\mathrm{Ref}}} \tag{2.84}$$

A perfect forecast results on a unitary SF, while performances which are equal to the reference model result on a null value of SF. If underperforming, the SF value is negative.

There are, generically, two risk indices, the Meteo-Risk-Index (MRI) [71],[128] and Normalised Prediction Risk Index (NPRI) [71],[129]. From the risk indices it is possible to have a previous hint for the magnitude of the forecasting errors and to do a critical analysis concerning the level of accuracy of the expected forecasts.

The MRI reflects the spread of the available NWP ensemble at a given time, which can be achieved by perturbing the initial conditions of the NWP model or by different NWP models

with equal initial conditions. The same spread can be created with lagged forecasts (same look-ahead time k but done at different t of $t+k|t$) applying different initial conditions to an unperturbed model.

Following [129], the NPRI results from the NWP ensemble forecasts converted to wind power. The spread is computed with a weighted standard deviation of the ensemble members and can be analysed as the ability of each ensemble member to provide information on predictability.

2.11 Summary and main conclusions

This overview gives a general idea about the met challenges in the scheduling with uncertainty. It is visible the interest that the scientific community still has concerning these issues. To fulfill the entire process there are several areas that must be investigated, each one conducting research areas addressed in this overview. The uncertainty associated to the power prediction gave a new interest to the scheduling, namely UC, ED and reliability assessment, introducing new models for the promotion of efficient analysis of the uncertainty. Follow-on from these problem there are some concerns about the need to increase the computational velocity. The reserves assessment created new challenges that have been investigated with good margin for future research.

Concerning the load and renewable power forecasts, the models which produced point forecasts have reached good performances. However, researchers are now focused on uncertainty modelling. Consequently a wide number of researches concerning probabilistic forecasts, scenarios generation and risk indices are available.

However, we were able to conclude that there is still space for research on complete scheduling tools in order to improve the robustness, velocity and computational burden reduction.

CHAPTER 3

Power forecast with uncertainty

Contents

In this chapter are presented some methodologies used in the forecasting of renewable power production, the load and the net load. Comparisons between probabilistic forecasting methods and evaluation criteria are also presented.

3. Power forecast with uncertainty

3.1 Introduction

In order to decrease the thermal generation fuel consumption and, consequently, decrease the power production costs in São Miguel Island, a large amount of renewable energy sources have been integrated. Nowadays, the generation capacity in São Miguel Island is ensured by 1 thermal power plant with 8 units (divided in 2 groups with different rated power), 2 geothermal power plants with 5 units, 7 small hydro power plants with 1 unit each and 1 wind power plant with 9 units. In table 3.1 the rated power to each power source is shown.

Table 3.1 – Rated power of each power source

Source	(# units) total power
Fuel	(4) 28 MW (4) 64 MW
Wind	(9) 9,4 MW
Small hydro	(7) 5 MW
Geothermal	(5) 29,6 MW
Other	(2) < 1 MW

To characterize the production and consumption in São Miguel Island, during 2012 were done hourly average measurements, and load variation between a minimum of 17,3 MW and a maximum of 70,2 MW was registered. The maximum renewable production reached was 43,8 MW. All this renewable production helps to decrease the thermal production during peak load periods but during off-peak periods the system is already saturated with RES power production. This situation leads to the necessity, most of the times, of limiting the wind power output in order to maintain the thermal generators operating above their technical minima. As an example, in figure 3.1 the load and production profile for a week in São Miguel Island is shown.

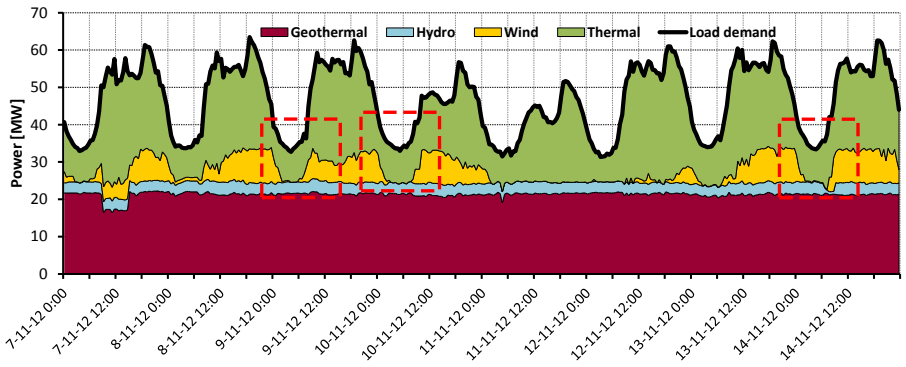

Figure 3.1 – Load/Production profile (one week)

As depicted in figure 3.1 the load follows the traditional consumption profile with clear differences between peak and off-peak periods and between working days and weekends.

In case of production, during almost all the time the geothermal power production is maintained constant and as the base of diagram, with only a slight decrease during a few hours on November 7th morning. As this happened in the peak load period, when more generation is required, it is expectable that this value is linked with some geothermal unit outage. Also, the hydro generation is generally constant. These hydro power plants have very low storage capacity, so the production is only dependent on the inflows and Azores Islands are characterized by frequent rains.

On the other hand, wind generation (as would be expected) presents considerable variability along the week. This cannot be explained only with wind variability. Despite wind generation reach remarkable production during the peak load periods, during the off-peak periods it is reduced almost to zero. This is a clear sign of wind curtailment during off-peak periods (and this is not a particular case of São Miguel Island, in [130] several case studies concerning wind power curtailment are presented). The areas highlighted with red squares seem to be periods were there was wind curtailment, mainly because the reduction of wind power generation was exactly during off-peak periods. Notice that throughout the periods before and after the off-peak period, the wind generation was high. Seeing that in those off-peak periods the wind power generation remains without curtailment, the thermal production should strongly be reduced or even turned-off (which is not acceptable following the conservative approach done by the grid operator and the units' operational limits). For operational security reasons it is mandatory that, at least, two thermal units must be on-line to avoid the complete loss of thermal production due to outages. It means that frequently, especially during off-peak periods, wind power production curtailments were necessary and, in some cases, to set the thermal units to work below their minimum technical limits. In figure 3.2, the hourly average thermal production, as well as the sum of minimum technical limits of 2 units, since 0h00 of December 1st up to 23h00 of December 31st is shown.

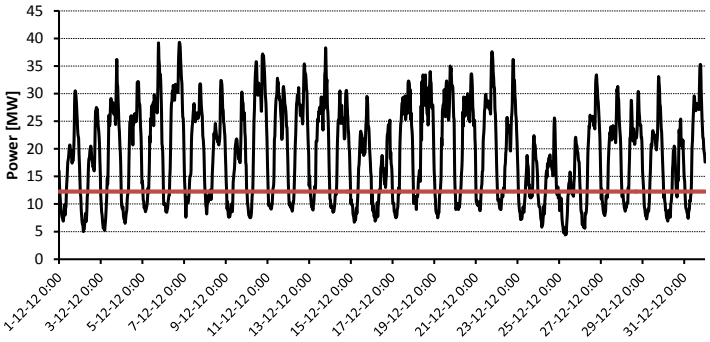

Figure 3.2 – Thermal production and minimum technical limits

In these cases the thermal units were forced to work with poor efficiency and high fuel consumption while renewable sources are wasted. In 2012 those occurrences happened during 745 hours (17% of the year).

As it is shown, during all over off-peak periods the thermal units worked below their minimum limits. To face this problem, it is clear the necessity of an efficient method to forecast load and renewable production in order to know the thermal production necessities. These forecasts, further than the spot values, must incorporate the uncertainty. This thermal production necessity is characterized as *net load* [31],[51] and [131]–[136], and it is calculated by the difference between forecasted load and the sum of forecasted renewable production. This way, the complete forecasting methodology involves the probabilistic forecasting of load and renewable production, in order to obtain the probabilistic forecasted values for the thermal production. It is intended to estimate the future conditional *pdf* of the random variable P_{t+k} for each look-ahead time step $t+k$, given a learning set with N samples summarizing all historical information available up to the instant t.

To develop this process, the data sets used in this work contain hourly average values since 0:00 of January 1st up to 23h00 of December 31st of 2012. The training/parameterization data set contain 7656 hourly average values since 0:00 of January 1st up to 23h00 of November 14th (87,2% of the total) and the test/validation set is composed by 1128 hourly averages values (12,8% of the total) since 0:h00 of November 15th up to 23h00 of December 31st. The NWP forecasts have 1 hour of temporal resolution and the forecast are available at 00h00 for 0h00 up to t+24.

3.2 Choice of forecast models

As discussed in 2.10, in the literature there are several probabilistic estimation models. The choice of the model used in this work is based on analysis and comparison between several approaches available in the literature.

In the case of point forecasts there are several standard error measures and evaluation criteria such as, Mean Error (resulting from systematic error), the Mean Square Error and Mean Absolute Error (resulting from systematic and random errors), Percentage Error, Mean Average Percentage Error (MAPE), and Standard Deviation Errors (SDE) (resulting from random errors). If calculated in function of installed capacity, it results on normalized values. Other error measures can be described as frequency distribution of the errors or coefficients of determination (R^2) [72],[137]. However, evaluating probabilistic forecasts is harder than the evaluation of point forecasts. To evaluate probabilistic forecasts, there are four indicators that are widely used, namely, the reliability, sharpness, resolution and skill score [1],[8],[9],[11],[13] and [138].

The reliability is a measure of the agreement between nominal proportions (forecasted probabilities) and the computed from evaluation samples. The reliability diagrams give the empirical coverage versus the nominal coverages (proportions) for various nominal coverage rates. The nearer the diagrams are to a diagonal, the better the results. In alternative the diagrams can be drawn in function of the deviation from the "perfect reliability" in order to calculate the bias. In this case the deviation of empirical coverage in relation to the nominal one should be null.

This is similar to the use of Probability Integral Transform (PIT) histograms, but in the reliability there is the added value to give the deviation magnitude to the "perfect reliability. The reliability is calculated with equations (3.1) up to (3.4).

$$\xi_k^{\alpha} = \begin{cases} 1 & if\ \ p_{t+k} \le \hat{q}_{t+k|t}^{\alpha} \\ 0 & otherwise \end{cases} \tag{3.1}$$

$$n_{k,1}^{\alpha} = \#\left\{\xi_{i,k}^{\alpha} = 1\right\} = \sum_{i=1}^{N} \xi_{i,k}^{\alpha} \tag{3.2}$$

$$n_{k,0}^{\alpha} = \#\left\{\xi_{i,k}^{\alpha} = 0\right\} = N - n_{k,1}^{\alpha} \tag{3.3}$$

$$\hat{\alpha}_k^{\alpha} = \frac{n_{k,1}^{\alpha}}{n_{k,1}^{\alpha} + n_{k,0}^{\alpha}} \tag{3.4}$$

In (3.1) p_{t+k} is the realization of the variable and $\hat{q}_{t+k|t}^{\alpha}$ the forecasted quantile with the nominal coverage proportion α_i. The result of this equation takes the value "1" if the realization of the variable p_{t+k} hits the forecasted quantile with the nominal coverage α_i and is "0" if it misses it. The number of "hits" and "misses" are counted by (3.2) and (3.3), $\hat{\alpha}_k^{\alpha}$ is calculated by equation (3.4) and gives the percentage of the hits . With the difference between empirical and nominal proportions it is possible to have an idea about the bias of the probabilistic forecasting methods and to measure the quality of the forecasts.

Other indicator is the sharpness, which represents the capacity of the model to forecast extreme values. This criterion evaluates the prediction independently of the observations and gives an indication of the level of predictions usefulness. It measures the probability of forecasting values with probability falling near 0 or 1 instead on 0,5 (which is the dispersion around the 0,5). Following the equation (3.5), the quantiles are gathered by pairs in order to obtain intervals with different nominal coverage rates from narrow intervals up to wider intervals. The sharpness of the predictive intervals is measured by the average interval size, equation (3.6), where $\delta_{t+k|t}^{\alpha}$ is the size of the interval forecast with nominal coverage rate 1-α estimated at time *t* for lead time *t+k*.

$$\delta_{t,k}^{\alpha} = \hat{q}_{t+k|t}^{1-\alpha/2} - \hat{q}_{t+k|t}^{\alpha/2} \tag{3.5}$$

$$\overline{\delta}_{k}^{\alpha} = \frac{1}{N}\sum_{t=1}^{N} \delta_{t,k}^{\alpha} \tag{3.6}$$

With larger intervals it is possible to predict values with large dispersion around the median or even outliers but this does not mean that it is a good prediction. Larger intervals mean that the approach is very conservative and it is not designed to "take risks".

The reliability and sharpness have contradictory results: generally good values of reliability conduce to bad values of sharpness and vice-versa. For this, a trade-off between reliability and sharpness has to be accepted.

The skill score, by equations (3.7) and (3.8), gives information about the model performance in a single measure for a set of *m* quantiles,

$$S_c\left(\hat{f}_{t+k|t}, p_{t+k}\right) = \sum_{i=1}^{m}\left(\xi^{\alpha_i} - \alpha_i\right)\left(p_{t+k} - \hat{q}_{t+k|t}^{\alpha_i}\right) \tag{3.7}$$

$$S_{ck}\left(\hat{f}_{t+k|t}, p_{t+k}\right) = \frac{1}{N}\sum_{t=1}^{N} S_c\left(\hat{f}_{t+k|t}, p_{t+k}\right) \tag{3.8}$$

where p_{t+k} is the realized forecasted, α_i is the quantile proportion, $\hat{q}_{t+k}^{\alpha_i}$ is the forecasted quantile and ξ^{α_i} is the indicator resulting from (3.1). The higher the value, the better the skill score with the maximum value of 0 for perfect probabilistic forecasts [6],[11].

Finally, the fourth indicator used for evaluating probabilistic forecasts is the resolution [6]. This indicator, used in case of intervals forecasting, can be calculated by the standard deviation of the size of the intervals. Similarly to other indicators, the resolution is dependent on the case being studied. A case with less uncertainty (small sharpness) generates less variability in intervals' size. In opposition to the sharpness, as higher is the resolution, the better is the model [6]. In conclusion, sharpness is related to the average size of prediction intervals, whereas resolution is measured with the variability of their size.

These indicators were used by several authors to study the performances of many probabilistic forecasts and will serve as base for the choice of the probabilistic forecasts used in this work. In [1] a comparison between Spline Quantile Regression (SQR), Quantile Regression Forest (QRF) and KDE is done, with the Linear Quantile Regression (LQR) serving as comparison base. Regarding the reliability, it is concluded that the QRF and KDE present equivalent performances whereas sharpness achieved nearly equal values for all approaches. In [6] the KDE and QRF were compared with B-splines Quantile Regression and it is concluded that KDE presents encouraging results of reliability and sharpness towards the remaining techniques. In [9] and [11] it is presented a time adaptive conditional KDE and its

performances are compared with other probabilistic forecasts approaches, namely LQR and SQR in terms of reliability, sharpness and skill score. As a result, KDE showed to have a trend to present a better reliability while quantile regression presents the tendency of better sharpness. The skill score was quite similar to both approaches. Also in [118] it is done a comparison between LQR, Local Gaussian model and KDE, concerning reliability and sharpness. It is concluded that the provided examples did not give any clear preference between methods. It was also stated that regarding simplicity and implementation, the results suggest the KDE estimator as a good choice. Facing these results, it can be concluded that there is not an approach that stands out with clear improvement over the others. Given these conclusions, in this work, the probabilistic forecasting method to define the *pdf* as well as the expected values for each time-ahead forecasts is based on KDE, whose mathematic formulation was presented in point 2.10.3 and from equation (2.73) up to equation (2.77).

3.3 Choice of the Kernel function

When using a KDE approach, the choice of kernel function is the first step. There are several possible functions that can be used for each variable. In the statistics literature are presented several kernel functions namely, Gaussian, Epanechnikov, Biweight, Triweight, Tricube, Cosine, Logistic, Silverman's, among others. Generally, the most broadly used is the Gaussian kernel function, though in [122] it is stated that the Epanechnikov kernel has a slight improvement regarding the Gaussian kernel. In reference [6] it was used the Biweight kernel instead of the classical Gaussian kernel just to decrease the computational efforts. Following [14], and considering the wind power as a bounded variable, both Gaussian and truncated Gaussian kernels were compared, but without any practical benefits. As conclusion, in [1] and [6] it is stated that the kernel function when compared with the selection of bandwidth *h* has a minor impact on the estimation quality.

On the other hand, and particularly to wind power forecast in [9] and [11], it is considered that the choice of the kernel function is a critical issue. The authors proposed different kernels to different forecasting variables, Beta kernel to the wind power (because it can be bounded between 0 and 1 p.u.), Gamma kernel to the wind speed (between 0 and + *Inf*.) and von Mises distribution to wind direction (circular between 0 and 2π).

Subsequently to this analysis it was decided to choose as kernel the Gaussian function; it is widely used in the literature and it is easy to implement. In comparison, the Epanechnikov, Biweight, Triweight, Tricube and Cosine kernel functions demand the standardization of the values between -1 and 1. Moreover, there are no strong signs of the superiority of the remaining approaches.

Nevertheless, it is consensual that after the choice of the kernel function, the choice of smoothing parameter is much more critical. Small bandwidth values lead to an over fitted prediction function, while high values generalize too much [122]. This aspect will be deeply explored in point 3.5.

3.4 Choice of explanatory variables

To forecast load or power generation based on renewable sources it is mandatory to understand which are the explanatory variables and their interdependences and identify those with enough statistical information to characterize the variables to be forecasted. Generally, the variables choice depends on their availability or some practical rules. Following a different approach, in [6] it is proposed the selection of the variables based on information theory, namely the entropy and mutual information. The entropy of a random variable permits to measure the quantity of information contained in that variable while the mutual information allows to quantify the information contained in one random variable about other random variable. As an example of mutual information usefulness, in [6] sixteen potential input variables were analysed in order to investigate the information contained in each one with capacity to describe the wind power. As result, wind speed presented 45% of the information, the wind direction 15% and the temperature below 10%. The remaining variables were considered independent from wind power production. Equation (3.9) represents an unbiased estimator of mutual information.

$$\hat{I}(x,y) = \frac{1}{N}\sum_{i=1}^{N} \log\left(\frac{f_{x,y}(x_i, y_i)}{f_x(x_i).f_y(y_i)} \right) \tag{3.9}$$

In equation (3.9) $f_{x,y}(x_i,y_i)$ is the joint *pdf* between variables X and Y and $f_x(x_i)$ and $f_y(y_i)$ are the marginal *pdf* of X and Y. This can be figured by density functions, calculated using kernel density estimators avoiding the integral formulation and reducing the high integration computation [6].

3.5 Wind power forecast

The wind power production in São Miguel Island is generated from a single power plant with 9 wind generators totalizing 9,4 MW of rated power. An historical dataset of wind power production and wind speed measures is available in the power plant, provided by the grid operator. There are also forecasted values of wind speed, wind direction and air density supplied by Weather Research Forecasting (WRF). Handling the available data and the mutual information values, the explanatory variables hourly average, wind speed and wind direction were chosen in this work. In figure 3.3 the relationship between wind speed and

direction forecasts and wind power measurement are shown. It can be verified that wind power output is strongly linked with wind speed and direction (although with less significance). Nevertheless, there is a significant level of randomness between the wind power and each explanatory variable.

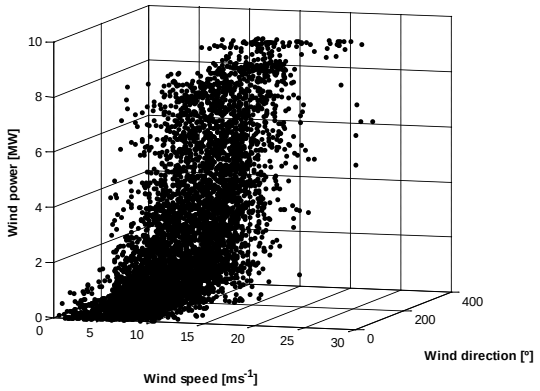

Figure 3.3 – Relation between measured power output and forecasted wind speed and direction

This fact can be easily understood when analysing figures 3.4 and 3.5. In figure 3.4 the measured values of wind power in function of wind speed forecasts are shown.

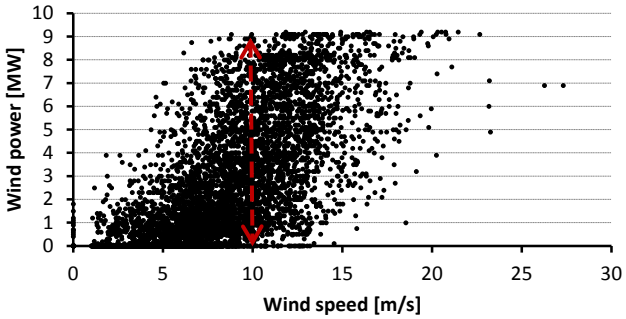

Figure 3.4 – Measured wind power in function of forecasted wind speed

It is clear the uncertainty of wind power associated to the wind speed forecasted. This means that when the wind speed is predicted by the WRF (for instance 10 ms^{-1}) historically, wind power values between zero and the rated power were already were measured. This figure gives a clear idea about the uncertainty associated and confirms that a single point forecast does not give enough information to accurately characterize the forecasted values. The same phenomenon can be analysed in figure 3.5, where the relationship between measured wind power and wind direction forecast is shown. It is verified that the relationship is not as clear as between power and wind speed. Analysing the wind direction dataset, it was concluded that there is no strong predominance of any direction, though being visible some differences between power productions in function of wind direction. These differences occur probably

due to some natural obstacles near the wind farm. Once again, when the wind blows from a forecasted direction there is a remarkable dispersion of the measured power.

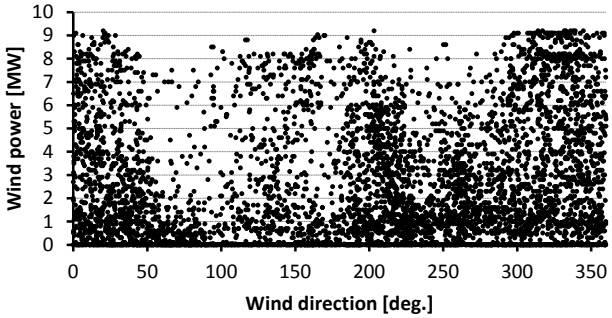

Figure 3.5 – Measured wind power in function of forecasted wind direction

Generically, there are several hypotesis to explain this uncertainty. However, the most common and with more significance are the errors of wind forecasted provided from WRF. The second source of error is the W2P conversion, due to the non-linearity between wind speed and power, which can introduce more or less error depending on the level of wind speed forecasted. It is common that from the rated power up to the cut-off, the error of wind forecasts is minimized due to the steadiness of power production. Between the cut-on velocity and rated power, due to the cubic relation between wind and power, any forecasting error of wind speed potentiates the deviation of wind power forecast. In the case of forecasted wind speed near maximum value, if the real wind speed is higher than the cut-off, the power production is null or, for more recent turbines, suffers a significant reduction in the production, which can introduce remarkable errors.

In the particular case of São Miguel Island, when there is the necessity of wind power curtailment, the errors can be noteworthy, as mentioned in point 3.1 and depicted in figure 3.2. This situation is exhibited in figure 3.6 where wind power production limits indicated by the grid operator, are presented, also the power production for a 168 hours case, from 0h00 of November 15th up to 23h00 of November 21st is depicted

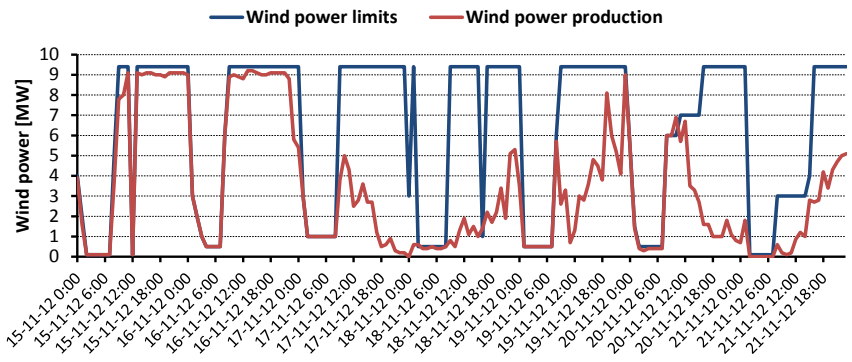

Figure 3.6 – Wind power limit vs. wind power production

During this time period, independently of the available wind speed, the maximum production was several times imposed, forcing curtailment, always in off-peak period. These limits are imposed in order to increase the need of thermal production, decreasing the risk of thermal generators to work below their minimum limits. This is a proceeding which has been done several times since 2012 and it creates a big challenge to the wind power forecast. The curtailment is not an explanatory variable and cannot be modelled for inclusion in the forecasting model. There are also three short periods (at 15th, 17th and 18th) where there were registered limitations without any direct explanation. These cases maybe result from issues with the measurements or wind generator outages. From the above, it is clear that the curtailment process also introduces very significant errors between the wind speed prediction and the power forecast, skewing the data set. In this case it was necessary to do some data pre-processing, gathering the information disclosed by the system operator about wind generation limits in each hour. It was considered that if the power output is equal to the imposed limit, it means that most likely there was wind power curtailment and an error was artificially created. Thus, there was the necessity to filter all these situations in the data set, replacing the wind power curtailed values by "real" values, which should be measured in absence of limitation. This can be achieved computing a theoretic W2P function. In figure 3.7 the relation between measured wind speed and measured wind power is shown. It's clear that there are several wind power values which do not correspond to measured wind. This means that those were wrong measures of wind speed, wind power or power curtailment. Very high values of wind speed are another source of uncertainty, since the installed turbines are equipped with "*software for storm regulation*". Instead of cutting the production to velocities above the maximum, it regulates the pitch angle of the blades in order to reduce the rotation velocity and, consequently, the power production. Without this information, the power forecasts for velocities above the maximum values become hard to forecast.

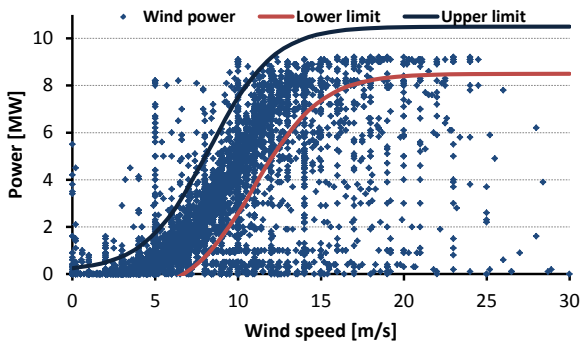

Figure 3.7 – Wind power and outlier filtering

As shown in figure 3.7, to overcome some of these problems, two sigmoid functions were modelled in order to act as filters. With these functions, it was intended to filter "abnormal"

wind power production values. This process must be done with measures instead of forecasted wind speed in order to avoid forecasting and W2P errors.

After filtering the values above and below the limits, with the least square method, it was possible to achieve a "theoretical" relation between wind speed and power production P_w, modelled by equation (3.10),

$$P_w = \frac{P^{\max}}{1+e^{(-0,6.v+5,5)}}, \qquad 0 < v \leq 25 \;\; ms^{-1} \tag{3.10}$$

where P^{max} is the rated power of the wind generators set and v is the measured wind speed in the wind power plant, resulting the "theoretical" power curve shown in figure 3.8. After the "polluted" values are removed from the data set, this power curve and forecasted wind speed allows the projection of the wind power forecasts without curtailment.

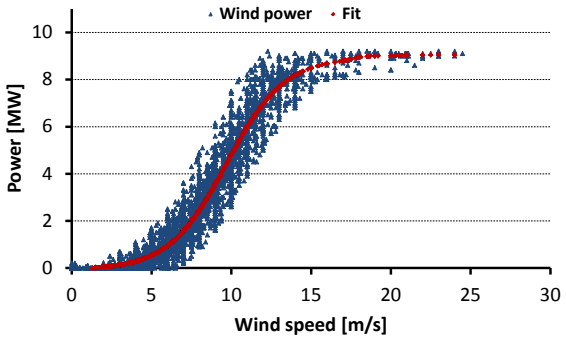

Figure 3.8 – Resulting "theoretical" power curve

Analysing figure 3.9, the theoretical wind power production which results from equation (3.10) and the measured wind power, it is observable that there are notorious differences. This is a clear sign that curtailment introduced remarkable errors in dataset.

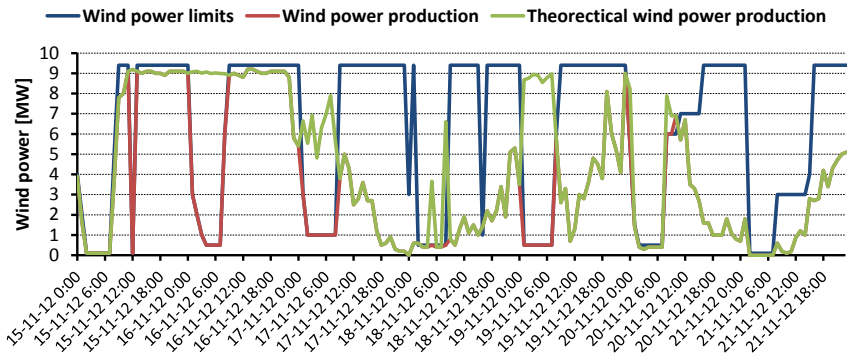

Figure 3.9 – Wind power limit, wind power production and theoretical power production

The theoretical wind power production should be understood as the wind power values that would be measured in the absence of limitation.

Still in figure 3.9, there are two occasions where the wind power production and the theoretical wind power are equal, namely at November 15th and 20th, 2012. In these two cases, beyond the limitation introduced by the grid operator, the wind speed was higher than the maximum allowed by the turbines which led to a natural cut-off. After pre-processing the dataset, it is already possible to do wind power forecasts.

As discussed in points 3.2 and 3.3 the chosen uncertainty estimator were the KDE being the kernel function defined by a Gaussian. In this technique, each Kernel acts as a filter, giving more to the power values registered near the forecasted explanatory variables. Following the equation (2.75), it is possible to calculate the joint and marginal distributions of explanatory variables. To define the conditional probability function of wind power forecasts by the equation (2.76) the wind power values were divided into 52 bins.

As indicated in point 3.3, the shape of the obtained conditional distribution is strongly linked with the choice of the smoothing parameter *h*, which has much more importance than the choice of the kernel function. To illustrate it, in figure 3.10 a) to c) the shape of wind power forecast probability distribution, obtained in function of smoothing parameters of the explanatory variables (wind speed and direction) and wind power are shown.

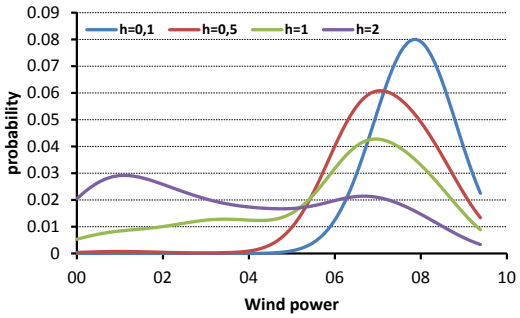

a) Wind speed

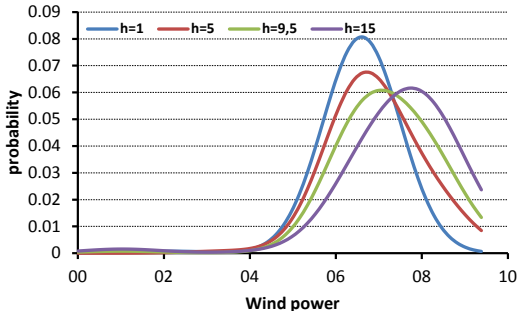

b) Wind direction

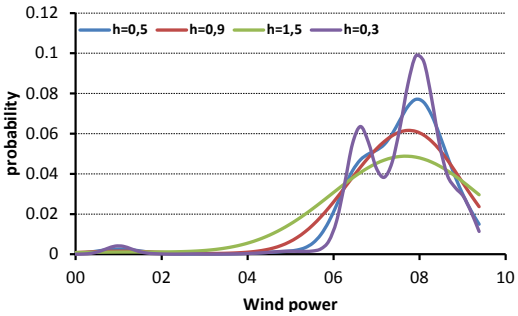

c) Wind power

Figure 3.10 – Probability distribution in function of smoothing parameter *h*

It's clear that the resulting probability distribution can take different shapes only due to the smoothing factor. If *h* is too large the distribution becomes too smooth, not giving enough information about the forecasted values. On the other hand if *h* is too small the distribution becomes very narrow and with a number of unjustified detail [122].

There are several techniques to optimize the values of *h* although many authors use a simple trial-and-error technique or some rules of thumb as the Silverman's rule. More sophisticated approaches can be used, as Leave-One-Out Cross Validations (LOOCV) presented in equation (3.11), [110] and [122].

$$h = \arg\min_{h} \left\{ \frac{1}{N} \sum_{i=1}^{N} \left[Y_i - \hat{f}_{h,[-i]}(X_i) \right]^2 \right\} \tag{3.11}$$

Where (Y_i,X_i) is the i^{th} observation and $\hat{f}_{h,[-i]}$ is the estimated function, omitting the i^{th} observation using bandwidth *h*.

In this work, wind speed and direction smoothing parameters were calculated by LOOCV while wind power was calculated by trial-and-error. In table 3.2 the smoothing parameters obtained are shown.

Table 3.2 – Bandwidth h_j for wind power forecast Kernel's

Variable	h_j
Wind speed	1,7
Direction	10
Wind power	0,8

As example, in figure 3.11 the conditional probability distribution of wind power forecast for forecasted wind speed of 12 ms^{-1} and direction of 247º is shown.

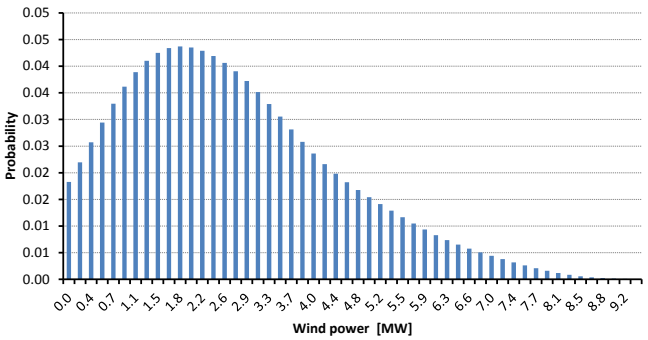

Figure 3.11 – Conditional probability distribution of wind power forecast

For each look-ahead time of the forecasting horizon, knowing the forecasted values of wind speed and direction, it is possible to compute a probability distribution for each time ahead. The point forecast value results from equation (2.77). In figure 3.12 the wind power forecasted and measured, as well as the 80% uncertainty interval is shown (following [13], a nominal coverage between 0,75 and 0,85 seems a good compromise). The forecasts were done at 0h00 up to 24 hours ahead and cover a time horizon of 168 hours.

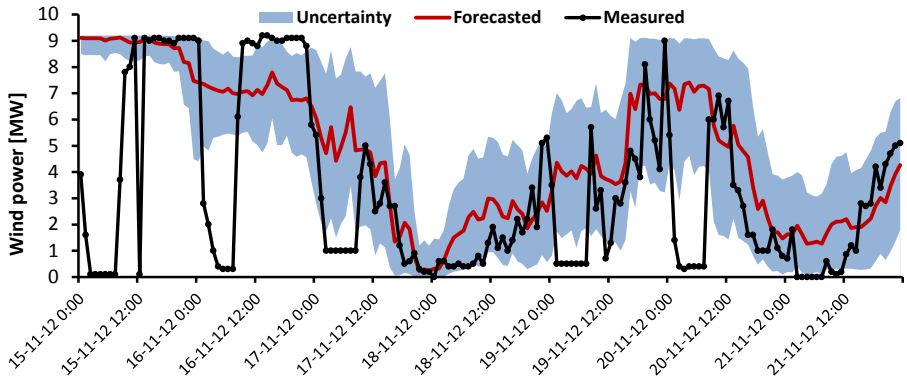

Figure 3.12 – Hourly measured and forecasted wind power generation

Outside the off-peak periods, where there was no limitation in production, the measured values are reasonably covered by the uncertainty interval. A more accurate forecast is particularly hard to do, since there is only one power plant throughout the island consequently there is no smoothing effect resulting from some errors compensation. The forecasting performances indicators cannot be directly applied, since measures do not depend exclusively of the explanatory variables.

3.6 Hydro power forecast

Despite the low rated power, compared with remain generation technologies implemented in São Miguel Island, the hydro power production was modelled and forecasted in order include its contribution to the generation mix. The total hydro production capacity is concentrated in 7 small hydro power plants (SHPP's), with only one unit each. Except one, all present a rated power less than 1 MW. In table 3.3 the rated capacity of each facility is shown.

Table 3.3 – Small hydro power capacity in São Miguel Island

	# units	Power [kW]
CHTN	1	1658
CHTB	1	94
CHFN	1	608
CHCN	1	400
CHFR	1	800
CHRP	1	800
CHSC	1	670

All the presented SHPP have low storage capacity and small watersheds, which means that the hydro production is strongly connected with rainfalls where the SHPP's areas are located. In figure 3.13 the aggregated hourly average power production and hourly average precipitation in São Miguel Island during 2012 is shown.

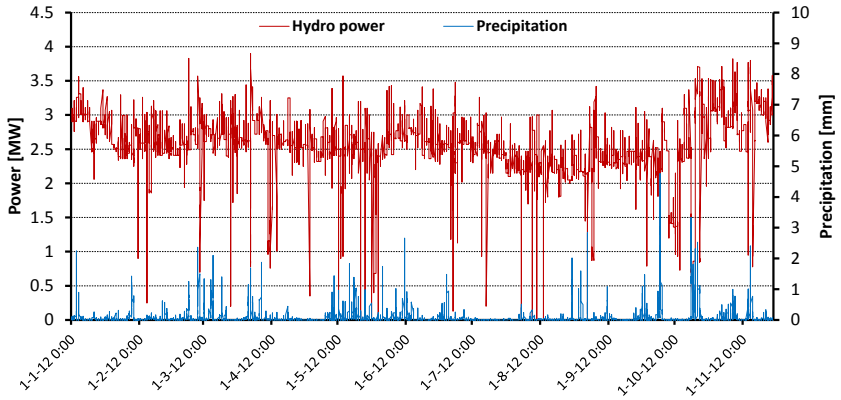

Figure 3.13 – Hourly average hydro power production and hourly forecasted precipitation

Observation of figure 3.13 allows the verification that some variability on power production is inconsistent, which may be related with failures on data acquisition or outages. On the other hand, as discussed in point 2.6.1, the empirical regularities or periodicity are very often masked by noise. As such, it is comprehensible that it is not easy to establish a direct mathematical regression between rainfall and electric power production. These difficulties are related with several issues, such as:

- Frequent phase-shift errors (temporal deviation between the forecasted and real moment of precipitation);
- Delay between the instant when the precipitation occurs and the instant that the hydro-resource arrives to the SHPP reservoirs (which depends of the watershed characteristics);
- The electric energy production is mainly influenced by the operation strategy of the SHPP's (the timing for generation is practically independent of the time of the precipitation).

These reasons suggest the use of a moving average filter in the hydro power production and precipitation, leading to a better understanding of the relationship between both variables, as shown in figure 3.14. The data was filtered by a 24 values moving average centred in an hour *h*, which lead to a smoothing of high frequency noise and possible wrong measures.

Although the aggregated production seems to be relatively constant throughout the year, there are some variations in hydro power production, with a fast increasing during periods with precipitation and decreases in production over dry periods.

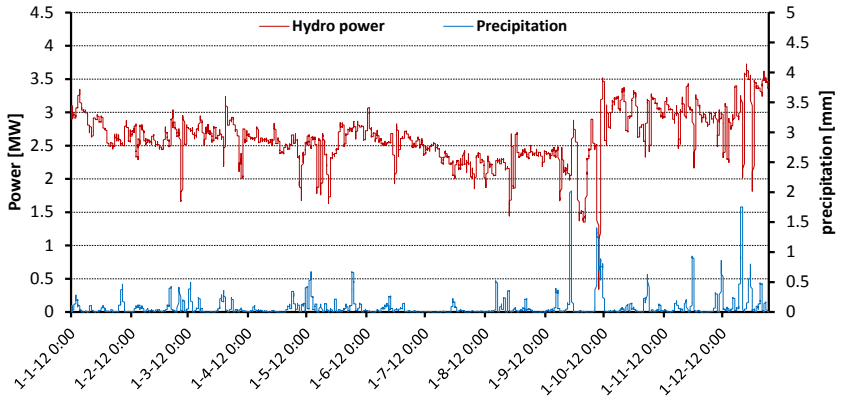

Figure 3.14 – Daily average hydro power precipitation and HPP

In this work the hydro power forecasts are based on the methodology proposed by [96], named H4C, which is composed of three modules. The first is used to estimate the daily average power production of the SHPP, the second takes into account the operation strategy of the SHPP and the third is an assimilation module. The methodology used in this work, uses as inputs variables, past values of power production of SHPP and precipitation as along with forecasted values of precipitation (from an NWP tool).

The first step, in order to create a relation between the forecasted values of precipitation and hydro power production, consists on the introduction of the concept of hydrological power Potential (HPP). The variable HPP represents the level of hydrological potentiality to produce electrical power and is defined by equation (3.12),

$$\hat{H}_h = B\left(H_{h-1} + A.\hat{R}_h\right) \tag{3.12}$$

where $\hat{H}_h$ is the forecasted HPP to the hour *h* and depends on the previous forecasted HPP, H_{h-1}. The parameter *A* is related with the incremental response of the electric power generation to the precipitation (MW/mm/h), parameter *B* is dimensionless and related with the speed of decrease of such generation in dry days (its value must be positive and lower than 1). The variable $\hat{R}_h$ is the forecasted precipitation for hour *h*, in mm/h. In other words, parameter *A* is connected with the incremental power production due to the precipitation, while parameter B represents the decrease of the power production in dry days. As the area of the Island is relatively small, the precipitation is considered uniform all over the island so it was chosen a point near all SHPP and it is considered the average precipitation of the set of the points. Figure 3.15 shows the temporal evolution of the hydro power aggregated production of all SHPP's, as well as its HPP. The parameters *A* and *B* were obtained by the least squares method where the fitness function was the absolute difference between the average power production and the corresponding HPP value.

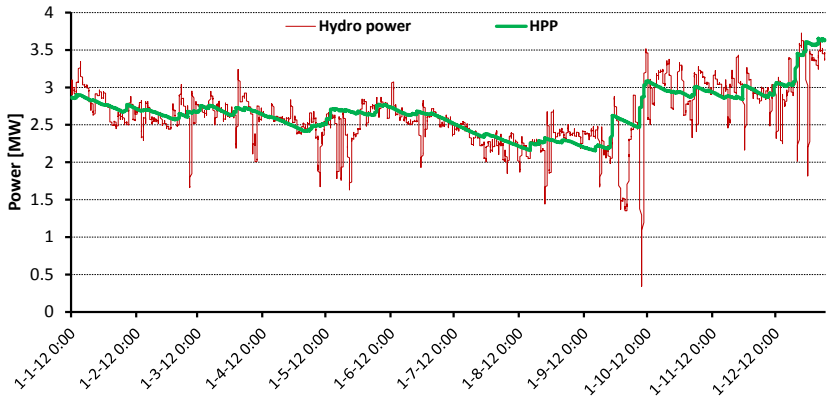

Figure 3.15 – Average hydro power production and HPP

It can be seen that the HPP presents a good adherence to the average hydro power production. Nevertheless, some differences between the evolution of HPP and power production can occur due to nonlinearities associated with the generation limits. Thus, to model this non-linearity, in [96], is proposed the function (3.13) to convert HPP in power production,

$$\hat{P}_{est\_h} = P^{\min} + \frac{P^{\max} - P^{\min}}{\left(1 + e^{\left(-8\frac{\hat{H}_h - h_c}{h_s}\right)}\right)} \tag{3.13}$$

where $\hat{P}_{est\_h}$ is the forecasted power production for hour h, by the explanatory variable H_h, and P^{max} and P^{min} are the maximum and minimum power production, respectively. The parameters h_c and h_s are calculated by the equation (3.14),

$$\begin{cases} h_c = \dfrac{h_o + h_m}{2} \\ h_s = h_m - h_o \end{cases} \tag{3.14}$$

where h_o is the value when HPP reaches the minimum value of power production and h_m is the value when it reaches the maximum. Following on from this process, the parameters used to calculate HPP and hydro power production are shown in table 3.4. These values were optimized by least squares method.

Table 3.4 – Parameters used to hydro power forecast

Parameter	Value
P^{min}	2,18
P^{max}	3,47
h_o	1,855
h_m	3,746
A	0,00855
B	0,99976

In figure 3.16 is depicted the measured hourly hydro power production during 2012 as well the calculated HPP and consequent hydro power point forecasts.

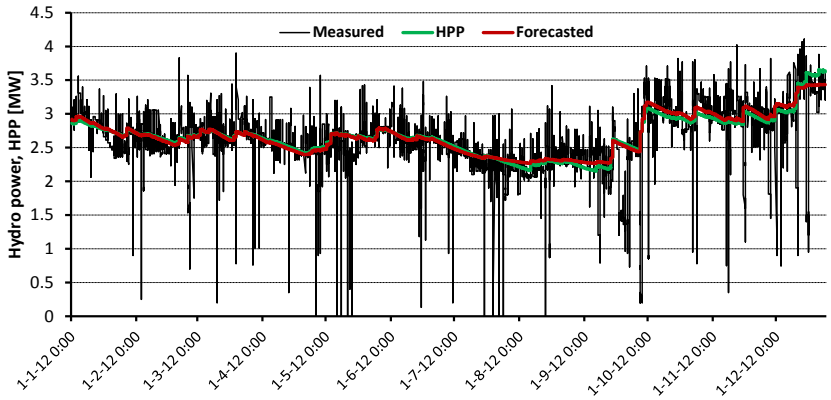

Figure 3.16 – Measures vs hydro power forecasted and HPP

Using equation (3.13), in the presented case, the fitting of power forecast to the measured values is slightly better than with HPP, reaching low MAPE values.

For a better perception about the results that this method is able to reach, a hydro power forecast was done for a period of 7 days (168 hours) divided in frames of 24 hours. To represent the uncertainty, the values of forecasted HPP were used as inputs of a KDE whose bandwidth values are depicted in table 3.5. Once again the bandwidth of HPP forecast was calculated by LOOCV method whereas for hydro power it was calculated by trial-and-error.

Table 3.5 – Bandwidth for hydro power forecast Kernel's

Variable	h_j
Hydro point forecast	0,08
Hydro power	0,1

The results are shown in the figure 3.17, namely the measured and hydro power forecasted with 80% uncertainty interval, as well as the measured precipitation.

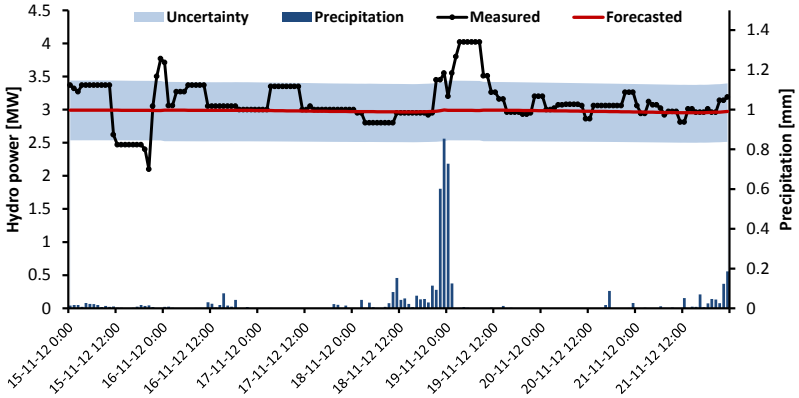

Figure 3.17 – Hourly measured and forecasted hydro power

During this period, the forecasted power production presented small variations and the uncertainty interval remained almost constant. The measured values fall inside the uncertainty interval except on two occasions: On the first, despite the weak rainfall, the big production loss resulted from two power plants outages or measurement failures. Opposed, on the second, there were heavy rains, which substantially increased the power production. With the data from figure 3.17 it is possible to understand that there is a strong correlation between the rainfall and the hydro power.

As in other methods, H4C can be affected by a BIAS error, due to possible errors in the forecasted precipitation which may imply significant deviations in the values of HPP. These deviations can be disseminated over the time, introducing significant forecast errors. The correction of HPP values allows reducing forecasting errors and can be done whenever new data is available. When the measured data of hydro power production is available for hour h (P_h), it can be used to adjust the HPP calculating H_{new_h} by equation (3.15) which represents the new adjusted HPP for hour h[96].

$$H_{new\_h} = h_c - \frac{h_s}{8}.\ln\left(\frac{1}{P_h - P^{\min}}.\left(P^{\max} - P^{\min}\right) - 1\right) \tag{3.15}$$

3.7 Geothermal power forecast

Geothermal power plants are considered as a renewable power source. Though, due to their specificities, they rarely are subject of study. Their implantation has to be done near areas with volcanic activity and as the resource is easy to control the variability is very low (when compared with other RES). In São Miguel Island there are two geothermal power plants namely: *central geotérmica da Ribeira Grande* (CGRG) and *central geotérmica do Pico Vermelho* (CGPV). The power capacity and number of units is depicted in table 3.6.

Table 3.6 – Geothermal power capacity in São Miguel Island

	units	Rated power/unit	Total capacity
CGRG	2	2,9 MW	16,6 MW
	2	5,4 MW	
CGPV	1	13 MW	13 MW

With 26,9 MW of power capacity it is the second source of energy in the island and, as depicted in figure 3.1, it ensures the base of load diagram. However, due to some over dimensioning, during the years, the production never reached the rated power, presenting an average production around 21 MW. In figure 3.18 the geothermal power production on *Ribeira Grande* and *Pico Vermelho*, during 2012 is shown.

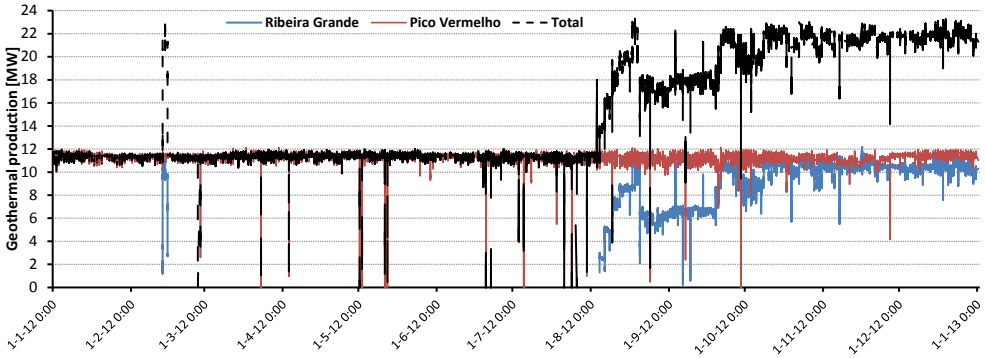

Figure 3.18 – Hourly average geothermal power production all over 2012

Generally, the geothermal power production does not present great variability and it remains relatively constant around the set point power. Exceptionally, during most of the time of 2012 the CGRG remained unavailable and, when it was online, the apparent variability resulted from malfunctions of the power plant. It only restarted the production in August and a more constant production was only achieved by October. Since this date, the higher variability of total production can be explained by unit's outages or errors in data acquisition. As the production is generally constant, the production forecast is based on a set point. In absence of information from the grid operator about the real set point, the spot forecast resulted from a moving average of the previous values. In order to model the uncertainty, the same proceedings as done in previous cases were implemented. The set point forecast is the unique explanatory variable and the bandwidths are shown in table 3.7.

Table 3.7 – Bandwidth for geothermal power forecast Kernel's

Variable	h_j
Point forecast	0,25
Geo power	0,5

In figure 3.19 the forecasted and measured geothermal power as well as the 80% uncertainty interval is shown.

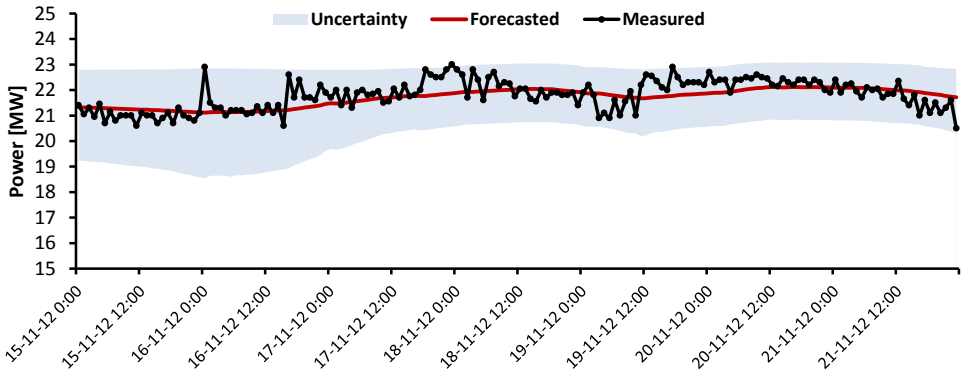

Figure 3.19 – Measured and forecasted geothermal with uncertainty

It is visible that the production present a much lower variability compared with the remaining RES.

3.8 Load forecast

Load forecast is one of the most important information for the scheduling process, being its knowledge fundamental to the UC, ED, security assessment and reserve capacity allocation, whether in deterministic or in stochastic formulations [4]. When the scheduling is deterministically formulated, the load forecasted values are generally provided as *spot* values (expected average demand) being the forecasted errors covered by a certain amount of pre-defined reserve [139]. In the case of stochastic formulation, due to the load (or production forecast uncertainty), the reserves can also be fixed or allocated dynamically in function of uncertainty sources [46],[59],[62],[63].

As in other forecasting process, the main concern is to choose the better explanatory variables which contain relevant information for better behaviour characterization of future load values. These explanatory variables are then used as inputs to a KDE in order to model the stochastic behavior of load forecast.

Generally, the load has a typical behavior all over the 24h of a day, with off-peak periods during the night, beginning to grow early morning up to peak load period during the industry working period and decreasing again by the evening up to the off-peak. Moreover, the load behaviour presents differences between working days, weekends and holidays. In figure 3.20 the load profile along the 24 hours of all days of 2012 in São Miguel Island, is shown. Different values registered for each hour along the day and within each hour are clearly shown. On the other hand, in figure 3.21 the load behaviour for each hour all over the weekends of 2012 is depicted. Clearly the behaviour during weekends is different with regards to amplitude and shape.

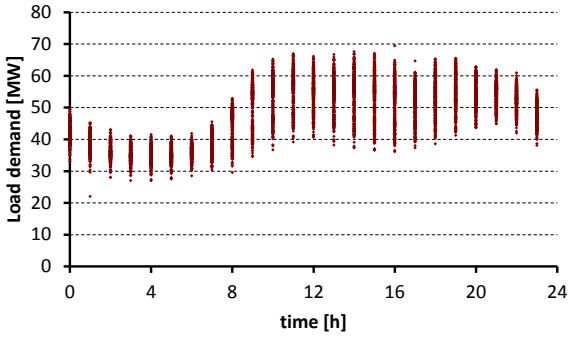

Figure 3.20 – Behaviour of load for each hour all over 2012 (all days)

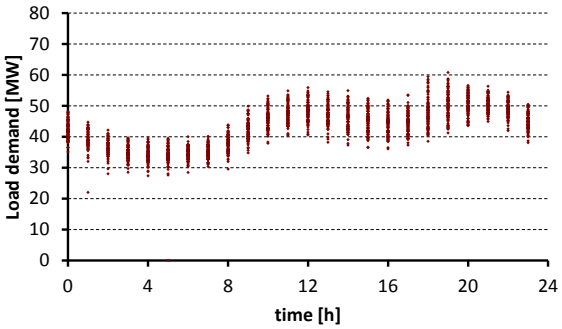

Figure 3.21 – Behaviour of load for each hour all over the weekends of 2012

As such, besides from the hour of the day, one of the explanatory variables should be the day of the week. In figures 3.22 a) to d), the load behaviour for different weeks of 2012 is depicted. It is shown that even for the same days of the week, the profile changes with different weeks along the year.

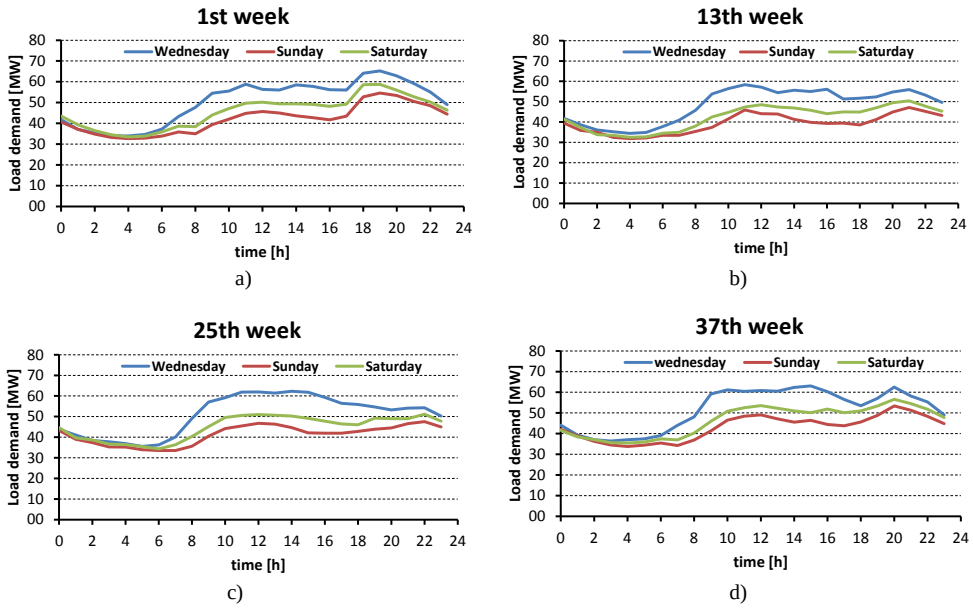

Figure 3.22 – Behaviour of load for different first weeks of 2012

This behaviour depends on many issues such as like weather conditions, summer or winter hours, holidays, school calendar, population growth due to tourism, among others. Following

[110], the weather conditions as temperature, humidity and wind speed are important sources of load variation. Within these meteorological variables, temperature is found to be the most important, being observed that the load/temperature relationship is highly non-linear. Generally, the relationship between load and temperature is characterized by an asymmetric function with the shape of a "V" where the minimum represents the transition point between the need of warming to cooling and vice-versa. To exemplify, figure 3.23 shows the relation between load and temperature in Crete Island, on two different hours (Crete Island is one of the cases studies of SINGULAR project) (*http://www.singular-fp7.eu*).

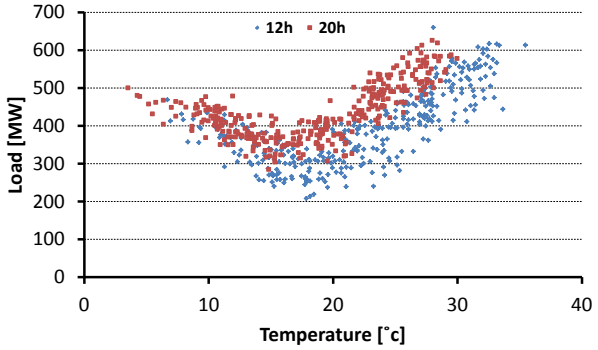

Figure 3.23 – Relation between load and temperature (Crete Island)

Analysing São Miguel Island case, due to the reduced temperature amplitude all over the year of 2012 (10,9ºC up to 24,7ºC) the behaviour of the relation between load and temperature is not so noticeable, as shown in figure 3.24.

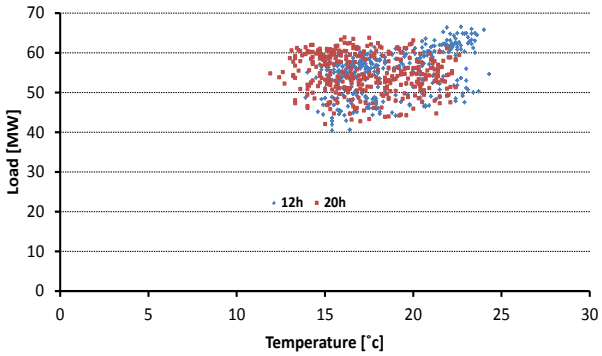

Figure 3.24 – Relation between load and temperature (S. Miguel Island)

However, even with this behaviour, the temperature was considered as an explanatory variable to this case study. As decision, the explanatory variables for the load forecast are the hour of the day, day of the week, week of the year and temperature.

In figures 3.25 a) to d) the probability distribution of load forecast in function of each explanatory variable is shown. Fixing the remaining explanatory variables, allows to study the behavior of the probability distribution for different values of the explanatory variable.

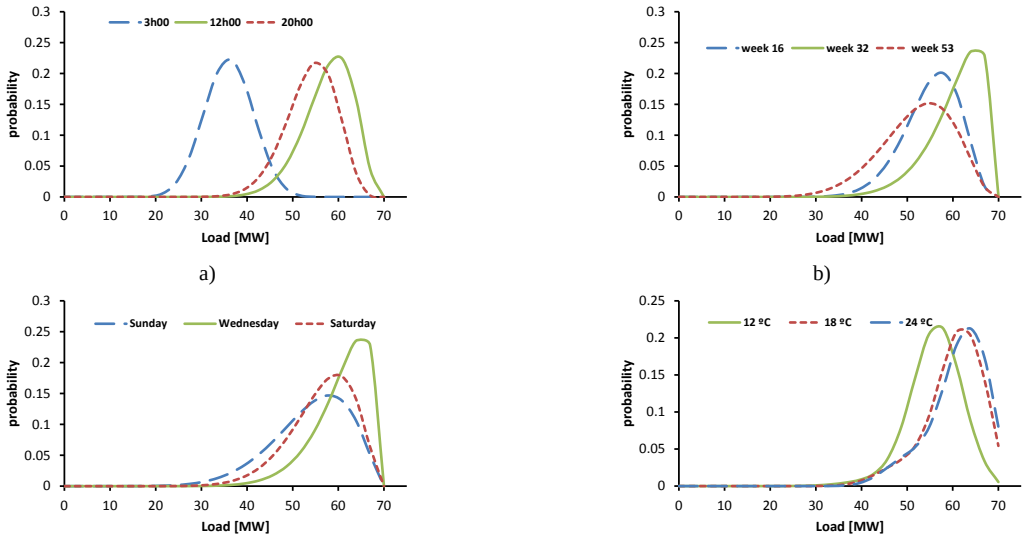

Figure 3.25 – Probability distribution of load
a) Wednesday, week 20, 20º; b)12h00, Wednesday, 20º; c) 12h00, week 32, 20º; d) 12h00, Wednesday, week 32

In figure 3.25 there is a clear influence of the explanatory variables on the probability distribution behavior. In the case of figure b), despite school vacations, as Azores is a touristic destination, the consumption during August was high (week 32). On the other hand, during the year's last week(week 53, due to 2012 to be leap year), there was a lower consumption, due to less tourism, school vacations, some companies closed for balance, among others. In the case of temperature in figure d), there are some differences between the probabilistic distribution for 12 ºC and 18 ºC. From 18 ºC up to 24 ºC the difference is negligible. One explanation is the fact that for 12ºC warming is necessary whereas for 18 ºC and 24 ºC it is not necessary.

As previous approaches, the bandwidth of each Gaussian kernel were calculated and shown in table 3.8, whereas in figure 3.26 the measured and forecasted load values with a confidence interval of 80% are shown.

Table 3.8 – Bandwidth for load forecast Kernel's

Variable	h_j
Hour	0,49
Day of week	0,3
Week	1,5
Temperature	2,2
Load	0,8

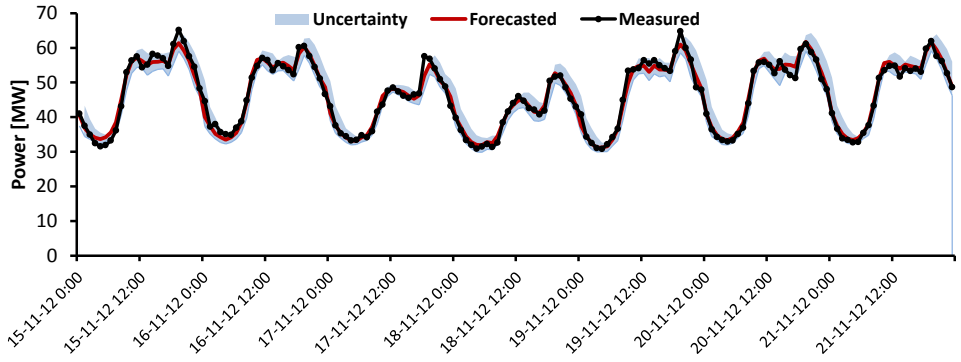

Figure 3.26 – Measured and forecasted load with uncertainty

As shown in figure 3.26 the load forecasting was able to capture the typical profile of the load and describes the differences between working days and weekends. It is noteworthy the fitting of the forecasted values to the measured, as well as the low uncertainty associated.

As specified in point 3.2, there are several methods to access the performances of point forecasts. In this work, to assess the systematic errors the Mean Error (BIAS) will be used, the Standard Deviation Errors (SDE) will be used to assess the random errors and to assess both errors the Mean Absolute Error (MAE) will be applied. Analysis of the performances of uncertainty forecast will be done in chapter 5. In table 3.9 the performances of point forecasts for each RES and load are shown. The values are normalized in function of rated power, or in the case of load, in function of the higher load measured during the week under study.

Table 3.9 – Performances of point forecasts

	Wind	Hydro	Geo	Load
BIAS	-17,1 %	6,5 %	0,4 %	-0,1 %
RMSE	35,0 %	13,4 %	2,2 %	2,2 %
SDE	30,6 %	11,7 %	2,1 %	2,2 %

Analysing the table 3.9 it is possible to verify that there is a noticeable negative mean error in the case of wind forecasts. However, in this case, the comparison is not proper since the power produced is limited and consequently it is natural a negative systematic error. Due to the variability of wind power production, the SDE is also appreciable. In case of hydro power forecasting errors, and due to the substantial deviations, both systematics and random are relatively high. In the case of geothermal and load forecast, random errors are the larger contributors.

3.9 Aggregation of random variables (*net load*)

After the definition of all forecasts (wind, geo, hydro and load) and their respective uncertainties, it is necessary to define the probability distribution of its aggregations. The result is the *net load*, which represents the power value that must be fed by the conventional

power plants. Following [66],[140] and [141], and assuming that all variables are statistically independent (renewable production and load), the probability distribution resulting from the sum (or subtraction) is calculated by convolution. The first step is to calculate the sum of all renewable productions for each look-ahead time step by equation(3.16). It represents the sum between wind production (P_W) and hydro production (P_H), which should later be added with the geothermal production. For obtaining the probability distribution of the *net load*, the probability distributions of load (P_L) and renewable production (P_{RES}) have to be subtracted with equation (3.17). For implementing the convolution represented by equation (3.16) the next steps must be followed:

1. Express the functions P_W and P_H in terms of a variable m (bins);
2. Reflect one of the functions $P_W(m) \rightarrow P_W(-m)$ (in case of subtraction the function should not be reflected as in equation (3.17)) ;
3. Add an offset n that allows $P_W(n-m)$ and slides over the m;
4. Wherever the functions intercept, sum their product; (weighted average of $P_W(m)$ where weighting function is $P_H(-m)$.

$$P\left(W+H=m\right)=\sum_{n=-\infty}^{\infty} P_W\left(W=m-n\right).P_H\left(H=n\right) \tag{3.16}$$

$$P\left(L-RES=m\right)=\sum_{n=-\infty}^{\infty} P_L\left(L=m+n\right).P_{RES}\left(RES=n\right) \tag{3.17}$$

In figure 3.27 are shown the measured and forecasted values of *net load*, as well as the uncertainty which results from the convolution. The interval forecast represents 80% of coverage rate and the point forecasts were calculated algebraically summing the remaining point forecasts. In other words, this is the power value that must be fed by the thermal power units and the generation scheduling must be done based on these forecasts.

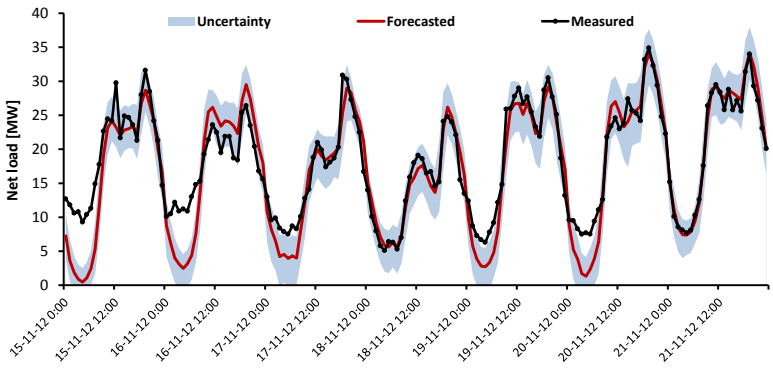

Figure 3.27 – Measured and forecasted *net load* with uncertainty

In figure 3.27 significant differences between the forecasted and measured values of *net load* are visible. These differences occur in periods where there was wind power curtailment, as in

figure 3.12. The obtained errors were 3,1% for the BIAS, 9,8% for the RMSE and 9,3% to the SDE. Despite being higher than the errors of load and geothermal, they are considerably lower than those from wind and hydro forecasts separately. As conclusion, in figure 3.28 it is shown a complete diagram about the forecasting process with the indication of the explanatory variables as well as the forecasting models.

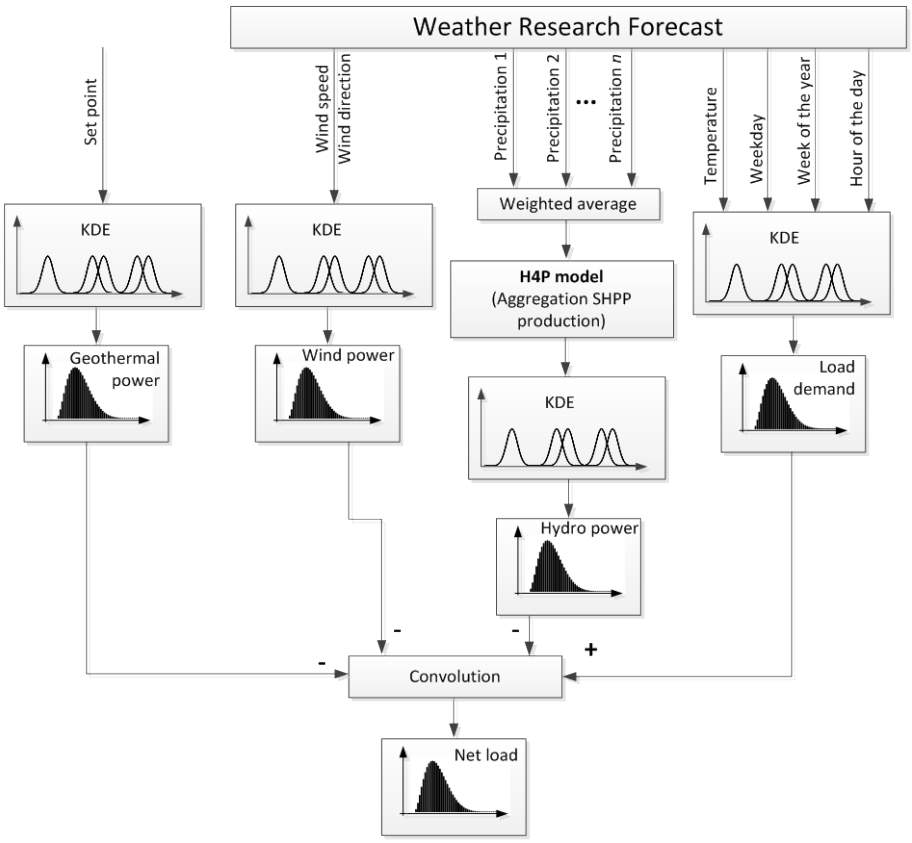

Figure 3.28 – Diagram of the *net load* forecasting

3.9.1 Fitting the probability distribution to a Beta *pdf*

In [126] it is proposed to model the wind power production with a Beta distribution. In this work, and as an extension, it is also proposed the fitting of the *net load* probability to a Beta distribution. This way, it is possible to evaluate the distributions in a continuous and parametric way. The usage of KDE in an initial stage allows dealing with multivariate forecasting problems when having more than one explanatory variable. Later, the probability distribution resulting from the Kernel is fitted to a Beta probability density function. Though being a parametric distribution, the use of the Beta *pdf* could present several advantages such as [20],[22],[114] and [126]:

- The *pdf* is superiorly and inferiorly bounded, which is very important when the random variable is limited, as in the case of power production;

- The Beta *pdf* can be represented only knowing two parameters (α, β);
- The inverse *pdf* is also parametric, being easier to obtain quantiles;
- The *pdf* has great flexibility, showing great fitting capacity.

The Beta *pdf* is defined by equation (3.18),

$$f(x,\alpha,\beta)=\frac{x^{\alpha-1}(1-x)^{\beta-1}}{B[\alpha,\beta]} \tag{3.18}$$

where $B[\alpha,\beta]$ is the Beta function and α and β are the shape parameters, which must be positives. The x is the random variable, which must be normalized in the interval [0,1]. The characteristic parameters α and β of Beta distribution (3.18) are calculated by the moment method as in (3.19) and (3.20),

$$\alpha=\frac{(1-E)E^2}{\sigma^2}-E \tag{3.19}$$

$$\beta=\frac{(1-E)}{E}\alpha \tag{3.20}$$

where E and σ^2 are the first and second moments calculated by (3.21) and (3.22) respectively, with E representing the expected value of the random data set and σ^2 the variance.

$$E=\frac{\sum f(x).x}{\sum f(x)} \tag{3.21}$$

$$\sigma^2=\frac{\sum f(x)x^2}{\sum f(x)}-E^2 \tag{3.22}$$

In figure 3.29 an example of Beta *pdf* applied to a probability distribution example is shown. Its fitting capacity is revealed by the results.

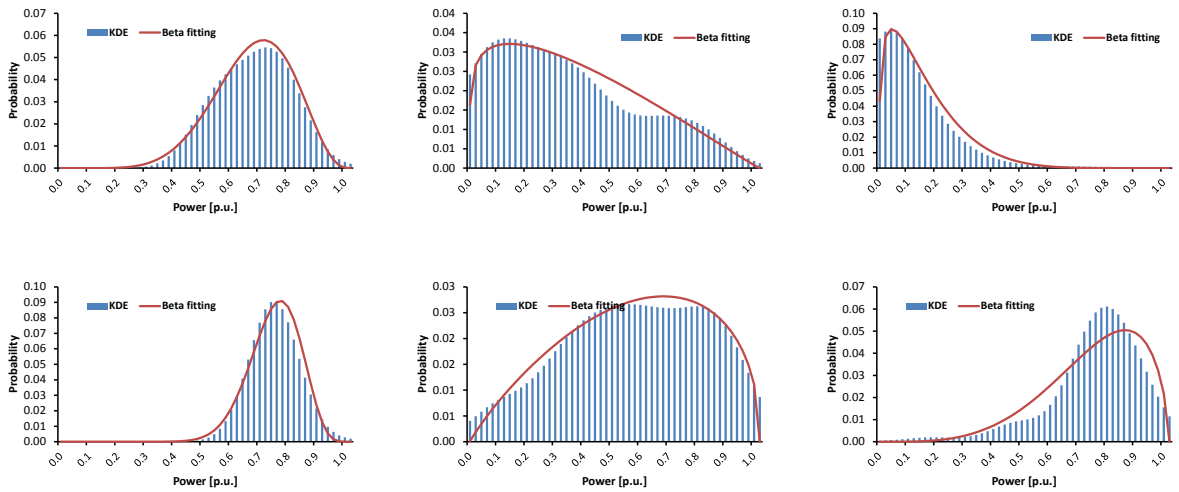

Figure 3.29 – Examples of Beta *pdf* fitting to the probability distributions

These parameters have to be calculated for every forecasted look-ahead time-step, since they are related with the expected value and variance of the distribution. The drawback is the time consuming, which can be reduced choosing a limited kernel as in [6]. In this work, in order to increase the speed, the model was programmed in a Graphic Processing Units (GPU) [142] by the *Smartwatt* team.

3.10 Summary and main conclusions

The necessity of forecasting the load and production to optimize the thermal production in the scheduling process is a clear need. The classical point forecasts are not enough to characterize the uncertainties associated with the load, and furthermore the renewable power, which is strongly characterized by uncertainty. Analysis of challenges and the critical importance of the forecasts was accomplished and the awareness that quality of the forecasts is mandatory is one of the main conclusions. There are several probabilistic forecasting techniques, all with comparable performances, including the widely disseminated technique based on *Nadaraya-Watson* estimator, with conditional and marginal probability densities calculated with KDE. There are several kernel functions, in this work it was chosen the Gaussian function because it is one of the most used.

In this work, wind generation reveals an extra challenge due to the wind curtailment, which is not an explanatory variable, forcing to take several approaches for dealing with it.

The small area of the island and the reduced number of wind power plants and hydro power plants do not allow a real smoothing effect for decreasing the variability. It is also concluded that the choice of the explanatory variables is fundamental to the success of the forecasts and a careful choice of the smoothing factor can strongly influence the shape of the probability distributions. It is shown that convolution allows to aggregate probability distributions in order to calculate the *net load* forecasting.

Finally, the probability distributions were approached to a Beta *pdf* in order to reduce the computational efforts and work with a very flexible and easy to implement parametric *pdf*.

The complete study done in this chapter allowed the creation of a set of tools and proceedings focused in São Miguel Island case, which will support the remaining studies along the work.

As conclusion, a good forecast of the *net load* could give trustable information to the grid operator in order to improve the grid operation. It is also notorious that the quality of the forecasts is essential to the success of the scheduling.

CHAPTER 4

Generation scheduling under uncertainty

Contents

In this chapter a full methodology for the generation scheduling under uncertainty, based on risk assessment is presented.

The concept of equivalent generator is introduced and an original contribution of a metaheuristic in order to solve economic dispatch is addressed.

4. Generation scheduling under uncertainty

4.1 Introduction

Increasing introduction of electric energy production with RES, and mostly those with high variability, has created several challenges to the energy networks operators, especially in the scheduling. This problem is boosted in low power networks, particularly in islands without any connection to continental networks. Large variations on renewable production can introduce stability problems in the network, which can originate generation or load shed and, at limit, black-outs a strong possibility. With this into consideration and for security, scheduling is generally done by a conservative way, with low risk, although sometimes far away from an optimal operation. As such there is the necessity to introduce uncertainty of load/RES in scheduling for achieving a better management of the thermal unit's commitment.

4.2 Generation scheduling under uncertainty

When available, the RES production allows thermal production decrease, especially during the peak load periods. Optimizing the number and the power of the on-line thermal units lowers cost and emissions. On the other hand, an extreme reduction of the thermal committed capacity can lead to a situation where the spinning reserves are not sufficient to handle with great variations of load, renewable production or generation outages. Therefore, due to the uncertainty in load and renewable production forecast, it is sometimes hard to find a completely robust/economic scheduling solution.

As analysed in chapter 2, the stochastic programming is an approach widely used to deal with the generation scheduling under uncertainty applying recourse problems, chance-constrained or robust optimization, with uncertainty described by scenarios [4],[15-16],[31-32] and [57-67]. The scenario-based approach demands a great number of realizations in order to capture the temporal interdependence of the probabilistic behaviour of the uncertainty. One of the main problems of this approach is that it is time consuming to solve all scenarios, being necessary to appeal to some kind of scenario reduction. In all of the approaches presented in the scheduling overview, the UC and the ED are solved for each scheduling scenario, increasing the computational efforts with the crescent number of scenarios. To overcome this problem, this work develops a short-term scheduling approach to be used in insular power grids based on risk assessment, addressing the increase of variability and uncertainty created by RES.

4.3 Description of the methodology

The proposed generation scheduling is designed to minimize the sum of the estimated costs based on risk cost analysis. These costs result from the estimated normal operation cost plus the estimated cost of operating outside normal conditions. It is understood as “abnormal” conditions if there is the necessity of load shed due to the lack of available thermal production or RES curtailment caused by the lack of load. Following [143], decisions have to be made to accept a risk as long as it can be technically and financially justified.

Contrary to widely used scenarios-based approach, in this work it is proposed the probabilistic estimation of costs based on estimation of risk, directly using the probability density function of the random variables. Stochastic programming allows the implicit determination of the reserves, by incorporating explicitly the stochastic nature of the uncertainty, with scenario-base. In the methodology proposed in this work it is also not considered a predefined value for the reserves, since reliability and operational risk minimization are expected to lead to solutions with enough levels of dynamic reserves.

It is intended to evaluate the adequacy of each possible thermal GENeration mix SET (GENSET) in the UC for each hour under a probabilistic *net load* forecast. This way, the need of development of a large number of scenarios, by modelling explicitly the uncertainty of the forecast is avoided. For each hour h of the scheduling period ($h = 1..H$), the ability of each thermal generation mix set (GENSET) to meet the *net load* is verified. The risk of load shed or RES curtailment and thermal production below the technical minimums are used to define the objective function, as well as the probability of the thermal generators operating inside the appropriated ranges. This process is done in an independent way for each hour ahead (single period) being hereafter the probability of unexpected outages and start-up costs incorporated in the problem. An N-1 contingency of thermal units is taken into account and the start-up costs are integrated using a dynamic programming, based on the values obtained from the single period approach. The main objective is to choose the best configuration of thermal units in order to minimize the costs of unit commitment up to H hours ahead.

The proposed methodology is divided into two stages; the first consists of a pre-processing which is done only once (offline) and the second, processed on-line.

In figure 4.1a) a block diagram resumes the procedures of pre-processing stage. The proceeding starts with the determination of the fuel consumption characteristic of each thermal unit. Knowing the specific consumption in function of the power production it is possible to define a mathematical expression.

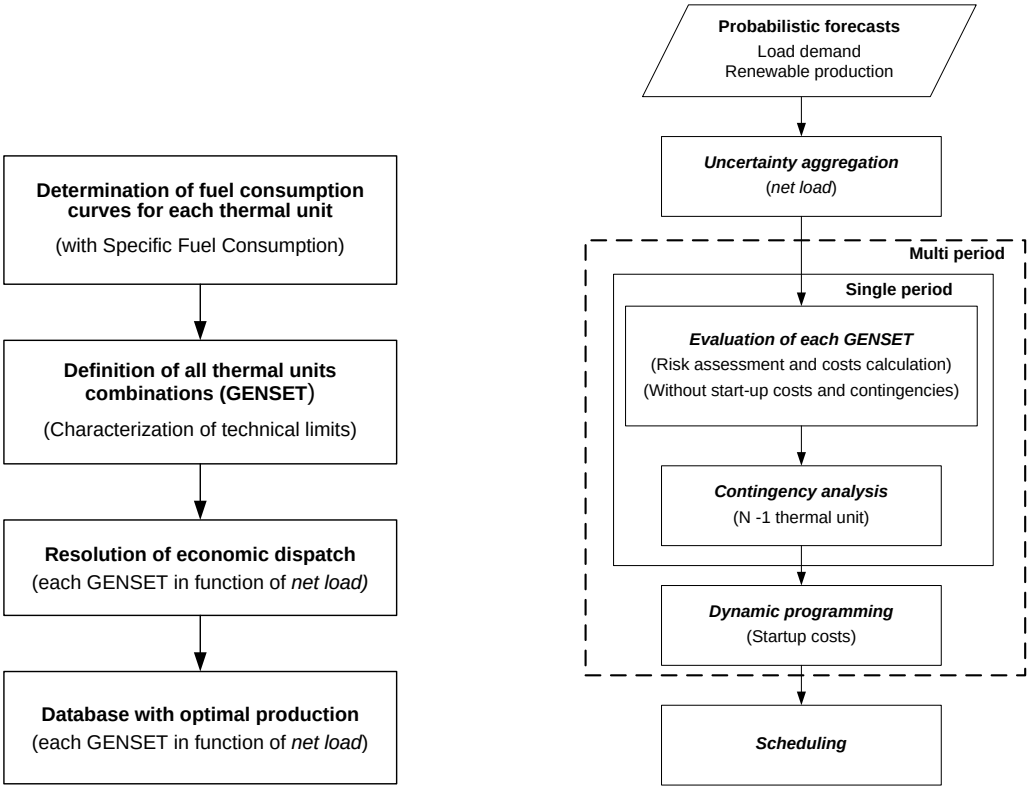

Figure 4.1 – Proposed methodology

Generally, these characteristics are given by the manufacturer and are evaluated by tests. With the set of thermal units it is created a dataset with all possible combinations of thermal mixes, defining a GENSET to each combination, with the respective maximum and minimum limits of generation. For each GENSET it is solved an ED for different values of *net load* allowing to define an equivalent generator. All results are stored in a database.

Although exhaustive and very time consuming, this procedure is done only once, being updated when there is a change in the number or rated power of thermal units.

The second stage procedure, shown in figure 4.1b), is always done whenever the scheduling performed. The load and RES production forecasts are received and aggregated as *net load,* which will be the procedure input. Knowing the probability density function (Beta) of the *net load* for each hour and all combinations of GENSET, it is done the risk assessment of each GENSET to be able to feed the *net load,* and the risk costs of the GENSET are computed. Next, is done a contingency analysis for (*N*-1). These procedures are recalculated to each hour of the scheduling period. At the end it is done a multi-period UC resulting in the solution with lower risk and lower cost with risk embedded.

4.3.1 Thermal generation characterization

In São Miguel Island the thermal power production is ensured by one power plant with eight generators divided in two sets, each one composed by four identical groups (prime mover plus generator) with the same rated power. The units are designated (1-4) for the set of machines with lower rated power while the designation (5-8) indicates the remaining units. The technical operation limits in steady-state of each set of groups are:

$$3848 \text{ kW} \leq P_{G1-G4} \leq 7200 \text{ kW}$$
$$8410 \text{ kW} \leq P_{G5-G8} \leq 16500 \text{ kW}$$

With exception of start-up and shutdown periods (where the fuel is common diesel), the synchronous generators are powered by an internal combustion machines fed with heavy fuel oil. More information concerning the generation units is given in table AI.1 at annex I.
In table 4.1 it is presented the specific consumption for each kind of machines for different values of power production. The production percentage in table 4.1 is calculated relatively to the maximum allowable power in steady-state of each generation unit.

Table 4.1 – Specific consumption for thermal units

% of rated power	Rated power [kW]		Specific consumption [g/kWh]	
	Units 1 - 4	Units 5 - 8	Units 1 - 4	Units 5 - 8
50	3848	8410	222	218
75	5772	12615	213	207
100	7696	16820	212	205

With the values of specific consumption it is now possible to define a continuous function, generally modelled by a second order polynominal. In figure 4.2 is depicted the specific fuel consumption of each type of thermal units in g/kWh.

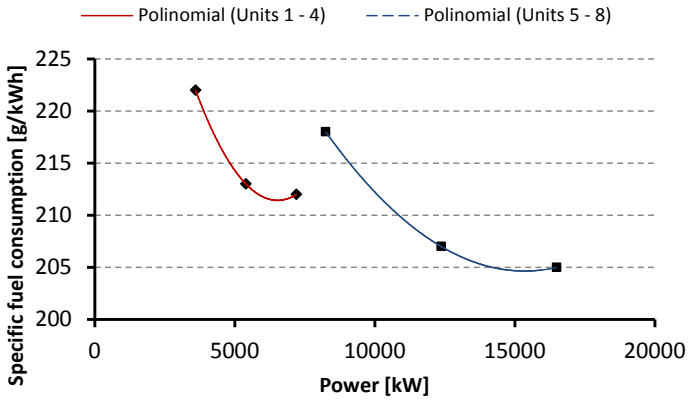

Figure 4.2 – Specific fuel consumption for each type of thermal units

These curves represent the relationship between the specific fuel consumption and the power generation [144]. Examining this figure it is visible that specific consumption is remarkably higher when the units are operating at low power. Considering that the specific consumption continues to increase for even lower power values, this means that, beyond other technical issues, when the units operate below minimum limit, the efficiency is even lower. On the other hand the efficiency increases with the power growth, meaning that the maximum efficiency is near the maximum power.

Given the specific fuel consumption (g/kWh) of each thermal unit and multiplying them by the power production (kW) it is possible to draw the fuel consumption curve (g/h). When the fuel price is known it is possible to create the cost function (€/h), characterizing the hourly cost of producing a certain amount of power. Generally, it is preferable to work with fuel consumption functions instead of cost functions because fuel costs are variable. Following [145], when the thermal units do not present valve-point effects, a second order trend line can be used to represent the fuel consumption values and consequently the generation costs. In figure 4.3 it is shown the fuel consumption for each type of thermal units.

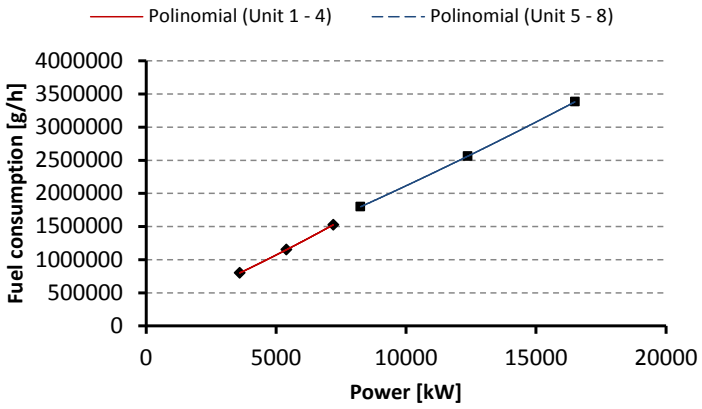

Figure 4.3 – Fuel consumption for each type of thermal units

Applying a second order trend line to the fuel consumption points of figure 4.3 results in equations (4.1) and (4.2), where P_i is the power production of each thermal unit. These functions can easily be converted in currency multiplying them by the fuel cost.

$$FC_{Units1-4}\left(P_i\right) = 3{,}89\times10^{-3}P_i^2 + 160P_i + 172800 \tag{4.1}$$

$$FC_{Unit5-8}\left(P_i\right) = 1{,}70\times10^{-3}P_i^2 + 150P_i + 445500 \tag{4.2}$$

4.3.2 Thermal units combinations (GENSET)

Once known the number of available thermal units in power system, together with minimum and maximum technical limits of each unit, it is possible to aggregate the units by defining all

the available combinations. In this work, as there are 8 units, it is possible to define 255 combinations of thermal production mix and subsequent available power to feed the *net load*. However, as there are only two types of generators, in a restricted analysis of available power, the number of combinations can be reduced to 24 regardless of which thermal unit is on-line, this allows to create a much more tractable data set. For a matter of simplicity and to an easier understanding, the units (1-4) will be represented by G_S (*small power*) and G_B (*big power*). Table 4.2 summarizes the 24 possible unit's combinations.

Table 4.2 – Possible combinations of GENSET's

GENSET	$1G_S$ $0G_B$	$2G_S$ $0G_B$	$3G_S$ $0G_B$	$4G_S$ $0G_B$	$1G_S$ $1G_B$	$1G_S$ $2G_B$	$1G_S$ $3G_B$	$1G_S$ $4G_B$	$2G_S$ $1G_B$	$2G_S$ $2G_B$	$2G_S$ $3G_B$	$2G_S$ $4G_B$	$3G_S$ $1G_B$	$3G_S$ $2G_B$	$3G_S$ $3G_B$	$3G_S$ $4G_B$	$4G_S$ $1G_B$	$4G_S$ $2G_B$	$4G_S$ $3G_B$	$4G_S$ $4G_B$	$0G_S$ $1G_B$	$0G_S$ $2G_B$	$0G_S$ $3G_B$	$0G_S$ $4G_B$
Max [kW]	7 200	14 400	21 600	28 800	23 700	40 200	56 700	73 200	30 900	47 400	63 900	80 400	38 100	54 600	71 100	87 600	45 300	61 800	78 300	94 800	16 500	33 000	49 500	66 000
Min [kW]	3 848	7 696	11 544	15 392	12 258	20 668	29 078	37 488	16 106	24 516	32 926	41 336	19 954	28 364	36 774	45 184	23 082	33 212	40 622	49 032	8 410	16 820	25 230	33 640

In figure 4.4 it is depicted the power production limits of each combination of thermal units. It is observable that, due to a finite set of GENSET's, small variations in the production limits force several changes in the unit commitment. For instance, in the case of $2G_S\_3G_B$, the minimum limit is 32,9 MW and for decreasing this limit to 32,2 MW (a 700 kW decrease), it is necessary to adopt the configuration $4G_S\_2G_B$, which implies 3 manoeuvres. In this particular case two thermal type G_S must by started and one type G_B must be switch off.

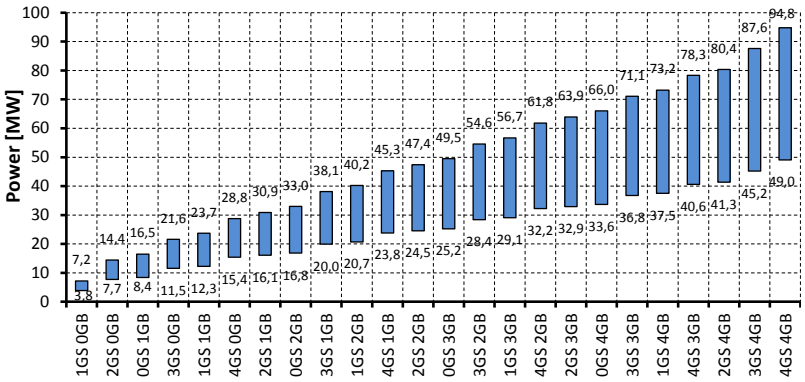

Figure 4.4 – Power production limits of the GENSET's

With the knowledge about of all possible GENSET's makes conceivable the computation of optimal power production for each unit in function of the *net load* that each GENSET is able to produce. Therefore, in this work, it is proposed the establishment of the concept of *equivalent optimal generation unit*. As such, each GENSET is considered as an equivalent

generator with an equivalent cost function. In figure AI.1 of annex I the specific consumption curves of all GENSET's are shown.

4.3.3 Equivalent optimal generation unit

As shown in figure 4.1a) calculation of equivalent generation unit is done offline for each GENSET merely once, and only if there are changes in the number of thermal power plants, units or in the rated power of the units recalculation is done.

There are several methodologies to solve the ED, mainly when the cost functions are continuous and convex [145]. Following figure 4.3 and equations (4.1) and (4.2) it is visible that fuel consumption functions are convex, continuous and differentiable. In case of a GENSET with units of the same type (equal technical limits and cost functions), the power production is divided equitably for all units of the GENSET. If the units have different cost functions an ED must be solved in order to establish the production of each unit. In this work, in order to get a solution to the problem defined by equation (4.3), the ED was solved by the Lagrange multipliers. Later it is proposed a methodology to be used in case of non-convex cost functions.

$$\begin{aligned} \min F_T &= \sum_{i=1}^{N_G} F_i\left(P_i\right) \\ &s.t. \\ & P_i^{\min} \le P_i \le P_i^{\max} \\ & \sum_{i=1}^{N_G} P_i = L_N \end{aligned} \tag{4.3}$$

Minimum and maximum production limits of each unit and the total production to be equal to the *net load* (L_N) requirement are the unique restrictions taken into account in this formulation. For simplicity, the problem is formulated and solved without considering transmission losses, which may be introduced later, together with some changes in the resolution procedure. Equations (4.4) up to (4.7) specify the mathematical formulation for solving the ED of a GENSET, taking for instance the units 4 (G_S) and 5 (G_B), in function of the *net load*.

The Lagrange function (4.4) is obtained when the equality restriction, equation (4.3), multiplied for an undetermined multiplier λ is added to the objective function [49]:

$$\mathscr{L}\left(P_4, P_5, \lambda\right) = \sum_{i=4}^{5} F_i\left(P_i\right) + \lambda\left(L_N - \sum_{i=4}^{5} P_i\right) \tag{4.4}$$

where $\mathscr{L}$ is the Lagrangian operator and λ the Lagrange multiplier.

The derivative of Lagrange function (4.5) gives the necessary conditions for the existence of a minimum cost operating condition for the GENSET. This happens when the incremental cost rates of all units are equal to some undetermined λ [49].

$$\frac{\partial \mathscr{L}(P_i,\lambda)}{\partial P_i} = \frac{\partial F_i(P_i)}{\partial P_i} - \lambda = 0 \tag{4.5}$$

In order to calculate the most economic production of each unit for each value of *net load*. Equations systems (4.6) and (4.7), resulting from (4.5), can be solved by any linear programming solver.

$$\begin{bmatrix} 2a_4 & 0 & -1 \\ 0 & 2a_5 & -1 \\ -1 & -1 & 0 \end{bmatrix} \begin{bmatrix} P_4 \\ P_5 \\ \lambda \end{bmatrix} = \begin{bmatrix} -b_4 \\ -b_5 \\ L_N - P_4 - P_5 \end{bmatrix} \tag{4.6}$$

$$\begin{bmatrix} P_4 \\ P_5 \\ \lambda \end{bmatrix} = \begin{bmatrix} 2a_4 & 0 & -1 \\ 0 & 2a_5 & -1 \\ -1 & -1 & 0 \end{bmatrix}^{-1} \begin{bmatrix} -b_4 \\ -b_5 \\ L_N - P_4 - P_5 \end{bmatrix} \tag{4.7}$$

Considering the coefficients a_i and b_i from equations (4.1) and (4.2) with *net load* varying between 12258 kW and 23730 kW (limits of the GENSET $1G_S\_1G_B$), several values of fuel consumption and power production were obtained. Regarding the *net load,* in figure 4.5 is shown the power production profile of each unit of the GENSET as well as the equivalent fuel consumption. Fitting the resulting points makes possible the definition of the mathematical functions of each unit production as well as the fuel consumption for each *net load* and it delivers a linear function for the power production and a second order function to the fuel consumption.

In figure 4.5 it can be clearly observed three distinct areas with different power production and fuel consumption functions. For smaller than 15594 kW *net load* values, the minimum production restriction of unit G_4 is activated, remaining its production constant whereas the unit G_5 continues to produce the lasting *net load.* With this, the fuel consumption function is also different. The opposite case happens when the *net load* is higher than 22425 kW. In this case G_5 reaches the maximum production and the remaining load has to be fed by G_4. Between the values of *net load* of 15594 kW and 22425 kW, both units are working inside their production limits. This procedure should be repeated to each GENSET combination and should be done only once and off-line.

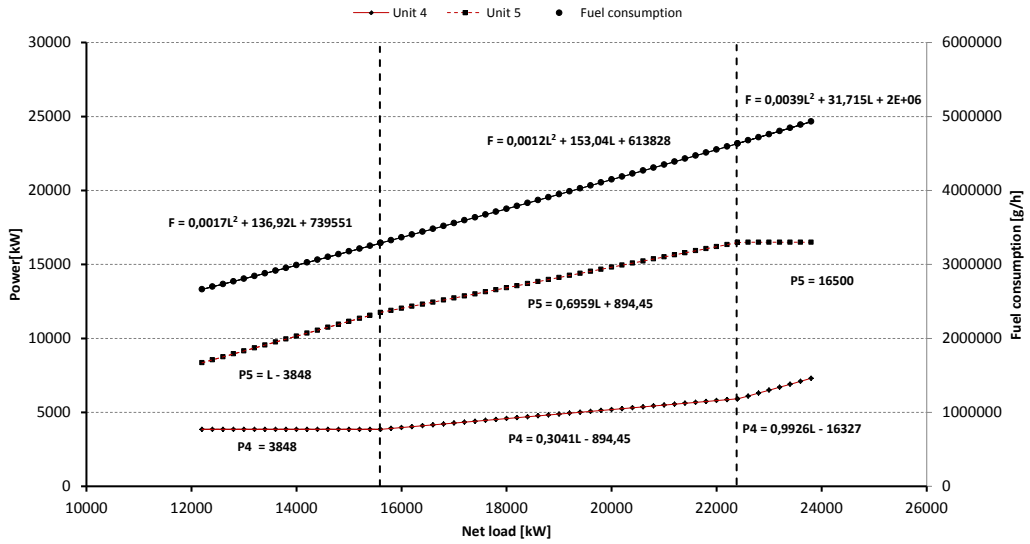

Figure 4.5 – Equivalent optimal generation unit

This technique eases the calculation of the power production that each unit must generate and simultaneously calculates the fuel consumption cost. The process computation time is reduced because it is no longer necessary to run any ED during the on-line scheduling.

In tables AII.5 up to AII.7 of annex II the database with the parameters of fuel consumption for each GENSET together with the parameters for the calculation of the production of each unit are shown.

As shown in figure 4.3 and described above, the fuel consumption and consequently, the cost functions of both type of units were approximated to a continuous and convex second order polynomial, which allowed the use of linear programming for solving the ED. On the other hand, there are cases were the thermal units may neither have continuous or differentiable cost functions as explained in equations (2.14) and (2.15) in point 2.2.2. To deal with these cases, this work proposes a novel metaheuristic optimization technique based on clouds of particles, called Sensing Cloud Optimization (SCO).

4.4 Sensing Cloud Optimization Algorithm

4.4.1 Concept of the algorithm

The developed algorithm can be characterized as a metaheuristic, since it is an iterative algorithm searching for optimal solution candidates; it is based on quality measures, namely the function fitness value. As other meta-heuristics, it does not require any kind of assumption about the problem to be studied.

It presents a stochastic technique based in a cloud of particles with parallel search, without presenting evolutionary strategies; there is no competition between the particles or self-

adaptation to their characteristics, it is a purely cooperative system where all are contributing to achieve the optimum value. During the optimization process, despite the existence (as in other metaheuristics) of random technique at a given moment, there is a high level of determinism in the particles' movements. As such, SCO presents appropriate heuristics characteristics for solving non-convex and non-differentiable constrained optimization problems, using different evaluation performance devices, as well as adjustments in search space in order to accelerate the convergence and avoid getting trapped in local minima. The SCO approach presents a progressive adaptation with efficient movements of the population based on gradient and intelligent concentration of computational effort and it has advantage in speed and accuracy of the convergence.The concept of central particle was defined: it represents the particle trying to find the optimal value, where the remaining particles of cloud spread around according with a Gaussian distribution. These particles will act as sensors "to fill" the search space and give "signals" to the central point for moving into the "right" direction. An exemplificative flowchart is shown in figure 4.6.

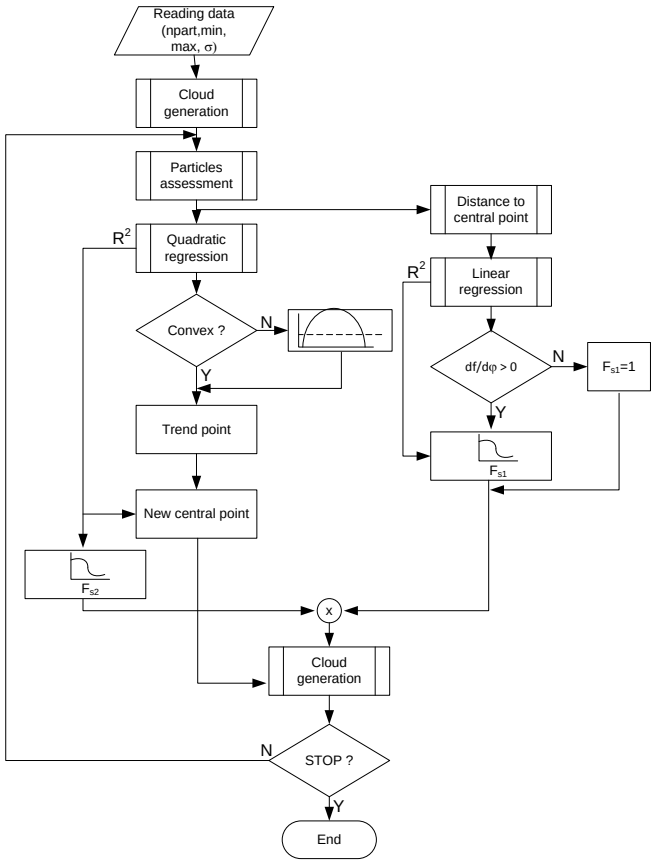

Figure 4.6 – SCO's flowchart

The algorithm can be characterized with two distinct steps: the cloud particles fitness evaluation and a statistical analysis, which allows determining the cloud's direction and dimension for the next iteration. The fitness values of each cloud particle will help the central

point moving in the search space. Concisely, the movement of central point is the response of a weighted mean between the second-order polynomial fit curve, defined by the cloud fitness values, and the best fitness points of the cloud. The weight is defined by the determination coefficient of the second-order polynomial fit curve. An adaptive adjustment of the current search space is performed by two inverted sigmoid functions given by equations (4.15) and (4.17), based in two different assessments, which allows a dynamic increase/decrease of cloud size in each iteration. The first evaluation is focused on the second-order polynomial fit curve and the second is focused on the normalized variation of the distance between the cloud central point and each particle. The complete algorithm is described by the following steps:

Reading data

In the reading data routine, all user inserted initial parameters are converted into the algorithm memory. These parameters include the cloud size, i.e. the number of particles, the minimum and maximum values of each dimension of search space, the initial variance σ^2 of the Gaussian distribution for each dimension and the stopping criteria (maximum number of iterations, goal or maximum number of iterations without improvement).

Cloud generation

The algorithm starts by defining a central point X_q at a randomly position (following an uniform distribution) in the search space, normalized by the *min-max* method, as in equation (4.8),

$$X_{q(i)} = Rnd(0,1).\left(x_{\max(i)} - x_{\min(i)}\right) + x_{\min(i)} \tag{4.8}$$

with $i = 1...N$, where N represents the problem dimension.
Thereafter is created a cloud of j particles ($j = 1\ldots M$) with N dimensions each, following a Gaussian normal distribution with mean centered in the central point and variance σ^2. In the first iteration, this value is defined by the user and in the next it is defined by a self-adaptive process estimation, according to some cloud statistical parameters and activation functions which will be explained ahead.

Particles assessment

Similarly to other heuristics techniques, the fitness evaluation of particles is carried out using parallel search. After the cloud generation, the fitness value of each particle is calculated $f(x_{(i,j)})$ also being registered the best fitness value of all particles $f(x_{b(i,j)})$ together with its

position in the search space $x_{b(i)}$. The originality of this methodology, which differs from other metaheuristics, relies in how the fitness values are addressed.

Quadratic regression

In this step it is appointed the least square method for estimating the second-order regression coefficients which best fit the fitness values of the cloud particles. Even if the search space is not continuous, the use of particles always makes possible the determination of regression coefficients from the fitness of the cloud particles as shown in figure 4.7. This fact shows the added value of the proposed technique. The use of a second order polynomial (in the case of being convex) has also an added value: it always allows the indication of a local or global minimum within the search space giving some information for the point where the central point should be moved.

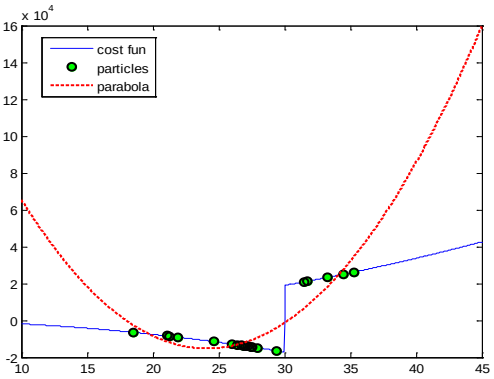

Figure 4.7 – Example of quadratic regression from cloud of particles fitness values (one dimension)

Depending on the search space, the regression may result on a concave function with a central point progressing toward the maximum. In this case the approach must be slightly different; the solution will be discussed later.

Distance to central point

To understand if the central point is near or far from the minimum in the search space, the Euclidean distance between each particle and the central point is calculated by equation (4.9).

$$\varphi_{(i,j)} = \left\| X_{q(i)} - x_{(i,j)} \right\| \tag{4.9}$$

Figures 4.8 a) and b), represent the graph with fitness values in function of the distance $\varphi_{(i,j)}$. In figure 4.8 a) it can be verified that the closer particles are to the central point the lower the fitness, while those farther have worse values. It means that the cloud is above a minimum in

the search space. Thus, the search should be more refined and the cloud should be focused in the search space near the central point.

The opposite case can be observed in b), where there are no clear differences of fitness values between particles close or far from the central particle. Said this, there is no sufficient information and decision capacity for determining if the cloud is far or close to a minimum. If this is the case, the search must be enlarged, spreading the cloud.

This situation can be evaluated calculating the determination coefficient $R^2_{\varphi(i)}$ of a first-order function which best fit the fitness values, as presented in figure 4.8. Simultaneously, the slope is calculated and normalized by equation (4.10), where $\sigma_{\varphi(i,j)}$ represents the standard deviation of $\varphi_{(i,j)}$ and $\sigma_{fitness(i,j)}$ the standard deviation of fitness values.

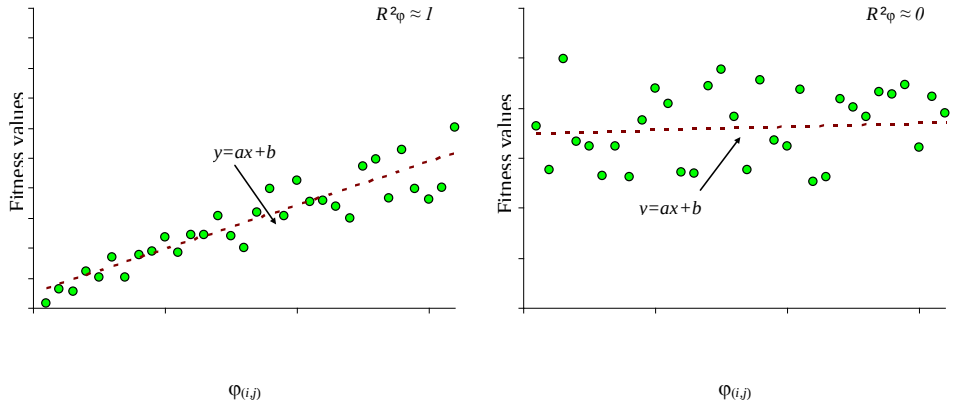

a) cloud over an optimal solution, **b)** cloud far from an optimal solution

Figure 4.8 – Evaluation of $\varphi_{(i,j)}$,

$$\nabla\varphi_{(i,j)} = \frac{\partial f\left(\varphi_{(i,j)}\right)}{\partial\varphi_{(i,j)}}\left(\sigma_{\varphi_{(i,j)}} \Big/ \sigma_{fitness_{(i,j)}}\right) \tag{4.10}$$

The slope $\nabla\varphi_{(i,j)}$ gives additional and important information, if it is high it means that the cloud is over a minimum in a narrow valley, otherwise it is over a wide valley. This information is given for each dimension *i*.

New central point

As mentioned above, if the second-order function defined by the particles fitness values, results in a convex function and if the new central point moves to the parabola vertex, the objective function tends to be equal or lower than the previous iteration. However, it is necessary to evaluate the quality of the given new central point location. This evaluation may be obtained with the calculation the determination coefficient of the second-order trend line,

$R^2_{fitness(i)}$. If the determination coefficient is low the adherence of quadratic fit curve is also low and the vertex may not provide reliable information about a supposed lower value of fitness function in the search space, as it is shown in figure 4.11.

According to these considerations, it is proposed that the position of the new central point must result from an weighted value using the value given by the quadratic fit curve vertex (trend point) and the position of the particle with the best fitness value $x_{b(i)}$, trough (4.11).

$$X_{q(i)} = R^2_{fitness_{(i)}} \left(t_{p(i)} \right) + \left(1 - R^2_{fitness(i)} \right) x_{b(i)} \qquad (4.11)$$

Analysing equation (4.11), when the limit $R^2_{fitness(i)}$ is equal to 0 the central point will move towards $x_{b(i)}$ value, on the other hand, if it is equal to 1 it is concluded that the parabola's vertex indicates the minimum inside the search space, bounded by the limits of each cloud's dimensions. To illustrate this concept, in figure 4.9, it is shown the contour plot of a *sphere* function with two dimensions, whose minimum $f(x_1,x_2) = 0$, it is defined by the coordinates $(x_1,x_2) = (0,0)$. It is also shown the particle cloud, the central point and the best fit particle $x_{b(i)}$. The *trend point* ($t_{p(i)}$) indicates the position defined only by the vertex of the second-order functions related with variables x_1 and x_2 as shown in figure 4.10 and 4.11. In this particular case the *trend point* has fitness values higher than the previous iteration. However, the new central point position is defined from the weighted average between the trend point and the particle with best fitness $x_{b(i)}$ as (4.11), resulting in a lower fitness value. This process allows a better convergence velocity as well as less oscillation.

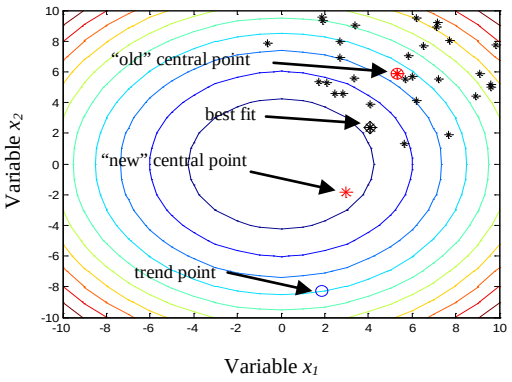

Figure 4.9 – Contour plot of *sphere* function with 2 dimensions

Figure 4.10 and 4.11 show the second-order function, defined for each cloud dimension as well as the vertex (*trend point*) and best particle $x_{b(i)}$. In case of variable x_1 from figure 4.10, the new position results from the average of the *trend point* and the best value, because the coefficient of determination was 0,50.

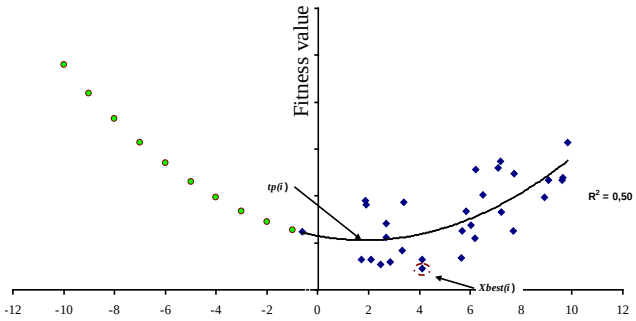

Figure 4.10 – Particle cloud behaviour for the variable x_1

In case of variable x_2 the determination coefficient has an important role, giving more weight to the best fitness particle than to the vertex of the function, making the new central point to move to a coordinate close to the minimum.

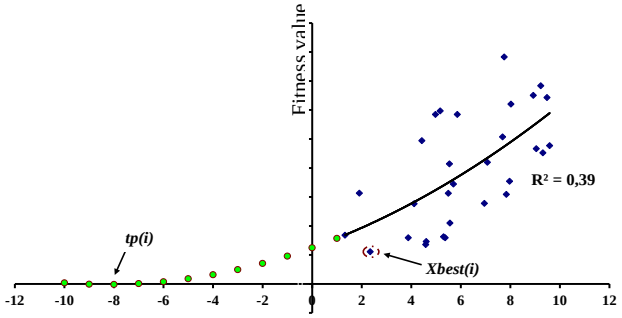

Figure 4.11 – Particle cloud behaviour for the variable x_2

Depending of the function to be optimized and the search space covered by the cloud, the second-order fitness function could be concave indicating a maximum instead of a minimum. In this case it is necessary to calculate the trend point in order to ensure that the central point continues to move towards a minimum. This is done calculating the roots of the concave function subtracted by the best fitness, as indicated in equation (4.12)

$$a_{0(i)} + a_{1(i)} x_{(i)} + a_{2(i)} x_{(i)}^2 - f\left(x_{b(i)}\right) = 0 \tag{4.12}$$

Then, the closest trend point $x_{b(i)}$ will be chosen using equation (4.13)

$$t_{p(i)} = \min\left\{\left|x_{1(i)} - x_{b(i)}\right|, \left|x_{2(i)} - x_{b(i)}\right|\right\} \tag{4.13}$$

To prevent a premature convergence into a local optimal and simultaneously to ensure a fast optimum search, the variance of the Gaussian distribution of the particles cloud must be dynamically adapted along the search space.

New cloud generation

After the definition of a new central point position in iteration (*k*+1), the cloud is centred in that point, with new variance values for each dimension *i* calculated by equation (4.14).

$$\sigma_{(i)}^{2(k+1)} = \sigma_{(i)}^{2(k)}.F_{s1(i)}^{(k)}.F_{s2(i)}^{(k)} \tag{4.14}$$

The changing in cloud distribution variance and consequently in the search space results from equations (4.15) and (4.17) represent both inverted sigmoid functions as shown in figures 4.12 and 4.13.

$$F_{s1(i)}^{(k)} = 1 + \frac{\Delta\varphi - 1}{1 + e^{\left(\frac{-8\left(R_{\varphi(i)}^2 - tc\right)}{ts}\right)}} \tag{4.15}$$

As seen in figure 4.12, if the value of $R_{\varphi(i)}^2$ is near to 0, the value of $F_{s1(i)}$ will remain near 1. If $R_{\varphi(i)}^2$ is near to 1 the central point is near to an optimal solution, so the value of $F_{s1(i)}$ will decrease depending from $\Delta\varphi_{(i)}$. This value is dynamic and it is calculated by equation (4.16).

$$\Delta\varphi_{(i)} = \frac{1}{1 + h.\nabla\varphi_{(i)}} \tag{4.16}$$

The slope calculated in (4.10) will define how narrow should be the next cloud, as depicted in figure 4.12. The *h* parameter of equation (4.16) can be used to speed up the search; however, if the value is too high, the search is faster, but not so accurate.

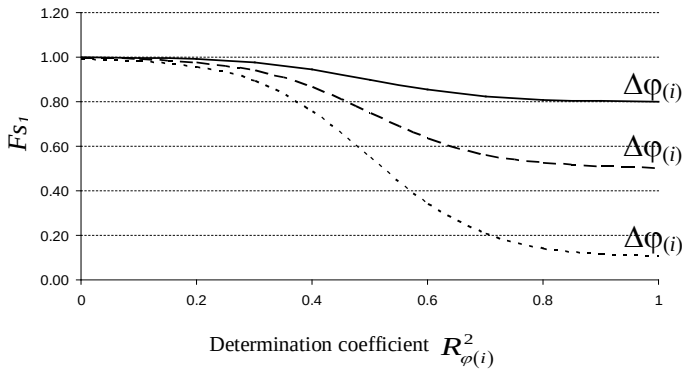

Figure 4.12 – Inverted sigmoid behaviour for different values of $\Delta\varphi$

On the other hand, the value F_{s2} in equation (4.14) intends to expand the cloud's variance. If the coefficient of determination $R_{fitness(i)}^2$, calculated in the quadratic regression, has very low values, it means that the search space delimited by the cloud is quite flat and the cloud should

be increased by a *K* value. Hence, if $R^2_{fitness(i)}$ is approximately 1, low or no variation will be verified in F_{s2}, as shown in figure 4.13.

$$F_{s2(i)}^{(k)} = 1 - \frac{(K-1)}{1+e^{\left(-aR^2_{fitness(i)}+b\right)}} \tag{4.17}$$

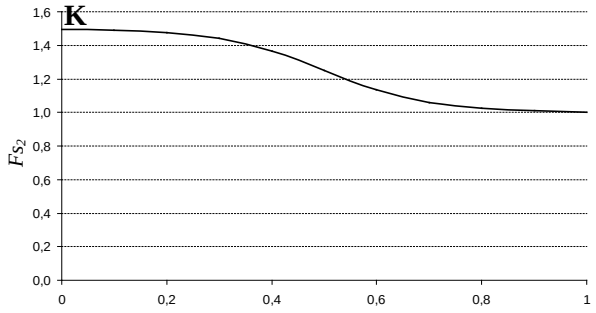

Figure 4.13 – Inverted sigmoid behaviour with *K*=1,5

The variance of the particles distribution to each dimension is given by (4.14), allowing the cloud to increase or decrease the space under search by a dynamic and automatic way.

Stopping criteria

In this algorithm several stopping criteria will be used. One stopping criterion is the definition of a fitness value to be reached, although there are no guarantees that the algorithm will reach the value, leading to a never-ending. On the other hand, the minimum value of the functions is sometimes unknown. For this, a variation is introduced for making the algorithm to run until the fitness value does not change in a certain amount during a determined number of iterations. The objective of this criterion is to decrease the processing time as long as the relation between processing time/results is considered acceptable. However, it can lead to premature stops in flat regions of the search spaces.

In case of none of the above criteria could stop the algorithm, there is a defined maximum number of iterations. This criterion is not a guarantee to find the global or even a local optimum before reaching the maximum of iterations.

In the proposed algorithm all these criteria can be used to stop the algorithm whenever one of them is met.

4.4.2 Evaluation of SCO's performance

To demonstrate the performances and behavior of SCO, among several benchmark functions to test heuristics [146], the *Rastrigin's* function (4.18) was used. Although being continuous, it is also multimodal, presenting several local minima which represent a big challenge to optimization algorithms.

$$f\left(x_i\right) = \sum_{i=1}^{2}\left(x_i^2 - 10\cos\left(2\pi x_i\right) + 10\right) \tag{4.18}$$

To an easier analysis, the function has only two dimensions in the range [-5,12 ; 5,12]. For the present example the chosen central point starting values were (5,0;5,0), close to the search space limits and far away from the global minimum $f(0,0) = 0$ (though in practice the starting values are randomly created). The initial value of variance for each cloud dimension was $\sigma^2 = 0{,}1$. The algorithm parameters and related equations are presented in table 4.3. As stopping criteria, a maximum number of 500 iterations or minimum fitness value of $1e^{-10}$ were chosen (the remaining stopping criteria were not applied).

Table 4.3 – Parameters of the SCO to solve *Rastrigin's* function

Parameter	value	Eq.
nº particles	50	-
h	10	(4.16)
t_c	0,5	(4.15)
t_s	1,0	(4.15)
K	1,01	(4.17)
a	50	(4.17)
b	5	(4.17)

With a small variance it is intended to create a small cloud far away from the global optimum to create particularly hard conditions and validate the search capacity of SCO. After the first iteration and as an example, the cloud dimensions were comprised between [4,1681;5,1098] for variable x_1 and [4,251;5,1172] for variable x_2. In figure 4.14 a) and b), it is shown the fitness value evolution together with cloud variance for each dimension. As seen in figure 4.14 b), the size of cloud greatly varies throughout the progress of the search. With an intentionally small initial cloud ($\sigma^2 = 0{,}1$), the gathered search space information is limited. So, in early iterations, (less than 100 iterations), the cloud expanded, and the variance of variable x_2 reached a value near 6.

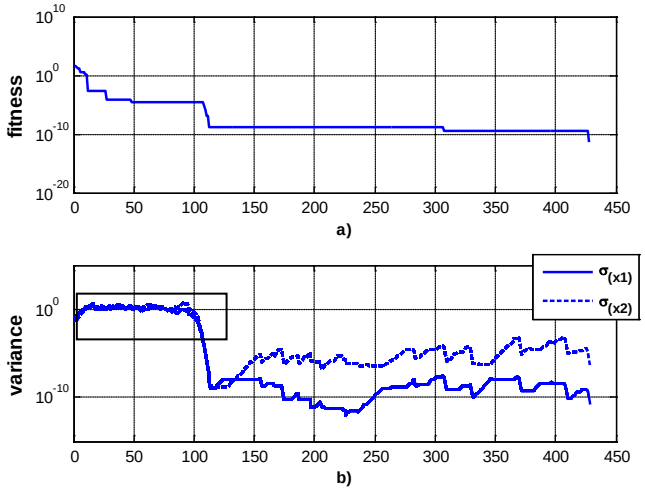

a) fitness evaluation and b) cloud's variance

Figure 4.14 – SCO's performance solving *Rastrigin's* function

This corresponds to an increase of about 60 times the initial variance, as it can be seen in figure 4.15, which shows the magnification of figure 4.14 b).

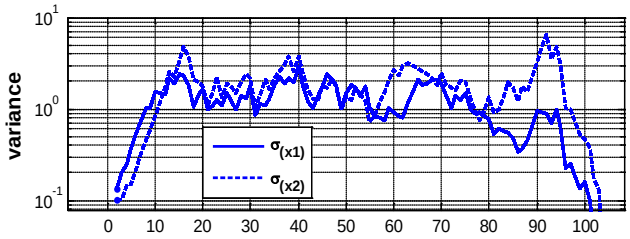

Figure 4.15 – Behaviour of cloud variance

Successive increases in cloud size allowed the perception of the direction to be taken for reaching the near-optimal global. Thus, when the cloud was positioned above the global minimum, the search was refined contracting the cloud to perform a narrow search, with the objective function reaching the value $1e^{-9}$. To reach the goal of $1e^{-10}$, the cloud once again changed its size and shape. Once more, the variance took different values to each dimension separately, until it reached the fitness value of $4{,}93e^{-12}$ and stopped the search. In this case it is clear the behavior of SCO and its capacity to find the minimum of fairly difficult problems with wide search space and large number of local minima.

4.4.3 Evaluation of SCO's in ED

To evaluate the SCO's performances for solving ED, several case studies with non-convex or non-continuous cost functions and non-continuous restriction, as presented in equation (2.14) and (2.15), were tested. To apply SCO to an ED problem, the following 12 steps must be done:

Step 1 Create randomly a central particle $P_{q(i)}$, with i=1..N_G dimensions, (each dimension represents a generation unit) and according to its technical limits, as in (4.19). If there are starting values, then $P_{q(i)} = P_{(i)}^{0}$.

$$P_{q(i)} = rand\,(0,1).\left(P_i^{\max} - P_i^{\min}\right) + P_i^{\min} \tag{4.19}$$

Step 2 Create the remaining cloud with [$N_G \times N_P$] dimensions, where j = 1..N_P particles and i = 1..N_G dimensions normally distributed. The remaining particles are normally distributed, centered in the central particle and with standard deviation $\sigma_{(i)}^{(k=1)}$, as in (4.20).

$$P_{(i,j)}^{(k)} \sim N\left(P_{q(i)}^{(k)}, \sigma_{(i)}^{(k)}\right) \tag{4.20}$$

Step 3 To each cloud's particle $P_{(j)}^{(k)}$, calculate the transmission losses $P_L^{(k)}$ by

$$P_L^{(k)} = \sum_{i=1}^{N_G}\sum_{z=1}^{N_G} P_i^{(k)} B_{iz} P_z^{(k)} + \sum_{i=1}^{N_G} B_{oi} P_i^{(k)} + B_{oo} \tag{4.21}$$

Step 4 Evaluate each particle with (4.22) and retain the best fitness value $P_{(j)BEST}^{(k)}$ position.

$$f_{(j)}^{(k)} = \sum_{i=1}^{N_G} F_i\left(P_{(i,j)}^{(k)}\right) + q\left|\sum_{i=1}^{N_G} P_{(i,j)}^{(k)} - D - P_L^{(k)}\right| \tag{4.22}$$

The fitness function (4.22) has a penalty factor q to decrease the deviation between the power production and the sum of power demand and active losses as in (4.4).

Step 5 Calculate the second-order regression coefficients to each dimension i, $\left[\beta o_{(i)}\ \beta 1_{(i)}\ \beta 2_{(i)}\right]$ and the determination coefficient $R_{q(i)}^{2(k)}$.

Step 6 Verify the convexity of polynomials. If it is convex, then $t_{p(i)}^{(k)} = -b_i \big/ 2a_i$. If not calculate $t_{p(i)}^{(k)}$ by (4.12) and (4.13).

Step 7 Generate new central particle by (4.23) and verify if it fulfils all constrains.

$$P_{q(i)}^{(k+1)} = t_{p(i)}^{(k)}.R_{q(i)}^{2} + \left(1 - R_{q(i)}^{2}\right).P_{(i)BEST}^{(k)} \tag{4.23}$$

If the central particle fulfils all the constraints, then it is a feasible solution (as remain particles act as sensors and are not candidates to a solution, there is no need to satisfy all constrains).

Step 8 Calculate the Euclidean distance for each particle *j* to the central particle, by (4.24)

$$\varphi_{(i,j)}^{(k)} = \left\| P_{q(i)}^{(k)} - P_{(i,j)}^{(k)} \right\| \tag{4.24}$$

Step 9 Calculate the linear regression coefficients [$\alpha_{0(i)}$ $\alpha_{1(i)}$] and the determination coefficient $R_{\varphi(i)}^{2(k)}$.

Step 10 Calculate the new standard deviation for each dimension *i* of new cloud by (4.14).

Step 11 If $k = it_{max}$ go to step 12, otherwise, $k=k+1$ and go to step 2.

Step 12 The central particle which generates the latest best fitness value represents the optimal power generation of each thermal unit and, consequently, the minimum total generation cost.

To verify the feasibility of the proposed method, some cases were studied to demonstrate the capacity of the algorithm to reach the optimal values as well as the capacity to solve highly constrained problems with growing dimension.
As any other heuristic method it may not converge to exactly the same solution at each run. Due to their stochastic behaviour, their performances could not be judged by the results of a single trial so all cases were performed 50 times keeping the average, maximum and minimum cost values.
Mainly, in power systems literature the convergence tests in ED problems are mostly related with number of iterations or generations [33],[36],[41] and [147] or CPU time per iteration/generation [35]. However, this way does not give adequate information about the computational effort to perform a task in order to have the same base of comparison with other techniques [43]. Thus, in this work, to compare the computational efforts independently of the CPU or number of iterations, the number of objective function evaluations is used [148], [149]. The proposed algorithm was implemented in *Matlab*® (R2010a) and executed on a Core (i2) 1,59 GHz processor.

First case study

The first test system consists of six thermal units with prohibited operation zones and ramp limits, as shown in tables 4.4 and 4.5, feeding a load of 1263 MW. The network has 26 buses and 46 transmission lines characterized by the losses coefficients matrices $\mathbf{B_{ij}}$, $\mathbf{B_{0j}}$ and $\mathbf{B_{00}}$, with 100 MVA capacity base. These matrices are shown in Annex II. This is a very common case study, largely used for comparison of performances between metaheuristics

[34],[36],[43],[150] and [151]. The units have cost functions defined by second order continuous and convex functions and the initial values of each unit are defined by P_i^0 .

Table 4.4 – Generating unit's data (first case study)

Unit	P_i^{min} (MW)	P_i^{max} (MW)	a_i ($/MW^2)	b_i ($/MW)	c_i ($)	UR_i (MW/h)	DR_i (MW/h)	P_i^o (MW)
1	100	500	0.0070	7.0	240	80	120	440
2	50	200	0.0095	10.0	200	50	90	170
3	80	300	0.0090	8.5	220	65	100	200
4	50	150	0.0090	11.0	200	50	90	150
5	50	200	0.0080	10.5	220	50	90	190
6	50	120	0.0075	12.0	190	50	90	110

Table 4.5 – Generating unit's prohibited zones (first case study)

Unit	*Prohibited zones* (MW)
1	[210 240] [350 380]
2	[90 110] [140 160]
3	[150 170] [210 240]
4	[80 90] [110 120]
5	[90 110] [140 150]
6	[75 85] [100 105]

In this case simulation, the central particle, as well as each individual particle of the cloud will have 6 dimensions (P_1...P_6), one for each generation unit. Depending on the number of particles N_P the dimension of cloud will be [6 x N_P]. The number of evaluations was limited to 5000 and each attempt was ran 50 times as in [34].

As explained above, the particles act as "sensors" of the search space and allow the calculation of the first and second order polynomials, as depicted in figures 4.7 and 4.8. Therefore, there are a minimum number of particles necessary to describe the curve fitting. On the other hand, a large number and the need of evaluation of each particle will slow down the algorithm. After some trials, the number of particles was set to 50.

In this case study, the value of *h* of (4.16) is 1 and the remaining values of the parameters are those presented in table 4.3. The penalty value *q* in (4.22) was set to 30.

Figure 4.16 shows the best solution obtained by SCO for this case study and the results obtained by the PSO and GA, proposed by [34] and New-PSO (NPSO), PSO with Local Random Search (PSO-LRS) and New PSO-LRS (NPSO-LRS) all proposed by [36].

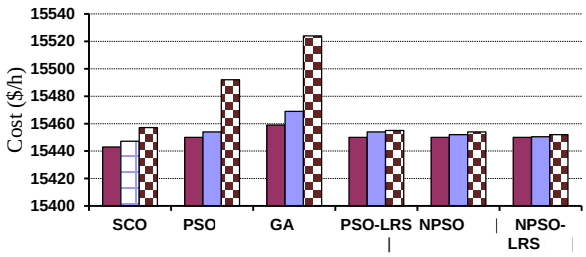

Figure 4.16 – Comparative minimum, maximum and average solutions (first case study)

In figure 4.17 the convergence behaviour of SCO's best solution is shown.

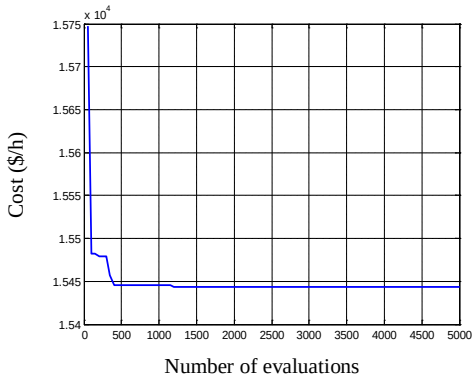

Figure 4.17 – Convergence behaviour of SCO for a 6-units problem

From figure 4.16, it can be observed that SCO reaches best solutions than the other 5 methods for the minimum and average costs. As in [36], with NPSO and NPSO-LRS, SCO it had a fast convergence to the cost value 15450$, (less than 400 evaluations), reaching a lower value few evaluations after. In addition, the losses obtained by SCO were fewer when compared to the remaining methods. The results are exposed in table 4.6. The algorithm demonstrated good velocity of convergence, reached a lower cost for the generation configuration and had lower losses.

Table 4.6 – Results obtained (6-units 1263 MW) (Best individual)

Power output (MW)	*Method*					
	SCO	*PSO [34]*	*GA [34]*	*PSO-LRS [36]*	*NPSO [36]*	*NPSO-LRS [36]*
P_{G1}	445,3	447,5	474,8	447,4	447,5	447,0
P_{G2}	176,8	173,3	178,6	173,3	173,1	173,4
P_{G3}	265,0	263,5	262,2	263,4	262,7	262,3
P_{G4}	135,3	139,1	134,3	139,1	139,4	139,5
P_{G5}	167,7	165,5	151,9	165,5	165,3	164,7
P_{G6}	85,3	87,1	74,2	87,2	88,0	89,0
P_T (MW)	1275,50	1276,01	1276,03	1275,95	1275,95	1275,94
P_{Loss} (MW)	12,50	12,96	13,02	12,96	12,95	12,94
Cost ($/h)	**15443**	15450	15459	15450	15450	15450

Second case study

The second test is an extent of the first. Consisting of 15 thermal units system, whose characteristics are presented in tables 4.7 and 4.8, feeding a load of 2630 MW [33],[34],[43] and [54]. The thermal units are connected to a 30-bus network with active losses matrices shown in annex II.

Table 4.7 – Generating unit's prohibited zones (second case study)

Unit	Prohibited zones (MW)
2	[185 225] [305 335] [420 450]
5	[180 200] [305 335] [390 420]
6	[230 255] [365 395] [430 455]
12	[30 40] [55 65]

Table 4.8 – Generating unit's data (second case study)

Unit	P_i^{min} (MW)	P_i^{max} (MW)	a_i ($/MW^2)	b_i ($/MW)	c_i ($)	UR_i (MW/h)	DR_i (MW/h)	P_i^o (MW)	
								[33]	[34]
1	150	455	0.000299	10.1	671	80	120	395	400
2	150	455	0.000183	10.2	574	80	120	450	300
3	20	130	0.001126	8.8	374	130	130	50	105
4	20	130	0.001126	8.8	374	130	130	104	100
5	150	470	0.000205	10.4	461	80	120	426	90
6	135	460	0.000301	10.1	630	80	120	208	400
7	135	465	0.000364	9.8	548	80	120	286	350
8	60	300	0.000338	11.2	227	65	100	262	95
9	25	162	0.000807	11.2	173	60	100	95	105
10	25	160	0.001203	10.7	175	60	100	134	110
11	20	80	0.003586	10.2	186	80	80	67	60
12	20	80	0.005513	9.9	230	80	80	30	40
13	25	85	0.000371	13.1	225	80	80	46	30
14	15	55	0.001929	12.1	309	55	55	15	20
15	15	55	0.004447	12.4	323	55	55	52	20

The parameters of SCO were similar to the first case study. The results obtained were compared with Fast Evolutionary Programming (FEP), Improved Fast Evolutionary Programming (IFEP), Swarm Direction Fast Evolutionary Programming (SFEP) proposed by [33], Particle Swarm Optimization (PSO) and Genetic Algorithms (GA) proposed by [34]. Figure 4.18 shows the total costs and it is clear the improvement of SCO over all other methods; it presents the lowest values for all indicators as well as the lowest average value after 50 trials.

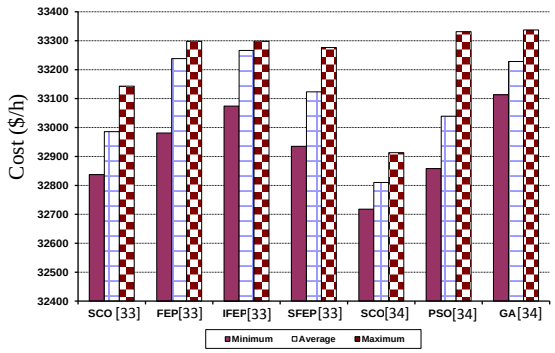

Figure 4.18 – Comparative minimum, maximum and average solution (second case study)

Although in [33] and [34] the unit's parameters were similar, the values of P_i^0 were different, as shown in table 4.8. This fact is enough to produce fairly different results as it can be observed in table 4.9. These differences are due to the ramps limits associated with starting

values P_i^0, leading to different production portfolios. In figure 4.19 it is shown the convergence speed of SCO in the case of [33].

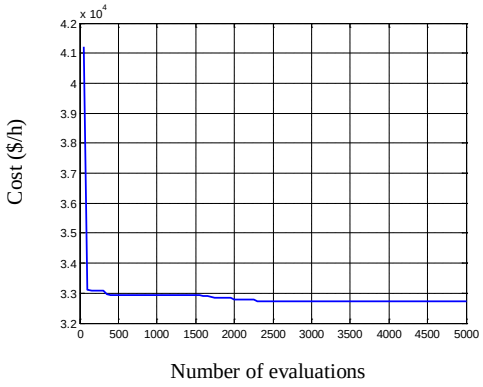

Figure 4.19 – Convergence behaviour of SCO for a 15-units problem

Table 4.9 – Results obtained (15-units 2630 MW) (Best individual)

Power output (MW)	*Method*						
	SCO [33]	*FEP* [33]	*IFEP* [33]	*SFEP* [33]	*SCO* [34]	*PSO* [34]	*GA* [34]
P_{G1}	455,0	389,9	333,8	343,7	455,0	439,1	415,3
P_{G2}	455,0	450,4	343,4	346,5	380,0	408,0	359,7
P_{G3}	130,0	89,8	85,3	127,9	130,0	119,6	104,4
P_{G4}	130,0	55,9	119,9	96,4	130,0	130,0	74,9
P_{G5}	355,2	272,6	457,0	426,1	170,0	151,1	380,3
P_{G6}	288,0	455,1	403,9	413,9	460,0	460,0	426,8
P_{G7}	353,9	457,9	464,1	452,3	430,0	425,6	341,3
P_{G8}	162,0	109,7	102,9	117,5	60,0	98,6	124,8
P_{G9}	25,0	90,5	103,8	42,5	51,3	113,5	133,1
P_{G10}	90,7	53,9	102,9	100,9	160,0	101,1	89,3
P_{G11}	80,0	79,9	28,3	79,1	78,4	33,9	60,1
P_{G12}	76,6	50,8	24,1	26,7	80,0	80,0	50,0
P_{G13}	27,4	54,9	50,0	36,1	31,7	25,0	38,8
P_{G14}	17,7	23,4	31,5	43,6	20,4	41,4	41,9
P_{G15}	19,1	26,2	21,6	15,0	22,6	35,6	22,6
P_T (MW)	2665,71	2668,2	2662,4	2663,4	2659,38	2662,4	2668,4
P_{Loss} (MW)	35,71	38,387	32,431	38,278	**29,38**	32,43	38,278
Cost ($/h)	**32837**	32981	33074	32935	**32718**	32858	33113

Once more the SCO reached the lowest cost value and in the case of [34] also reached the lowest losses.

Deeper tests in the case of [34] showed that increasing the maximum of evaluations up to 25000, an even lower cost value was obtained (32708$) with a total production of 2659,58 MW and 29,58 MW of losses after 16200 evaluations. On the other hand, with 100 particles and a maximum of 20000 evaluations, the value of (32703$) was reached. These results are in line with those obtained in [40] with PSO with Chaotic Sequences (CSPSO),

PSO with Crossover Operation (COPSO) and PSO with both Chaotic sequences and Crossover operation (CCPSO).

Third case study

In this case study, the objective was to investigate the behavior of large power systems, where all units present valve-point effects [36],[42],[54],[55] and [152]–[154]. In this case, the traditional quadratic and convex cost functions are transformed into non-convex functions. The system presents 40 units feeding a load of 10500 MW, the grid losses were not considered and the units do not have ramp limits or prohibited zones.

To elucidate the valve-point effect, in figure 4.20 a) it is shown the first unit cost function from the set of 40 under study, as well as its derivative in b). From figure 4.20 it is clear that the cost function is not convex and its derivative is not continuous. The information concerning the units' cost functions is described in table AII.1 in annex II.

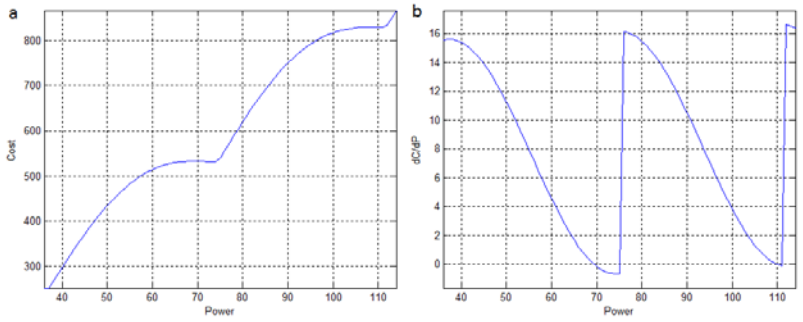

Figure 4.20 – a) non-convex cost function with valve point effect; b) its derivative

As deepen in point 2.2.2, commercial tools able to solve economical dispatch for thermal units generally require convex cost functions. Further, algorithms based on particles, due to their nature, should be able to explore non-convex search spaces, finding an optimal solution without the need of cost functions pre-processing. Because of this problem's complexity, the number of particles was increased to 100 and the maximum number of evaluations to 50000. The remaining parameters of SCO are found in table 4.2. Figure 4.21 shows the convergence behavior, reaching a minimum in less than 50000 evaluations.

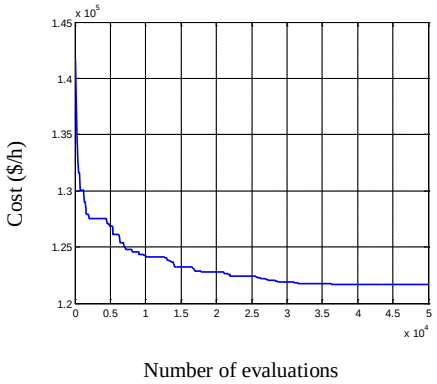

Figure 4.21 – Convergence behaviour of SCO for a 40-units problem

When compared with other algorithms, the minimum cost value is lower than several optimizations techniques such as PSO [36],[42], Classical Evolutionary Programming (CEP), PSO Embebbed in CEP (CEP_PSO) [42], Improved Fast Evolutionary programing (IFEP), Modified PSO (MPSO), Evolutionary Strategy Optimization (ESO), PSO Local Random Search (PSO_LRS), New PSO (NPSO), NPSO_LRS [36] and CTPSO [54]. The results are shown in figure 4.22 and table 4.10. The unit's production values are not indicated in the text due to the large amount of data, being shown in table AII.2 in annex II.

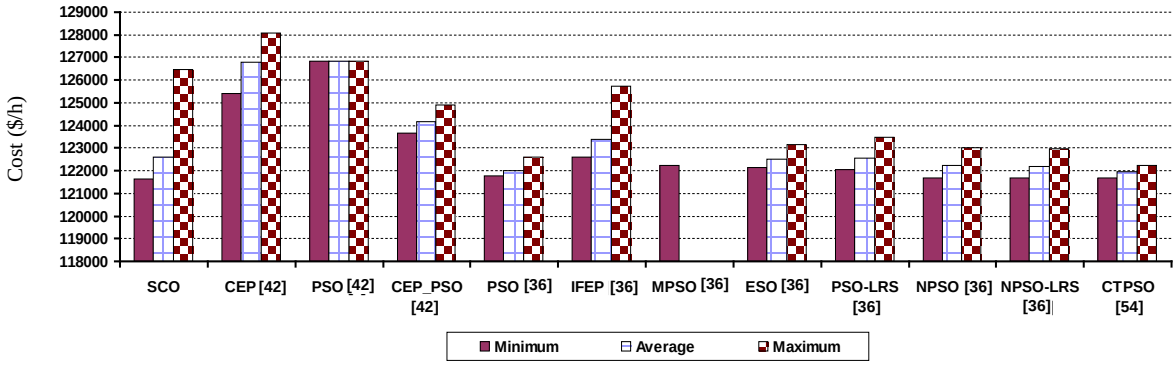

Figure 4.22 – Comparative minimum, maximum and average solutions (third case study)

Table 4.10 – Results obtained (40-units 10500 MW) (Best individual)

Method	SCO	CEP [42]	PSO [36]	CEP_PSO [42]	PSO [42]	IFEP [36]
Cost ($/h)	**121632**	125420	126849	123670	121751	122624
Method	MPSO [36]	ESO [36]	PSO-LRS [36]	NPSO [36]	NPSO-LRS [36]	CTPSO [54]
Cost ($/h)	122252	122122	122036	121704	121664	121695

Fourth case study

The fourth case study intends to study a system with 10 thermal units with valve-point effects and multi-fuels [36],[54] and [147]. In this case the cost functions are non-convex nor continuous and so non-differentiable along the domain. Thus, the cost functions of each thermal unit can be described by equation (2.14), where each branch is the cost for burning

the fuel *k*, which depends on the decision variable P_i. Due to the large amount of information, the required data is available in table AII.3 and AII.4 in annex II [147].

In the present case study, one unit burns 2 types of fuels and the remaining units burn 3 types. If considering this case study being solved by traditional software packages used by the system operators (where the cost functions must be convex), the cost functions should be split in fuels and transformed into convex functions. Next, all the combinations should be tested and should be 59049, which is a massive number where some are feasible and others are not. The best solution must be found inside the set of feasible solution [155].

Restrictions are not including forbidden operation zones, ramp limits or power losses in transmission lines. The load considered was 2700 MW.

As referred in the first case study, the number of particles has not excessive importance because it does not exist a direct relationship between the increase of its number and the increase of performances. With this, once again, after some experiences the number of particles was set to 10 and the number of evaluations was limited to 2000. The remaining parameters are found in table 4.3. In figure 4.23 the convergence behavior is shown. The best value was reached after 1800 evaluations.

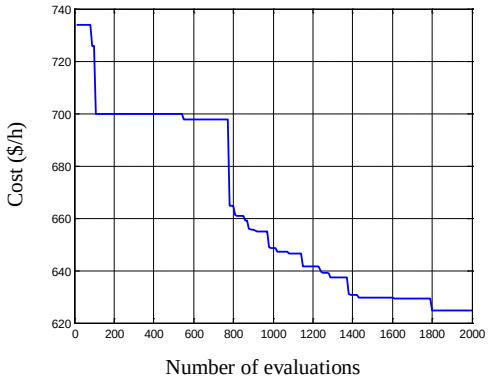

Figure 4.23 – Convergence behaviour of SCO for a 10-units problem

The reached results with SCO were compared with Conventional Genetic Algorithm with Multiplier Updating (CGA_MU) and Improved Genetic Algorithm with Multiplier Updating (IGA_MU) as well as with PSO-LRS, NPSO and NPSO_LRS [147]. The results are shown in table 4.11. It can be concluded that all the proposed methods reach the same combination of fuels and SCO reached comparable results with other proposed metaheuristics. Despite CGA_MU and IGA_MU not giving information about the number of evaluations, when comparing with remaining algorithms SCO needed less evaluations to reach the optimal.

Table 4.11 – Results obtained (10-units 2700 MW) (Best individual)

Power (*MW*)	*Method*						
	SCO	*CGA_MU*[147]	*IGA_MU*[147]	*PSO-LRS*[147]	*NPSO*[147]	*NPSO-LRS*[147]	*fuel*
P_{G1}	225,612	222,0108	219,1261	219,1261	220,6570	223,3352	2
P_{G2}	207,103	211,6352	211,1645	211,1645	211,7859	212,1957	1
P_{G3}	281,576	283,9455	280,6572	280,6572	280,4026	276,2167	1
P_{G4}	237,912	237,8052	238,4770	238,4770	238,6013	239,4187	3
P_{G5}	271,667	280,4480	276,4179	276,4179	277,5621	274,6470	1
P_{G6}	242,476	236,0330	240,4672	240,4672	239,1204	239,7974	3
P_{G7}	284,633	292,0499	287,7399	287,7399	292,1397	285,5388	1
P_{G8}	243,321	241,9708	240,7614	240,76,14	239,1530	240,6323	3
P_{G9}	432,693	424,2011	429,3370	429,3370	426,1142	429,2637	3
P_{G10}	273,006	269,9005	275,8518	275,8518	274,4637	278,9541	1
P_T (MW)	2700	2700	2700	2700	2700	2700	
Cost ($/h)	624,65	624,72	624,52	624,23	624,16	624,13	
Evaluations	1800	N/A	N/A	3440	3240	2120	

Succeeding the achieved results this new optimization algorithm is adequate to solve high constrained ED problems. The obtained results are comparable or even better than several metaheuristics. As a conclusion, SCO is a useful tool, but like other metaheuristics they only should be used when it is really necessary. Otherwise the linear programming is precise and fast enough.

So far it was described the pre-proceeding that must be done off-line in order to create the database with the optimal production of each unit of the GENSET's in function of the *net load*. This database is one of the main information and must be available to the UC which is run one or more times a day following the procedure shown in figure 4.1b).

4.5 Unit commitment based on risk assessment

Following the flowchart of figure 4.1b), after the information about the *net load* values for each hour ahead of the scheduling horizon, it is necessary to evaluate each GENSET to determine which should be allocated for each hour. For this it is required to know the *net load* probabilistic forecast, (presented in point 3.9) together with the GENSET characteristics (technical limits from table 4.2) and fuel consumption curves (as presented in figure 4.3).

The *pdf* of *net load* (*L-RES*) represents the amount of power that must be produced by the thermal units. In [32] it is done a similar approach described as *net demand*, defined as the load minus the total wind power and it represents the power that must be produced by other generators of the system. Despite wind power forecast errors of a single wind farm, not generally following a normal distribution (due to the W2P nonlinearity), the errors were assumed as following a normal distribution, considering several wind generators geographically dispersed and taking into account the central limit theorem. As load forecast

errors were also considered normally distributed and uncorrelated with wind power errors, in [32] it was assumed that net demand errors follow a normal distribution with null expected value and standard deviation given by the square root of the sum of variances. In [31] the same concept of *net load* was presented: both wind and load were considered uncorrelated with the forecasts errors normally distributed.

In figure 4.24 it is depicted an example of a risk assessment proposed in this work, showing an example of six different theoretical thermal generation mixes (GENSET's). In the present work, due to the low number of wind turbines and all in the same wind farm without appreciable geographic smoothing effect, the errors could not be considered as normally distributed. However, as shown in point 3.9.1, after the aggregation the *net load* can be sufficiently well described by a Beta *pdf*.

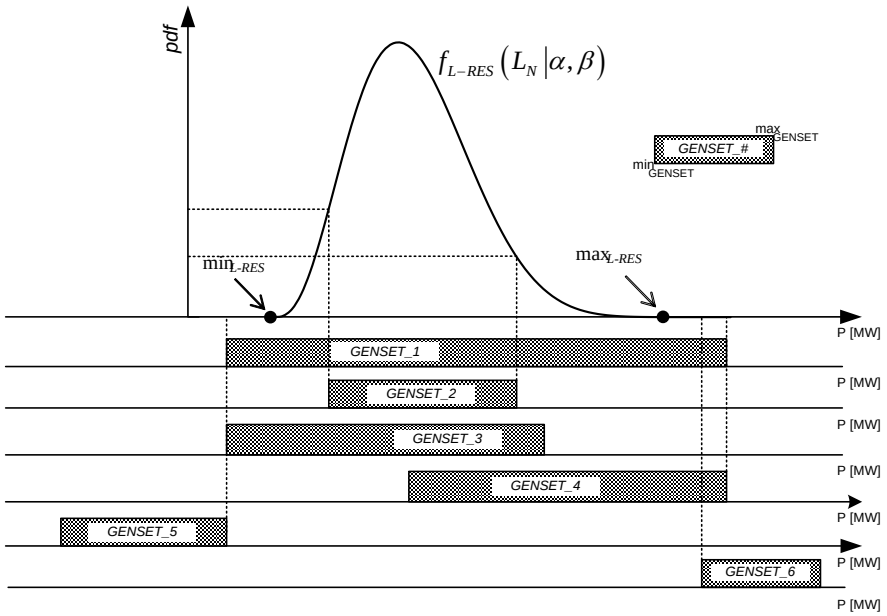

Figure 4.24 – Example of single period unit commitment based on risk assessment

Depending on the technical minimum and maximum limits (generation capacity) of each unit, the mixes are able to cover a certain amount of *net load*.

Analysing the case of GENSET_1 it is verified that the minimum generation limit is lower than the $min_{L\text{-}RES}$, meaning that the probability of the GENSENT_1 to work below the minimum is zero. On the other hand, the maximum generation capacity is higher than $max_{L\text{-}RES}$ meaning that the mix has enough available power to feed the entire *net load*; GENSET_1 is a thermal mix which can be chosen to feed the *net load* without any additional actions as load shed or wind curtailment.

The GENSET_2 shows a mix that does not have the capacity to feed all the range of *net load,* existing some probability of load shed due to the lack of thermal power capacity and some probability of the thermal units to work below the minimum generation capacity.

In the case of GENSET_3 there is a probability of the *net load* to be higher than the available production and, consequently, a certain probability of load shed to avoid blackouts. GENSET_4 shows the opposite case, the mix has enough power capacity to feed the maximum value of net load, but at same time some probability of the thermal units work below the minimum generation capacity exists. One possibility is RES curtailment which will increase the *net load* in order to exceed min_{GENSET} (or at least bring closer the two values) to decrease the probability of working below the minimum. It should be noticed that even with RES curtailment, the minimum generation capacity can be higher than $min_{L\text{-}RES}$. As shown in figure 4.3, the fuel consumption is higher near the minimum and, as a consequence, low efficiency and high production costs.

The case of GENSET_5 the probability of load shed equals one, this means that GENSET does not have the capacity to feed any *net load*. Finally, in the case of GENSET_6 the *net load* is so reduced that the GENSET has a very high probability to work below the minimum, even with RES curtailment.

Ideally, to each value of *net load*, the most convenient solution is the closest to GENSET_1, but it must be perceived that the set of possible thermal mixes are limited and consequently it would not be possible to cover the entire *net load* necessities without load or wind curtailment.

4.5.1 Risk of operation areas

To analyze the risk of load shed, RES curtailment or to prevent operation of thermal units above or below technical limits, all configurations of GENSET must be tested. As verified previously in point 4.3.2, though there are 255 different combinations, as there are two sets of units with equal characteristics allow the combinations to be reduced to 24, decreasing the computational effort.

As indicated in point 3.9.1, the probability density function of *net load* can be described by a Beta distribution. In this kind of *pdf* is mandatory that the random variable is normalized between 0 and 1. In this work, the *net load* was normalized by the *min-max* method as shown in equation (4.25).

$$L_{N[p.u.]} = \frac{L_{N[MW]} - \min_{L-RES[MW]}}{\max_{L-RES[MW]} - \min_{L-RES[MW]}} \tag{4.25}$$

Figures 4.25 and 4.26 show a possible Beta *pdf* and *cdf* with the parameters α_h and β_h concerning the *net load* for an hour *h*, $f_{L\text{-}RES}(L_N|\alpha_h,\beta_h)$ and $F_{L\text{-}RES}(L_N|\alpha_h,\beta_h)$.

In this specific case, the analysis is divided into three different possible operation areas, namely RES curtailment or below the min_{GENSET} (area 1), normal operation (area 2) and load shed (area 3) above max_{GENSET}.

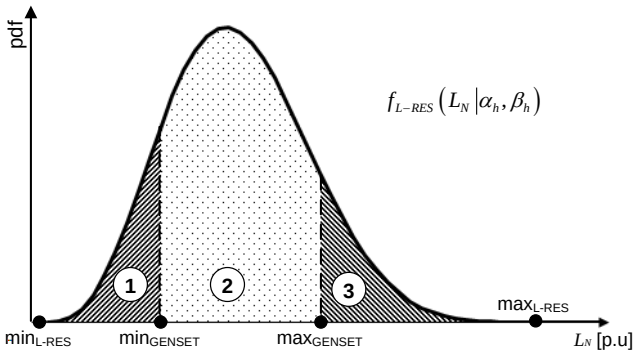

Figure 4.25 – Uncertainty associated to a specific committed GENSET (*Load-RES*)

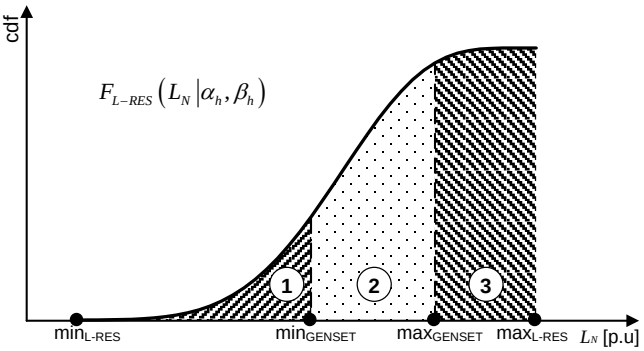

Figure 4.26 – Cumulative distribution function associated to a specific GENSET (*Load-RES*)

4.5.2 Probability of operation below the minimum GENSET limit

In figure 4.25, area 1 represents the risk of thermal units to operate under its technical minimum ($min_{L\text{-}RES} < min_{GENSET}$) and represents the risk of RES curtailment or the storage activation (when it exists) too. In the case study addressed in this work, there is no significant storage capacity, so this will not be addressed; only the RES curtailment question is analyzed. The probability of RES curtailment $prob(WC)_h$ in hour h is the same probability of generators violate its minimum limit and can be calculated by equation (4.26).

$$prob(WC)_h = \begin{cases} 0, & if \quad \min_{GENSET} \le \min_{L-RES,h} \\ \dfrac{1}{B(\alpha_h,\beta_h)} \displaystyle\int_{\min_{L-RES,h}}^{\min_{GENSET}} L_N^{\alpha_h-1}(1-L_N)^{\beta_h-1}\,dL_N, & if \quad \min_{L-RES,h} < \min_{GENSET} < \max_{L-RES,h} \\ 1, & if \quad \min_{GENSET} \ge \max_{L-RES,h} \end{cases} \tag{4.26}$$

Observing figure 4.25 it is clear that if the minimum value of *net load* is higher than the GENSET minimum generation, there is no risk of RES curtailment. On the other hand, the risk is maximum if the minimum of GENSET is higher than the maximum of *net load*.

4.5.3 Probability of operation above the maximum GENSET limit

In figure 4.25, area 3 corresponds to the probability of the *net load* being greater than max_{GENSET} (total thermal capacity of the mix). Therefore, there is the probability of some load not to be supplied in hour *h* (probability of load shed), calculated by equation (4.27).

$$prob(LS)_h = \begin{cases} 1, & if \quad \max_{GENSET} \le \min_{L-RES,h} \\ 1 - F_{L-RES,h}\left(\max_{GENSET} \middle| \alpha_h, \beta_h\right), & if \quad \min_{L-RES,h} < \max_{GENSET} < \max_{L-RES,h} \\ 0, & if \quad \max_{GENSET} \ge \max_{L-RES,h} \end{cases} \quad (4.27)$$

4.5.4 Probability of operation inside GENSET limit

The area bounded by the RES curtailment probability and load shed probability is the area of GENSET's normal operation (NO) and it is defined by GENSET technical limits (max_{GENSET} and min_{GENSET}). As the integral of *cdf* is 1 the $prob(NO)_h$ can be calculated by equation (4.28).

$$prob(NO)_h = 1 - \left[prob(WS)_h + prob(LS)_h \right] \quad (4.28)$$

At the end of this analysis it is concluded that if the thermal limits' stay under $min_{L\text{-}RES}$ and above $max_{L\text{-}RES}$ there is no need of load and RES shed. However, as depicted in figure 4.4 and table 4.2 and due to limited solution set, these conditions could not be often achieved.
In case of load shed the room for maneuver is reduced; it is not recommended thermal units to work in steady state beyond the maximum limits. On the other hand, when the *net load* is lower than the GENSET minimum and if there is RES production available at that moment, there is the possibility of RES curtailment in order to increase the value of $min_{L\text{-}RES}$ to closer values to the GENSET minimum.

4.5.5 Wind power curtailment

Analyzing the production behavior of RES and due to technical reasons, tradition is to keep the production in the geothermal power plants constant. Hydro power plants, because of lacking storage capacity and having low rated power, do not have worth mentioning capacity of control and are strictly connected with the available resource. So, the RES with an effective

and noticeable capacity of control is the wind power production with curtailment capacity. By this, when there is the risk of thermal units to work below their minimums, the wind curtailment is an option to take in consideration. Even so, it is necessary to determine if there still is the risk of thermal units to operate under the technical limits after total wind curtailment. As a consequence, and considering load and wind generation independent and random variables, another indicator is introduced, L_{NW}, which represents the resulting *net load* after the partial or total wind curtailment. This variable will give place to another Beta *pdf* defined by the parameters α_{h1} and β_{h1}.

With wind curtailment, the amount of RES is reduced and, consequently, the need of thermal production is increased, as depicted in figures 4.27. In figure 4.28 it is presented the *cdf* with and without wind curtailment. Depending on the available wind power production for the hour *h*, the curtailment capacity should be different. Given this, and once again, the performances of the forecast play an important role.

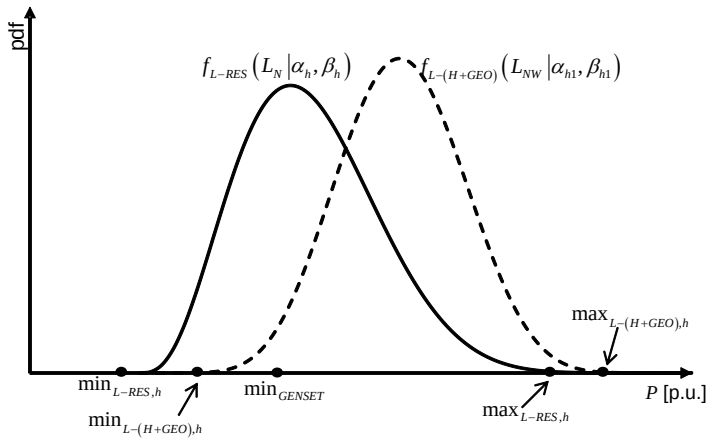

Figure 4.27 – *Pdf* of *net load* with (*L*-(*H*+*GEO*)) and without wind curtailment (*L*-*RES*)

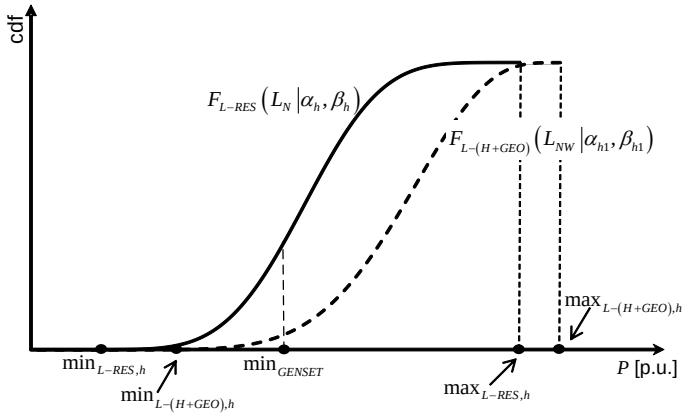

Figure 4.28 – *Cdf* of *net load* with (*L*-(*H*+*GEO*)) and without wind curtailment (*L*-*RES*)

Depending on the situation and even with wind curtailment, it could not be enough to raise the minimum value of the *net load* to a value higher than min_{GENSET} as depicted in figures 4.29

and 4.30. This situation reduces, but does not avoid, the risk of thermal units to continue to operate below their minimums, during the hour *h*. Thus, it is necessary to calculate the new risk, by calculating the new probability *prob*(min|*WC*)$_h$.

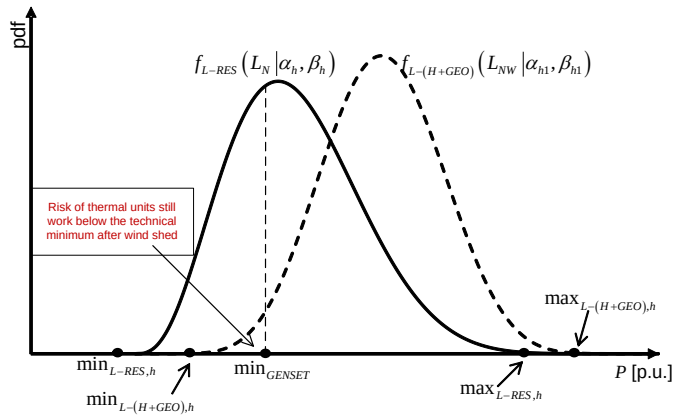

Figure 4.29 – Probability of thermal units work below the minimum (*pdf*)

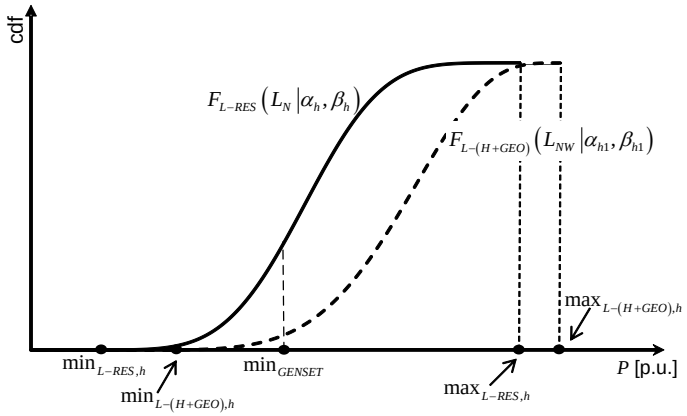

Figure 4.30 –Probability of thermal units work below the minimum (*cdf*)

This is done with the formulation of equation (4.26) using the Beta *pdf* defined by parameters α_{h1} and β_{h1}.

After the definition of the different risk areas for all GENSET, the power values must be computed in order to calculate the cost assigned to each area and calculate the total cost associated to each hour *h*.

4.6 Power calculation for different operation risks areas

Starting with the case of wind curtailment risk, when the probability of wind curtailment is higher than zero, it is necessary to determine which quantity of wind power should be curtailed. In this situation there are two hypotheses: the quantity of available wind production is higher than the curtailment necessity (being necessary to curtail only a percentage of

available power) or the wind power capacity to curtail is lower than the needed. With this, the calculation of wind power curtailment $P(WC)_h$ should be the minimum of equation (4.29).

$$P(WC)_h = \begin{cases} 0 & ,if \quad prob(WC)_h = 0 \\ \min_{GENSET} - \min\left[F^{-1}_{L-RES,h}\left(\dfrac{prob(WC)_h}{2}, \alpha_h, \beta_h \right), \hat{P}_w \right] & ,\ if \quad prob(WC)_h > 0 \end{cases} \tag{4.29}$$

To estimate $P(WC)_h$, it is necessary to obtain the inverse of the Beta *cdf* of *net load* $F^{-1}_{L-RES,h}\left(prob(WC)/2, \alpha_h, \beta_h \right)$ and wind power forecast. With this inverse function it is possible, assigning some probability, to know the power to curtail. The result of the equation (4.29) will be the minimum of these values because the wind power available to curtail is limited by the wind power forecast. In figure 4.31 the inverse *cdf* of *net load* with and without curtailment is shown.

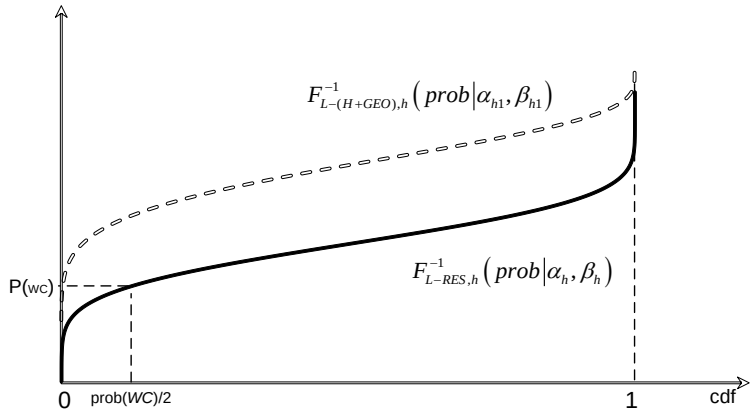

Figure 4.31 – Inverse *cdf* of *net load* with (L-(H+GEO)) and without wind curtailment L-RES

If, with the previous reasoning, the wind curtailment is not enough to guarantee that the thermal units are not operating below the minimum, it is possible to estimate the $P(\Delta prob|WC)_h$ by the equation (4.30). This represents the value that the thermal units are producing below the limits after the wind curtailment, in hour *h*.

$$P\left(\Delta prob|WC\right)_h = \begin{cases} 0 & ,if\ \min_{GENSET} \le \min_{L-(H+GEO),h} \\ \min_{GENSET} - \left\{ F^{-1}_{L-(H+GEO),h}\left[\dfrac{prob(\min|WC)}{2} | \alpha_{h1}, \beta_{h1} \right] \right\} & ,if\ \min_{L-(H+GEO),h} < \min_{GENSET} < \max_{L-(H+GEO),h} \\ \min_{GENSET} - F^{-1}_{L-(H+GEO),h}\left(0{,}5 | \alpha_{h1}, \beta_{h1}\right) & ,if\ \min_{GENSET} \ge \max_{L-(H+GEO),h} \end{cases} \tag{4.30}$$

On the opposite case, if there is a risk of load shed, the calculation of load shed $P(LS)_h$, is calculated by equation (4.31).

$$P(LS)_h = \begin{cases} 0 & ,if\ \ prob(LS)_h = 0 \\ F_{L-RES}^{-1}\left(1 - prob(LS)_h + \dfrac{prob(LS)_h}{2} \middle| \alpha_h, \beta_h\right) - \max_{GENSET} & ,if\ \ prob(LS)_h > 0 \end{cases} \quad (4.31)$$

In the end, the calculation of power produced under normal operation of thermal units is done by (4.32):

$$P(NO)_h = \begin{cases} 0 & ,if\ prob(WC)_h = 1\ \ or\ \ prob(LS)_h = 1 \\ F_{L-RES}^{-1}\left[\dfrac{1 - prob(LS)_h + prob(WC)_h}{2}, \alpha_h, \beta_h\right] & ,if\ 0 < prob(WC)_h < 1\ \ and\ \ 0 < prob(LS)_h < 1 \end{cases} \quad (4.32)$$

4.6.1 Risk-based cost analysis (without contingencies)

To conclude the evaluation of performances of each GENSET (So far without contingencies), the risk costs related with each risk assessment done so far are computed. The risk cost of wind curtailment is calculated by (4.33) whereas the risk cost of load shed is done by (4.34),

$$C_{WC,h} = prob(WC)_h \times P(WC)_h \times C_{WC} \quad (4.33)$$

$$C_{LS,h} = prob(LS)_h \times P(LS)_h \times C_{LS} \quad (4.34)$$

where, C_{WC} and C_{LS} are, respectively, the wind curtailment and load shed cost. These costs, in €/MWh, are constants and independent from the amount curtailed.
When, after wind curtailment, there still is violation of the minimum limits of a GENSET, the risk cost is calculated by equation (4.35), where the cost C_{MIN_GEN} is considered constant (there is not enough information concerning the consumption below the minimum power).

$$C_{\min|WC,h} = prob(\min|WC)_h \times P(\Delta prob|WC)_h \times C_{MIN\_GEN} \quad (4.35)$$

The thermal generators' risk cost of normal operation are calculated by (4.36), where F[.] is the equivalent optimal generation unit (GENSET) fuel consumption function, presented in point 4.3.3. and as referred, the resulting function gives the fuel consumption which has to be multiplied by the fuel cost C_{FUEL}.

$$C_{NO,h} = \left\{ \begin{array}{l} prob(NO)_h \times F\left[P(NO)_h\right] + prob(LS)_h \times F\left(\max_{GENSET}\right) + \\ prob(WC)_h \times F\left(\min_{GENSET}\right) + prob(\min|WC)_h \times F\left(\min_{GENSET}\right) \end{array} \right\} \times C_{FUEL} \quad (4.36)$$

At the end, the risk cost for a given GENSET at hour *h* based on risk assessment is calculated by equation (4.37)

$$C_{GENSET} = C_{WC,h} + C_{LS,h} + C_{\min|WC,h} + C_{NO,h} \tag{4.37}$$

These calculations must be done for all GENSET's in function of the *net load* of each period $h = 1..H$, where H is the time horizon to be scheduled.
Yet, there is an important issue that should be highlighted; the results from equation (4.37) are not the real costs. They are only risk costs and are calculated in order to define the scheduling. The final real costs must be calculated with measured values.

4.6.2 Contingencies analysis

In this work the contingency analysis is limited to one unexpected thermal unit outage (*N*-1). Due to the small rated power capacity, the absence of interconnections, low spinning reserve and fast response units, the outage of more than one thermal unit may lead to a blackout.
Following [156] there are two types of outages, dependent and independent. In the case of independent outages, the outages can be classified as:

- Forced outages
- Planned outages
- Semiforced outages
- Partial failure mode
- Multiple failure mode

The forced outages, which can happen randomly and are totally uncontrollable, can still be divided in repairable and non-repairable forced failures. Planned outages create the "must out unit" restriction indicated in point 2.2.1.
To the contingencies analysis of this work, only independent forced and repairable outages are studied and they can be modeled using a steady up-down-up cycle process as shown in figure 4.32 [32],[143].

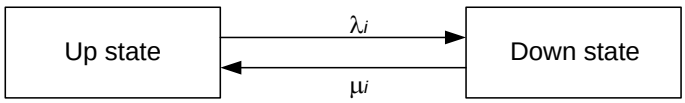

Figure 4.32 – State space diagram of a repairable component

Mathematically, the average unavailability in the long-term process can be defined by equation (4.38),

$$U_i = \frac{\lambda_i}{\lambda_i + \mu_i} \tag{4.38}$$

where U_i is the average unavailability, λ_i is the failure rate (failures/year) and μ_i is the repair rate (repairs/year) of unit *i*.

During the single-period analysis it is considered that a failure of a unit cannot be repaired or replaced within this period. In absence of real values, the value used in this work was defined as 0,015. Following this approach, the evaluation of a *N*-1 contingency (the outage of a single unit) is done by equation (4.39). The parameter n_S and n_B represent the number of units of type G_S and G_B, respectively, while indices $_{(n\text{-}1)S,h}$ and $_{(n\text{-}1)B,h}$ represent the outage of a unit of each type, at hour *h*, of the GENSET under evaluation. The parameter n_{UNIT} represents the total units of the GENSET under evaluation.

$$C_{GENSET(N-1),h} = (1-U)^{n_{UNIT}} \times C_{GENSET\_nS\_nB,h} + (1-U)^{n_{UNIT}-1}\left[n_S \times U \times C_{GENSET\_(n-1)S\_nB,h} + n_B \times U \times C_{GENSET\_nS\_(n-1)B,h}\right] \quad (4.39)$$

With this technique, and with the database created off-line, it is possible to calculate the outage cost, since the equivalent cost functions of each GENSET are already known, being the recalculation very easy and fast. For instance, if the GENSET_$3G_S$_$3G_B$, lose a unit type G_S, the new cost can be calculated searching in the database the cost related with the GENSET_$2G_S$_$3G_B$.

Previous evaluations have two exceptions, which happen when there only is one on-line unit, as GENSET_$0G_S$_$1G_B$ or GENSET_$1G_S$_$0G_B$. It is considered that the loss of all thermal generation will conduce to a blackout. In this case, it is considered a constant blackout cost (C_{BO}) plus the cost of *net load* shed, as shown in equation (4.40).

$$C_{GENSET(N-1),h} = (1-U) \times C_{GENSET,h} + U\left[E(L_N) \times C_{LS,h} + C_{BO}\right] \quad (4.40)$$

One of the key ideas of the proposed approach is that there are no infeasible solutions. All solutions are possible as long as the cost is acceptable. After calculating all risk costs to each hour *h*, an ordered priority list (from lower to higher price) is created.

4.7 Multi-period unit commitment

Until now, the costs resulting from risk assessment were evaluated only considering a single step ahead. However, considering startup and shutdown costs as well as the constraints of minimum time up, minimum time down, among others, as described in point 2.2.1., the power systems scheduling process is done over a larger time horizon. So, it is necessary to implement a multi-period UC in order to incorporate the transitions between the single periods. From the several approaches described in [37] and [157], in this work it is used the dynamic programming method.

4.7.1 Dynamic programming

Dynamic programming (DP) was one of the first optimization techniques to be applied to solve the UC problem [37],[49]. One of the dynamic programming advantages is the capacity of solving problems of various sizes and the ease to be modified for incorporation of the characteristics of different units. It is relatively easy to add constraints mainly for those that affect the economic dispatch. One of the disadvantages of DP is that beyond the calculation of the transitions along the time periods (states), all units' combinations must be addressed in order to define the feasible solutions.

The total number of solutions is calculated by $(2^{NG}\text{-}1)^{Ns}$ being N_G the units' number and *Ns* the number of states during the scheduling period.

Generally, the constraints on the units and the load/capacity relationships of typical power systems are such that this huge number is never completely reached. If the sum of the maximum is lower than the load or if the sum of all minimum is highergreat than the load, these solutions are infeasible. Nevertheless, the real practical barrier in the UC is the high dimension of the possible solution space [37],[49],[50] and [157].

The DP algorithm can also be solved by forward or backward approach, where the major difference is that the forward approach does not deal with the cold or hot starting costs. For this, when forward DP is used, it should be assumed that [49]:

- A state consists of an array of units with specified units on-line and the remaining off-line;
- The start-up costs are independent from the time since the unit was shut down;
- There are no cost for shutting down the units;
- There is a strict priority order and in each state a specified minimum amount of capacity must be operating.

A feasible state is the one where the committed units can supply the required load and meet the minimum amount of capacity for each period.

In equation (4.40) the generic mathematic representation of a forward DP approach, is shown [49]. The state (*K*,*I*) represents the I^{th} units' combinations at each hour *K* of scheduling period and $\{L\}$ is the set of feasible states.

$$FC(K,I) = \min_{\{L\}}\left[P_{COST}(K,I) + S_{COST}(K-1,L:K,I) + FC(K-1,L)\right] \qquad (4.40)$$

$FC(K,I)$ is the least total cost to arrive at state (*K*,*I*), $P_{COST}(K,I)$ is the production cost for the state (*K*,*I*) and $S_{COST}(K\text{-}1,L{:}K,I)$ are the transition costs related with units' starting in the transition from the feasible state (*K*-1,*L*) up to the state (*K*,*I*). When *K* is equal or greater

than 1, $FC(K\text{-}1,L)$ is the total accumulated cost to arrive at state (K-1,I). As seen in equation (4.40) the calculation of the transition costs from K-1 to K *is* only done for the feasible solutions $\{L\}$ at K-1. This problem is solved recursively in order to compute the minimum cost accumulated up to the end of scheduling period. At the end, a backtracking is used to find the optimal multi-period UC. Departing from combinations of units with the minimum accumulated cost, the best path is traced hourly until reaching the beginning of the scheduling period.

In figure 4.33 the flowchart with UC via forward DP,(based on [49] and [157]) with the introduced changes is shown.

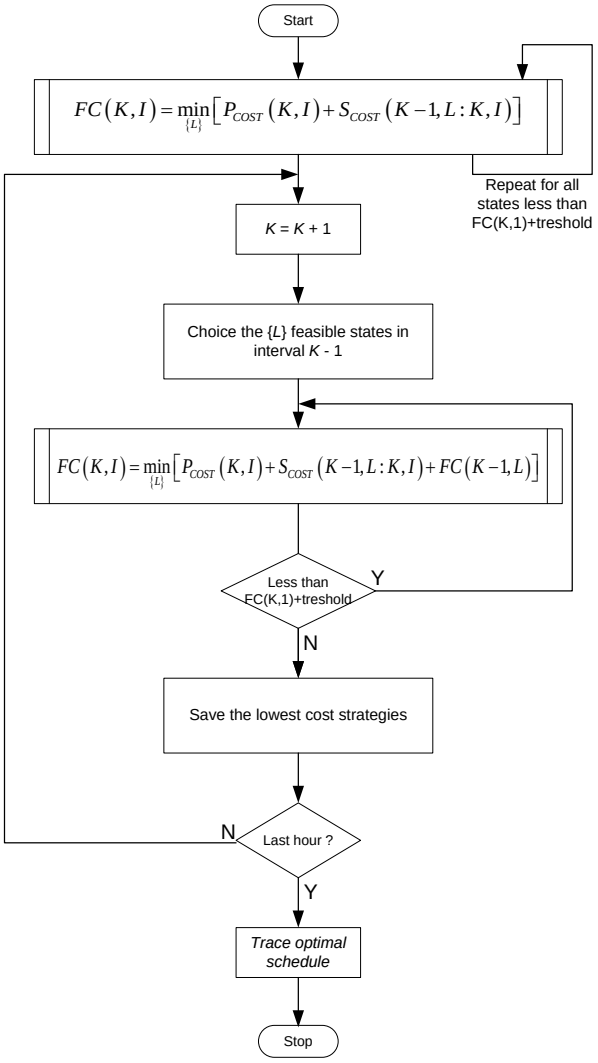

Figure 4.33 – Unit commitment via forward dynamic programming

It should be noticed that in a dynamic programming all the combinations in each state are evaluated but the transitions are only done between feasible combinations. Still, in the proposed approach, all combinations are always considered feasible because the assessment is based on risk. For this and considering 8 units (255 combinations) for a 24h scheduling, there

are $5{,}71 \times 10^{57}$ possible solutions, which represent impracticable time consumption. To overcome this problem it is proposed a heuristic method.

In each state (*K*,*I*) all the 255 solutions, resulting from the single period UC, are ordered from the lowest to the highest cost. Knowing the best solution of each state (*K*,*I*), only the closer "paths" are tested. Considering *FC*(*K*,1), the cheapest solution at time *K*, all solutions in that state not respecting the condition of equation (4.41) are excluded from the multi-period analysis.

$$FC(K,I) \leq FC(K,1) + threshold \tag{4.41}$$

This way, only the solutions near the best solution at each state are tested, with paths not fulfilling the entire scheduling being eliminated. However, as all heuristics, there is no certainty that the most economical solution is achieved, the compensation is the velocity of the process.

As conclusion, to an overall perception of the proposed scheduling approach, in figure 4.34 a flowchart of the proceeding is shown.

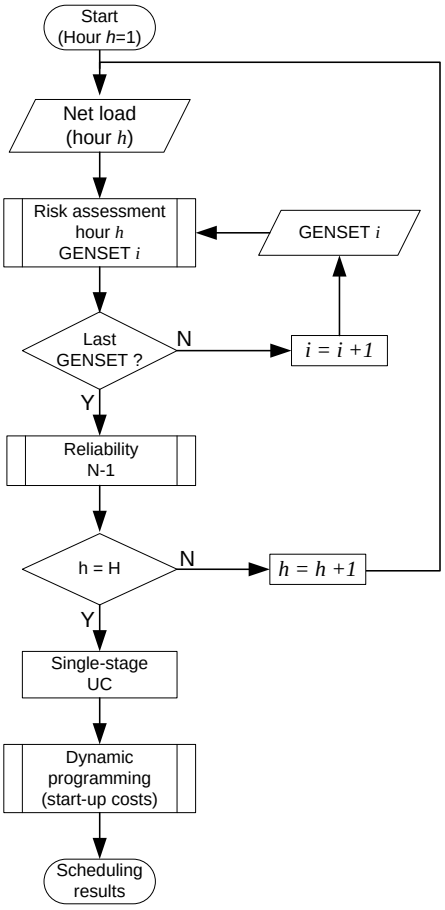

Figure 4.34 – Flowchart of proposed methodology

4.8 Summary and main conclusions

In this chapter it is proposed an innovative and advanced stochastic UC and ED based on risk assessment, addressing the increase of uncertainty and variability introduced by RES in the short-term of insular electricity power networks. The difference between this methodology and the latest published methods relies on the fact that the uncertainty and variability of RES are not modeled by scenarios. This allows the reduction of computational efforts, particularly, with the introduction of off-line pre-processing. In this process it is introduced the equivalent optimal generation unit concept. In generic approaches, the production costs in each state are calculated on-line by an ED, allocating the power generation for each on-line unit. In the methodology proposed this step is already completed off-line, being the cost calculation and power allocation done by a simple arithmetic process which is faster than a traditional ED. Also a new metaheuristic is proposed to solve ED, mainly for units with non-convex cost functions and it demonstrated its good convergence and search capacity.

Other noticeable difference is related with the *N*-1 reliability assessment. Contrary to the proposed methodologies based on scenarios, with the incorporation of the *N*-1 reliability in the risk costs, there is no necessity of multi-stage stochastic programming (which is time consuming). In the scheduling formulation, the network model was not considered as well as minimum up or minimum down time for the thermal units. However, these changes could be introduced without major efforts.

At the end, the methodology will allow a more effective proceeding to deal with uncertainty and variability of RES and it can be an important tool to be used by the grid operators in insular environment.

CHAPTER 5

Application of the developed methodology to a power system of an island

Contents

In this chapter case studies based on the proposed methodology are presented. A net load forecasting is done followed by a single-period and a multi-period unit commitment based on risk assessment. The scheduling proposed by the system operator in São Miguel Island is presented and compared with the results from the proposed methodology. At the end some reliability indices are presented and discussed.

5. Application of the developed methodology to a power system of an island

5.1 Introduction

This chapter presents case studies regarding the proposed methodology for the generation scheduling with large penetration of renewable energy sources. The case studies are based in São Miguel Island and result from a narrow collaboration between the system operator *Electricidade dos Açores* (EDA) and *Smartwatt, Solutions for Energy Systems* under the scope of SINGULAR project (*http://www.singular-fp7.eu*). The power production (wind, thermal, geothermal, and hydro), wind power limitation and load data was provided by EDA, while the renewable power forecasts for wind, hydro and geothermal were provided by *Smartwatt, Solutions for Energy Systems*.

The complete study will go throughout the *net load* forecasting and its analysis. A single and a multi-period unit commitment covering 7 days between 0h00 of February 25th up to 23h00 of March 3rd 2014 are analyzed.

The forecasting horizons provided by the forecasting tool may be from 24 hours up to 7 days ahead, refreshed each 6 hours. In the cases studies the forecasting horizon was 24 hours ahead. The choice of a 7 days study intends to test the behavior of the proposed method for different days of the week (working days and weekends). The results obtained such as, scheduling, number of startup, spinning reserve, partial and total cost will then be compared with those resulting from the system operator decisions. It is intended to compare the approach proposed in this work with a real environment of a real power system and to conclude about the added value of the developed methodology.

5.2 Net load forecasting

Following the proposed methodology presented in chapter 4, to do the scheduling of thermal units it is mandatory to have the knowledge of the *net load* that has to be fed by the thermal units. As explained in chapter 3, the forecasts of *net load* result from the convolution of the various forecasting probabilistic distributions. In the case of São Miguel Island: load minus the sum of the productions from wind, hydro and geothermal (renewable production).

The load, hydro and geothermal production forecasts do not exhibit considerable challenges since they all are based in historical datasets, which are strongly connected with the explanatory variables. In the case of load greater errors may arise if the real conditions are not sufficiently envisaged in the dataset for a certain forecast moment. For instance, national or regional holidays, abnormal temperatures for a certain period of the year, general strike, among others.

In the case of geothermal units, the power production is dependent on a renewable, but easy to control, resource. The production is defined by set points and rarely suffers big changes. For this reason it is used as the base of the load diagram. In this case, the main source of the deviation between what was forecasted and the real production is the unexpected outages of some units.

In the case of hydro production, in São Miguel Island the hydro storage capacity is negligible; due to this, the power production cannot be delayed from the moment when it rains until the moment when there is the necessity of power production. On the other hand, as the watersheds are not big enough to introduce a significant delay between the rain period and the production, the hydro power forecast depends only from the rain forecasts, which are the main source of errors.

The wind power forecasts introduce a different kind of problem, because the measured values of production could not be fully linked with the explanatory variables due to wind power curtailment. Even with accurate forecasts of the explanatory variables, remarkable errors can occur. As proposed in chapter 3, a filtering technique was introduced in order to produce "real" wind power forecasts. The scheduling processes presented in the case studies are carried out on the assumption that the *net load* forecast results from wind power forecasts without curtailment. As the measured values of wind power, and consequently the *net load* provided by the system operator, may present wind curtailment, the comparison of the results achieved by the forecasts and measures may not be fair. To support this allegation, the measured and the estimated wind power without curtailment are shown in figure 5.1. This situation will be highlighted during all case studies.

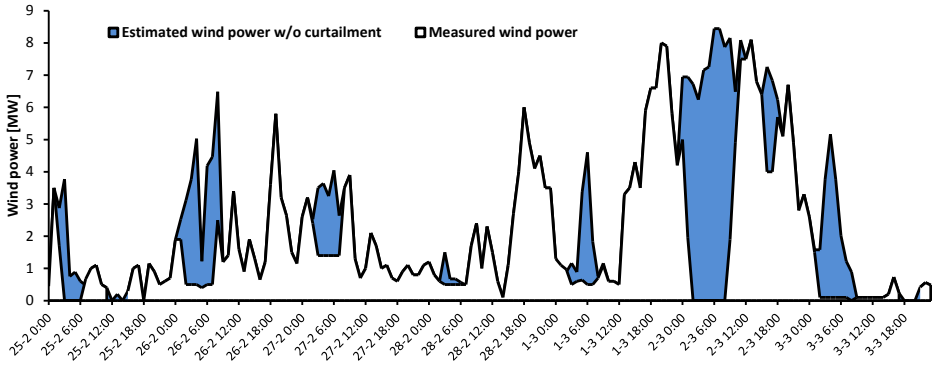

Figure 5.1 – Estimated wind power without curtailment and measured

The estimated values of wind power without curtailment were based on the procedures described in point 3.5 and calculated when information of wind power restrictions was available. Despite possible errors introduced by the approximated power curve of equation (3.10), the amount of wind power which is not used (wasted) is noteworthy. The wind energy

wasted during the period under analysis can be estimated in approximately 143 MWh. Reducing the waste of "clean" energy and, consequently, reducing the production costs is one of the main objectives of this research.

Figure 5.2 shows the forecasted *net load* with the interval forecast with a nominal coverage rate (1-α) equal to 0,8, as well as the measured values. To feature the wind curtailment accomplished during the period under study, the wind power limitations decided by the system operator are also depicted. Additionally, the possible measured values that the *net load* could present, in absence of wind curtailment are shown. Under this conditions the BIAS of calculated errors was -0,5%, while RMSE and the SDE were 7,5%. As base for the percentage, it was chosen the highest value of *net load* during the case study.

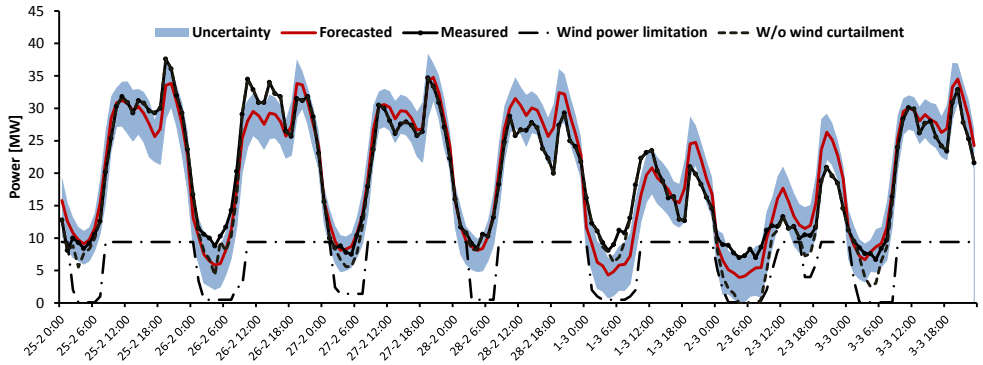

Figure 5.2 – Measured and predicted values of *net load* for the case study

In a first analysis it is clear that the system operator opted for wind power limitation during all off-peak periods. Considering that when there is effective wind curtailment, the *net load* tends to grow, it is explained why, in some cases, in off-peak periods the *net load* with wind curtailment tends to be higher than those forecasted, as it happened in February 26th and March 1st and 2nd. Notice that this analysis is done under the assumption that there were no notable errors in the remaining load, hydro and geothermal forecasts. A deeper analysis can be done regarding the impact that the wind power limitation has in *net load* forecasts.

5.2.1 Net load probabilistic forecasting assessment

As noted in chapter 3, the performances of the *net load* probabilistic forecast can be assessed by some indicators. In this case the reliability, sharpness and resolution will be assessed. The dataset under study was composed by hourly forecasted and measure values of *net load* with and without wind curtailment, between January 1st and March 3rd 2014 (the dataset to training the model was composed by the hourly average values of 2012 and 2013). In figure 5.3 the

reliability of the *net load* probabilistic forecast is shown. In addition, the "ideal" reliability is shown too.

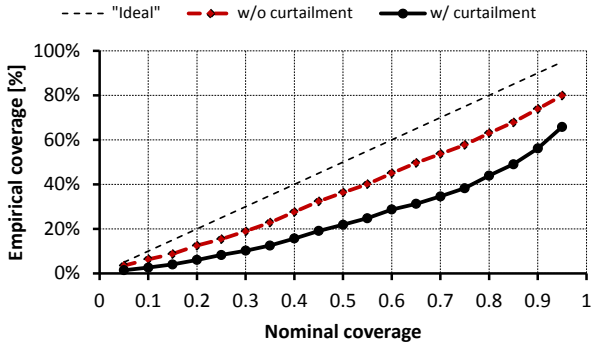

Figure 5.3 – Reliability diagram of the probabilistic *net load* forecast

From the figure 5.3 it is clear that the forecasting method used in this approach tends to systematically underestimate the uncertainty [9],[13] and [52] since forecasted quantiles proportions are lower than the empirical ones. Thus, the measured values of *net load* outperform all estimated quantiles, meaning that the probabilistic forecasts have an associated bias. These considerations are done based on the historical dataset between January 1st and March 3rd. In the case of a larger dataset, the results could be different (generally presenting less bias). Besides, after an analysis of all the forecasts from which results the *net load*, it was concluded that the geothermal forecasts presented a very significant error (during 202 hours) when the geothermal power plant of *Ribeira Grande* was offline. This situation was not reported by the system operator, allowing the forecasting error to persist. This fact confirms the importance of the measures provided by SCADA systems in order to incorporate more recent values to improve the forecasting models. In figure 5.4 the forecast and measured geothermal power production are shown.

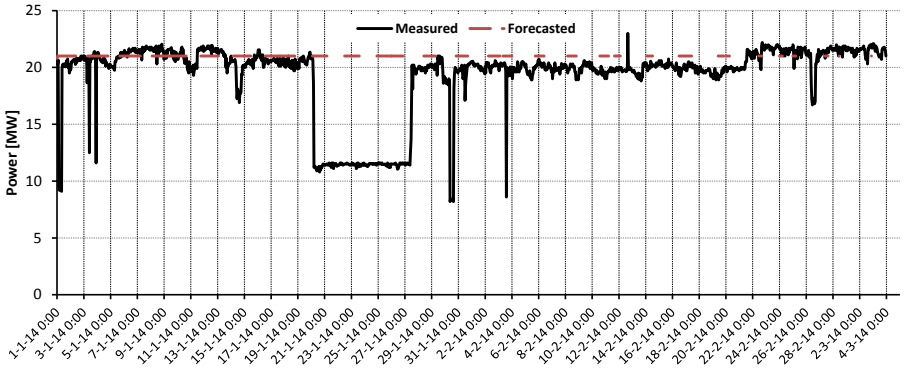

Figure 5.4 – Geothermal power production (January 1st up to March 3rd)

This situation occurred during almost 15% of the time used to calculate the reliability which introduced a remarkable error. In figure 5.5, the reliability calculated after the elimination of these "unexpected" values from the dataset is shown.

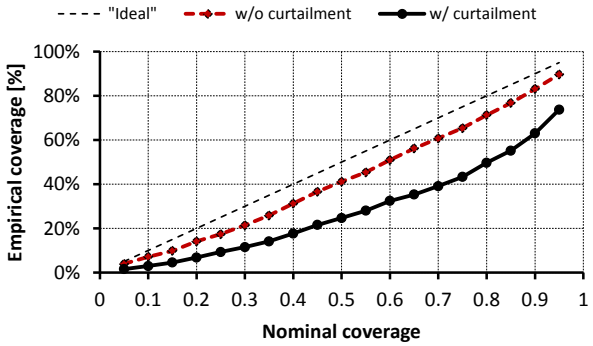

Figure 5.5 – Reliability diagram (with the removed values)

Although the continued underestimation, there are noticeable differences, with the bias reduction. Equation (5.1) allows a more intuitive way to analyse the bias of the probabilistic forecasting methods, representing it as a deviation from the "ideal" reliability,

$$\bar{b}^{(\alpha)} = \frac{1}{k_{\max}} \sum_{k} \left(\alpha - \hat{a}_k^{(\alpha)} \right) \tag{5.1}$$

where $\bar{b}^{(\alpha)}$ is the bias, α the nominal proportion, $\hat{a}_k^{(\alpha)}$ is the empirical coverage and k_{max} is the forecasting length. Applying equation (5.1) to the above data set results in the reliability diagram shown in figure 5.6.

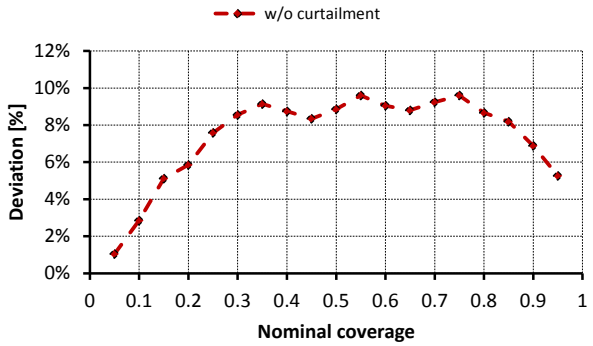

Figure 5.6 – *Net load* forecasting reliability diagram (deviations from "ideal" reliability)

In figure 5.6 it is visible that the uncertainty was underestimated for all predicted quantiles. It should be noticed that the *net load* results from four different variables forecasts, with different values and profiles of uncertainty.

For the same data set of the previous analysis, it was calculated the sharpness, as shown in figure 5.7.

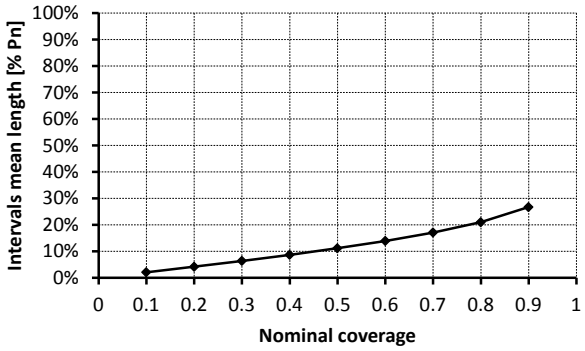

Figure 5.7 – Sharpness diagram of the probabilistic *net load* forecast

The values of the sharpness are relatively low, with a nominal coverage of 0,9, corresponding to 27% of the rated *net load*. For rated *net load*, it was considered the highest value registered in the data set (36,8 MW).

Until now it is clear that it must be a trade-off between the reliability and the sharpness, because improving reliability will usually worsen the sharpness [7],[9],[13] and [52]. Low values of sharpness can lead to "narrow" uncertainty intervals which can result in underestimation or overestimation of the uncertainty, with consequent degradation of the reliability. An indication to narrow intervals is when there is an overestimation to nominal coverages below 0,5 and underestimation above 0,5 [13],[138]. On the other hand, high values of sharpness could increase the uncertainty interval thus improving the agreement between the nominal proportions and the empirical ones. The drawback is that too high values could cover extreme prediction errors or even outliers. Summarizing, all measured values would fall inside the uncertainty interval. This question can be overcome with a deeper investigation concerning the kernel's bandwidth, which should be object of a future investigation. The fact of the evaluation set is reduced can influence the values of the reliability and sharpness, thus with a larger evaluation set is expected to witness better results.

Another criterion which can be used for the evaluation of probabilistic forecasts is the resolution [6],[8]. It represents the capacity of the forecasting model to provide situation dependent forecasts and it can be measured by the standard deviation of the predictive intervals size since it is not possible to directly verify this property. Figure 5.8 shows the resolution of the probabilistic *net load* forecast. In general and contrarily to sharpness, increasing the resolution gives more value to the probabilistic forecasting method [116]. Large standard deviations reveal that the probabilistic forecasting method has the capacity to represent a wide set of real situations.

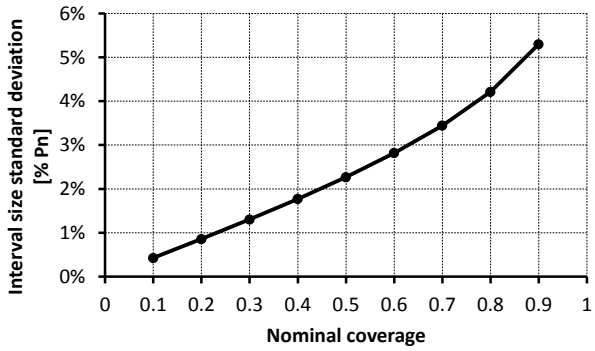

Figure 5.8 – Resolution of the probabilistic *net load* forecast

As seen in figure 5.8 the standard deviation interval size is relatively low with a resolution of 5,4% to a nominal coverage of 0,9. This value results from the smoothing effect of the aggregation of renewable production and load forecasts. Throughout the data set it is verified that the *net load* does not reveal notable changes when submitted to identical inputs and, consequently, the uncertainty profile does not significantly change along the data set.

Considering the proposed methodology for UC based on risk assessment on point 4.5, it is clear that the reliability, sharpness and resolution provide meaningful information to evaluate the potential impact of the *net load* forecast. Following the analysis of [9], reliability is important because the quantiles are related with the energy and power generated. Sharpness provides significant information: shapes of distributions tails have a crucial role for the calculation of the risks of load shed and wind curtailment.

As overall conclusion, this analysis is quite revealing of the *net load* forecasting challenges in this work and the implications on the scheduling process.

5.3 Unit commitment under uncertainty based on risk assessment

The case study will be divided into two cases. In the first, the unit commitment is solved on a single-period approach in order to evidence, in a real environment, the logic behind the proposed approach. As it is a single period approach, the transition costs between time periods (startup costs) are not included. Said this, the analysis is faced as a snapshot for each hour. Blackout costs, as well as unexpected outages of thermal units are not included.

The second case study presents a multi-period approach where all the previously mentioned costs and outages are integrated. In both studied cases the power grid is not contemplated and thus, there are no power losses, power grid congestions or lines outages. This kind of question could be integrated in future works. In table 5.1 some parameters used in the studied cases are presented.

Table 5.1 – Parameters for each case study

Case study parameters	Case 1	Case 2
$Cost_{Load\ shed\ €/MWh}$	1200	1200
$Cost_{Wind\ Curtailment\ €/MWh}$	150	150
$Cost_{Minimum\ violation\ €/MWh}$	157.5	157.5
$Cost_{Fuel\ €/g}$	0.0007	0.0007
$Probability_{Contingency\ \%}$	-	1.5
$Cost_{Blackout\ €}$	-	10 000
$Cost_{Start\text{-}up\ GS\ €}$	-	100
$Cost_{Start\text{-}up\ GB\ €}$	-	150
Threshold	-	1000

The economic impact of an energy interruption, due to load shed for instance, depends on the interruption cost (€MWh^{-1}) and the amount of unserved energy (MWh) [158],[159]. The interruption cost must be obtained from specific studies which assess the damages caused by the supply interruption to each class of consumers like residential, commercial or industrial. It also depends on several characteristics such as duration, frequency, duration of occurrence, depth of curtailment, the existence of a warning time, and geographical coverage [158],[159]. As in this work these issues were not a subject of study, the unit interruption cost was assumed as 1200 €/MWh.

The wind curtailment is an operational issue which will result on a costly operation to the system operator (because the thermal units have to cover the power curtailed). Considering the average cost of thermal production, it was assumed a penalty of 150€ for each MWh of wind curtailed (average marginal cost of thermal units).

In São Miguel Island there are thermal units that have to guarantee the constancy of the frequency. The loss of the total thermal production should lead to a blackout, which must be avoided at all costs and for this the blackout cost was set to 10000 €.

The thermal units are projected to work within their production limits, burning heavy fuel oil, and the efficiency is strongly dependent on the production level. When the units have to work below the minimum, they generally burn diesel. Following this and for not extrapolating the cost function to production values below the minimum, it was chosen a constant value of 157,5 € for each MWh. Within the technical limits the fuel cost was set to 0,0007 €/g (maximum price in 2012). This value, multiplied by the consumption equation of each GENSET defined in point 4.3.3, will give the thermal cost production. The parameters of consumption equations were determined off-line and are shown in tables AII.5 up to AII.7 in annex II. Remark that parameters presented in these tables will be constant, at least until the construction or decommissioning of some thermal unit. In case of some unit remains off-line for an extended period, minimal changes are needed and it is enough to cut the GENSET $4G_S\_4G_B$ option. Only on the second case study the starting costs of the thermal units were defined, as well as the probability of unexpected outages of thermal units. The threshold of

equation (4.42) used in the dynamic programming, as explained in point 4.7.1, is also referred and set to 1000.

In order to assess the performances of the proposed approach, a comparison towards the scheduling decided by the system operator for the same period under study will be done. This analysis comprises the total operation costs, number of maneuvers (startups), spinning reserves, wind curtailment, load shed and thermal production below the minimum limits.

The single-period UC was implemented in *Microsoft Excel* and the multi-period in *Matlab*®.

5.3.1 Single period unit commitment

To illustrate the analysis which is behind the risk assessment methodology, in a first approach it was considered that a constant GENSET was maintained online during 24h, independently of the dynamic of the *net load*. In figure 5.9 an example of *net load* forecast for a 24 h period is shown. The point forecast and the maximum and minimum values of the uncertainty probability distribution, respectively $max_{(L\text{-}RES)}$ and $min_{(L\text{-}RES)}$, are represented by L-(W+H+Geo). In the same figure the minimum values of probability distribution resulting from the complete wind curtailment (L-H-Geo) are also shown.

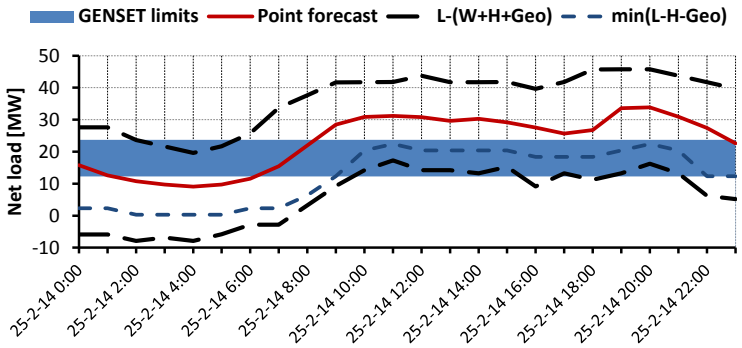

Figure 5.9 – *Net load* forecasting for 24 hours ahead

During this time period it was considered that only the GENSET $1G_S\_1G_B$ was maintained on-line, with its production comprised between 12,3 MW and 23,7 MW, corresponding respectively to the minimum and maximum production. Considering the example at 4:00, in analogy with figures 4.25 and 4.29, it is visible that the minimum *net load* is lower than the GENSET limits, which results in a certain probability of wind power curtailment (Loss Of Wind curtailment Probability - LOWP). It's also visible that even with total wind curtailment the new value of *net load* calculated by (L-H-Geo) is still lower than the GENSET limits. It means that with this GENSET, at this hour, even with total wind curtailment, the thermal units should work below their technical limits with a certain probability (Below Minimum Generation Probability - BMGP). Furthermore, there is no necessity of load shed because the

net load limit is lower than the GENSET maximum, meaning null probability (Loss Of Load Probability - LOLP).

Analyzing the case at 8:00 and concerning the wind curtailment, it is similar to the case at 4:00. In addition there is also a probability of load shed, once the GENSET maximum limit is lower than the maximum of *net load*. Summarizing, at the same hour there is a probability of the *net load* to fall within the GENSET limits (Normal Operation Probability - NOP), probability of wind curtailment (LOWP), load shed (LOLP) and unit's to work below the minimum (BMGP).

At 20:00 there is no necessity of wind curtailment corresponding to a null probability. On the other hand the probability of load shed is high due to the large difference between the $max_{(L\text{-}RES)}$ and the maximum production available by the GENSET. Finally, there is the case at 23:00, where the minimum of (L-H-Geo) is higher than the minimum of GENSET. Consequently, although the necessity of wind curtailment being present, the wind power available to curtail is enough to guarantee that thermal units do not work below the minimum.

In figure 5.10, the risks associated of the probability distribution of L-(W+H+Geo) with the GENSET $1G_S\_1G_B$ for a 24h example are shown.

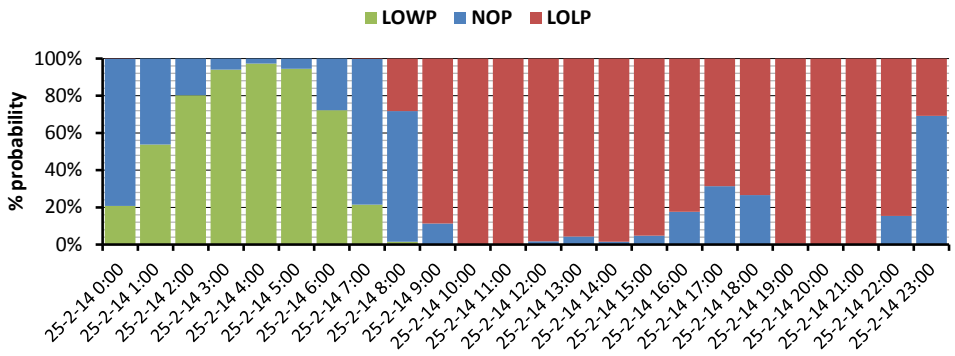

Figure 5.10 – Risk associated to GENSET $1G_S\_1G_B$ operation

It is visible that the major risk of wind curtailment occurs from 1:00 up to 6:00 with a probability greater than 50%. On the other hand there is a high risk of load shed between 9:00 and 22:00. The periods with lower LOLP and LOWP occur at 0:00, 7:00 up to 8:00 and 23:00. With the risk values and the cost penalties presented in table 5.1, it is possible, using equations (4.33) up to (4.36), to calculate the different contributions to the total risk cost. In figure 5.11 the percentage of the total risk cost associated to each risk value is shown, where (BMGC) represents the cost of the units to work below the minimum, (LOWC) the cost of wind curtailment and (NOPC) and (LOLC) are the costs of normal operation and load shed, respectively.

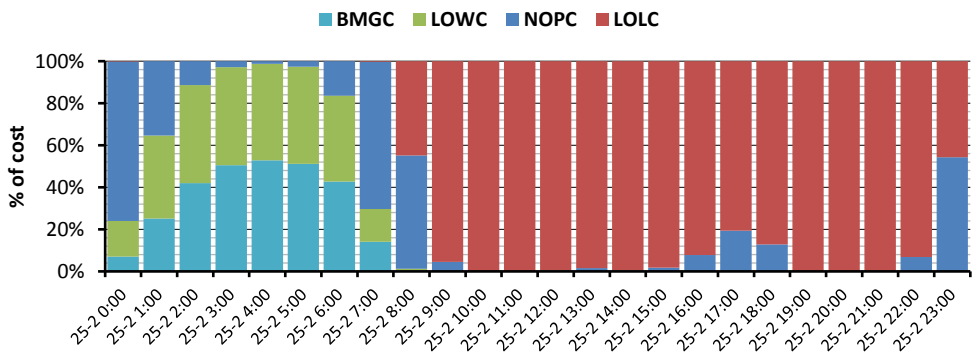

Figure 5.11 – Percentage of risk costs associated to GENSET $1G_S$_$1G_B$

As expected, in off-peak periods (mainly since 1:00 up to 6:00) the penalties related with wind curtailment have an important role to the total cost. Although the high probability of wind curtailment, the quantity of wind power able to cut is small. Because of this fact, the necessity of the thermal units to work below the minimum is present, leading to high associated costs. In the case of load shed, due to its high unitary cost, the associated percentage of the total cost is higher than the associated probability. For instance at 23:00 the probability of load shed is approximately 0,308 but the cost associated is 45,7% of the total cost. Obviously, this analysis is strongly dependent from the associated costs to each risk. At the end, the risk cost associated to each hour of the GENSET functioning is shown in figure 5.12. During the off-peak period the costs are fundamentally associated with excess of thermal power, while in the rest of the day there is a clear lack of available power, conducing to load shed with high costs. Notice that the calculated costs are risk costs, widely different from the real costs calculated *a posteriori* with the measured values.

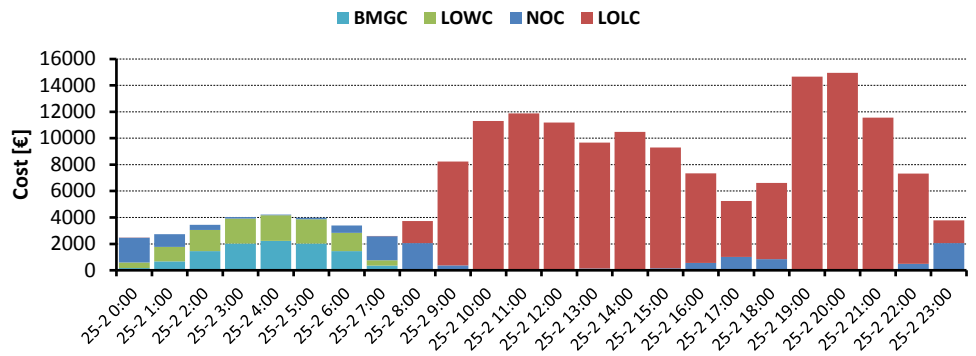

Figure 5.12 – Cost associated to GENSET $1G_S$_$1G_B$

A resume of the study done is presented in table 5.2.

Table 5.2 – Probability and risk costs for GENSET $1G_S\_1G_B$

	Net load		Probability				Risk costs [€]				
hour	Min	Max	NOP	LOWP	LOLP	BMGP	NOC	LOWC	LOLC	BMGC	Total
4	-7,88	19,61	0,028	0,972	0,000	0,949	53,6	1937,8	0,00	2226,07	4217,47
8	3,24	37,65	0,703	0,015	0,282	0,009	2011,1	28,58	1675,34	28,58	3732,58
20	16,25	45,75	7,1e-6	0,000	0,999	0,000	0,02	0,00	14950,87	0,00	14950,89
23	6,02	41,71	0,691	0,001	0,308	0,000	2054,99	2,65	1733,26	0,00	3789,90

Research continued with another study being envisaged, here it is considered an hour period (8:00 of February 25th) where all GENSET's are assessed. Following the minimum and maximum of forecast uncertainty distribution, the *net load* can vary between 3,24 MW and 37,65 MW. In figure 5.13 the risks associated to each GENSET at 8:00 are shown.

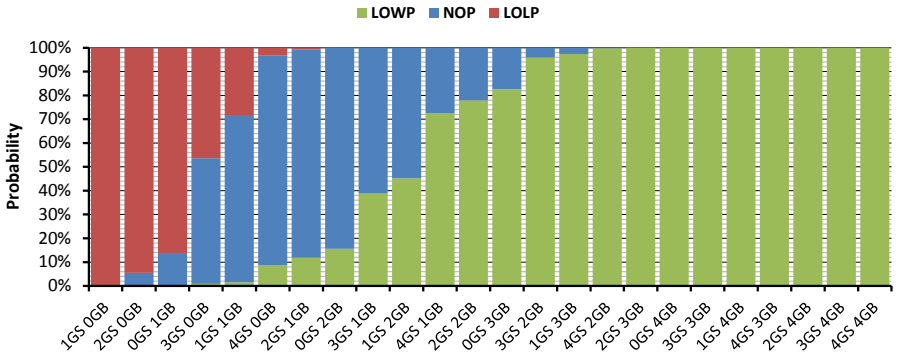

Figure 5.13 – Risk assessment for all GENSET's at 8:00

It is clear that the GENSET's with lower rated power have the high risk of load shed while in those with high rated power the high risk is related with wind curtailment. The GENSET's $4G_S\_0G_B$ and $2G_S\_1G_B$ are those presenting the lowest risk of load shed and wind curtailment and, consequently, the lower penalties and risk costs, as shown in figure 5.14.

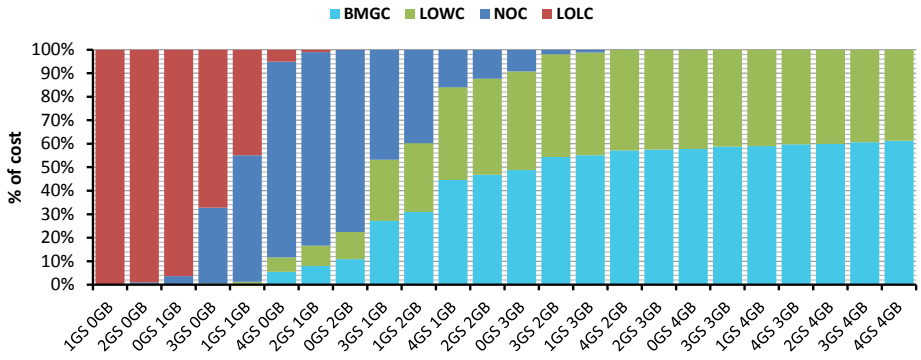

Figure 5.14 – Percentage of total risk costs for all GENSET's at 8:00

From the GENSET $4G_S\_2G_B$ the percentage of risk costs related with wind curtailment does not increase significantly. The power value for wind curtailment reaches the limit of available wind to curtail (forecasted) as shown in equation (4.29). At this point the risk cost of the wind curtailment only depends from the LOWP as shown in equation (4.33). From where the

maximum of wind curtailment is reached the risk cost related with the unit's operating below the minimum starts to increase. In figure 5.15 the risk costs associated to each GENSET are shown.

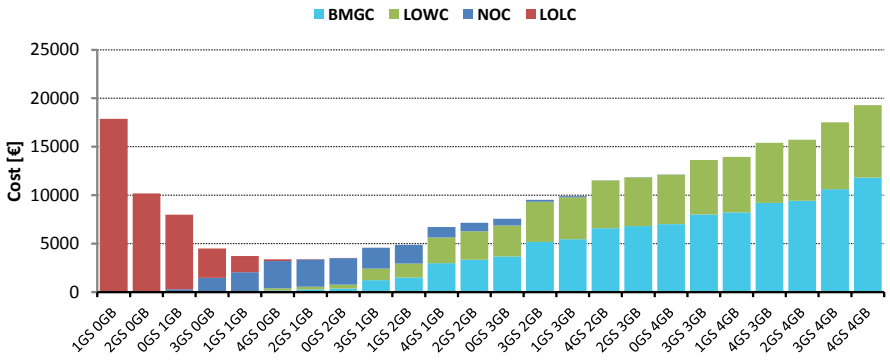

Figure 5.15 – Total risk cost to all GENSET at 8:00

As analysed in figure 5.15, the GENSET $4G_S\_0G_B$ is the one which presents the lowest risk cost. However, it must be noticed that it has as limits 15,39 MW and 28,8 MW and the *load net* 3,25 MW and 37,65 MW. There is always a probability of the thermal production not to be enough to feed the load or to be excessive when compared with the load necessities. Yet and despite of significant difference between maximum *net load* value and the GENSET's maximum, the LOLP is low (0,03). On the other hand the LOWP, associated to the difference between minimum *net load* and GENSET's minimum, is (0,09). Due to the differences between the penalties, the risk cost of load shed is comparable with the wind curtailment cost, clearly reflecting the weight given to the load shed.

This is a study that has to be done to each hour and to each GENSET in order to evaluate, by equation (4.37), the lowest cost to each *net load* forecast. As in the traditional approaches, it is mandatory to solve the ED to evaluate the power allocated to each GENSET's unit. With the equivalent cost generator proposed in 4.3.3 this process is very fast. The risk cost and the power allocated to each unit of the GENSET are evaluated by a simple calculation in function of *net load*. With this information it is possible to define the committed units to each hour ahead. The process presented in figures 5.13 up to 5.15 was computed to a 168 hours period resulting in the single-period UC. In the figure 5.16 are represented the *net load* forecasts as well as the uncertainty associated (nominal coverage of 0,98) and the GENSET's power limits.

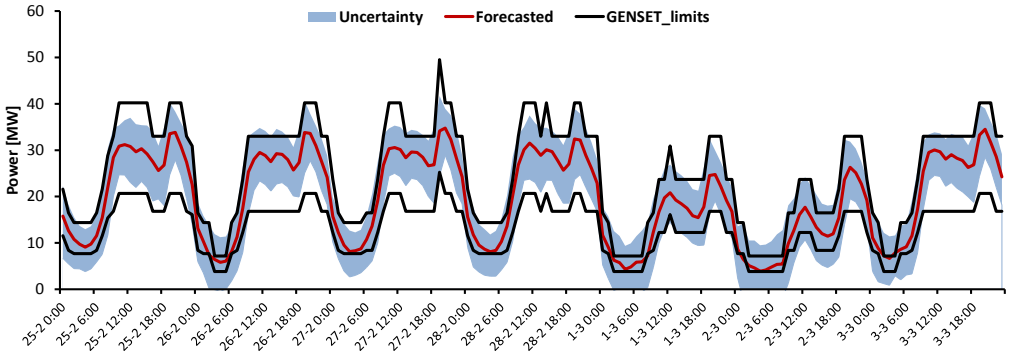

Figure 5.16 – Single-period unit commitment

The first conclusion taken from the figure 5.16 is the high number of manoeuvres. This happens due to the inexistence of starting costs, not adding any additional cost to the scheduling. For this, during the time period under study there were 70 changes in the committed GENSET's, resulting in 47 start-ups of units of type G_S and 19 of type G_B, which is a very significant number.

It is also seen that the *net load* uncertainty is relatively well covered by GENSET's available power, but it is evident that there always is a risk associated, mainly when GENSET's with narrow limits are chosen. This situation is mainly evident in off-peak periods and when there is only a single thermal unit on-line. To a better comprehension, in table AIII.2 of annex III, the chosen GENSET for each hour is shown. This situation is possible because the contingency criterion *N*-1 was not assessed and the blackout cost was not included.

The important information that must be retained is the resulting reserves in order to deal with unexpected changes in *net load* or power production. These changes can have different natures, such as outages related with equipment's malfunctioning, accidents (generation units or transmission lines) or forecasting errors.

In figure 5.17 the upward and downward reserves resulting from the scheduling are shown. Upward and downward reserves have different roles. The first intends to answer to a loss of power production due to generation outages or forecasting errors (when the forecasted power production is lower than the real one or if the load forecasted is lower than the real one). The second is generally related to forecasting errors when the power production is higher than the predicted or the load is lower than the forecasted.

An issue that must be highlighted is the fact that there was no predefined value for the reserves, as it occurs in several approaches listed in bibliography. These reached reserves are dynamic and implicitly result from the uncertainty and proposed methodology.

From figure 5.17 it is visible that with the obtained scheduling, both upward and downward reserves do not have the same profile, with an average forecasted upward reserve of 5,75 MW and average forecasted downward reserve of 6,63 MW.

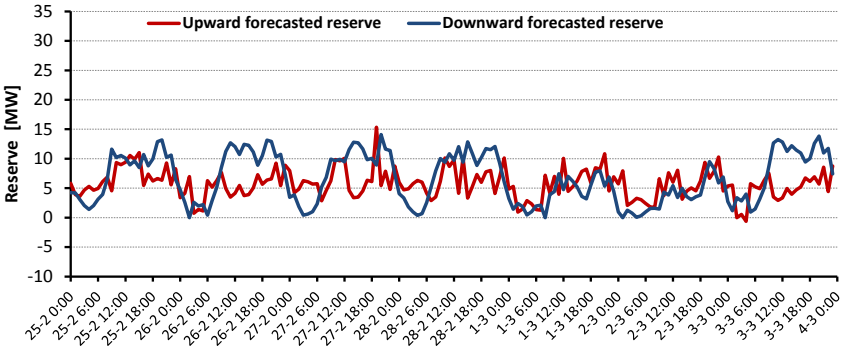

Figure 5.17 – Upward and downward forecasted reserves

In this first case study the *N*-1 criterion was not taken into account, thus the reserves should only cover the *net load* forecasting. Negative values for the reserves in some short periods of time are noticed. It is considered that the regulating reserves are defined by the thermal units, however, in case of lack of downward reserves, wind curtailment can be done to avoid thermal production to be below the minimum. As a consequence, if there is any negative downward reserve (thermal production higher than the *net load*) during the scheduling, wind production can be limited to avoid reserve negative value. In case of upward reserves there is a prediction of 2 hours of load shed. In case of downward reserves there are no negative values because 3 hours of wind curtailment are predicted. According to forecasts there is enough wind power production to curtail during these periods. Thermal units can work below the minimum only if there is not enough wind power to curtail. The expectable value of energy shed for the entire case study is 0,66 MWh and the wind curtailment is 1,95 MWh. Concerning the production below the minimum of thermal units, the predicted value is 0 MWh.

5.3.1.1 Validation of single-period unit commitment

In order to assess the performances of the proposed methodology, in figure 5.18 the single-period UC and perspective measurement of *net load* without curtailment is shown.

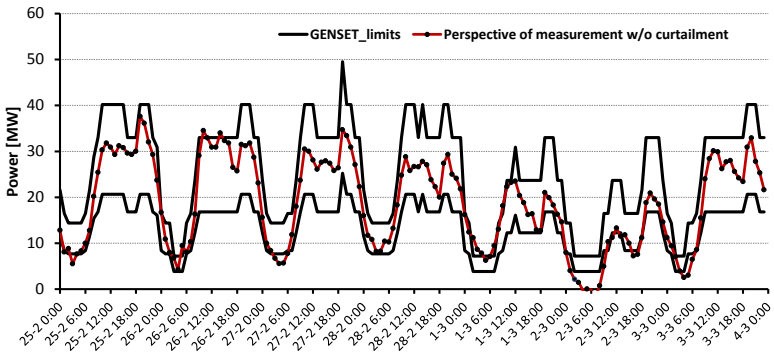

Figure 5.18 – Single-period unit commitment and perspective measurement of *net load*

It is observed that, generically, though there is an increment of the load shed and wind curtailment caused by forecasting errors, the obtained UC is still adequate to feed the *net load*. This means that the effectiveness of the reserves is strongly dependent on the *net load* forecasting performances. The measured values follow adequately the forecasted values despite *net load* point forecasts being generally greater than those measured (approximately in 68% of the time). In figure 5.19 the forecasted *net load* and the perspective of measured *net load* when considering absence of wind curtailment are shown.

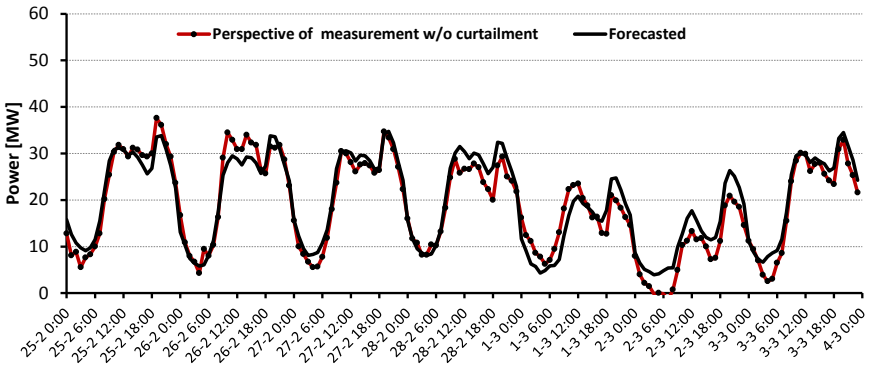

Figure 5.19 – Net load point forecast and perspective of measurement without curtailment

Both curves have the same profile. However, there are some prediction errors which can have some impact in the reserves. In table 5.3, the forecasted values and the measures of load shed, wind curtailment and thermal production below minimum, are shown.

Table 5.3 – Measured and forecasted energy below and above the GENSET limits

	Load shed [MWh]	Wind curtailment [MWh]	G < min [MWh]
Measured	14,92	50,28	0,90
Forecasted	0,66	1,95	0

Deviations introduced by the forecasting errors, both in load shed and in wind curtailment are observable with wind curtailment having more impact.

By the forecasting, 2 hours with load shed, 3 hours with wind curtailment and none with the thermal units working below the minimum were expected. In reality there were 7 episodes with a total of 9 hours of load shed and 8 episodes with a total of 24 hours of wind curtailment. There was only one hour where the wind curtailment was not enough, forcing the units to work below the minimum. Because of this, the reserves have suffered changes in their behaviour. In figures 5.20 up to 5.22 the upward and downward reserves are shown together with the comparison between forecasted and measured values.

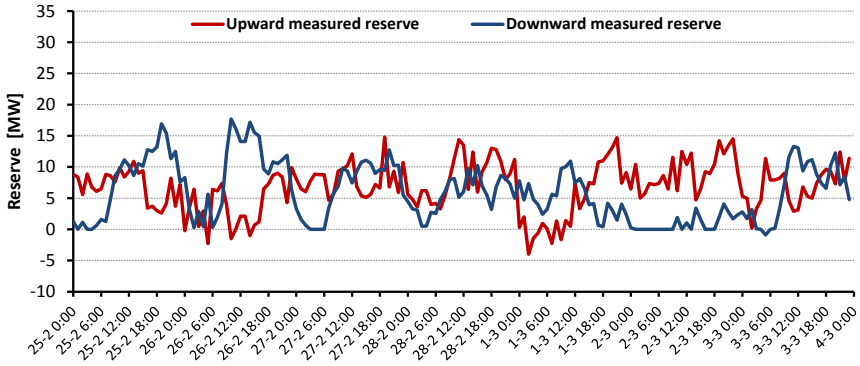

Figure 5.20 – Upward and downward measured reserves

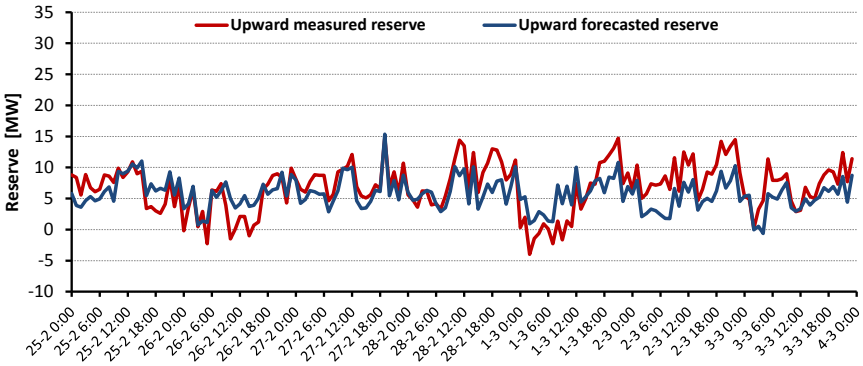

Figure 5.21 – Forecasted and measured upward reserves

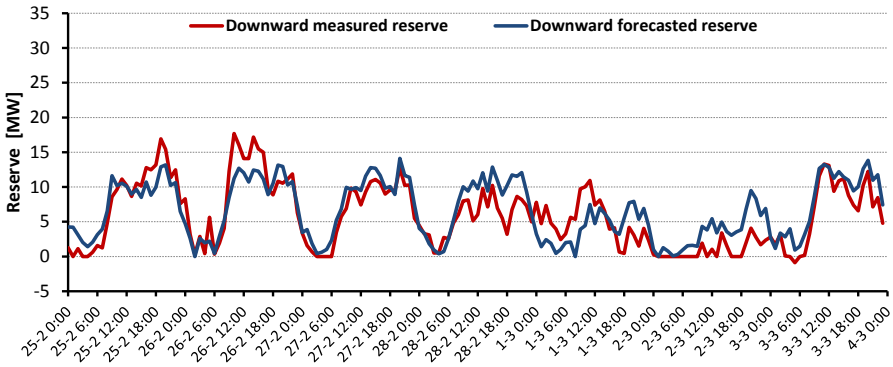

Figure 5.22 – Forecasted and measured downward reserves

Apart the increment of load shed and wind curtailment (waste of renewable resources) there were deviations of the average reserves. The forecasted downward reserve decreased from 6,63 MW to 5,58 MW, while the upward reserve increased from 5,75 MW up to 6,80 MW.

5.3.1.2 Comparison with system operator scheduling

Despite the acceptable results obtained in the previous approach, in this point a comparison with the solutions chosen by the São Miguel system operator to the same time period will be done. In this analysis it is considered that the scheduling solutions are not based on *net load*

forecasts, being all decisions supported by some rules of thumb. The larger impact, probably belongs to the obligation of maintaining at least one thermal unit type G_S and another G_B ($1G_S\_1G_B$) online, which results in a minimum limit of 12,26MW. In figure 5.23 the São Miguel system operator's committed thermal units' limits and real measured *net load* are shown. It should be noticed that the measured values were provided by the system operator without any handling.

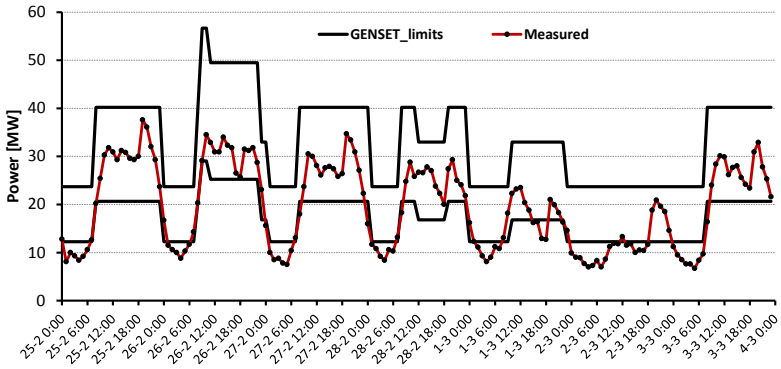

Figure 5.23 – Measures of *net load* and committed GENSET limits

Compared with the previous scheduling, there are three main differences; the first is the reduced number of manoeuvres, with the same set of units working during larger periods. This is clearly visible during March the 2nd, where the same configuration was maintained during 33 consecutive hours, even with multiple episodes of *net load* being below the minimum of thermal units. During a 168 hours period were only registered 16 changes in the thermal unit configuration, varying between 5 and 0 manoeuvres a day. During a 168 hours period, 3 start-ups of units type G_S and 7 of units type G_B were counted, against the 47 and the 19, respectively, of the previous approach. The second big difference is the number of hours where the *net load* was lower than GENSET limits. This aspect may reveal a concern about the number of start-ups (in order to decrease the costs), the number of hours where the units must be online or crew restrictions for start-up or shutdown manoeuvres. The system operator did not deliver any relevant information about these issues and, therefore, it was considered that only monetary issues were taken into account. The third is related with systematic wind power limitation during off-peak periods. In figure 5.24 the wind power limitation, as well as the measured production, and the perspective of power production without curtailment are shown.

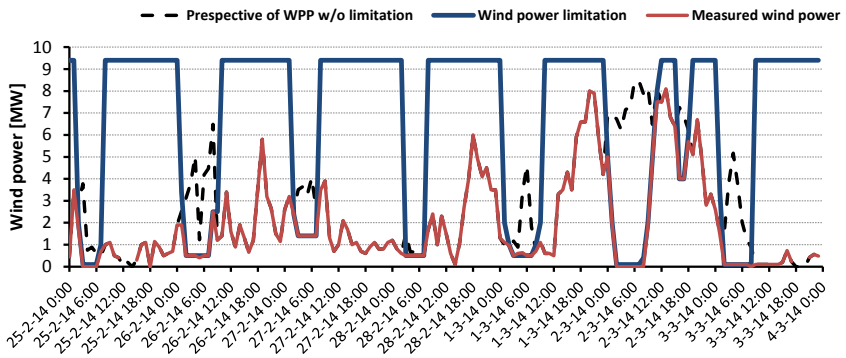

Figure 5.24 – Measures and perspective of wind power production (WPP) with limitation

Contrary to the approach proposed in this work, where the wind power production should only be limited to avoid the production below the minimum, the system operator's scheduling allows wind power limitation and, at same time, units to work below the minimum limit. In figure 5.25 the resulting upward and downward reserves are shown.

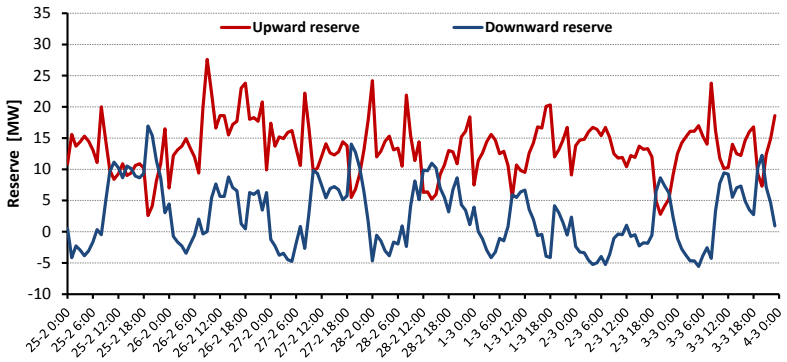

Figure 5.25 – System operator upward and downward reserves

It must be noticed that during all the periods of wind limitation showed in figure 5.24, there were also units working below the minimum. This fact led to negative values of downward reserves.

The calculated average reserve for the period under study is 13,39 MW for upward reserves and 2,63 MW for downward reserves. Compared with those obtained by risk assessment approach it is verified that the upward reserve is higher than the previous one (6,80 MW) and the downward is lower than the previous one (5,58 MW). These differences have dissimilar impacts. For instance, with a larger upward reserve the system operator had never the need of load shed, while the risk assessment approach presented a not supplied energy of 14,92 MWh. On the other hand, the low values of downward reserve result from 143,6 MWh of wind curtailment and 176,37 MWh of thermal units working below the minimums, against 50,28 MWh and 0,9 MWh from the risk assessment.

To a better comprehension, in figures 5.26 and 5.27 a comparison between the reserves obtained by system operator and risk assessment approach is shown.

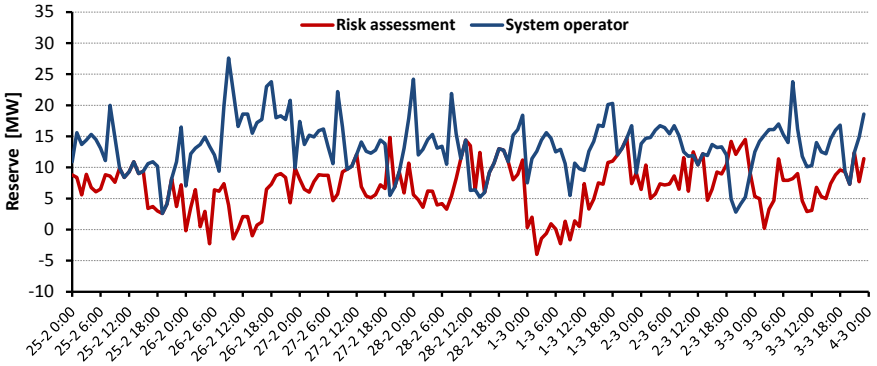

Figure 5.26 – Comparison between upward reserves

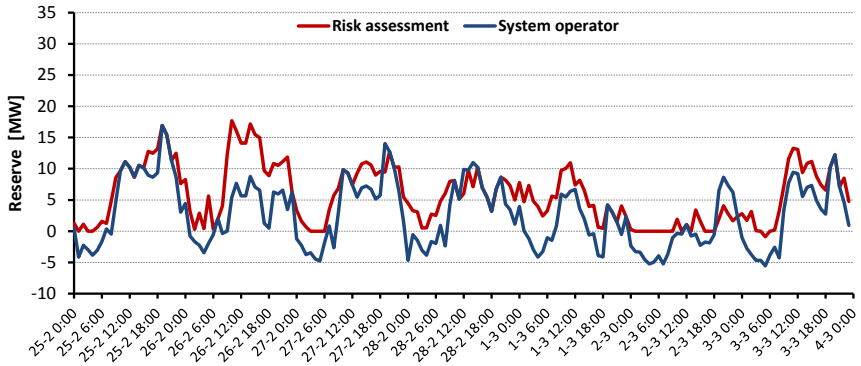

Figure 5.27 – Comparison between downward reserves

From figure 5.26 it can be observed that, generally, the upward reserves obtained by risk assessment are smaller than those obtained by the system operator. Apart from this, also some episodes of negative reserves, which actually is load shedding, were present. On the other hand, in figure 5.27 the downward reserves show the opposite tendency, with reserves achieved by risk assessment showing higher values. At this point, it is visible the difference between both approaches. The risk assessment approach considers that it is preferable to curtail the wind generation instead of the thermal machines to operate below the minimum. It should be remembered that, below the minimum, the efficiency of the thermal units is very low with consequent higher fuel consumption. Also, apparently, the system operator prefers to limit the wind production in a preventive way during the off-peak periods and, when necessary, to decrease the thermal production up to below the minimum. The option of the minimum commitment always being the GENSET_$1G_S$_$1G_B$ potentiates this situation.

This is the first drawn conclusion from the results showed in figures 5.26 and 5.27. Yet, another important conclusion is that, as the choices of the GENSET's are done based uniquely on risk assessment and total cost, there are no infeasible solutions. Due to this, in the case of

risk assessment, there were some hours where the upward reserves were negative, which means that it was cheaper to pay penalties for energy not supplied than to choose a GENSET with more power capacity. Table 5.4 is a summary of the number of hours where both approaches operated below or above the GENSET's limits.

Table 5.4 – Number of hours operating outside the GENSET's limits

	L_shed [h]	W_curt [h]	G < min [h]
Risk assessment	9	24	1
System operator	0	54	68

Besides the number of hours, a more important indicator is the quantity of *net load* which was not fed or fed at the expense of wind curtailment or even with the thermal units below the minimum. In the case of risk assessment, the value of *net load* is based on the assumption that there was no wind curtailment, while in the system operator approach it is the real measured value. Consequently, the comparisons shown in figure 5.28 are done in percentage of the total *net load* of each approach and summarized in table 5.5.

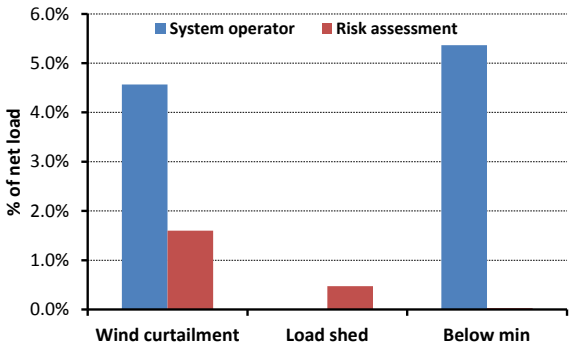

Figure 5.28 – Values outside the GENSET limits, in percentage of total *net load*

Table 5.5 – Values outside the GENSET limits, in percentage of total *net load*

	L_shed	W_curt	G < min
Risk assessment	0,47 %	1,60%	0,03 %
System operator	0,00 %	4,57 %	5,37 %

Except for the of load shed, where the system operator approach presents a null value, the risk assessment approach presents better results for the remaining indicators. Even when the *net load* was lower than the GENSET's limits, it was enough to proceed to wind curtailment to maintain the thermal units operating within their limits. In this case, and deep inside, it was "only" waste of "clean" energy.

Furthermore, in the case of the system operator, the scheduling indicates a special care with the load shed, with a high value of upward reserve even if meaning low downward reserves. So, even with strong wind power limitation, there was a remarkable quantity of energy produced by the thermal units below the limits. In the case of risk assessment the situation is

the opposite. The value of power produced below the minimum is very low but on the other hand, although being relatively small, there is load shed.

So far it can be concluded that this is a problem hard to be solved. If on one side, investment on the avoidance of load shed leads to an increase of the production below the minimum, on the other side the opposite is also true. Once it is known the risk costs to each GENSET and for each hour, it is possible to calculate the total risk cost reached by the system operator solution. The risk cost for the two approaches is shown in figure 5.29. Even with a high penalty due to the load shed, the risk cost from risk assessment reveals to be lower than that resulting from the system operator's scheduling of.

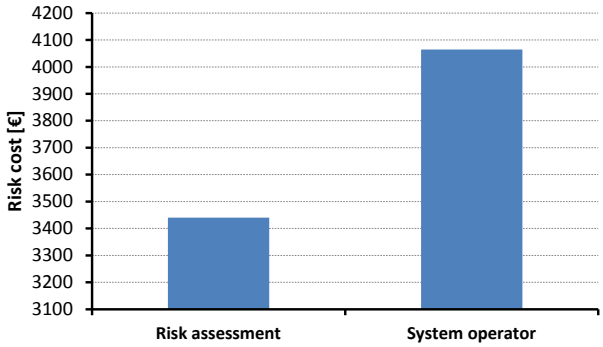

Figure 5.29 – Risk costs for both approaches

At the end, a comparison of the real costs between both approaches is done under some considerations. When the *net load* is outside of the thermal unit limits, the total cost is calculated by the sum of fuel cost (at maximum or minimum) and the remaining *net load* is multiplied by the penalty costs shown in table 5.1. Within the production limits only the fuel costs are taken into account. In figure 5.30 a comparison between the real costs derived from both approaches is shown. Beyond the total cost, also the partial costs are shown in table 5.6 in order to understand the weight each parameter has on the final cost.. The first conclusion is that cost of system operator solutions is 30,98% higher than that obtained by the risk assessment. It is also clear that the bigger portion is resultant from fuel costs.

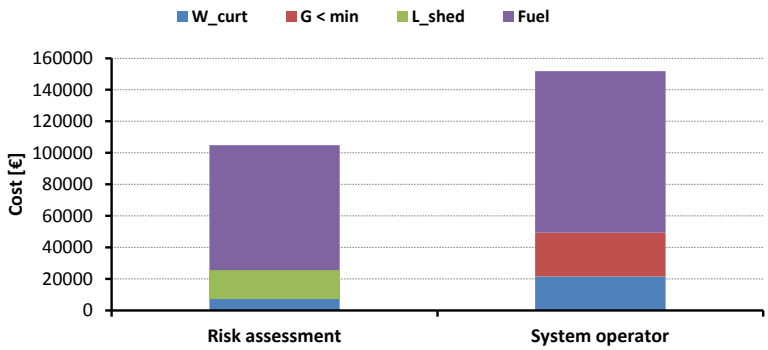

Figure 5.30 – Comparison between total costs for both approaches

The partial costs obtained by the system operator are all higher than those obtained by the risk assessment approach, with exception of load shed. Naturally, the fuel consumption costs are directly related to the commitment of thermal units and the load allocated to each unit. As in the risk assessment approach, the scheduling had as base the *net load* forecasting, allowing a more objective unit commitment. The same happened with the wind limitation. In this case, the system operator, apparently, prefers a preventive action with consequent higher costs. Other important point for taking into account is the high cost of load shed. Although the energy shed value (ENS) was relatively low (0,48% of *net load* or 14,92 MWh) due to its high penalty cost it is fairly close to the cost resulting from 143,6 MWh of wind curtailed when in the case of system operator. With this, it is clear that the load shed must be avoided, since it can, and even for low values of load shed, compromise the entire process,.

Table 5.6 – Comparison between total costs for both approaches

	ENS	W_curt	G < min	Fuel
Risk assessment	17903 €	7542 €	141 €	79204 €
System operator	0 €	21542 €	27778 €	102505 €

Up to this point the UC was done based on single periods, startup costs and unit's outages were not contemplated. For this reason, there were no restrictions to the starting of units and, as such, the number of manoeuvres was much higher than the presented by the system operator. Concerning the online units, because the rated power of thermal unit's type G_S is lower than G_B, its operation is more flexible, due to that, the number of startups of units type G_S was 47% higher than the number of startups of units G_B. The blackout cost was also not contemplated and, consequently, there were several registered cases with only one on-line unit ($1G_S\_0G_B$ or $0G_S\_1G_B$). For a deep analysis of the number of start-ups and committed GENSET's, tables AIII.1 and AIII.2 in annex III show the complete scheduling for both approaches.

To implement an *N*-1 contingency, in case of thermal outages, the predefined GENSET naturally has to change to a more expansive one. This way, the GENSET cost (considering *N*-1) results from the weighted sum of the predefined GENSET and those resulting after the outage, as depicted in equation (4.39). The value used to weight the sum is the contingency probability from table 5.1. In cases when only one unit is on-line, it is assumed that a single unit contingency leads to a system blackout, so equation (4.39) is replaced by equation (4.40) where the blackout costs and the costs of not supplying energy are taken into account.

5.3.2 Multi period unit commitment

The single-period unit commitment discussed in previous cases allows for demonstration, with some detail, the concept of the scheduling based on risk assessment. Obviously an UC is always solved to an extended time period, since the stages must be temporally interconnected. If a decision is taken in one hour it will have consequences to the ones following it, as explained in chapter 2. In this case study the results of a multi-period UC, with starting costs and contingency criterion *N*-1 are presented and assessed. The starting costs, the contingency probability, and the blackout cost are shown in table 5.1. The UC was solved for 24 hours periods beginning at 0:00, which is the time when the *net load* forecasts are available. In figure 5.31 the technical limits of the GENSET's arising from multi-period UC are shown, as well as the *net load* point forecasting and the uncertainty distribution.

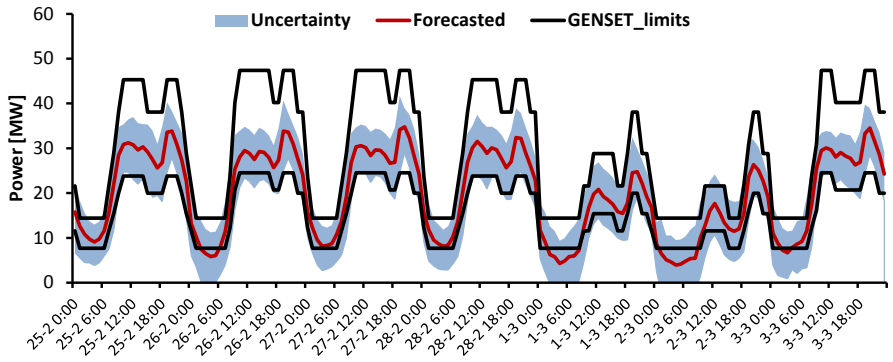

Figure 5.31 – Multi-period unit commitment

The first impression from the multi-period case study is the decrease of the number of manoeuvres, with less starts. In table AIII.3, in annex III, it is possible to compare the number of manoeuvres with those obtained by the single period approach (table AIII.2) and by the system operator (table AIII.1). As during working days (25th up to 28th February and 3rd March), the *net load* had a similar shape, the committed units exhibited approximately an identical profile. On the weekend, the behaviour was quite different, obligating a higher number of manoeuvres. The starting costs reduced the number of start-ups, but nonetheless there were more than when the system operator approach is used, as shown in table 5.7.

Table 5.7 – Number of start-ups for both approaches

	G_S	G_B
Risk assessment	29	10
System operator	3	7

From the results depicted in figure 5.31 it is visible that, except for during some off-peak periods, the GENSET limits are able to cover the forecasted *net load* necessities as well as some of the uncertainty. Contrary to the single period approach, where the wind power

curtailment is strongly avoided, in the multi-period case, due to the (*N*-1) criterion, it was preferred to curtail some wind power than to increase the risk of blackout (penalized with 10000€), as seen in Feb. 26th, and March 1st and 2nd.

As a consequence, whereas in single-period it was allowed to work with only one unit (1GS_0GB), in the multi-period at least two must be online ($2G_S\_0G_B$). This solution can, however, create a problem and mainly in off-peak periods. Following figure 5.31, with more than one online unit, the minimum limits of the GENSET increase and so increase the risk of wind curtailment or even units operating below their minimums. Nevertheless, due to the high penalty resulting from the *N*-1 criterion and the risk of blackout, it becomes more economical to keep on-line two units instead of one. In this approach it is preferred to manage the production with units type G_S because they have lower start-up costs. Furthermore, an outage of a unit type G_S has less impact on risk costs than the outages of a unit type G_B with a higher rated power. This way, it was possible, in off-peak periods, to decrease the technical minimum with the GENSET $2G_S\_0G_B$ and still ensure the condition *N*-1. In comparison, the limit of GENSET $2G_S\_0G_B$ is 7,69 MW instead 12,26 MW of the GENSET $1G_S\_1G_B$ used traditionally by the system operator. On the other hand, the system operator prefers making the production management at the expense of units type G_B since they present more rated power and more production range. It should be noticed that the system operator has a conservative approach in the scheduling, giving more weight to the security than to the starting costs. Other conclusion indicates a generic increment of the upward reserves due to high number of on-line units, especially during off-peak periods.

5.3.2.1 Validation of multi-period unit commitment

In figure 5.32 the generation limits of the committed GENSET's and the perspective of *net load* measurement without curtailment are shown. Once again the forecasting errors have an important role on the performances of the proposed method.

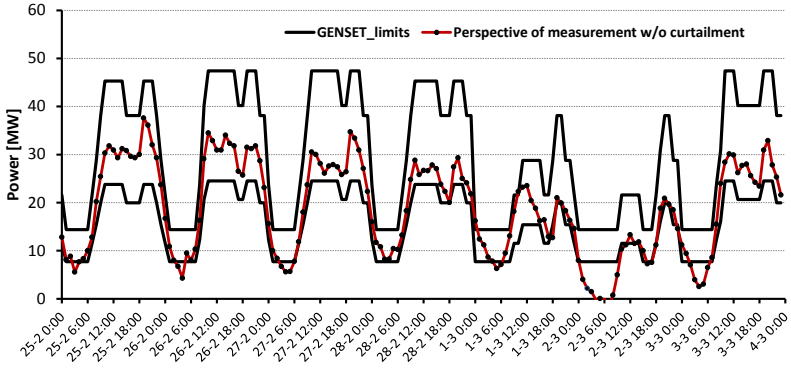

Figure 5.32 – GENSET power limits and measured *net load*

Comparing with *net load* forecasting of figure 5.31, there was only one off-peak period where the *net load* was not lower than the minimum of thermal units, namely on February 28th. The great deviations occur on March 2nd and 3rd, precisely during the weekend and mainly in off-peak periods. Notice that March 2nd was a Carnival Saturday which, although being different from a traditional holiday, can present specific forecasting challenges. During the forecast process this day was processed as a normal Saturday.

Analysing figures 5.23 and 5.32 there are clear differences between the scheduling resulting by the risk assessment approach and the solution done by the system operator. Our approach allows the usage of 2 units type G_S instead of the classical approach of $1G_S\_1G_B$, which represents a higher cost and a higher minimum limits, obligating to wind curtailment and the production below the minimum. Figure 5.33 shows the upward and downward reserves obtained by the multi-period UC.

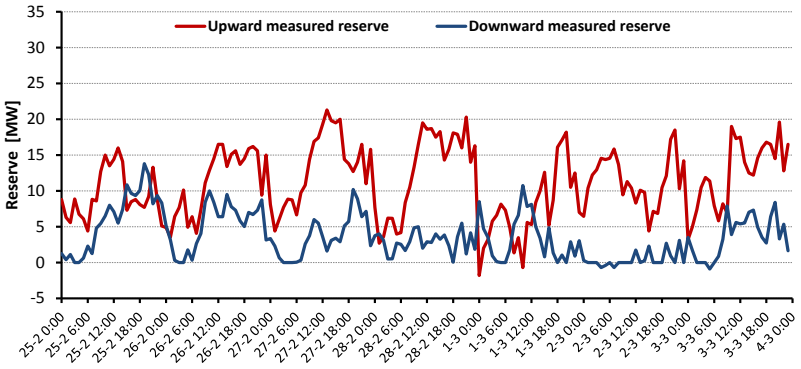

Figure 5.33 – Upward and downward in multi-period approach

As expected, due to contingency criterion *N*-1 the upward reserves increased while the downward decreased. Nevertheless, comparing with the scheduling proposed by the system operator, the average downward reserve is slightly superior while the upward reserves are inferior, as shown in table 5.8.

Table 5.8 – Average reserves in multi-period UC

	Upward reserve [MW]	Downward reserve [MW]
Risk assessment	11,16	3,58
System operator	13,39	2,63

The average value of the reserves can give important overall information concerning the reserves, but an hourly analysis shows that even with a comfortable upward reserve there are two hours in March 1st where it was negative, revealing load shed. Analysing figure 5.33 it can be seen that the load shed periods happened at 0:00 and 10:00. Consulting the figure 5.32 it is visible that the first was during the transition to the off-peak period, with an important decrease on the available power due to the transition from GENSET $3G_S\_1G_B$ to

GENSET $2G_S\_0G_B$. It should be noted it was considered that both units were turned off at the same instant and the dynamic within the hour was not considered. Probably with a finer scheduling it would be possible to delay the shutdown of one of the units and this way to avoid the load shed. The second episode, reveals a lack of available power since it occurred before the transition from the GENSET $3G_S\_0G_B$ to $4G_S\_0G_B$. This transition could be done one hour earlier, but at that moment it was less expensive to shed the load than to start another unit. To face this problem, the thermal units may use a boost which allows the increasing of the power during a short period of time in order to avoid, or at least to decrease the amount of load shed. This technical information is shown in table A.I in annex I.

Regarding the downward reserves, despite the average being 2,63 MW, there were some periods where the reserves were negative, caused mainly by the necessity of having at least 2 thermal units on-line even in off-peak periods.

In figure 5.34 a comparison between downward reserves from risk assessment approach and system operator approach is shown.

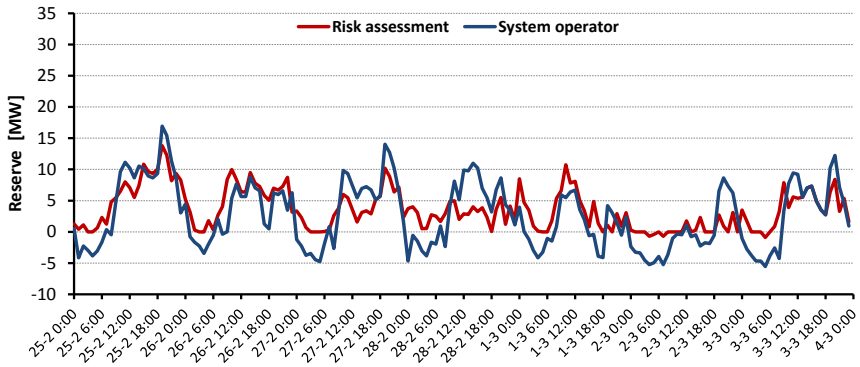

Figure 5.34 – Risk assessment and system operator downward reserves for a multi-period approach

The proposed method showed to be often able to avoid downward negative reserves imposing wind curtailment. Nevertheless, 4 hours of production below the minimum still happened, because a complete wind curtailment was not enough to avoid it.

On the other hand, the system operator without access to forecasts production prefers a preventive approach, limiting the wind generation and, in the case of necessity, to operate with the thermal units below the minimum.

A deeper analysis allowed concluding that in line with the conclusions from single period case, the risk assessment allowed once again to present less wind curtailment than the system operator approach. Also the energy produced by the thermal units working below the minimum is remarkably lower when compared with those obtained by the system operator as shown in table 5.9 and figure 5.35. The maximum capacity of the on-line units dispatched by the grid operator was sufficient to meet the load, however, during some periods (mainly off-

peak periods), the minimum power capacity of committed units is higher than the necessary. On the other hand there was no need of load shed.

Table 5.9 – Values outside the GENSET limits for multi-period UC (in percentage of total *net load*)

	L_shed	W_curt	G < min
Risk assessment	0,08 %	2,98 %	0,09 %
System operator	0,00 %	4,57 %	5,37 %

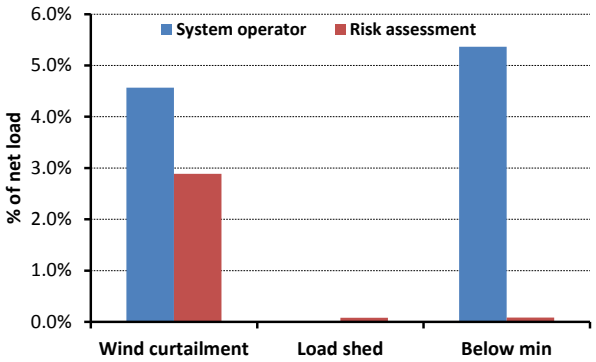

Figure 5.35 – Multi-period unit commitment

The main observation drawn from table 5.9, is the increase of wind curtailment from 1,60% (table 5.5) up to 2,98% in the case of risk assessment approach. This increment is linked with the fact that there were more units committed in off-peak periods and errors in forecasts. The production below the minimum, despite being low, increases 3 times. With the unit commitment defined in the multi-period case it was possible to reduce the amount of low shed 6 times, from 0,48% (table 5.5) to 0,08%, though at expense of wind power curtailment. As concluded previously, in single period case, this is a hard problem to be solved since a balancing point between the necessities of load shed, wind power curtailment and production below the minimum must be found.. To support this analysis, in table 5.10 the number of hours where the *net load* was lower or higher to the GENSET limits is shown. Unsurprisingly, there was a decrease on the hours of load shed and an increase of remaining values.

Table 5.10 – Number of hours operating outside the GENSET's limits

	L_shed [h]	W_curt [h]	G < min [h]
Risk assessment	2	33	4
System operator	0	54	68

To support these conclusions, in figures 5.36 and 5.37 the wind energy curtailed and the energy produced below the unit's minimum, for both approaches, is shown.

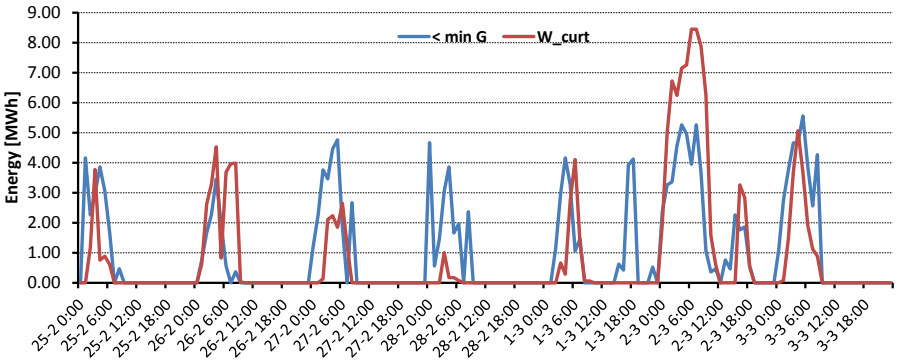

Figure 5.36 – Wind energy curtailed and produced below the minimum by system operator

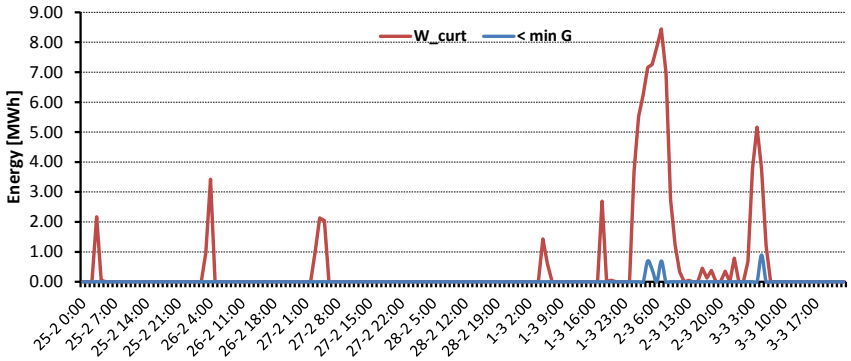

Figure 5.37 – Wind energy curtailed and produced below the minimum by the risk assessment approach

Differences are well visible, showing more episodes of wind curtailment and production below minimum by the system operator scheduling than those resulting by the risk assessment. It is clear that the deviation between the minimum of GENSET and the expected *net load* (without curtailment) registered during off-peak period of March 2nd introduced an important quantity of wind energy curtailed which conditioned the results.

Regarding the real costs obtained by both approaches, the costs from the system operator scheduling revealed, once again, to be higher than those obtained by the scheduling based on risk assessment as shown in figure 5.38.

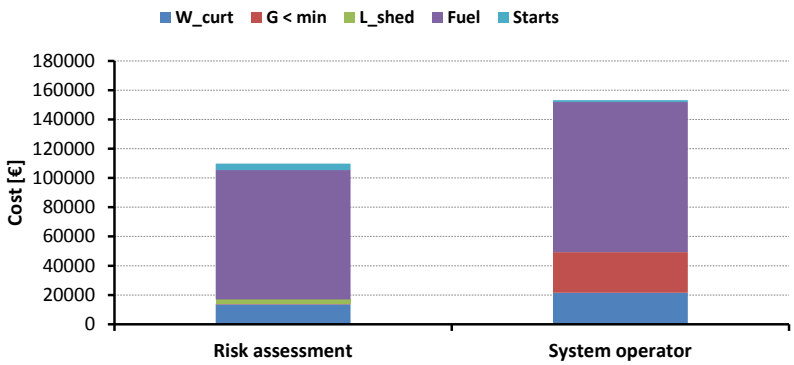

Figure 5.38 – Multi-period operation costs

There is a new portion regarding the start-up costs but it does not markedly influence the total cost. Despite the big difference in the number of startups, as in risk assessment approach the starting of units type GS (with lower cost) prevail, their impact is relatively low.

Although the slight increment of the energy produced below the thermal unit's limits, it is still much lower than the registered by the system operator approach. In the case of wind power curtailment, the increment was higher but, like in the generation below minimum, it is much lower than the registered by the system operator approach.

In the end, remains the conclusion that the great effort to the total cost is the fuel cost. In these 168 hours period under analysis, the costs reached by the risk assessment approach represent 71,7% of those presented by the system operator. Once again, it is concluded that there is the "waste" of "clean" energy, but the requirement of producing below the minimum is maintained low. Said this, the results can be considered very satisfactory. In table 5.11 the comparison of each contribution to the final cost are shown.

Table 5.11 – Comparison between total costs for both approaches

	ENS	W_curt	G < min	Fuel	Start-ups
Risk assessment	3000 €	13609 €	423 €	88349 €	4400 €
System operator	0 €	21542 €	27778 €	102505 €	1350 €

In order to present a consistent comparison between the risk analysis approach and the system operator approach, the results were concentrated in order to ease the comparison. Tables 5.12 up to 5.14 shows some evaluation regarding load shed, wind curtailment and work below the minimum. These comparisons can be done based on the reliability indices definitions, as presented in [143],[158]–[161] (namely, state sampling method and state duration sampling method), however, the temporal unit of these indices is usually a year, a season or a month. In this case, the temporal period is much reduced, specifically 168h, and so the amount of information for calculating those indices is also reduced.

Table 5.12 – Comparison regarding load shed

	Risk assessment	System operator
Nº of hours with load shed [h/168]	2	0,00
Load shed [MW]	1,25	0,00
Energy shed [MWh/168h]	2,50	0,00
Frequency of load shed [occ./168h]	2,00	0,00
Duration of load shed [h/occ.]	1,00	0,00

Table 5.13 – Comparison regarding wind curtailment

	Risk assessment	System operator
Nº of hours with wind curtailment [h/168]	33	54
Wind curtailment [MW]	2,75	3,99
Wind energy curtailed [MWh/168h]	90,73	143,61
Frequency of wind curtailment [occ./168h]	12	8
Duration of wind curtailment [h/occ.]	2,75	7,25

Table 5.14 – Comparison regarding thermal units working below the minimum

	Risk assessment	System operator
Nº of hours generation below min. [h/168]	4	68
Generation below minimum [MW]	0,67	3,20
Energy generation below min. [MWh/168h]	2,68	176,40
Frequency of generation below min. [occ./168h]	3	14
Duration of generation below min. [h/occ.]	1,33	3,90

From tables 5.12 up to 5.14, several conclusions can be stressed out. For instance, in the case of wind curtailment, there were more occurrences in the risk assessment approach but the duration was much lower. It means that in the case of system operator the curtailment occurrences were more extended (generally during all off-peak periods). In average, the wind power curtailed by the risk assessment approach is also lower than that from system operator. The same conclusions can be extrapolated to the thermal production below the minimum, with the exception of the number of occurrences.

Other important conclusions can be addressed analysing figure 5.39. In this figure is shown the evolution of the risk cost in function of the forecasted *net load*.

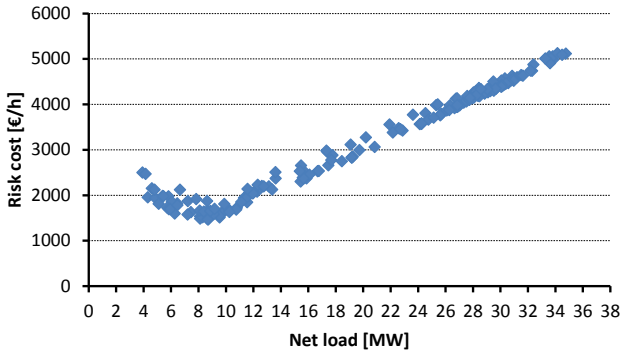

Figure 5.39 – Risk costs in function of *net load*

It is verified that, naturally, the costs grow with the *net load* increment, because there is the necessity to burn more fuel in thermal power plants. However, to lower values of *net load* approximately below 8 MW the cost starts to increase again. This happens due to the increment of the cost related with the penalties of wind curtailment and the thermal units operate below the minimum.

The trend of the costs increasing linearly with the *net load* indicates that there is no increment on costs due to load shed, which means that there is no significant load shed. The rated capacity of thermal production is 94,8 MW and the *net load* never exceeded 36 MW during the week under study. Since 2012 the maximum registered of *net load* was 62 MW, meaning that currently the thermal system is overestimated for more than 30 %.

Analyzing figure 5.39 it is possible to verify that for equal values of *net load* there is more than one cost. It means that despite the net load point forecast to be the same, the difference in uncertainty associated (different probability distribution) can lead to different solutions.
This curve can also be used for the demand response. To values of *net load* below the minimum risk cost, the energy prices can suffer an adequacy, reducing the tariffs of energy. With this way, the energy consumption should increase to a higher net load and consequently, reduce the operational costs. If there is a hydro power plant with pumping and storage capacity, it is possible to calculate the value of *net load* since it is advantageous to pump.

5.4 Summary and main conclusions

The scope of this chapter was to present some case studies to assess the performances of a scheduling of thermal units under uncertainty based on risk assessment. The first part presented a probabilistic *net load* forecast where it was highlighted the problematic of the wind power curtailment to the forecasting proceeding. It was concluded that the database which supports the forecasts have an important role, with the possibility of introducing important errors. This situation was shown with the case of geothermal power prediction. The success of this approach, and the generality of the approaches, is strongly dependent on the forecasting quality, otherwise the results may be compromised. It is believed that increasing the available dataset forecasting models can be improved and so, the reliability of the net load forecasts is also improved.
Concerning the UC under uncertainty it was shown that an approach based on risk assessment is a technique which allows reaching acceptable results. The assessment of the approach was based on forecasts with the assumption that the *net load* did not present any kind of wind curtailment. All these cases were studied based on real environmental, adding additional complexity. It means some parameters that are not controllable (as errors in the measures and forecasts) are always present. It should be noticed that all the assessment was done in basis of hourly average values, meaning that intra hour phenomena might have occurred and this was not taken into account. It was considered that the units start in the beginning of the hours and the starting time is neglected (in reality when pre-heated, the units G_S need 8 minutes to produce above the minimum and the G_B need10 minutes).
When comparing with the procedures adapted by the system operator is was shown that, for the time period under study, the approach based in risk assessment presented a lower cost both for single-period and for the multi-period approaches, mostly with the reduction of fuel consumption. It was also concluded that the forecasting errors strongly influenced the final results, because the values of wind curtailment were severely penalized by the deviations registered in a single day. Nevertheless, the quantity of energy produced by the thermal units

working below the minimum was markedly reduced, due to the possibility of committing solutions constituted by only with units G_S during the off-peak periods.

Concerning the spinning reserves, in general, they were acceptable except in the cases of load curtailment.

It was observed that the scheduling of the thermal units in São Miguel Island is a remarkable challenge, being very hard to determine an appropriate scheduling to avoid simultaneously wind curtailment and load shed. With the present formulation, the approach based on risk assessment could not avoid load shed despite reducing the production below the minimum. In practice, the load shed can be reduced or even avoided if appealing to unit's boost, this can increase the rated power with more 4,2% and 9,2% of additional power during 30 min, for units G_S and G_B respectively.

CHAPTER 6

General Conclusions

Contents

In this chapter the overall conclusions and the original contribution are presented. Conclusions concerning the research questions and formulated hypothesis are addressed.

Future research perspectives are also discussed.

6. Conclusions

6.1 Overall conclusions

Power systems scheduling although being done daily and throughout the world, it is a challenging problem and it encourages continuous research work. The emergent power generation done with variable power plants lead to new challenges, pushing new and strenuous research.

This work intended to develop a complete methodological suit for giving a complete answer to the energy systems with integration of highly variable power sources scheduling. The chosen case study is focused on an island under real context, adding some more challenges not existent in mainland grids. A few of these challenges are related with lower and limited rated power, limited diversity of power plants, power plants with low flexibility, highly variable power sources, small geographic area and absence of connections with other power systems. The covering of all these issues was ensured by the presented case study. São Miguel Island has a small area and smoothing effect in renewable production variability (wind and hydro) is low or inexistent. Its low capacity of regulation makes the geothermal power plants to be maintained constant. To overcome these problems, a trustable forecasting tool which allows correct operational decisions is essential for efficient power scheduling. For this task, the major problem was related with operational issues, such as wind power curtailment. Wind power curtailment skews the data set and creates wind power forecasting difficulties. This is one main hurdle and had to be solved. When under real context, faults in measurements make the available data to be of poor quality and this is another issue that had to be addressed along this work; incorrect measures and lack of information do not allow the accomplishment of better results.

Optimization of the thermal production was also an issue. Commonly, this kind of units is used as the base of load diagram. In São Miguel they have to follow the load diagram profile which demands an accurate scheduling, once although there are several units, they have a relatively limited rated power.

To overcome all these challenges the overall problem was split into two small actions. The first specified the characteristics of forecasting systems which best suited the problem and mathematical models including uncertainty were chosen. The second developed a new generation scheduling process based on risk assessment, attempting the reduction of operational costs and speeding up computational process. Power forecasts, uncertainty, optimization and power scheduling were covered in this work. The final result, is the development of an integrated set of mathematic techniques for optimizing the electric energy systems operation in the presence of significant penetrations of renewable generation. The

innovation of this thesis is spread on several parts of the problem. Aggregation of all components in the global scheduling approach is the added value brought by the present research work.

Research questions were posed for developing the work and they were used as the base for the investigation. The first research question was [*Which is the most adequate probabilistic forecasting model to each forecast horizon ?*]. During the research we found in the literature several models to be likely used for forecasting, both parametric and nonparametric. All of them, regardless how, can be used but its choice is fundamentally dependent on the application.

It was concluded that nonparametric forecasting techniques such as quantile regression, prediction intervals and kernel density forecasts presented similar results on the uncertainty representation. As such, the kernel density forecasting model was chosen based on the *Nadaraya-Watson* conditional estimator because it allows to have some sensibility in relation to the weight each explanatory variable has in the forecasted random variable. It was verified that the great challenge of this technique is the determination of the bandwidth of each kernel, since the impact of the kernel function is minor. This technique was used to forecast all random variables (renewable production and load) which were aggregated by convolution, resulting in the *net load*.

To ease manipulation of probability distributions of *net load* in the scheduling problem, the fitting of the probability distribution obtained by the kernel to a parametric Beta distribution was done. With a parametric solution it was very simple and fast to calculate the *pdf*, *cdf* and the inverse of the *cdf* even if losing some details of the original probability distribution. The Beta *pdf*, with fundamentally two parameters, becomes very easy and light to manipulate.

Although some studies to trying to recognize which should be the better distributions in function of temporal horizons and power amplitude or wind velocity are found in the literature, the obtained results fundamentally depend on the cases studies. There is no strong evidence supporting visible improvements. Other approaches generally connected to scheduling under uncertainty, for simplicity, and based on the central value theorem; characterize the uncertainty by a Normal distribution. Yet, in this case study, due to the small data sets and the nonlinearity of W2P, the forecasting errors could not be characterized by Normal distributions.

As a conclusion it was verified that for the scheduling problem, the Beta distribution was a good choice, though other more complex mathematical approaches could also be used.

This was one of the main objectives of this thesis, forecast of renewable sources with associated uncertainties.

The second research question was [*What is the aggregation role of RES for the scheduling process?*]. This question is intrinsically linked with the previous one. As understood above, the renewable production forecasting has always an associated uncertainty, which can be reduced with its aggregation. In this work it was verified that the major forecasting errors (in percentage) belong to the wind power forecasting, followed by the hydro power forecasting. The lowest errors were achieved by the geothermal and load forecasting.

It is well known the added value of power production aggregation due to the spatial smoothing effect, whether they are wind, hydro or photovoltaic generation. In this case as there is only one wind power plant, the smoothing effect was not applicable. Furthermore, in the case of hydro production and due to the small island area, the spatial smoothing was also negligible.

Still, considering different power sources statistically not correlated, it is expectable that, somehow, the variability and the forecasting error can cancel each other. Considering this aggregate production as a negative load permits the calculus of the *net load* and forecast the necessity of thermal production. The resulting *net load* already incorporates all the forecasting uncertainties, which are substantially lower than those presented by the wind and hydro power separately. With this, it was possible to reduce the uncertainty amplitude, to have more confidence in the forecasts and to low variability of the main variable of the scheduling problem.

The last research question was [*Which optimization tools should be used?*]. In recent literature, related with scheduling under uncertainty, stochastic programming models with the uncertainty modeled by scenarios are generally proposed. The use of scenarios is done to model the uncertainty as well as the random variables temporal interdependence. Theoretically, only with an infinite number of scenarios uncertainty could be fully modelled. In order to transform it into a more tractable problem, cost functions are linearized and the number of scenarios is reduced. Still, even with the reduction, the algorithms are computational expensive. Once the problem is formulated, generally the MILP algorithm is selected.

In this work it is proposed a complete different approach: the uncertainty of random variables is defined by the full *pdf* and the optimization method is based on risk assessment. Unlike traditional approaches, in the proposed method the UC and the ED are disaggregated. With this, there was no necessity to run the ED problem for each temporal interval and for each feasible set of units.

A pre-processing where the ED was solved off-line for each GENSET and for several values of *net load* made possible this disaggregation. As the thermal units had convex cost functions,

it was considered that the linear programming was sufficiently fast and precise to calculate the ED off-line.
With this approach the UC is faster because the ED was previously calculated. With this way it is possible to calculate the costs and the allocated load to each unit quicker than with those obtained running traditional numerical methods. This technique gains strength in cases where it is mandatory to calculate the UC repetitively and in very short time intervals.

Improving the algorithm's velocity was another of this thesis' main objectives.

Likewise, interval optimization requires less computational efforts to generate upper and down bounds of the objective value. However, the choice of the uncertainty interval coverage rate can dramatically change the optimal solutions. For this, it was chosen the utilization of the full *pdf*.

In the scheduling classical approach, the demand is known and the algorithm tries to find a set of generation units (feasible solutions) which are able to feed the load with minor cost or with the lowest penalties when imbalances occur. This work proposes the opposite paradigm: when available production of each GENSET is known, based on risk assessment and associated costs, it was found which portion of load could be fed. With this approach there are no infeasible solutions. Provided the risk and consequent cost is acceptable, all solutions are accepted. This way the attempt to find the trade-off between economy and reliability of the system was pursued. The trade-off is based on risk assessment, where the risk of wind curtailment, load shed, unit's normal operation together with the units working below the minimum is taken into account.

Finally, aiming an even better scheduling improvement, it was proposed a simple heuristic to increase the velocity of the dynamic programming to solve the UC for all time horizons.
As regards to the security criteria, when the uncertainty is modeled by scenarios, two or more stages stochastic programming approaches are generally used. In the case of intervals optimization it is not appropriated to simulate discrete variables. In this work this issue was solved introducing the assessment of N-1 security criterion in the risk costs, avoiding the use of discrete variables. The risk cost of each GENSET is already incorporating the value related with any unexpected outage. The last objective of this work was to propose an innovative optimization approach and to create a scheduling optimization tool.

After careful analysis of the case study results it was shown that the methodology proposed in this thesis is able to answer the above research questions. The complete methodology establishes the capacity to achieve the scheduling of a power system with the integration of high power sources. As a final conclusion we dare say that, in an island environment, the

scheduling based on risk assessment, using the full probability distributions could be a better alternative compared with those based on scenarios which are widely presented in the literature.

Compared with the system operator proposed scheduling, two analyses can be done; the first based in single-period UC and the second based on multi-period UC. In both analyses the proposed methodology reached lower total costs, primarily in the fuel consumption. The wind energy curtailed quantity was low as well as the thermal production was below the minimum limits. On the other hand, the results also showed that the risk assessment approach had more maneuvers than those obtained by the system operator and also presented some marginal values of load shed. A deep analysis about the load shed showed that this problem can be outperformed by the power plant operators, delaying some maneuvers or using the boost of the thermal units.

Concerning the reserves, it was concluded that the proposed approach allows the implicitly determination of the reserves because they are already incorporated in the uncertainty. In average, the amount of upward reserves was lower than those resulting from the system operator proposal, while in the case of downward reserves it was the opposite. As shown above, this is a hard solving problem due to the difficulty of reaching solutions with lower cost and robustness.

Other important conclusion is that the success of the proposed method is deeply connected with the quality of the forecasts. Without accurate forecasts this methodology is compromised. Overcoming this problem may imply the implementation of a SCADA system in order to improve the very short term forecasting.

Other generic conclusions can be addressed: It is clear that the wind power plant was oversized regarding the actual needs of production. This problem has the well-known effect to the thermal power plants. If the geothermal power plants are able to impose the frequency, the number of thermal units operating in off-peak periods could be reduced or even totally turned off. Outside of the island’s environment, perhaps some thermal units could be decommissioned.

It also can be concluded that the introduction of some sort of storage to store the energy excess during off-peak periods is mandatory. With some storage capacity it should be possible to avoid the wind power curtailment, the waste of clean energy and units working below the minimum, with simultaneous enough capacity to cover eventual load shed. As a suggestion, V2G and reversible hydro power plants could be good solutions. Another way could be the implementation of a policy of demand response.

6.2 Contributions

This work presents several and important original contributions. The most important contribution was the methodology based on risk assessment, using the full probability distributions.

The developed methodology is a good alternative compared with those based on scenarios, widely presented in the literature. With this approach the computation time is reduced, since it is not necessary to run the UC and ED to each scenario. In the power systems scheduling, the processing time is a very important issue, predominantly when there is the need to often refresh.

Concerning the resolution ED of complex problems with non-convex cost functions or non-continuous spaces, it was presented as an original contribution a metaheuristic based on a cloud of particles. Through the tests presented in literature, the performances are acceptable, as well as the speed and robustness.

The presentation of a complete methodology to *net load* forecast under uncertainty in a real environment is also an important contribution. In the thesis was also shown the importance of the aggregation of the RES in order to reduce the uncertainty.

One of the biggest challenges was the fact the work had to be applied in real environment. There were some values which had to be presumed due to the lack of better information. The lack of measures on time and inadequate values were additional found problems.

6.3 Perspectives of future research

The natural continuity of this work should be researching the capacity or tractability of the proposed method in power systems with bigger dimensions and in non-isolated systems. This could be one of the drawbacks of this approach.

In this specific work it was not included the grid model. With its inclusion several issues can be addressed, such as power losses, congestions and line outages.

Other weakness felt in this work, and it should be overcome is the lack of SCADA in order to obtain recent past measured values. With this value it should be possible to verify the performances of the forecasts and take corrective actions when large deviations are present.

As perspective of future research, it would be important to implement some type of storage in the system.

Another line for research may be the demand response for investigation of which tariff's scheme could be proposed in order to increase the consumption in off-peak periods.

In the case of forecasts, time adaptive models could be studied, though little improvements take place in absence of major changes in the power system.

References

[1] J. Juban, “Uncertainty estimation of wind power forecasts: Comparison of Probabilistic Modelling Approaches,” in *EWEC - European Wind Energy Conference & Exhibition*, 2008.

[2] M. Sengupta and J. Keller, “PV Ramping in a Distributed Generation Environment : A Study Using Solar Measurements,” in *38th IEEE Photovoltaic Specialists Conference (PVSC), 2012*, 2011, pp. 586–589.

[3] Y. Gao, K. Zhao, and C. Wang, “Economic dispatch containing wind power and electric vehicle battery swap station,” *Pes T&D 2012*, pp. 1–7, May 2012.

[4] J. Wang, A. Botterud, V. Miranda, C. Monteiro, and G. Sheble, “Impact of wind power forecasting on unit commitment and dispatch,” in *8th Int. Workshop on Large-Scale Integration of Wind Power into Power Systems, Bremen, Germany*, 2009, p. 8.

[5] A. Botterud, A. Zhou, J. Wang, and R. J. Bessa, “Use of Wind Power Forecasting in Operational Decisions - Report - Argonne National Laboratory,” 2011.

[6] J. Juban, L. Fugon, and G. Kariniotakis, “Probabilistic short-term wind power forecasting based on kernel density estimators,” in *European Wind Energy Conference*, 2007, no. May, pp. 1–11.

[7] J. Juban, N. Siebert, and G. N. Kariniotakis, “Probabilistic Short-term Wind Power Forecasting for the Optimal Management of Wind Generation,” pp. 683–688, 2007.

[8] P. Pinson, J. Juban, and G. N. Kariniotakis, “On the Quality and Value of Probabilistic Forecasts of Wind Generation,” in *Probabilistic Methods Applied to Power Systems, 2006. PMAPS 2006. International Conference on*, 2006, pp. 1–7.

[9] R. J. Bessa, V. Miranda, A. Botterud, and J. Wang, “Time Adaptive Conditional Kernel Density Estimation for Wind Power Forecasting,” *IEEE Trans. Sustain. Energy*, vol. 3, no. 4, pp. 660–669, 2012.

[10] M. Lydia and S. Suresh Kumar, “A comprehensive overview on wind power forecasting,” *2010 Conf. Proc. IPEC*, pp. 268–273, Oct. 2010.

[11] R. Bessa, J. Sumaili, V. Miranda, A. Botterud, J. Wang, and E. Constantinescu, “Time-adaptive kernel density forecast: A new method for wind power uncertainty modeling,” in *17th Power System Computation Conference*, 2010.

[12] B. Lange, K. Rohrig, and F. Schlögl, “Wind power forecasting,” 2007.

[13] P. Pinson, H. A. Nielsen, J. K. Møller, H. Madsen, and G. N. Kariniotakis, “Non-parametric probabilistic forecasts of wind power: required properties and evaluation,” *Wind Energy*, vol. 10, no. 6, pp. 497–516, Nov. 2007.

[14] J. Jeon and J. W. Taylor, “Using Conditional Kernel Density Estimation for Wind Power Density Forecasting,” vol. 44, no. 0, 2012.

[15] E. Constantinescu, V. Zavala, M. Rocklin, and S. Lee, “Unit commitment with wind power generation: integrating wind forecast uncertainty and stochastic programming.,” *New York*, 2009.

[16] J. Wang, a. Botterud, R. Bessa, H. Keko, L. Carvalho, D. Issicaba, J. Sumaili, and V. Miranda, “Wind power forecasting uncertainty and unit commitment,” *Appl. Energy*, vol. 88, no. 11, pp. 4014–4023, Nov. 2011.

[17] P. Bacher, H. Madsen, and H. A. Nielsen, “Online short-term solar power forecasting,” *Sol. Energy*, vol. 83, no. 10, pp. 1772–1783, Oct. 2009.

[18] P. Pinson, G. Reikard, and J.-R. Bidlot, “Probabilistic forecasting of the wave energy flux,” *Appl. Energy*, vol. 93, pp. 364–370, May 2012.

[19] Hanz Bludszuweit, “Reduction of the uncertainty of wind power predictions using energy storage,” PhD Thesis, Universidad de Zaragoza, 2009.

[20] H. Bludszuweit, J. A. Domínguez-navarro, and A. Llombart, "Statistical Analysis of Wind Power Forecast Error," *IEEE Trans. Power Syst.*, vol. 23, no. 3, pp. 983–991, 2008.

[21] H. Bludszuweit and J. Domínguez, "Probabilistic energy storage sizing for reducing wind power forecast uncertainty," in *International Conference on Renewable Energies and Power Quality*, 2010, p. 5.

[22] A. T. Al-Awami and M. a. El-Sharkawi, "Statistical characterization of wind power output for a given wind power forecast," in *41st North American Power Symposium*, 2009, vol. 0, no. 1, pp. 1–4.

[23] M. D. L. Leite and J. S. Das Virgens Filho, "Ajuste de modelos de distribuição de probabilidade a séries horárias de velocidade do vento para o município de Ponta Grossa, Estado do Paraná," *Acta Sci. Technol.*, vol. 33, no. 4, pp. 447–455, Sep. 2011.

[24] S. Soman, H. Zareipour, O. Malik, and P. Mandal, "A review of wind power and wind speed forecasting methods with different time horizons," in *North American Power Symposium (NAPS), 2010*, 2010, pp. 1–8, 26 – 28 Sept. 2010.

[25] G. Fu, F. Y. Shih, and H. Wang, "A kernel-based parametric method for conditional density estimation," *Pattern Recognit.*, vol. 44, no. 2, pp. 284–294, Feb. 2011.

[26] G. Papaefthymiou and P. Pinson, "Modeling of spatial dependence in wind power forecast uncertainty," in *Proc. of 10th International Conference on Probabilistic Methods Applied to Power Systems*, 2008, pp. 1–9.

[27] F. Adam, T., Cadieux, "Wind Power in Ontario: Quantifying the benefits of geographic diversity," in *2nd Climate Change technology Conference*, 2009.

[28] U. Focken, M. Lange, K. Mönnich, H. P. Waldl, H. G. Beyer, and A. Luig, "A statistical analysis of the reduction of the wind power prediction error by spatial smoothing effects," *J. Wind Eng. Ind. Aerodyn.*, vol. 90, no. July 2001, pp. 231–246, 2002.

[29] L. Costa, "Simulação e Otimização da Gestão de Portfólio de Agentes de Mercado Agregadores," M. Sc Thesis, Faculty of Engineering, University of Porto.

[30] H. Zhang and L. L. Lai, "Research on Wind and Solar Penetration in a 9- bus Network," in *Power and Energy Society General Meeting, 2012 IEEE*, 2012, pp. 1–6.

[31] D. Pozo and J. Contreras, "A Chance-Constrained Unit Commitment With an Security Criterion and Significant Wind Generation," *ieeexplore.ieee.org*, vol. 28, no. 3, pp. 2842–2851, 2013.

[32] G. Liu and K. Tomsovic, "Quantifying Spinning Reserve in Systems With Significant Wind Power Penetration," *IEEE Trans. Power Syst.*, vol. 27, no. 4, pp. 2385–2393, 2012.

[33] Z.-L. Gaing and T.-C. Ou, "Dynamic economic dispatch solution using fast evolutionary programming with swarm direction," *2009 4th IEEE Conf. Ind. Electron. Appl.*, no. 1, pp. 1538–1544, May 2009.

[34] Z.-L. Gaing, "Particle swarm optimization to solving the economic dispatch considering the generator constraints," *IEEE Trans. Power Syst.*, vol. 18, no. 3, pp. 1187–1195, Aug. 2003.

[35] W. Lin, F. Cheng, and M. Tsay, "An improved tabu search for economic dispatch with multiple minima," *IEEE Trans. Power Syst.*, vol. 17, no. 1, pp. 108–112, 2002.

[36] A. I. Selvakumar and K. Thanushkodi, "A New Particle Swarm Optimization Solution to Nonconvex Economic Dispatch Problems," *IEEE Trans. Power Syst.*, vol. 22, no. 1, pp. 42–51, Feb. 2007.

[37] N. Padhy, "Unit commitment-a bibliographical survey," *Power Syst. IEEE Trans.*, vol. 19, no. 2, pp. 1196–1205, 2004.

[38] A. B. D. S. Serapião, “Fundamentos de otimização por inteligência de enxames: uma visão geral,” *Sba Control. Automação Soc. Bras. Autom.*, vol. 20, no. 3, pp. 271–304, 2009.

[39] J. Hazra and A. Sinha, “Application of soft computing methods for Economic Dispatch in Power Systems,” *Int. J. Electr. Electron. Eng.*, no. 2, pp. 538–543, 2009.

[40] J. Park, Y. Jeong, J. Shin, and K. Y. Lee, “An Improved Particle Swarm Optimization for Nonconvex Economic Dispatch Problems,” *IEEE Trans. Power Syst.*, vol. 25, no. 1, pp. 156–166, 2010.

[41] N. Sinha, R. Chakrabarti, and P. . Chattopadhyay, “Evolutionary programming techniques for economic load dispatch,” *IEEE Trans. Evol. Comput.*, vol. 7, no. 1, pp. 83–94, 2003.

[42] N. Sinha and B. Purkayastha, “PSO embedded evolutionary programming technique for nonconvex economic load dispatch,” *Power Syst. Conf. Expo. 2004. IEEE PES*, vol. 1, pp. 66–71, 2004.

[43] I. Ciornei and E. Kyriakides, “A GA-API Solution for the Economic Dispatch of Generation in Power System Operation,” *IEEE Trans. Power Syst.*, vol. 27, no. 1, pp. 233–242, 2012.

[44] S. J. Nanda and G. Panda, “A survey on nature inspired metaheuristic algorithms for partitional clustering,” *Swarm Evol. Comput.*, vol. 16, pp. 1–18, Jun. 2014.

[45] J. P. S. Catalão, “Electric Power Systems: Advanced Forecasting Techniques and Optimal Generation Scheduling.” CRC Press, Covilhã, 2012.

[46] A. Botterud, J. Sumaili, H. Keko, J. Mendes, R. Bessa, and V. Miranda, “Demand dispatch and probabilistic wind power forecasting in unit commitment and economic dispatch: A case study of Illinois,” *2013 IEEE Power Energy Soc. Gen. Meet.*, vol. 4, no. 1, pp. 250–261, 2013.

[47] A. Botterud, J. Wang, V. Miranda, and R. J. Bessa, “Wind Power Forecasting in U.S. Electricity Markets,” *Electr. J.*, vol. 23, no. 3, pp. 71–82, Apr. 2010.

[48] M. Carrión and J. M. Arroyo, “A Computationally Efficient Mixed-Integer Linear Formulation for the Thermal Unit Commitment Problem,” *IEEE Trans. Power Syst.*, vol. 21, no. 3, pp. 1371–1378, 2006.

[49] Allen J. Wood and B. F. Wollenberg, *Power generation, and control*, 2nd ed. New York, 1984.

[50] A. Bhardwaj, V. K. Kamboj, V. K. Shukla, B. Singh, and P. Khurana, “Unit Commitment in Electrical Power System-,” in *PEOCO20122012 IEEE International Power Engineering and Optimization Conference*, 2012, no. June, pp. 275–280.

[51] J. Kiviluoma, M. O’Malley, A. Tuohy, P. Meibom, M. Milligan, B. Lange, H. Holttinen, and M. Gibescu, “Impact of wind power on the unit commitment, operating reserves, and market design,” in *2011 IEEE Power and Energy Society General Meeting*, 2011, pp. 1–8.

[52] R. J. Bessa, M. Matos, I. C. Costa, L. Bremermann, I. G. Franchin, R. Pestana, N. Machado, H.-P. Waldl, and C. Wichmann, “Reserve Setting and Steady-State Security Assessment Using Wind Power Uncertainty Forecast: A Case Study,” *IEEE Trans. Sustain. Energy*, vol. 3, no. 4, pp. 827–836, Oct. 2012.

[53] X. Xia and A. M. Elaiw, “Dynamic Economic Dispatch : A Review,” *Online J. Electron. Electr. Eng.*, vol. 2, no. 2, pp. 234–245.

[54] K. Y. Lee, “An Improved Particle Swarm Optimization for Nonconvex Economic Dispatch Problems,” *IEEE Trans. Power Syst.*, vol. 25, no. 1, pp. 156–166, Feb. 2010.

[55] J.-B. Park, K.-S. Lee, J.-R. Shin, and K. Y. Lee, “A Particle Swarm Optimization for Economic Dispatch With Nonsmooth Cost Functions,” *IEEE Trans. Power Syst.*, vol. 20, no. 1, pp. 34–42, Feb. 2005.

[56] V. Botterud, A.; Zhou, Z.; Wang, J.; Valenzuela, J.; Sumaili, J.; Bessa, R.J.; Keko, H.; Miranda, "Unit commitment and operating reserves with probabilistic wind power forecasts," in *PowerTech, 2011 IEEE Trondheim*, 2011, pp. 1–7.

[57] M. Shahidehpour, "Security-Constrained Unit Commitment With Volatile Wind Power Generation," *IEEE Trans. Power Syst.*, vol. 23, no. 3, pp. 1319–1327, Aug. 2008.

[58] L. . Chen and Z. Y. Li, "Optimal reserve dispatch and security-constrained unit commitment considering volatile wind," *2013 IEEE Int. Conf. IEEE Reg. 10 (TENCON 2013)*, pp. 1–6, Oct. 2013.

[59] B. Zhou and Quanyuan Jiang, "Security-Constrained Unit Commitment with Wind Power Generation by Using Interval Linear Programming," in *Power and Energy Society General Meeting, 2012 IEEE*, 2012, pp. 1–6.

[60] H. Wu and M. Shahidehpour, "Stochastic SCUC Solution With Variable Wind Energy Using Constrained Ordinal Optimization," *Sustain. Energy, IEEE Trans.*, vol. 5, no. 2, pp. 379–388, 2013.

[61] Qianfan Wang; Yongpei Guan; Jianhui Wang, "A Chance-Constrained Two-Stage Stochastic Program for Unit Commitment With Uncertain Wind Power Output," *Power Syst. IEEE Trans.*, vol. 27, no. 1, pp. 206–215, 2012.

[62] L. Wu, M. Shahidehpour, and Z. Li, "Comparison of Scenario-Based and Interval Optimization Approaches to Stochastic SCUC," *IEEE Trans. Power Syst.*, vol. 27, no. 2, pp. 913–921, 2012.

[63] M. E. Khodayar, M. Shahidehpour, L. Wu, and A. Variables, "Enhancing the Dispatchability of Variable Wind Generation by Coordination With Pumped-Storage Hydro Units in Stochastic Power Systems," vol. 28, no. 3, pp. 2808–2818, 2013.

[64] H. Chen, H. Li, R. Ye, and B. Luo, "Robust scheduling of power system with significant wind power penetration," in *Power and Energy Society General Meeting, 2012 IEEE*, 2012, pp. 1–5.

[65] A. Kalantari, J. F. Restrepo, and F. D. Galiana, "Security-Constrained Unit Commitment With Uncertain Wind Generation : The Loadability Set Approach," vol. 28, no. 2, pp. 1787–1796, 2013.

[66] M. Matos and R. J. Bessa, "Setting the Operating Reserve Using Probabilistic Wind Power Forecasts," *IEEE Trans. Power Syst.*, vol. 26, no. 2, pp. 594–603, May 2011.

[67] N. Di Domenica, G. Mitra, P. Valente, and G. Birbilis, "Stochastic programming and scenario generation within a simulation framework: An information systems perspective," *Decis. Support Syst.*, vol. 42, no. 4, pp. 2197–2218, Jan. 2007.

[68] N. Di Domenica, G. Birbilis, G. Mitra, and P. Valente, "Technical Report Stochastic Programming and Scenario Generation within a Simulation Framework : An Information Systems Perspective," Brunel University, Uxbridge, Middlesex, 2003.

[69] S. Ahmed, A. Shapiro, and E. Shapiro, "The sample average approximation method for stochastic programs with integer recourse," in *Submitted for publication*, 2002, no. Dmii, pp. 1–24.

[70] J. Mayer, *Stochastic linear programming algorithms : A comparison based on a model management system*, IX. Australia: Gordon and Breach Science Publishers, 1998.

[71] C. Monteiro, R. Bessa, V. Miranda, A. Botterud, J. Wang, and G. Conzelmann, "Wind Power Forecasting : State-of-the-art 2009 Technical Report," 2009.

[72] G. Kariniotakis, P. Pinson, and N. Siebert, "The State of the Art in Short-term Prediction of Wind Power - From an Offshore Perspective," in *Proc. of 2004 SeaTechWeek*, 2004, pp. 1–13.

[73] J. Zack, "Overview of Wind Energy Generation Forecasting - Technical Report," New York, 2003.

[74] G. Giebel, "Equalizing Effects of the Wind Energy Production in Northern Europe Determined from Reanalysis Data - Riso technical Report," Roskilde, 2000.
[75] C. Pérez-llera, M. C. Fernández-baizán, J. L. Feito, and V. González, "Local Short-Term Prediction of Wind Speed : A Neural Network Analysis," in *iEMSs'02*, pp. 124–129.
[76] K. S. Dietachmayer, "Application of continuous dynamic grid adaptation techniques to meteorological modeling," *Am. Meteorol. Soc.*, vol. 120, pp. 1707–1722, 1992.
[77] R. C. Retallack, "Meteorologia," in *–Compêndio para a formação profissional de pessoal meteorológico de classe IV (Volume II), Instituto Nacional de Meteorologia e Geofisica, Lisboa, Portugal, 1979*, vol. II, no. Volume II, 1979.
[78] Y.-K. Wu and J.-S. Hong, "A literature review of wind forecasting technology in the world," *2007 IEEE Lausanne Power Tech*, pp. 504–509, Jul. 2007.
[79] I. J. Ramirez-Rosado, L. A. Fernandez-Jimenez, C. Monteiro, J. Sousa, and R. Bessa, "Comparison of two new short-term wind-power forecasting systems," *Renew. Energy*, vol. 34, no. 7, pp. 1848–1854, Jul. 2009.
[80] D. a. Bechrakis and P. D. Sparis, "Correlation of Wind Speed Between Neighboring Measuring Stations," *IEEE Trans. Energy Convers.*, vol. 19, no. 2, pp. 400–406, Jun. 2004.
[81] C. M. Zealand, D. H. Burn, and S. P. Simonovic, "Short term streamflow forecasting using artificial neural networks," *J. Hydrol.*, vol. 214, no. 1–4, pp. 32–48, 1999.
[82] T. Ludermir and R. D. Gouveia, "Self-Organizing Modeling in Forecasting Daily River Flows," in *Proceedings of Vth Brazilian Symposium on Neural Networks*, pp. 210–214.
[83] C. Liu and W. Liu, "Study on forecasting discharge of hydropower station with backwater effect based on improved EBP neural network," in *Power Engineering Society General Meeting, 2003, IEEE*, vol. 3, pp. 1451–1454.
[84] M. Valenca and T. Ludermir, "Monthly stream flow forecasting using an neural fuzzy network model," in *Proceedings Sixth Brazilian Symposium on Neural Networks*, 2000, pp. 117–119.
[85] T. Stokelj, D. Paravan, and R. Golob, "Short and mid term hydro power plant reservoir inflow forecasting," in *PowerCon 2000. 2000 International Conference on Power System Technology*, vol. 2, pp. 1107–1112.
[86] I. N. Sacchi, R., Ozturk, M.C., Principe, J.C., Carneiro, A.A.F. da Silva, "Water inflow forecasting using the Eco State Network: A Brasilian case Study," in *Proc. of International Joint Conference on Neural networks*, 2007, pp. 2403 – 2408.
[87] D. Paravan, T. Stokelj, and R. Golob, "Selecting input variables for HPP reservoir water inflow forecasting using mutual information," in *2001 IEEE Porto Power Tech Proceedings*, 2001, vol. vol.2, pp. 1–6.
[88] D. Paravan, "Improvements to the water management of a run-of-river HPP reservoir: methodology and case study," *Control Eng. Pract.*, vol. 12, no. 4, pp. 377–385, Apr. 2004.
[89] R. Golob, T. Štokelj, and D. Grgič, "Neural-network-based water inflow forecasting," *Control Eng. Pract.*, vol. 6, no. 5, pp. 593–600, May 1998.
[90] N. Estoperez and K. Nagasaka, "A month ahead micro-hydro power generation scheduling using artificial neural network," *IEEE Power Eng. Soc. Gen. Meet. 2005*, pp. 1330–1336.
[91] R. J. Kuligowski and A. P. Barros, "Experiments in Short-Term Precipitation Forecasting Using Artificial Neural Networks," *Mon. Weather Rev.*, vol. 126, no. 2, pp. 470–482, Feb. 1998.
[92] O. Kişi, "Streamflow Forecasting Using Different Artificial Neural Network Algorithms," *J. Hydrol. Eng.*, vol. 12, no. 5, p. 532, 2007.

[93] W. Huang, B. Xu, and A. Chan-Hilton, “Forecasting flows in Apalachicola River using neural networks,” *Hydrol. Process.*, vol. 18, no. 13, pp. 2545–2564, Sep. 2004.
[94] Y. B. Dibike and D. P. Solomatlne, “River Flow Forecasting Using Artificial Neural Networks,” *Phys. Chem. Earth, Part B Hydrol. Ocean. Atmos.*, vol. 26, no. 1, pp. 1–7, 2001.
[95] P. Coulibaly, F. Anctil, and B. Bobee, “Daily reservoir inflow forecasting using artificial neural networks with stopped training approach,” *J. Hydrol.*, vol. 230, no. 3–4, pp. 244–257, May 2000.
[96] C. Monteiro, I. J. Ramirez-Rosado, and L. A. Fernandez-Jimenez, “Short-term forecasting model for electric power production of small-hydro power plants,” *Renew. Energy*, vol. 50, pp. 387–394, Feb. 2013.
[97] A. Sfetsos, “Univariate and multivariate forecasting of hourly solar radiation with artificial intelligence techniques,” *Sol. Energy*, vol. 68, no. 2, pp. 169–178, 2000.
[98] F. Hocaoglu, O. Gerek, and M. Kurban, “Hourly solar radiation forecasting using optimal coefficient 2-D linear filters and feed-forward neural networks,” *Sol. Energy*, vol. 82, no. 8, pp. 714–726, Aug. 2008.
[99] M. K. S. Hokoi, M. Matsumoto, “Stochastic models of solar radiation and outdoor temperature,” in *ASHRAE Transactions*, 1990, pp. 245–252.
[100] C. Mustacchi, V. Cena, and M. Rocchi, “Stochastic simulation of hourly global radiation sequences,” *Sol. Energy*, vol. 23, no. 1, pp. 47–51, Jan. 1979.
[101] R. Aguiar and M. Collares-Pereira, “TAG: A time-dependent, autoregressive, Gaussian model for generating synthetic hourly radiation,” *Sol. Energy*, vol. 49, no. 3, pp. 167–174, Sep. 1992.
[102] R. Aguiar and M. Collares-Pereira, “Statistical properties of hourly global radiation,” *Sol. Energy*, vol. 48, no. 3, pp. 157–167, Jan. 1992.
[103] L. L. Mora-Lopez and M. Sidrach-de-Cardona, “Multiplicative ARMA models to generate hourly series of global irradiation,” *Sol. energy*, vol. 63, no. 5, pp. 283–291, 1998.
[104] M. Hassanzadeh, M. Etezadi-Amoli, and M. Fadali, “Practical approach for sub-hourly and hourly prediction of PV power output,” in *North American Power Symposium (NAPS), 2010*, pp. 1–5.
[105] M. L. Roderick, “Estimating the diffuse component from daily and monthly measurements of global radiation,” *Agric. For. Meteorol.*, vol. 95, no. 3, pp. 169–185, Jun. 1999.
[106] J. et. al. Soares, “Modeling hourly diffuse solar-radiation in the city of São Paulo using a neural-network technique,” *Appl. Energy*, vol. 79, no. 2, pp. 201–214, Oct. 2004.
[107] E. Lorenz, J. Hurka, D. Heinemann, and H. G. Beyer, “Irradiance Forecasting for the Power Prediction of Grid-Connected Photovoltaic Systems,” *IEEE J. Sel. Top. Appl. Earth Obs. Remote Sens.*, vol. 2, no. 1, pp. 2–10, Mar. 2009.
[108] E. A. Feinberg and D. Genethliou, “Load Forecasting,” in *Power electronics and power systems - Applied mathematics for restructured electric power systems*, 2005, pp. 269–285.
[109] M. Ramezani, H. Falaghi, M. Haghifam, and G. A. Shahryari, “Short-Term Electric Load Forecasting Using Neural Networks,” in *EUROCON 2005 - The International Conference on Computer as a Tool, 2005.*, 2005, vol. 00, pp. 1525–1528.
[110] J. M. Liu, R. Chen, L.-M. Liu, and J. L. Harris, “A semi-parametric time series approach in modeling hourly electricity loads,” *J. Forecast.*, vol. 25, no. 8, pp. 537–559, Dec. 2006.
[111] R. Hostache, P. Matgen, M. Montanari, C. Fosty, and L. Pfister, “Assessment and reduction of hydro-meteorological model forecasting uncertainty using an

autoregressive error model and bivariate meta-gaussian density," in *4th IASME / WSEAS International Conference on Water Resource, Hydraulics & Hydrology*, 2009, pp. 110–118.

[112] P. Pinson, G. Papaefthymiou, B. Klockl, and H. A. Nielsen, "Generation of Statistical Scenarios of Short-term Wind Power Production," in *IEEE Power TECH*, 2007, no. 2, pp. 491–496.

[113] X. Ma, Y. Sun, and H. Fang, "Scenario Generation of Wind Power Based on Statistical Uncertainty and Variability," *IEEE Trans. Sustain. Energy*, vol. 4, no. 4, pp. 894–904, 2013.

[114] A. Luig, S. Bofinger, and H. G. Beyer, "Analysis of confidence intervals for the prediction of the regional wind power output," 1996.

[115] G. Giebel, J. Badger, L. Landberg, H. A. Nielsen, H. Madsen, K. Sattler, and H. Feddersen, "Wind Power Forecasting Using Ensembles," in *2004 Global Wind Power Conference and Exhibition*, 2004, vol. 101295, no. Fu 2101.

[116] P. Pinson, G. Kariniotakis, T. S. Nielsen, and H. Madsen, "Properties of Quantile and Interval Forecasts of Wind generation and their Evaluation," in *Europe's Premier Wind Energy Event*, 2006, no. 1.

[117] a Botterud, J. Wang, R. J. Bessa, H. Keko, and V. Miranda, "Risk management and optimal bidding for a wind power producer," *IEEE PES Gen. Meet.*, pp. 1–8, Jul. 2010.

[118] J. B. Bremnes, "A comparison of a few statistical models for making quantile wind power forecasts," *Wind Energy*, vol. 9, no. 1–2, pp. 3–11, Jan. 2006.

[119] H. A. Nielsen, H. Madsen, and T. S. Nielsen, "Using quantile regression to extend an existing wind power forecasting system with probabilistic forecasts," *Wind Energy*, vol. 9, no. 1–2, pp. 95–108, Jan. 2006.

[120] J. B. Bremnes, "Probabilistic wind power forecasts using local quantile regression," *Wind Energy*, vol. 7, no. 1, pp. 47–54, Jan. 2004.

[121] A. Botterud, J. Wang, R. Bessa, H. Keko, J. Sumaili, and V. Miranda, "Advances in Probabilistic Forecasting with Application to Wind Power Trading," 2010.

[122] S. Demir and O. Toktamis, "On The Adaptive Nadaraya-Watson Kernel Regression Estimators," *Hacettep J. Math. Stat.*, vol. 39, no. 3, pp. 429–437, 2010.

[123] O. Kramer, B. Satzger, and J. Lässig, "Power prediction in smart grids with evolutionary local kernel regression," *Hybrid Artif. Intell. Syst.*, pp. 262–269, 2010.

[124] G. Papaefthymiou and D. Kurowicka, "Using Copulas for Modeling Stochastic Dependence in Power System Uncertainty Analysis," *IEEE Trans. Power Syst.*, vol. 24, no. 1, pp. 40–49, Feb. 2009.

[125] R. J. Bessa, V. Miranda, a. Botterud, Z. Zhou, and J. Wang, "Time-adaptive quantile-copula for wind power probabilistic forecasting," *Renew. Energy*, vol. 40, no. 1, pp. 29–39, Apr. 2012.

[126] Á. J. Duque and J. Sánchez, Ismael Castronuovo, Edgardo Usaola, "Simulation scenarios and prediction intervals in wind power forecasting with the Beta distribution," in *11th Spanish-Portuguese Conference on Electrical Engineering*, 2009.

[127] G. Anastasiades and P. McSharry, "Quantile Forecasting of Wind Power Using Variability Indices," *Energies*, vol. 6, no. 2, pp. 662–695, Feb. 2013.

[128] P. Pinson and G. Kariniotakis, "On-line assessment of prediction risk for wind power production forecasts," *Wind Energy*, vol. 7, no. 2, pp. 119–132, Apr. 2004.

[129] P. Pinson, H. A. Nielsen, H. Madsen, and G. Kariniotakis, "Skill forecasting from ensemble predictions of wind power," *Appl. Energy*, vol. 86, no. 7–8, pp. 1326–1334, Jul. 2009.

[130] S. Fink, C. Mudd, K. Porter, and B. Morgenstern, "Wind Energy Curtailment Case Studies May 2008 — May 2009," 2009.

[131] Y. V Makarov, P. V Etingov, and J. Ma, “Incorporating Uncertainty of Wind Power Generation Forecast Into Power System Operation , Dispatch , and Unit Commitment Procedures,” *IEEE Trans. Sustain. Energy*, vol. 2, no. 4, pp. 433–442, 2011.
[132] Y. V Makarov, S. Lu, N. Samaan, K. Subbarao, P. V Etingov, J. Ma, R. P. Hafen, R. Diao, and N. Lu, “Integration of Uncertainty Information into Power System Operations,” in *Power and Energy Society General Meeting*, 2011, pp. 1–13.
[133] N. Menemenlis, M. Huneault, and a. Robitaille, “Integration of new generation and load technology in the computation of risk over the operations planning time-horizon,” *2010 IEEE PES Innov. Smart Grid Technol. Conf. Eur. (ISGT Eur.*, pp. 1–8, Oct. 2010.
[134] S. Jin, A. Botterud, and S. M. Ryan, “Temporal Versus Stochastic Granularity in Thermal Generation Capacity Planning With Wind Power,” *IEEE Trans. Power Syst.*, pp. 1–9, 2014.
[135] J. J. Hargreaves and B. F. Hobbs, “Commitment and Dispatch With Uncertain Wind Generation by Dynamic Programming,” *IEEE Trans. Sustain. Energy*, vol. 3, no. 4, pp. 724–734, Oct. 2012.
[136] H. Holttinen, P. Meibom, A. Orths, and B. Lange, “Impacts of large amounts of wind power on design and operation of power systems, results of IEA collaboration,” *Wind*, no. November 2009, pp. 179–192, 2011.
[137] H. Madsen, P. Pinson, G. Kariniotakis, H. A. Nielsen, and T. Skov, “A Protocol for Standardazing the performance evaluation of short term wind power prediction models,” in *Wind Engineering, Multi-Science Publishing*, 2005, pp. 475–489.
[138] P. Pinson and G. Kariniotakis, “Conditional prediction intervals of wind power generation,” *IEEE Trans. Power Syst.*, no. August, pp. 1–12, 2010.
[139] G. S. Lauer, N. R. Sandell, D. P. Bertsekas, and T. A. Posbergh, “Solution of Large-Scale Optimal Unit Commitment Problems,” *Power Appar. Syst. IEEE Trans.*, vol. PAS-101, no. 1, pp. 79–86, 1982.
[140] R. C. Williamson, “Probabilistic Arithmetic,” Ph.D. - University of Queensland, 1989.
[141] M. Matos and R. Bessa, “Operating reserve adequacy evaluation using uncertainties of wind power forecast,” *2009 IEEE Bucharest PowerTech*, pp. 1–8, Jun. 2009.
[142] P. D. Michailidis, “Accelerating Kernel Density Estimation on the GPU Using the CUDA Framework,” *Appl. Math. Sci.*, vol. 7, no. 30, pp. 1447–1476, 2013.
[143] W. Li, *Risk Assessment of Power Systems, Models, methods, and applications*, 1st ed. Piscataway: IEEE Press, 2005.
[144] P. Yadav, R. Kumar, S. K. Panda, and C. S. Chang, “An Improved Harmony Search algorithm for optimal scheduling of the diesel generators in oil rig platforms,” *Energy Convers. Manag.*, vol. 52, no. 2, pp. 893–902, Feb. 2011.
[145] X. Xia and a. M. Elaiw, “Optimal dynamic economic dispatch of generation: A review,” *Electr. Power Syst. Res.*, vol. 80, no. 8, pp. 975–986, Aug. 2010.
[146] A. Stefek, “Benchmarking of heuristic optimization methods,” in *Mechatronika, 2011 14th International Symposium*, 2011, pp. 68–71.
[147] C.-L. Chiang, “Improved Genetic Algorithm for Power Economic Dispatch of Units With Valve-Point Effects and Multiple Fuels,” *IEEE Trans. Power Syst.*, vol. 20, no. 4, pp. 1690–1699, Nov. 2005.
[148] P. M. Fonte, C. Monteiro, and F. P. Maciel Barbosa, “Sensing Cloud Optimization applied to a non-convex constrained economical dispatch,” *IECON 2013 - 39th Annu. Conf. IEEE Ind. Electron. Soc.*, no. 3, pp. 2163–2168, Nov. 2013.
[149] P. Fonte, C. Monteiro, and F. Barbosa, “Sensing Cloud Optimization to Solve ED of Units with Valve-Point Effects and Multi-fuels,” in *Technological Innovation for the Internet of Things*, 2013, no. 1, pp. 477–484.

[150] M. H. Sulaiman, M. W. Mustafa, Z. N. Zakaria, O. Aliman, and S. R. A. Rahim, “Firefly Algorithm Technique for Solving Economic Dispatch Problem,” in *2012 IEEE International Power Engineering and Optimization Conference (PEOCO 2012)*, 2012, no. June, pp. 90–95.

[151] B. Mahdad, K. Srairi, and T. Bouktir, “Improved Parallel PSO Solution to Economic Dispatch with Practical Generator Constraints,” in *MELECON 2010 - 2010 15th IEEE Mediterranean Electrotechnical Conference*, 2010, pp. 314–319.

[152] S. Coelho and V. C. Mariani, “Combining of Chaotic Differential Evolution and Quadratic Programming for Economic Dispatch Optimization With Valve-Point Effect,” *Power*, vol. 21, no. 2, pp. 989–996, 2006.

[153] S. Aronoff and G. Mackinney, “Brief Papers: Pyrrole Derivatives and Iron Chlorosis in Plants.,” *Plant Physiol.*, vol. 18, no. 4, pp. 713–5, Oct. 1943.

[154] S. B. Nejad, S. H. Elyas, and A. Khamseh, “Hybrid CLONAL Selection Algorithm with PSO for Valve- Point Economic Load Dispatch,” no. 1, pp. 1147–1150, 2012.

[155] J. Pontes, P. M. Fonte, and R. Pestana, “Solving non-Convex and Restricted Problems Using Swarms – Economic Dispatch Case,” *Procedia Technol.*, vol. 17, pp. 502–509, 2014.

[156] R. N. Billinton, R. and Allan, *Reliability Evaluation of Power Systems*, 2nd Ed. Springer, New York, 1996.

[157] P. K. Singhal and R. N. Sharma, “Dynamic programming approach for solving power generating unit commitment problem,” in *2011 2nd International Conference on Computer and Communication Technology (ICCCT-2011)*, 2011, no. 5, pp. 298–303.

[158] A. M. L. da Silva, G. Perez A., J. W. Marangon Lima, and J. C. O. Mello, “Loss of load costs in generating capacity reliability evaluation,” *Electr. Power Syst. Res.*, vol. 41, no. 2, pp. 109–116, May 1997.

[159] L. Manso, A. Silva, and J. Mello, “Comparison of alternative methods for evaluating loss of load costs in generation and transmission systems,” *Electr. Power Syst. Res.*, vol. 50, pp. 107–114, 1999.

List of publications

Conferences:

P. M. Fonte, C. Monteiro, and F. Barbosa, "Sensing Cloud Optimization to Solve ED of Units with Valve-Point Effects and Multi-fuels," in *Proc. of DoCEIS'13 - Doctoral Conference on Computing, Electrical and Industrial Systems*, 2013, pp. 477–484, Costa da Caparica, Portugal

P. M. Fonte, C. Monteiro, and F. P. Maciel Barbosa, "Sensing Cloud Optimization applied to a non-convex constrained economical dispatch," *IECON 2013 - 39th Annu. Conf. IEEE Ind. Electron. Soc.*, no. 3, pp. 2163–2168, Nov. 2013.

P. M. Fonte, B. Santos, C. Monteiro, J. Catalão, and F. P. Maciel Barbosa, "Renewable Power Forecast to Scheduling of Thermal Units," in *Proc. of DoCEIS'14 - Doctoral Conference on Computing, Electrical and Industrial Systems*, 2014, pp. 361-368, Costa da Caparica, Portugal

J. Pontes, **P.M. Fonte**, and R. Pestana,"Solving non-Convex and Restricted Problems Using Swarms – Economic Dispatch Case," *Procedia Technology*, vol 17, pp 502-509,2014

Book Chapter:

C. Monteiro, B. Santos, T. Santos, C. Soares, **P. M. Fonte**, G. Sannino, A. Carello and R. Medina, "Smart and Sustainable Power Systems: Operations, Planning and Economics of Insular Electricity Grids", João P. S. Catalão (Editor) Taylor & Francis/CRC Press (*in press*)

Annex I – Technical characteristics of thermal units

Table AI.1 – Technical characteristics of thermal units

	Units 1-4	Units 5-8
Generator Model	Siemens 1 DK5726 - 4DE 07	ABB AMG 1600
Motor Model	Krupp MAK 8M601	Wartsila V46
Rated Power (kW)	7696	16820
Maximum power (boost) (kW) (<30 minutes)	7500	18015
Maximum power in steady-state (kW)	7200	16500
Minimum technical	3848	8410
Cold starting time (from 0 to 50%) (minutes)	30	30
Pre-heated Starting time (from 0 to 50%) (minutes)	8	10

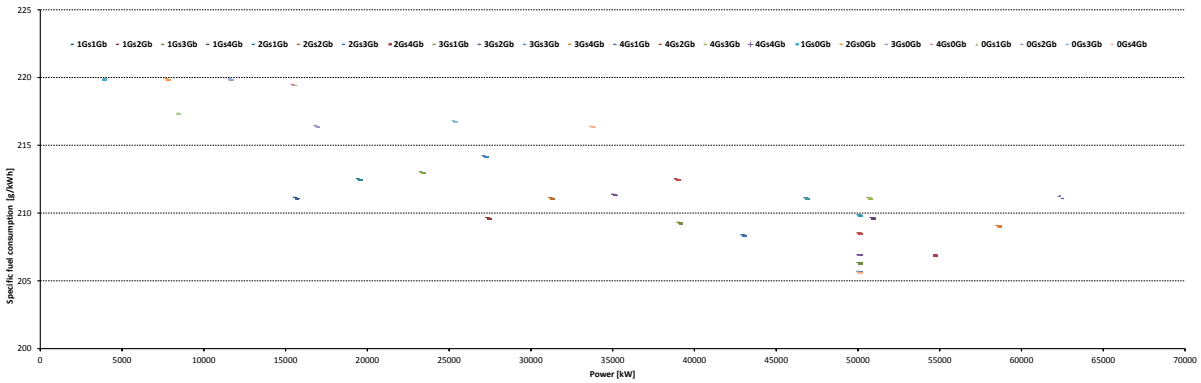

Figure AI.1 – Specific consumption of each GENSET

Annex II – Results of economic dispatch

Active power losses matrices for the first case study (6 units)

$$Bij = \begin{vmatrix} 0.0017 & 0.0012 & 0.0007 & -0.0001 & -0.0005 & -0.0002 \\ 0.0012 & 0.0014 & 0.0009 & 0.0001 & -0.0006 & -0.0001 \\ 0.0007 & 0.0009 & 0.0031 & 0 & -0.001 & -0.0006 \\ -0.0001 & 0.0001 & 0 & 0.0024 & -0.0006 & -0.0008 \\ -0.0005 & -0.0006 & -0.001 & -0.0006 & 0.0129 & -0.0002 \\ -0.0002 & -0.0001 & -0.0006 & -0.0008 & -0.0002 & 0.015 \end{vmatrix}$$

$$B0j = \begin{vmatrix} -0.0003908 & -0.0001297 & 0.0007047 & 0.0000591 & 0.0002161 & -0.0006635 \end{vmatrix}$$

$$B00 = \begin{vmatrix} 0.056 \end{vmatrix}$$

Active power losses matrices for the second case study (15 units)

$$Bij = \begin{vmatrix} 0.0014 & 0.0012 & 0.0007 & -0.0001 & -3E-04 & -0.0001 & -0.0001 & -0.0001 & -3E-04 & 0.0005 & -0.0003 & -0.0002 & 0.0004 & 0.0003 & -0.0001 \\ 0.0012 & 0.0015 & 0.0013 & 0 & -5E-04 & -0.0002 & 0 & 0.0001 & -2E-04 & -4E-04 & -0.0004 & 0 & 0.0004 & 0.001 & -0.0002 \\ 0.0007 & 0.0013 & 0.0076 & -0.0001 & -0.001 & -0.0009 & -0.0001 & 0 & -8E-04 & -0.001 & -0.0017 & 0 & -0.0026 & 0.0111 & -0.0028 \\ -0.0001 & 0 & -1E-04 & 0.0034 & -7E-04 & -0.0004 & 0.0011 & 0.005 & 0.0029 & 0.0032 & -0.0011 & 0 & 0.0001 & 0.0001 & -0.0026 \\ -0.0003 & -0.0005 & -0.001 & -0.0007 & 0.009 & 0.0014 & -0.0003 & -0.0012 & -0.001 & -0.001 & 0.0007 & -0.0002 & -0.0002 & -0.002 & -0.0003 \\ -0.0001 & -0.0002 & -9E-04 & -0.0004 & 0.0014 & 0.0016 & 0 & -0.0006 & -5E-04 & -8E-04 & 0.0011 & -0.0001 & -0.0002 & -0.002 & 0.0003 \\ -0.0001 & 0 & -1E-04 & 0.0011 & -3E-04 & 0 & 0.0015 & 0.0017 & 0.0015 & 0.0009 & -0.0005 & 0.0007 & 0 & -2E-04 & -0.0008 \\ -0.0001 & 0.0001 & 0 & 0.005 & -0.001 & -0.0006 & 0.0017 & 0.0168 & 0.0082 & 0.0079 & -0.0023 & -0.0036 & 0.0001 & 0.0005 & -0.0078 \\ -0.0003 & -0.0002 & -8E-04 & 0.0029 & -0.001 & -0.0005 & 0.0015 & 0.0082 & 0.0129 & 0.0116 & -0.0021 & -0.0025 & 0.0007 & -0.001 & -0.0072 \\ -0.0005 & -0.0004 & -0.001 & 0.0032 & -0.001 & -0.0008 & 0.0009 & 0.0079 & 0.0116 & 0.02 & -0.0027 & -0.0034 & 0.0009 & -0.001 & -0.0088 \\ -0.0003 & -0.0004 & -0.002 & -0.0011 & 0.0007 & 0.0011 & -0.0005 & -0.0023 & -0.002 & -0.003 & 0.014 & 0.0001 & 0.0004 & -0.004 & 0.0168 \\ -0.0002 & 0 & 0 & 0 & -2E-04 & -0.0001 & 0.0007 & -0.0036 & -0.003 & -0.003 & 0.0001 & 0.0054 & -0.0001 & -4E-04 & 0.0028 \\ 0.0004 & 0.0004 & -0.003 & 0.0001 & -2E-04 & -0.0002 & 0 & 0.0001 & 0.0007 & 0.0009 & 0.0004 & -0.0001 & 0.0103 & -0.01 & 0.0028 \\ 0.0003 & 0.001 & 0.0111 & 0.0001 & -0.002 & -0.0017 & -0.0002 & 0.0005 & -0.001 & -0.001 & -0.0038 & -0.0004 & -0.0101 & 0.0578 & -0.0094 \\ -0.0001 & -0.0002 & -0.003 & -0.0026 & -3E-04 & 0.0003 & -0.0008 & -0.0078 & -0.007 & -0.009 & 0.0168 & 0.0028 & 0.0028 & -0.009 & 0.1283 \end{vmatrix}$$

$$B0j = \begin{vmatrix} -0.0001 & -0.0002 & 0.0028 & -0.0001 & 0.0001 & -0.0003 & -0.0002 & -0.0002 & 0.0006 & 0.0039 & -0.0017 & 0 & -0.0032 & 0.0067 & -0.0064 \end{vmatrix}$$

$$B00 = \begin{vmatrix} 0.0055 \end{vmatrix}$$

Table AII.1 – Generating unit's data (third case study)

Unit	P_i^{min} [MW]	P_i^{max} [MW]	a_i	b_i	c_i	e_i	f_i
1	36	114	0,0069	6,73	94,705	100	0,084
2	36	114	0,0069	6,73	94,705	100	0,084
3	60	120	0,02028	7,07	309,54	100	0,084
4	80	190	0,00942	8,18	369,03	150	0,063
5	47	97	0,0114	5,35	148,89	120	0,077
6	68	140	0,01142	8,05	222,33	100	0,084
7	110	300	0,00357	8,03	287,71	200	0,042
8	135	300	0,00492	6,99	391,98	200	0,042
9	135	300	0,00573	6,6	455,76	200	0,042
10	130	300	0,00605	12,9	722,82	200	0,042
11	94	375	0,00515	12,9	635,2	200	0,042
12	94	375	0,00569	12,8	654,69	200	0,042
13	125	500	0,00421	12,5	913,4	300	0,035
14	125	500	0,00752	8,84	1760,4	300	0,035
15	125	500	0,00708	9,15	1728,3	300	0,035
16	125	500	0,00708	9,15	1728,3	300	0,035
17	220	500	0,00313	7,97	647,85	300	0,035
18	220	500	0,00313	7,95	649,69	300	0,035
19	242	550	0,00313	7,97	647,83	300	0,035
20	242	550	0,00313	7,97	647,81	300	0,035
21	254	550	0,00298	6,63	785,96	300	0,035
22	254	550	0,00298	6,63	785,96	300	0,035
23	254	550	0,00284	6,66	794,53	300	0,035
24	254	550	0,00284	6,66	794,53	300	0,035
25	254	550	0,00277	7,1	801,32	300	0,035
26	254	550	0,00277	7,1	801,32	300	0,035
27	10	150	0,52124	3,33	1055,1	120	0,077
28	10	150	0,52124	3,33	1055,1	120	0,077
29	10	150	0,52124	3,33	1055,1	120	0,077
30	47	97	0,0114	5,35	148,89	120	0,077
31	60	190	0,0016	6,43	222,92	150	0,063
32	60	190	0,0016	6,43	222,92	150	0,063
33	60	190	0,0016	6,43	222,92	150	0,063
34	90	200	0,0001	8,95	107,87	200	0,042
35	90	200	0,0001	8,62	116,58	200	0,042
36	90	200	0,0001	8,62	116,58	200	0,042
37	25	110	0,0161	5,88	307,45	80	0,098
38	25	110	0,0161	5,88	307,45	80	0,098
39	25	110	0,0161	5,88	307,45	80	0,098
40	242	550	0,00313	7,97	647,83	300	0,035

Table AII.2 – Results obtained (40-units 10500 MW)(Best individual)

Unit	Power output (MW)	Unit	Power output (MW)
PG1	114	PG21	550
PG2	114	PG22	550
PG3	120	PG23	550
PG4	190	PG24	550
PG5	97	PG25	550
PG6	140	PG26	550
PG7	300	PG27	10
PG8	300	PG28	10
PG9	300	PG29	10
PG10	130	PG30	97
PG11	94	PG31	190
PG12	94	PG32	190
PG13	125	PG33	190
PG14	271.67	PG34	200
PG15	266.66	PG35	200
PG16	266.66	PG36	200
PG17	500	PG37	110
PG18	500	PG38	110
PG19	550	PG39	110
PG20	550	PG40	550
PL =	10500 MW		

Table AII.3 – Generating unit's data (fourth case study)

Unit	P_i^{min} (MW)	P_i^{max} (MW)	fuel 1	fuel 2	fuel 3
1	100	250	[150 196]	[197 250]	
2	50	230	[158 230]	[50 114]	[115 157]
3	200	500	[200 332]	[333 388]	[389 500]
4	99	265	[99 138]	[139 200]	[201 265]
5	190	490	[190 338]	[339 407]	[408 490]
6	85	265	[139 200]	[85 138]	[201 265]
7	200	500	[200 331]	[332 391]	[392 500]
8	99	265	[99 138]	[139 200]	[201 265]
9	130	440	[214 370]	[371 440]	[130 213]
10	200	490	[200 362]	[408 490]	[363 407]

Table AII.4 – Generating unit's data (fourth case study)

Unit	fuel	a_i	b_i	c_i	e_i	f_i
	1	0,002176	-0,3975	26,97	0,02697	-3,975
	2	0,001861	-0,3059	21,13	0,02113	-3,059
2	1	0,004194	-1,269	118,4	0,1184	-12,69
	2	0,001138	-0,03988	1,865	0,001865	-0,3988
	3	0,00162	-0,198	13,65	0,01365	-1,98
3	1	0,001457	-0,3116	39,79	0,03979	-3,116
	2	0,00001176	0,4864	-59,14	-0,05914	4,864
	3	0,0008035	0,03389	-2,875	-0,002876	0,3389
4	1	0,001049	-0,03114	1,983	0,001983	-0,3114
	2	0,002758	-0,6348	52,85	0,05285	-6,348
	3	0,005935	-2,338	266,8	0,2668	-23,38
5	1	0,001066	-0,08733	13,92	0,01392	-0,8733
	2	0,001597	-0,5206	99,76	0,09976	-5,206
	3	0,0001498	0,4462	-53,99	-0,05399	4,462
6	1	0,002758	-0,6348	52,85	0,05285	-6,348
	2	0,001049	-0,03114	1,983	0,001983	-0,3114
	3	0,005935	-2,338	266,8	0,2668	-23,38
7	1	0,001107	-0,1325	18,93	0,01893	-1,325
	2	0,001165	-0,2267	43,77	0,04377	-2,267
	3	0,0002454	0,3559	-43,35	-0,04335	3,559
8	1	0,001049	-0,03114	1,983	0,001983	-0,3114
	2	0,002758	-0,6348	52,85	0,05285	-6,348
	3	0,005935	-2,338	266,8	0,2668	-23,38
9	1	0,001554	-0,5675	88,53	0,08853	-5,675
	2	0,007033	-0,04514	15,3	0,01423	-0,1817
	3	0,0006121	-0,01817	14,23	0,01423	-0,1817
10	1	0,001102	-0,09938	13,97	0,01397	-0,9938
	2	0,00004164	0,5084	-61,13	-0,06113	5,084
	3	0,001137	-0,2024	46,71	0,04671	-2,024

Table AII.5 – Cost functions parameters of GENSET's

GENSET	Min (MW)	Max (MW)	Interval (kW)		Unit 1		Unit 2		Unit 3		Unit 4		Unit 5		Unit 6		Unit 7		Unit 8		Cost (g/kWh)		
			From	Up to	ax	b	ax	b	ax	b	ax	b	ax	b	ax	b	ax	b	ax	b	a	b	c
0GS 1GB	8,41	16,5	8410	16500	0,00	0,00	0,00	0,00	0,00	0,00	0,00	0,00	1,00	0,00	0,00	0,00	0,00	0,00	0,00	0,00	0,0017	150	445500
0GS 2GB	16,82	33	16820	33000	0,00	0,00	0,00	0,00	0,00	0,00	0,00	0,00	0,50	0,00	0,50	0,00	0,00	0,00	0,00	0,00	0,00085	150	891000
0GS 3GB	25,23	49,5	25230	49500	0,00	0,00	0,00	0,00	0,00	0,00	0,00	0,00	0,33	0,00	0,33	0,00	0,33	0,00	0,00	0,00	0,00055	150	1336500
0GS 4GB	33,64	66	33640	66000	0,00	0,00	0,00	0,00	0,00	0,00	0,00	0,00	0,25	0,00	0,25	0,00	0,25	0,00	0,25	0,00	0,0004	150	1782000
1GS 0GB	3,848	7,2	3848	7200	1,00	0,00	0,00	0,00	0,00	0,00	0,00	0,00	0,00	0,00	0,00	0,00	0,00	0,00	0,00	0,00	0,0039	160	172800
2GS 0GB	7,696	14,4	7696	14400	0,50	0,00	0,50	0,00	0,00	0,00	0,00	0,00	0,00	0,00	0,00	0,00	0,00	0,00	0,00	0,00	0,00195	160	345600
3GS 0GB	11,544	21,6	11544	21600	0,33	0,00	0,33	0,00	0,33	0,00	0,00	0,00	0,00	0,00	0,00	0,00	0,00	0,00	0,00	0,00	0,0013	160	518400
4GS 0GB	15,392	28,8	15392	28800	0,25	0,00	0,25	0,00	0,25	0,00	0,25	0,00	0,00	0,00	0,00	0,00	0,00	0,00	0,00	0,00	0,00095	160	691200
1GS 1GB	12,258	23,7	15594,3	22425,4	0,30	-894,45	0,00	0,00	0,00	0,00	0,00	0,00	0,70	894,45	0,00	0,00	0,00	0,00	0,00	0,00	0,001183	153,0411	613827,72
1GS 2GB	20,668	40,2	27340,6	38925,4	0,18	-1054,85	0,00	0,00	0,00	0,00	0,00	0,00	0,41	527,43	0,41	527,43	0,00	0,00	0,00	0,00	0,000698	151,79	1058525,74
1GS 3GB	29,078	56,7	39086,9	55425,4	0,13	-1121,91	0,00	0,00	0,00	0,00	0,00	0,00	0,29	373,97	0,29	373,97	0,29	373,97	0,00	0,00	0,000495	151,2715	1,50E+06
1GS 4GB	37,488	73,2	50833,2	71925,4	0,10	-1158,75	0,00	0,00	0,00	0,00	0,00	0,00	0,23	289,69	0,23	289,69	0,23	289,69	0,23	289,69	0,000383	150,9849	1949006,26
2GS 1GB	16,106	30,9	19442,3	28350,9	0,23	-685,87	0,23	-685,87	0,00	0,00	0,00	0,00	0,53	1371,74	0,00	0,00	0,00	0,00	0,00	0,00	0,000907	154,6639	784241
2GS 2GB	24,516	47,4	31188,6	44850,9	0,15	-894,45	0,15	-894,45	0,00	0,00	0,00	0,00	0,35	894,45	0,35	894,45	0,00	0,00	0,00	0,00	0,000592	153,0411	1227655,46
2GS 3GB	32,926	63,9	42934,9	61350,9	0,11	-995,36	0,11	-995,36	0,00	0,00	0,00	0,00	0,26	663,57	0,26	663,57	0,26	663,57	0,00	0,00	0,000439	152,2561	1672146,45
2GS 4GB	41,336	80,4	54681,2	77850,9	0,09	-1054,85	0,09	-1054,85	0,00	0,00	0,00	0,00	0,21	527,43	0,21	527,43	0,21	527,43	0,21	527,43	0,000349	151,7932	2117051,48
3GS 1GB	19,954	38,1	23290,3	34276,3	0,19	-556,17	0,19	-556,17	0,19	-556,17	0,00	0,00	0,43	1668,52	0,00	0,00	0,00	0,00	0,00	0,00	0,000736	155,673	955557,4
3GS 2GB	28,364	54,6	35036,6	50776,3	0,13	-776,40	0,13	-776,40	0,13	-776,40	0,00	0,00	0,30	1164,60	0,30	1164,60	0,00	0,00	0,00	0,00	0,000514	153,9596	1397754,04
3GS 3GB	36,774	71,1	46782,9	67276,3	0,10	-894,45	0,10	-894,45	0,10	-894,45	0,00	0,00	0,23	894,45	0,23	894,45	0,23	894,45	0,00	0,00	0,000395	153,0411	1841483,18
3GS 4GB	45,184	87,6	58529,2	83776,3	0,08	-968,05	0,08	-968,05	0,08	-968,05	0,00	0,00	0,19	726,04	0,19	726,04	0,19	726,04	0,19	726,04	0,00032	152,4685	2285879,19
4GS 1GB	23,802	45,3	27138,3	40201,8	0,16	-467,73	0,16	-467,73	0,16	-467,73	0,16	-467,73	0,36	1870,91	0,00	0,00	0,00	0,00	0,00	0,00	0,000619	156,3611	1127345,46
4GS 2GB	32,212	61,8	38884,6	56701,8	0,12	-685,87	0,12	-685,87	0,12	-685,87	0,12	-685,87	0,27	1371,74	0,27	1371,74	0,00	0,00	0,00	0,00	0,000454	154,6639	1568482,58
4GS 3GB	40,622	78,3	50630,9	73201,8	0,09	-812,13	0,09	-812,13	0,09	-812,13	0,09	-812,13	0,21	1082,84	0,21	1082,84	0,21	1082,84	0,00	0,00	0,000358	153,6816	2011457,44
4GS 4GB	49,032	94,8	62377,2	89701,8	0,08	-894,45	0,08	-894,45	0,08	-894,45	0,08	-894,45	0,17	894,45	0,17	894,45	0,17	894,45	0,17	894,45	0,000296	153,0411	2455310,91

Table AII.6 – Cost functions parameters of GENSET's

GENSET	Min (MW)	Max (MW)	Interval (MW)		Unit 1		Unit 2		Unit 3		Unit 4		Unit 5		Unit 6		Unit 7		Unit 8		Custo (gr/kW)		
			From	Up to	ax	b	ax	b	ax	b	ax	b	ax	b	ax	b	ax	b	ax	b	ax^2	bx	c
0GS 1GB	8.41	16.5																					
0GS 2GB	16.82	33																					
0GS 3GB	25.23	49.5																					
0GS 4GB	33.64	66																					
1GS 0GB	3.848	7.2																					
2GS 0GB	7.696	14.4																					
3GS 0GB	11.544	21.6																					
4GS 0GB	15.392	28.8																					
1GS 1GB	12.258	23.7	12258.0	15594.3	0	3848	0	0	0	0	0	0	1	-3848	0	0	0	0	0	0	0.0017	136.9168	739551.71
1GS 2GB	20.668	40.2	20668.0	27340.6	0	3848	0	0	0	0	0	0	0.5	-1924	0.5	-1924	0	0	0	0	0.00085	143.4584	1172465.7
1GS 3GB	29.078	56.7	29078.0	39086.9	0	3848	0	0	0	0	0	0	0.333	-1282.67	0.333	-1282.67	0.333	-1282.67	0	0	0.0005665	145.63893	1613770.3
1GS 4GB	37.488	73.2	37488.0	50833.2	0	3848	0	0	0	0	0	0	0.25	-962	0.25	-962	0.25	-962	0.25	-962	0.000425	146.7292	2057172.7
2GS 1GB	16.106	30.9	16106.0	19442.3	0	3848	0	3848	0	0	0	0	1	-3848	0	0	0	0	0	0	0.0017	123.8336	1083947.6
2GS 2GB	24.516	47.4	24516.0	31188.6	0	3848	0	3848	0	0	0	0	0.5	-1924	0.5	-1924	0	0	0	0	0.00085	136.9168	1479103.4
2GS 3GB	32.926	63.9	32926.0	42934.9	0	3848	0	3848	0	0	0	0	0.333	-1282.67	0.333	-1282.67	0.333	-1282.67	0	0	0.0005665	141.27787	1907822
2GS 4GB	41.336	80.4	41336.0	54681.2	0	3848	0	3848	0	0	0	0	0.25	-962	0.25	-962	0.25	-962	0.25	-962	0.000425	143.4584	2344931.4
3GS 1GB	19.954	38.1	19954.0	23290.3	0	3848	0	3848	0	3848	0	0	1	-3848	0	0	0	0	0	0	0.0017	110.7504	1478687.6
3GS 2GB	28.364	54.6	28364.0	35036.6	0	3848	0	3848	0	3848	0	0	0.5	-1924	0.5	-1924	0	0	0	0	0.00085	130.3752	1810913.3
3GS 3GB	36.774	71.1	36774.0	46782.9	0	3848	0	3848	0	3848	0	0	0.333	-1282.67	0.333	-1282.67	0.333	-1282.67	0	0	0.000567	136.9168	2218655.1
3GS 4GB	45.184	87.6	45184.0	58529.2	0	3848	0	3848	0	3848	0	0	0.25	-962	0.25	-962	0.25	-962	0.25	-962	0.000425	140.1876	2645276.1
4GS 1GB	23.802	45.3	23802.0	27138.3	0	3848	0	3848	0	3848	0	3848	1	-3848	0	0	0	0	0	0	0.0017	97.6672	1923771.8
4GS 2GB	32.212	61.8	32212.0	38884.6	0	3848	0	3848	0	3848	0	3848	0.5	-1924	0.5	-1924	0	0	0	0	0.00085	123.8336	2167895.2
4GS 3GB	40.622	78.3	40622.0	50630.9	0	3848	0	3848	0	3848	0	3848	0.333	-1282.67	0.333	-1282.67	0.333	-1282.67	0	0	0.000567	132.55573	2546269.6
4GS 4GB	49.032	94.8	49032.0	62377.2	0	3848	0	3848	0	3848	0	3848	0.25	-962	0.25	-962	0.25	-962	0.25	-962	0.000425	136.9168	2958206.9

Table AII.7 – Cost functions parameters of GENSET's

GENSET	Min (MW)	Max (MW)	Interval (MW)		Unit 1		Unit 2		Unit 3		Unit 4		Unit 5		Unit 6		Unit 7		Unit 8		Custo (gr/kW)		
			From	Up to	ax	b	ax	b	ax	b	ax	b	ax	b	ax	b	ax	b	ax	b	ax^2	bx	c
0GS 1GB	8.41	16.5																					
0GS 2GB	16.82	33																					
0GS 3GB	25.23	49.5																					
0GS 4GB	33.64	66																					
1GS 0GB	3.848	7.2																					
2GS 0GB	7.696	14.4																					
3GS 0GB	11.544	21.6																					
4GS 0GB	15.392	28.8																					
1GS 1GB	12.258	23.7	22425.45	23700	1	-16500	0	0	0	0	0	0	0	16500	0	0	0	0	0	0	0.00389	31.63	1975177.5
1GS 2GB	20.668	40.2	38925.45	40200	1	-16500	0	0	0	0	0	0	0	16500	0	16500	0	0	0	0	0.00389	-96.74	5895660
1GS 3GB	29.078	56.7	55425.45	56700	1	-16500	0	0	0	0	0	0	0	16500	0	16500	0	16500	0	0	0.00389	-225.11	11934248
1GS 4GB	37.488	73.2	71925.45	73200	1	-16500	0	0	0	0	0	0	0	16500	0	16500	0	16500	0	16500	0.00389	-353.48	20090940
2GS 1GB	16.106	30.9	28350.9	30900	0.5	-8250	0.5	-8250	0	0	0	0	0	16500	0	0	0	0	0	0	0.001945	95.815	1618451.3
2GS 2GB	24.516	47.4	44850.9	47400	0.5	-8250	0.5	-8250	0	0	0	0	0	16500	0	16500	0	0	0	0	0.001945	31.63	3950355
2GS 3GB	32.926	63.9	61350.9	63900	0.5	-8250	0.5	-8250	0	0	0	0	0	16500	0	16500	0	16500	0	0	0.001945	-32.555	7341311.3
2GS 4GB	41.336	80.4	77850.9	80400	0.5	-8250	0.5	-8250	0	0	0	0	0	16500	0	16500	0	16500	0	16500	0.001945	-96.74	11791320
3GS 1GB	19.954	38.1	34276.35	38100	0.333	-5500	0.333	-5500	0.333	-5500	0	0	0	16500	0	0	0	0	0	0	0.001297	117.21	1614742.5
3GS 2GB	28.364	54.6	50776.35	54600	0.333	-5500	0.333	-5500	0.333	-5500	0	0	0	16500	0	16500	0	0	0	0	0.001297	74.42	3417120
3GS 3GB	36.774	71.1	67276.35	71100	0.333	-5500	0.333	-5500	0.333	-5500	0	0	0	16500	0	16500	0	16500	0	0	0.001297	31.63	5925532.5
3GS 4GB	45.184	87.6	83776.35	87600	0.333	-5500	0.333	-5500	0.333	-5500	0	0	0	16500	0	16500	0	16500	0	16500	0.001297	-11.16	9139980
4GS 1GB	23.802	45.3	40201.799	45300	0.25	-4125	0.25	-4125	0.25	-4125	0.25	-4125	0	16500	0	0	0	0	0	0	0.000973	127.9075	1699288.1
4GS 2GB	32.212	61.8	56701.799	61800	0.25	-4125	0.25	-4125	0.25	-4125	0.25	-4125	0	16500	0	16500	0	0	0	0	0.000972	95.815	3236902.5
4GS 3GB	40.622	78.3	73201.799	78300	0.25	-4125	0.25	-4125	0.25	-4125	0.25	-4125	0	16500	0	16500	0	16500	0	0	0.000972	63.7225	5304043.1
4GS 4GB	49.032	94.8	89701.799	94800	0.25	-4125	0.25	-4125	0.25	-4125	0.25	-4125	0	16500	0	16500	0	16500	0	16500	0.000972	31.63	7900710

Annex III – Results of unit commitment

Table AIII.1 – Unit commitment for single period (system operator)

	0:00	1:00	2:00	3:00	4:00	5:00	6:00	7:00	8:00	9:00	10:00	11:00	12:00	13:00	14:00	15:00	16:00	17:00	18:00	19:00	20:00	21:00	22:00	23:00
1	1Gs	1Gs	1Gs	1Gs	1Gs	1Gs	1Gs	1Gs	1Gs	1Gs	1Gs	1Gs	1Gs	1Gs	1Gs	1Gs	1Gs	1Gs	1Gs	1Gs	1Gs	1Gs	1Gs	1Gs
	1GB	1GB	1GB	1GB	1GB	1GB	1GB	1GB	2GB	2GB	2GB	2GB	2GB	2GB	2GB	2GB	2GB	2GB	2GB	2GB	2GB	2GB	2GB	2GB
2	1Gs	1Gs	1Gs	1Gs	1Gs	1Gs	1Gs	1Gs	1Gs	1Gs	1Gs													
	1GB	1GB	1GB	1GB	1GB	1GB	1GB	1GB	2GB	3GB	3GB	3GB	3GB	3GB	3GB	3GB	3GB	3GB	3GB	3GB	3GB	3GB	3GB	2GB
3		1Gs	1Gs	1Gs	1Gs	1Gs	1Gs	1Gs	1Gs	1Gs	1Gs	1Gs	1Gs	1Gs	1Gs	1Gs	1Gs	1Gs	1Gs	1Gs	1Gs	1Gs	1Gs	1Gs
	2GB	1GB	1GB	1GB	1GB	1GB	1GB	1GB	2GB	2GB	2GB	2GB	2GB	2GB	2GB	2GB	2GB	2GB	2GB	2GB	2GB	2GB	2GB	2GB
4	1Gs	1Gs	1Gs	1Gs	1Gs	1Gs	1Gs	1Gs	1Gs	1Gs	1Gs	1Gs								1Gs	1Gs	1Gs	1Gs	1Gs
	2GB	1GB	1GB	1GB	1GB	1GB	1GB	1GB	2GB	2GB	2GB	2GB	2GB	2GB	2GB	2GB	2GB	2GB	2GB	2GB	2GB	2GB	2GB	2GB
5	1Gs	1Gs	1Gs	1Gs	1Gs	1Gs	1Gs	1Gs	1Gs	1Gs														1Gs
	1GB	1GB	1GB	1GB	1GB	1GB	1GB	1GB	1GB	1GB	2GB	2GB	2GB	2GB	2GB	2GB	2GB	2GB	2GB	2GB	2GB	2GB	2GB	1GB
6	1Gs	1Gs	1Gs	1Gs	1Gs	1Gs	1Gs	1Gs	1Gs	1Gs	1Gs	1Gs	1Gs	1Gs	1Gs	1Gs	1Gs	1Gs	1Gs	1Gs	1Gs	1Gs	1Gs	1Gs
	1GB	1GB	1GB	1GB	1GB	1GB	1GB	1GB	1GB	1GB	1GB	1GB	1GB	1GB	1GB	1GB	1GB	1GB	1GB	1GB	1GB	1GB	1GB	1GB
7	1Gs	1Gs	1Gs	1Gs	1Gs	1Gs	1Gs	1Gs	1Gs	1Gs	1Gs	1Gs	1Gs	1Gs	1Gs	1Gs	1Gs	1Gs	1Gs	1Gs	1Gs	1Gs	1Gs	1Gs
	1GB	1GB	1GB	1GB	1GB	1GB	1GB	1GB	2GB	2GB	2GB	2GB	2GB	2GB	2GB	2GB	2GB	2GB	2GB	2GB	2GB	2GB	2GB	2GB

Table AIII.2 – Unit commitment for single period (Risk assessment)

	0:00	1:00	2:00	3:00	4:00	5:00	6:00	7:00	8:00	9:00	10:00	11:00	12:00	13:00	14:00	15:00	16:00	17:00	18:00	19:00	20:00	21:00	22:00	23:00
1	3GS	0GS	2GS	2GS	2GS	2GS	0GS	3GS	4GS	0GS	1GS	1GS	1GS	1GS	1GS	1GS	0GS	0GS	0GS	1GS	1GS	1GS	0GS	2GS
	0GB	1GB	0GB	0GB	0GB	0GB	1GB	0GB	0GB	2GB	2GB	2GB	2GB	2GB	2GB	2GB	2GB	2GB	2GB	2GB	2GB	2GB	2GB	1GB
2	0GS	2GS	2GS	1GS	1GS	1GS	2GS	0GS	1GS	0GS	0GS	0GS	0GS	0GS	0GS	0GS	0GS	0GS	0GS	1GS	1GS	1GS	0GS	0GS
	1GB	0GB	0GB	0GB	0GB	0GB	0GB	1GB	1GB	2GB	2GB	2GB	2GB	2GB	2GB	2GB	2GB	2GB	2GB	2GB	2GB	2GB	2GB	2GB
3	1GS	0GS	2GS	2GS	2GS	2GS	0GS	0GS	1GS	0GS	1GS	1GS	1GS	0GS	0GS	0GS	0GS	0GS	0GS	0GS	1GS	1GS	0GS	0GS
	1GB	1GB	0GB	0GB	0GB	0GB	1GB	1GB	1GB	2GB	2GB	2GB	2GB	2GB	2GB	2GB	2GB	2GB	2GB	3GB	2GB	2GB	2GB	2GB
4	3GS	0GS	2GS	2GS	2GS	2GS	2GS	0GS	1GS	0GS	1GS	1GS	1GS	0GS	1GS	0GS	0GS	0GS	0GS	1GS	1GS	0GS	0GS	0GS
	0GB	1GB	0GB	0GB	0GB	0GB	0GB	1GB	1GB	2GB	2GB	2GB	2GB	2GB	2GB	2GB	2GB	2GB	2GB	2GB	2GB	2GB	2GB	2GB
5	0GS	2GS	1GS	1GS	1GS	1GS	1GS	1GS	2GS	0GS	1GS	1GS	2GS	1GS	1GS	1GS	1GS	1GS	1GS	0GS	0GS	0GS	1GS	1GS
	1GB	0GB	0GB	0GB	0GB	0GB	0GB	0GB	0GB	1GB	1GB	1GB	1GB	1GB	1GB	1GB	1GB	1GB	1GB	2GB	2GB	2GB	1GB	1GB
6	2GS	2GS	1GS	1GS	1GS	1GS	1GS	1GS	1GS	0GS	0GS	1GS	1GS	1GS	0GS	0GS	0GS	0GS	3GS	0GS	0GS	0GS	0GS	1GS
	0GB	0GB	0GB	0GB	0GB	0GB	0GB	0GB	0GB	1GB	1GB	1GB	1GB	1GB	1GB	1GB	1GB	1GB	0GB	2GB	2GB	2GB	2GB	1GB
7	0GS	2GS	1GS	1GS	1GS	2GS	2GS	0GS	1GS	0GS	0GS	0GS	0GS	0GS	0GS	0GS	0GS	0GS	0GS	1GS	1GS	1GS	0GS	0GS
	1GB	0GB	0GB	0GB	0GB	0GB	0GB	1GB	1GB	2GB	2GB	2GB	2GB	2GB	2GB	2GB	2GB	2GB	2GB	2GB	2GB	2GB	2GB	2GB

Table AIII.3 – Unit commitment for multi-stage period (Risk assessment)

	0:00	1:00	2:00	3:00	4:00	5:00	6:00	7:00	8:00	9:00	10:00	11:00	12:00	13:00	14:00	15:00	16:00	17:00	18:00	19:00	20:00	21:00	22:00	23:00
1	3GS 0GB	2GS 0GB	2GS 0GB	2GS 0GB	2GS 0GB	2GS 0GB	2GS 0GB	3GS 0GB	4GS 0GB	3GS 1GB	4GS 1GB	4GS 1GB	4GS 1GB	4GS 1GB	4GS 1GB	3GS 1GB	3GS 1GB	3GS 1GB	3GS 1GB	4GS 1GB	4GS 1GB	4GS 1GB	3GS 1GB	4GS 0GB
2	3GS 0GB	2GS 0GB	2GS 0GB	2GS 0GB	2GS 0GB	2GS 0GB	2GS 0GB	2GS 0GB	1GS 1GB	1GS 2GB	2GS 2GB	2GS 2GB	2GS 2GB	2GS 2GB	2GS 2GB	2GS 2GB	2GS 2GB	1GS 2GB	1GS 2GB	2GS 2GB	2GS 2GB	2GS 2GB	3GS 1GB	3GS 1GB
3	1GS 1GB	2GS 0GB	2GS 0GB	2GS 0GB	2GS 0GB	2GS 0GB	2GS 0GB	3GS 0GB	4GS 0GB	3GS 1GB	2GS 2GB	2GS 2GB	2GS 2GB	2GS 2GB	2GS 2GB	2GS 2GB	2GS 2GB	1GS 2GB	1GS 2GB	2GS 2GB	2GS 2GB	2GS 2GB	3GS 1GB	3GS 1GB
4	1GS 1GB	2GS 0GB	2GS 0GB	2GS 0GB	2GS 0GB	2GS 0GB	2GS 0GB	3GS 0GB	4GS 0GB	3GS 1GB	4GS 1GB	4GS 1GB	4GS 1GB	4GS 1GB	4GS 1GB	4GS 1GB	3GS 1GB	3GS 1GB	3GS 1GB	4GS 1GB	4GS 1GB	4GS 1GB	3GS 1GB	3GS 1GB
5	2GS 0GB	2GS 0GB	2GS 0GB	2GS 0GB	2GS 0GB	2GS 0GB	2GS 0GB	2GS 0GB	2GS 0GB	3GS 0GB	3GS 0GB	4GS 0GB	4GS 0GB	4GS 0GB	4GS 0GB	4GS 0GB	3GS 0GB	3GS 0GB	4GS 0GB	3GS 1GB	3GS 1GB	4GS 0GB	4GS 0GB	3GS 0GB
6	2GS 0GB	2GS 0GB	2GS 0GB	2GS 0GB	2GS 0GB	2GS 0GB	2GS 0GB	2GS 0GB	2GS 0GB	2GS 0GB	3GS 0GB	3GS 0GB	3GS 0GB	3GS 0GB	3GS 0GB	2GS 0GB	2GS 0GB	2GS 0GB	3GS 0GB	2GS 1GB	3GS 1GB	3GS 1GB	4GS 0GB	4GS 0GB
7	2GS 0GB	2GS 0GB	2GS 0GB	2GS 0GB	2GS 0GB	2GS 0GB	2GS 0GB	2GS 0GB	1GS 1GB	2GS 1GB	2GS 2GB	2GS 2GB	2GS 2GB	1GS 2GB	1GS 2GB	1GS 2GB	1GS 2GB	1GS 2GB	1GS 2GB	2GS 2GB	2GS 2GB	2GS 2GB	3GS 1GB	3GS 1GB